Activated mTOR signaling promotes the expression of PGC1α and mortalin in pancreatic neuroendocrine tumours

Dissertation

To obtain the academic degree

Doctor of Natural Sciences (Dr. rer. nat.)

Completed at the University Medical Center Mainz in the

Institute of Pathology

Submitted to the Department of Biology-Faculty 10

Johannes Gutenberg University Mainz

Submitted by Jessika Valeska Buchwaldt

Born on July 18, 1995 in Wiesbaden

Mainz, 2025

1st Examiner: Dr. Wilfried Roth

2nd Examiner: Dr. Thomas Hankeln

Date of the Oral Examination: 27.03.2026

Index

List of abbreviations

4E-BP1	eIF4E Bindeprotein
Bp	Basenpaare (DNA)
BSA	Bovines Serumalbumin
cDNA	complementary DNA
DEPTOR	DEP domain containing mTOR interacting protein
DMSO	Dimethyl sulfoxide
DNA/ RNA	deoxyribonucleic acid/ ribonucleic acid
dNTP	Desoxyribonucleotide triphosphate
eIF4E	eucaryotic translation initiation factor
ES	Enrichment score
FCS	Fetal calf serum
FDR	False *Discovery Rate*
FFPE	Formalin-fixiertes Paraffin-eingebettetes Gewebe
GSEA	Gene Set Enrichment Analysis
KRAS	Kirsten Rat Sarcoma
MEN1	Multiple endokrine Neoplasie Typ 1
mRNA	Messenger-RNA
mTOR	mechanistic Target of Rapamycin
mTORc1/ mTORc2	mTOR Complex 1 / 2
NES	Normalized enrichment score
NET	Neuroendocrine tumors
NGS	Next generation Sequencing
panNET	Neuroendocrine Tumours of the Pancreas
PGC1α	Peroxisome proliferator-activated receptor γ co-activator 1α
PI3K	Phosphatidylinositol-3 kinase-related kinases
PRAS40	proline-rich Akt substrate of 40 kDa
pS6	Phosphorylated ribosomale protein S6
rCRS	Cambridge Reference Sequence
Rictor	rapamycin insensitive companion of mTOR
rpm	Rounds per minute
S6	Ribosomales Protein S6
S6K1	p70S6 Kinase 1
SBS	Sequencing by synthesis
SDS	Sodium dodecyl sulfate
TMA	Tissue microarray
WHO	World Health Organization

List of illustrations

List of tables

Abstract

Pancreatic neuroendocrine tumors (panNETs) are a rare malignancy that is difficult to treat. Since a considerable number of panNETs exhibit high mTOR pathway activity, current therapeutic strategies for advanced panNETs often involve the use of mTOR inhibitors. Recently, there has been discussion regarding the potential benefits of combining mTOR inhibition with therapies targeting cellular metabolism. These are based on observations that mTOR signalling also impacts mitochondrial functions and the expression of nuclear-encoded mitochondria-related genes. However, the precise interaction between mTOR and mitochondrial function, particularly in the context of panNETs, remains poorly understood. Consequently, the objective of this study is to identify proteins that connect these two systems and assess the functional implications of this relationship.

In the present study, a well-characterized cohort of 157 panNETs was established. We identified pS6 as a reliable biomarker for the mTOR pathway activity in panNET, as we revealed that 22 % of the investigated panNET exhibit mTOR pathway activity by expression analysis of pS6. We could verify this finding by identifying the mTORc1 pathway as the most upregulated pathway in panNET with activated mTOR pathway using RNA-sequencing and gene set enrichment analysis (GSEA). In addition, we were able to identify two mitochondria related proteins as targets of mTOR in panNET. RNA sequencing of panNET tissue and cell lines highlighted PGC1α as the most significantly upregulated gene in tumors with activated mTOR and in the BON1 cell line control group that was compared to BON1 cells treated with mTOR inhibitors. Furthermore, mortalin was found to be highly upregulated in high-grade panNETs with elevated mTOR activity. Interestingly, PGC1α was shown to influence mTOR pathway activity, while mortalin did not impact mTOR signaling. We could not find any correlation between somatic mutations in the mitochondrial DNA and the mTOR pathway activity

In summary, these findings offer valuable insights into the molecular interactions between mTOR signalling and the mitochondria-related proteins mortalin and PGC1α in panNETs. This may pave the way for new treatment options for this rare tumor entity, offering benefits for patients.

Zusammenfassung

Pankreatische neuroendokrine Tumore (panNETs) stellen eine seltene, schwer behandelbare Krebserkrankung dar. Ein erheblicher Anteil dieser Tumoren weist eine erhöhte Aktivität des mTOR-Signalwegs auf, weshalb Inhibitoren dieses Signalwegs Teil der Therapie bei fortgeschrittenen panNETs sind. In den letzten Jahren wurde diskutiert, ob eine Kombination aus mTOR-Inhibitoren und Therapien, die den Zellstoffwechsel gezielt ansprechen, zusätzliche Vorteile bieten könnte. Diese Überlegungen basieren auf der Erkenntnis, dass der mTOR-Signalweg auch mitochondriale Funktionen und die Expression mitochondrialer nukleär kodierter Gene beeinflusst. Die genaue Wechselwirkung zwischen mTOR und mitochondrialen Faktoren, insbesondere in panNETs, ist jedoch bislang wenig erforscht. Ziel dieser Studie war es daher, Gene und Proteine zu identifizieren, die diese beiden Systeme miteinander verbinden.

In der vorliegenden Arbeit wurde eine Kohorte von 157 panNETs untersucht. pS6 wurde als zuverlässiger Biomarker für die mTOR-Aktivität identifiziert, wobei in 22 % der Tumore ein aktivierter mTOR-Signalweg nachgewiesen werden konnte. Dieses Ergebnis wurde mittels RNA-Sequenzierung und GSEA-Analyse bestätigt. Es konnte nachgewiesen werden, dass der mTORc1-Signalweg in Tumoren mit erhöhter mTOR-Aktivität der am stärksten hochregulierte Signalweg ist. Im Rahmen der RNA-Sequenzierung wurde außerdem PGC1α als das am stärksten hochregulierte Gen in Tumoren mit aktiviertem mTOR-Signalweg identifiziert. Eine vergleichbare Hochregulation von PGC1α zeigte sich auch in unbehandelten BON1-Zellen im Vergleich zu BON1-Zellen, die mit mTOR-Inhibitoren behandelt wurden. Zudem war Mortalin in fortgeschrittenen panNETs mit erhöhter mTOR-Aktivität stark hochreguliert. Interessanterweise konnte außerdem gezeigt werden, dass PGC1α Einfluss auf den mTOR-Signalweg nimmt, während Mortalin keinen Einfluss zu haben scheint. Eine Korrelation zwischen somatischen Mutationen in der mitochondrialen DNA und der mTOR-Aktivität konnte nicht nachgewiesen werden. Zusammenfassend liefern diese Ergebnisse wertvolle Einblicke in die molekularen Interaktionen zwischen dem mTOR-Signalweg und mitochondrialen Proteinen, die potenziell neue therapeutische Ansätze für diese seltene Tumorform eröffnen.

1. Introduction

1.1 Neuroendocrine tumours of the pancreas (panNET)

1.1.1 The Pancreas

The pancreas is located behind the stomach in the retroperitoneal space (Fig. 1, Manser, 2013). The organ is 15 to 20 cm long and consists of three anatomical parts: the tail (*Cauda*), body (*Corpus*), and head (*Caput*) (Fig. 1, Manser, 2013). The head is connected to the duodenum via the pancreatic duct (Fig. 1, Manser, 2013). Histologically and functionally, the pancreas is divided into an exocrine and endocrine component (Schünke et al., 2018). The exocrine part of the pancreas consists of multiple glands that produce digestive enzymes (Schünke et al., 2018). These enzymes are needed for the breakdown of nutrients like carbohydrates or fats in the small intestine (Schünke et al., 2018). The endocrine component of the pancreas consists of clusters of epithelial cells known as islets of Langerhans, which are scattered along the exocrine part (Schünke et al., 2018). These epithelial cells can be divided into five different endocrine cell types that are named after the Greek alphabet (alpha, beta, delta, epsilon, upsilon; Schünke et al., 2018). These five endocrine cell types can secret a wide variety of hormones, with insulin and glucagon being the most important ones, as they regulate blood sugar levels (Schünke et al., 2018).

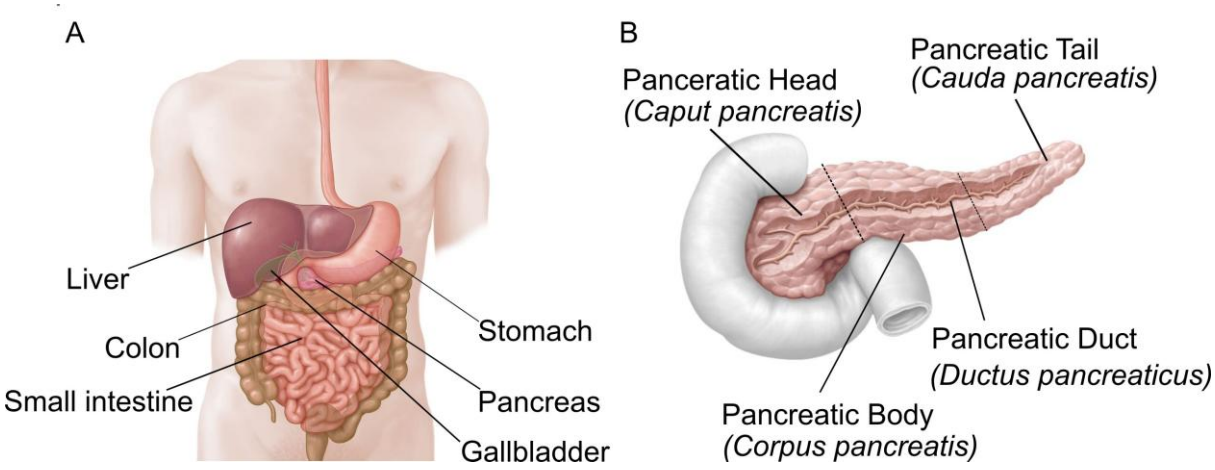

Figure 1: Localization and anatomy of the pancreas.

A) Localization of the pancreas. The pancreas is located behind the stomach, underneath the liver and above the colon in the retroperitoneal space. B) Anatomy of the pancreas. The pancreas consists of the three anatomical parts head, body and tail. (modified according to Schünke et al., 2018)

1.1.2 Epidemiology of panNET

Neuroendocrine tumours (NET) are a heterogeneous group of slowly growing cancers that arise from the diffuse neuroendocrine system (Scott & Howe, 2019; Storni et al., 2021). In comparison to other tumour entities they are rare malignancies with an incidence of about 7 per 100.000 people per year (Storni et al., 2021). NETs can be located in a variety of organs but up to 70 % occur in the gastrointestinal tract and pancreas (Maharjan et al., 2021; Oronsky et al., 2017; Storni et al., 2021). With regard to the pancreas, that means that 2 % of all tumours occurring in this organ are defined as NETs (Dasari et al., 2017). Most panNETs are sporadic but up to 10% are associated with inherited cancer syndroms like the Multiple endocrine neoplasia type 1 or the von-Hippel-Lindau syndrome (Jensen et al., 2008; Lehnert, 2015; Maharjan et al., 2021). While hereditary panNETs are more common in younger patients, sporadic panNETs are most frequently diagnosed in patients between the ages of 30 and 60 years (Lehnert, 2015). In total, the mean age at diagnosis is between 57 and 58 years without clear differences between the sexes regarding the occurrence of tumours (Greenberg et al., 2022; Scott & Howe, 2019).

1.1.3 Classification of panNET

Classification of NET is based on three categories: site of origin, proliferation index and the appearance of hormone release (Giuseppe Lamberti et al., 2018).

The proliferation index is identified by immunohistochemical staining of the proliferation marker Ki-67 according to the guidelines of the World Health Organization (WHO; Rindi et al., 2022). Based on this classification, NETs are divided into G1, G2 or G3 tumours (Table 1).

Table 1: Grading of NET according to the WHO-classification from 2019.

Grading	Ki-67 [%]
G1	< 3
G2	3 – 20
G3	> 20

In addition to this proliferation-based classification, the European Neuroendocrine Tumour Society (ENETS) and the American Joint Committee on Cancer/Union for International Cancer Control (AJCC/UICC) brought the TNM-staging system to life.

This system covers more information about the tumour, including size and extend of the primary tumour (T), the appearance of lymph node metastasis (N) and the presence of distant metastasis (M) (Table 2; Klöppel et al., 2010).

Table 2: TNM-Classification of NET.

(and Ferreira-Silva et al., 2024; modified according to Wittekind, 2017)

T (primary tumour)			
T_0		No primary tumour	
T_1 to T_4		Primary tumour detected Classification according to size and extend of the primary tumour	
N (lymph node metastasis)			
N_0		No lymph node metastasis	
N_1 bis N_3		Lymph node metastasis detected Classification according to localization and frequency	
M (distant metastasis)			
M_0		No distant metastasis	
M_1		Distant metastasis detected	
Anatomic stage			
Stage I	T_1	N_0	M_0
Stage IIA	T_2	N_0	M_0
Stage IIB	T_3	N_0	M_0
Stage IIIA	T_4	N_0	M_0
Stage IIIB	Any T	N_1	M_0
Stage IV	Any T	Any N	M_1

1.1.3.1 Hormonal release and clinical symptoms of panNET

Beside the proliferation index, panNETs can be categorized according to their ability to release hormones into the surrounding tissue. They can be divided into two groups: functional and non-functional tumours. Around 60 to 90% of panNET are non-functional, which means that they can secrete hormones but in a quantity that do not trigger any specific symptoms (Guilmette & Nosé, 2019; Maharjan et al.,

2021). In contrast, functional panNET also secrete hormones but in a quantity that leads to unspecific symptoms like shortness of breath, diarrhoea and rapid heartbeat as well as hormone specific symptoms in patients (Guilmette & Nosé, 2019; Lehnert, 2015; Storni et al., 2021). The hormone specific symptoms are listed in Table 3.

Table 3: Classification of functional panNET.

(Paniccia et al., 2015)

Tumour	Hormone	Symptom	Incidence [%]
Insulinoma	Insulin	Hypoglycemic	35 - 40
Gastrinoma	Gastrin	Zollinger-Ellison syndrome	16 - 30
Glucagonoma	Glucagon	Rashes, Malfunction of the glucose balance	<10
VIPoma	Vasoactive intestinal polypeptide	Verner-Morrison-Syndrome	<10
Somatostatinoma	Somatostatin	Diabetes	<5

1.1.4 Therapy of panNET

Besides early diagnosis, effective therapy is critical for survival of patients. The only curative therapy for panNET consist of the resection of the tumour, which is mostly implemented for primary, non-metastatic tumours (Akirov et al., 2019; Ro et al., 2013; Storni et al., 2021). Systematic therapies are often used for disease control and minimization of symptoms in patients with metastases and residual disease (Maharjan et al., 2021; Scott & Howe, 2019). These therapies include so called somatostatin analogues that are mostly used in functional panNETs as they are effective against hormone production (Ro et al., 2013). Although there is no clear evidence that these analogues are beneficial for patients with non-functional panNET, they seem to suppress tumour growth in this group (Lamberts, 1988; Sidéris et al., 2012). In the last few years, inhibitors of the mechanistic Target of Rapamycin (mTOR) have become important for the therapy of panNET.

1.2 The mTOR signalling pathway

The mTOR signalling pathway is a network that integrates a wide variety of biological processes that contribute to cellular homeostasis and metabolism (Laplante & Sabatini, 2012; Panwar et al., 2023; Saxton & Sabatini, 2017). The centre of this pathway is the mTOR protein that has a dual kinase activity as it

phosphorylates serine/threonine or tyrosine kinases (Panwar et al., 2023). Moreover, the mTOR protein forms the catalytic subunit of the two functional complexes mTOR-complex1 (mTORc1) und mTOR-complex2 (mTORc2) (Liu & Sabatini, 2020; Panwar et al., 2023). The exact structure of the complexes is shown in Figure 2.

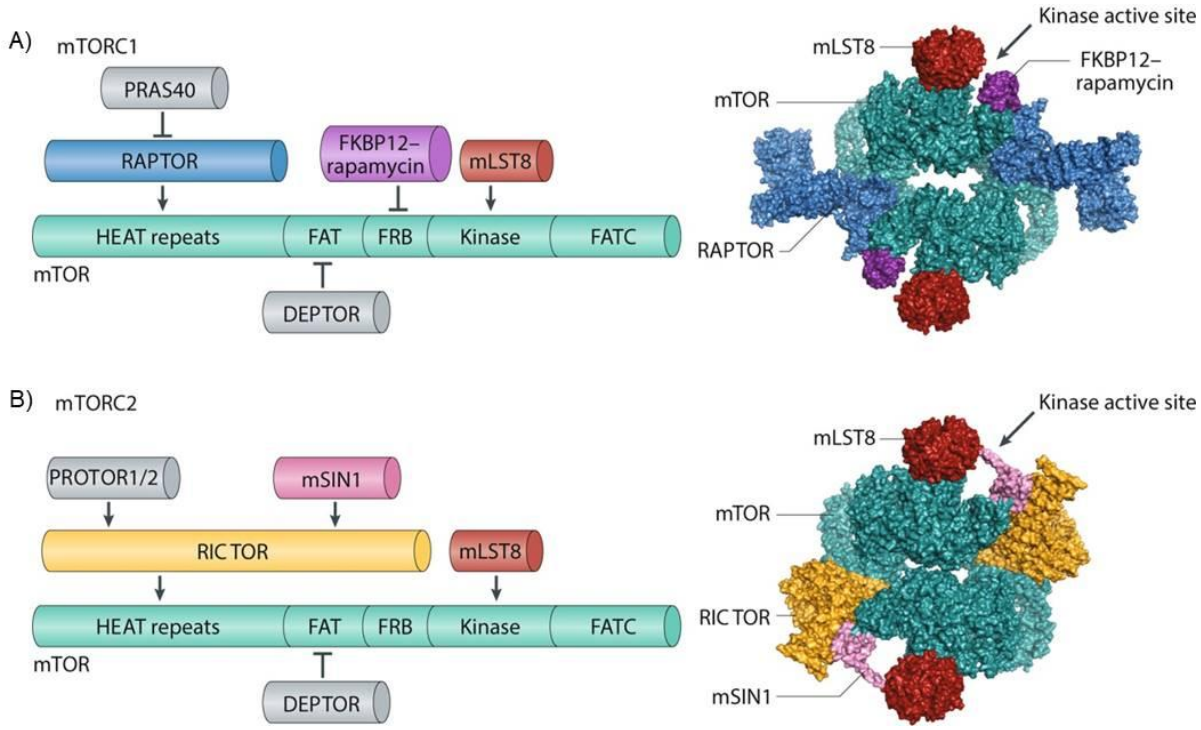

Figure 2: Structure of mTORc1 and mTORc2.

The domain structure of the catalytic subunit mTOR (in green) includes various binding sites for the subunits of mTORC1 (A) and mTORC2 (B). The catalytic subunit of mTOR consists, in both complexes, of HEAT repeats (comprising clusters of Huntingtin, the elongation factor 3, a subunit of protein phosphatase 2A, and TOR1 or TOR2), followed by a FRAP, ATM, and TRRAP (FAT) domain, as well as the FKBP12-Rapamycin-binding domain (FRB), the catalytic kinase domain, and the C-terminal FATC domain. Additionally, the structure of mTORC1 (A) includes Raptor as a defined subunit, which recruits PRAS40 (an insulin-regulated mTORC1 inhibitor). In mTORC2 (B), the additional subunits of the multiprotein complex comprise mLST8, DEPTOR, and RICTOR as defined components. Moreover, RICTOR recruits the protein associated with rictor 1 or 2 (PROTOR1/2) along with the MAPK-interacting protein (mSIN1) as scaffold proteins. (modified according to Liu & Sabatini, 2020).

Besides their slightly different composition, both complexes differ in their activation, function, and sensitivity against the mTOR-inhibitor rapamycin. While both complexes can be activated by signals from growth factors, mTORc1 mainly processes information about nutrients, hormones, amino acids and hypoxia (Tian et

al., 2019). In terms of their functions, the mTORc1 is well known for its role in the protein biosynthesis, nucleotide synthesis and the regulation of different metabolism, whereas mTORc2 regulates the organization of the cytoskeleton, cell survival and cell proliferation (W. Fu & Hall, 2020; Panwar et al., 2023; Saxton & Sabatini, 2017). It has been shown that the function of mTORc1 can be prevented by inhibition using rapamycin (Kang et al., 2013). For mTORc2 it has long been postulated that this inhibitor has no impact on its activity. Nevertheless, a study from Sarbassov *et al.* showed that extended incubation with rapamycin (up to 24 hours) can lead to inhibition of mTORc2 in a variety of carcinoma cell lines (Dos D. Sarbassov et al., 2006).

1.2.1 Downstream of mTORc1

The mTORc1 integrates stimuli from a variety of nutrients and growth factors for promotion of the synthesis of nucleotides, lipids and proteins (Saxton & Sabatini, 2017). At the same time, mTORc1 supresses catabolic processes like autophagy (Saxton & Sabatini, 2017).

In case of the protein synthesis, the p70S6 Kinase 1 (S6K1) and eIF4E Binding Protein (4EBP1) are the two most well-known downstream targets of mTORc1. The S6K1 is directly phosphorylated by mTORc1 at T389, leading to phosphorylation of the ribosomal protein S6 (S6), a component of the 40S subunit of ribosomes (Dennis et al., 1998; Meyuhas, 2015). The S6 protein than activates different targets that are involved in mRNA translation initiation, leading to increased protein synthesis (Holz et al., 2021; Saxton & Sabatini, 2017). The second downstream target of mTORc1, 4EBP1, promotes 5′cap-dependent mRNA translation by preventing the assembly of the eIF4F complex trough binding of the eIF4E (Saxton & Sabatini, 2017).

In case of the lipid/nucleotide and glucose metabolism, the mTORc1 controls different transcription factors. Two interesting targets in this context are the Hypoxia-inducible factor 1α (HIF1α) and the sterol responsive element binding protein (SREBP) (Saxton & Sabatini, 2017). While the SREBP controls the expression of genes involved in fatty acid and cholesterol biosynthesis (Porstmann et al., 2008), the HIF1α promotes the expression of a variation of glycolic enzymes (Düvel et al., 2010). Both transcription factors are directly activated by mTORc1 trough phosphorylation or indirect trough interaction of mTORc1 with target related inhibitors (Düvel et al., 2010; Peterson et al., 2011).

In addition to controlling these anabolic processes, mTORc1 also influences a variation of catabolic systems. One catabolic process that is suppressed by mTORc1 to promote cell survival and growth is the autophagy. The mTORc1 controls this process through the interaction with key activators like the 5' AMP-activated protein kinase or through impairment of transcription factors like TFEB (J. Kim et al., 2011; Martina et al., 2012).

1.2.2 Downstream of mTORc2

Although the role of mTORc2 is not well understood, one of the main functions of mTORc2 is to control the organization of the cytoskeleton (Saxton & Sabatini, 2017). This duty is mediated by the interaction of complex 2 with several members of the Protein kinase C family (Saxton & Sabatini, 2017). For example, mTORc2 controls PKCα and PKCγ (Saxton & Sabatini, 2017). These two proteins have been described to contribute to remodelling of the actin cytoskeleton and cell migration in different fibroblasts as well as brain and Purkinje cells (Jacinto et al., 2004; Thomanetz et al., 2013).

Besides its role in the organization of the cytoskeleton, mTORc2 is also described in the context of the PI3K/AKT pathway (D. D. Sarbassov et al., 2005). This pathway is one of the most important intracellular systems in cells, contributing to a variety of cell survival related biological processes like proliferation, growth and metabolism (D. D. Sarbassov et al., 2005). The mTORc2 phosphorylates and activates the Protein kinase B (AKT), a key component of this pathway (D. D. Sarbassov et al., 2005). Although mTORc2 seems to be one of the main control points of AKT, it should be mentioned that mTORc2-dependent phosphorylation does not seem to be required for all AKT related interactions (D. D. Sarbassov et al., 2005). For example, it has been shown that the phosphorylation of TSC2 trough AKT seems to be independent of the protein complex (Guertin et al., 2006; Jacinto et al., 2006).

1.2.3 mTOR and cancer

The mTOR signaling pathway is one of the most frequently mutated pathways in a wide variety of tumour entities. Especially the upregulation of the mTOR pathway activity has been connected to high tumour growth and progression in different studies (Hua et al., 2019; Saxton & Sabatini, 2017). In panNET, immunohistochemical examinations revealed a high percentage of tumours with upregulated mTOR pathway activity, whereby the exact numbers differ between 33

% in a study from Lamberti et al. and 26 to 52 % in a study from Komori et al. (Komori et al., 2014; G. Lamberti et al., 2017). In both studies, the dysregulation of mTOR was correlated with high invasion, high proliferation and an advanced-stage of panNET (Komori et al., 2014; G. Lamberti et al., 2017).

In general, overexpression of mTOR in cancer can be associated with three different biological reasons: mutations in the *mTOR* gene itself, mutations in different components of mTOR and mutations of upstream targets of mTOR. Mutations in the *mTOR* gene itself are rarely found in human cancer types but studies showed that these mutations are correlated with the activation of the mTOR signaling pathway in colorectal cancer cells and mice fibroblasts (Edinger & Thompson, 2004; Sekulić et al., 2000). Moreover, a comparison of different tumour genome sequencing data revealed 33 mutations in the C-terminal region of mTOR that have the potential to induce pathway hyperactivation (Grabiner et al., 2014). Grabiner *et al.* showed that these mutations appear in a wide variety of cancer types and they suggest that the activation of the mTOR complex may be attributed to an inhibited interaction between mTOR and its regulatory subunit DEPTOR (Grabiner et al., 2014).

Besides mutations in the *mTOR* gene itself, genetic aberrations in different components of the two mTOR complexes have also been associated with elevated mTOR pathway activity (Conciatori et al., 2018). Especially the subunit RICTOR of mTORc2 seems to be linked to pathway hyperactivation (Conciatori et al., 2018). Enrichment of RICTOR has been observed in non-small-cell lung cancer and breast cancer (Cheng et al., 2015; Morrison Joly et al., 2016; Pilotto et al., 2017).

The most frequently reason for hyperactivation of the mTOR pathway is the occurrence of mutations in various upstream targets of mTOR. These mutations manifest as loss-of-function mutations in tumour suppressor genes and gain-of-function mutations in oncogenes (Conciatori et al., 2018; Tian et al., 2019). For example, mutations in the tumour suppressor PTEN, KRAS and BRAF are associated with upregulated mTOR pathway activity and could be observed in breast cancer, kidney cancer and NETs (Conciatori et al., 2018; DeGraffenried et al., 2004; Scarpa et al., 2017; Zoncu et al., 2011). In panNET, a whole-genome sequencing analysis also identified PTEN as one of the most frequently mutated genes taken together with MEN1, DAXX and ATRX (Jiao et al., 2011; Scarpa et al., 2017). This observation is supplemented by the finding that the mTOR signaling pathway is one

of the top three upregulated pathways in 102 primary panNETs, right after chromatin remodelling and DNA damage repair (Scarpa et al., 2017).

1.2.4 Inhibitors of the mTOR signaling pathway

Inhibitors of the mTOR signaling pathway are a central element in the targeted drug therapy of well or moderately differentiated and metastatic panNET. In general, there are three different groups of inhibitors that are already used for treatment of patients or are in clinical trial.

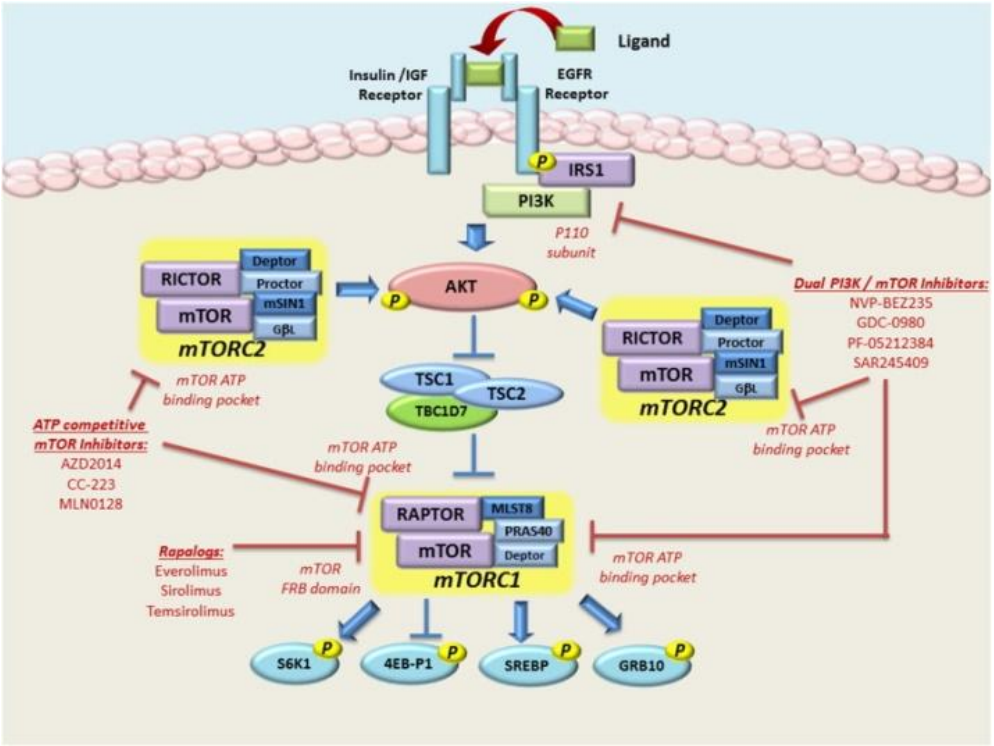

Figure 3: Inhibition of the mTOR signaling pathway.

There are three categories of inhibitors of the mTOR signaling pathway. Firstly, the rapalogs that consists of derivate of rapamycin and mainly inhibit the activity of the mTORc1 through impairment of the mTOR-Raptor relationship. Secondly, ATP competitive inhibitors that perform allosteric interaction with the ATP-binding pocket and therefore inhibit mTORc1 and mTORc2. Thirdly, dual PI3K/mTOR inhibitors that inhibit both mTOR complexes as well as PI3K, due to the sequence homology of PI3K and mTOR. (Malley & Pidgeon, 2016)

The first group of mTOR inhibitors consists of rapalogs, which are water-soluble derivates of rapamycin with a good pharmacokinetic (Hua et al., 2019). They inhibit the mTOR pathway by impairing the relationship between mTOR and its subunit Raptor through interaction with the 12 kDa FK506-binding protein (FKBP12) (J. Chen

et al., 1995; Chiarini et al., 2019). Interestingly, these substances do not induce apoptosis or other cell death related mechanisms, they only lead to cell growth arrest (Hua et al., 2019). As Raptor is a subunit of mTORc1, this inhibition leads to downregulation of the mTORc1 activity without affecting mTORc2. The best-known rapalogs are everolimus (trade name: Afinitor®) and temsirolimus (trade name: Torisel®), which were initially used to treat renal cell carcinoma but were later approved for the treatment of advanced breast cancer and panNET (Figure 3, Hua et al., 2019; Roskoski, 2022). Although the efficiency of rapalogs has been clinically proven in different tumour entities, there are no established biomarkers for the response of patients to these substances. There has been a study that postulate KRAS as a prognostic marker for resistance of patients to rapalog induced mTOR inhibition (Yeung et al., 2017).

The second group of mTOR inhibitors consists of ATP competitive inhibitors. These substances inhibit both mTOR complexes, as they directly target the ATP-binding pocket of mTORc1 and mTORc2 trough allosteric interaction (Amin et al., 2021; Neil et al., 2016). In comparison to rapalogs, ATP competitive inhibitors not only lead to cell growth arrest, they also induce apoptosis. Two known ATP competitive mTOR inhibitors are MLN018 (Sapanisertib) and AZD2014 (Vistusertib), which are being investigated for use in various tumour entities such as leukaemia, breast cancer and colorectal cancer (Figure 3, Gökmen-Polar et al., 2012; Guichard et al., 2015; Rashid et al., 2018).

The third and last group consists of dual PI3K/mTOR inhibitors. These inhibitors are based on the observation that the lipid kinase PI3K has high sequence homology with mTOR in its hinge-region (Feldman & Shokat, 2010; Panwar et al., 2023; Schenone et al., 2011). Therefore, these inhibitors not only inhibit both mTOR complexes, they also impair the activity of PI3K (Feldman & Shokat, 2010; Schenone et al., 2011). Representatives of this group include NVP-BEZ235 (Dactolisib) and GDC-0980 (Apitolisib) that are still in clinical trial (Figure 3, Dolly et al., 2016; Shi et al., 2018).

In addition to these specific inhibitors of the mTOR signaling pathway, multikinase inhibitors such as sunitinib (trade name: Sutent®) are also used in the treatment of panNET. Especially kinases that influence tumour growth, angiogenesis and metastasis are of interest in this context (Chow & Eckhardt, 2007). Furthermore, there has been recent discussion regarding the potential benefits of combined

treatment of mTOR inhibitors with inhibitors targeting cellular metabolism for patients (Tsoli et al., 2018).

1.3 Mitochondria and cancer

The development and formation of malignant tumours as a consequence of neoplastic disease is very complex. For a better understanding of this process, the most important characteristics of tumour formation have been summarized under the term “hallmarks of cancer” (Figure 4), including resistance of cell death, activation of invasion/metastasis and deregulation of cellular energetics (Hanahan, 2022).

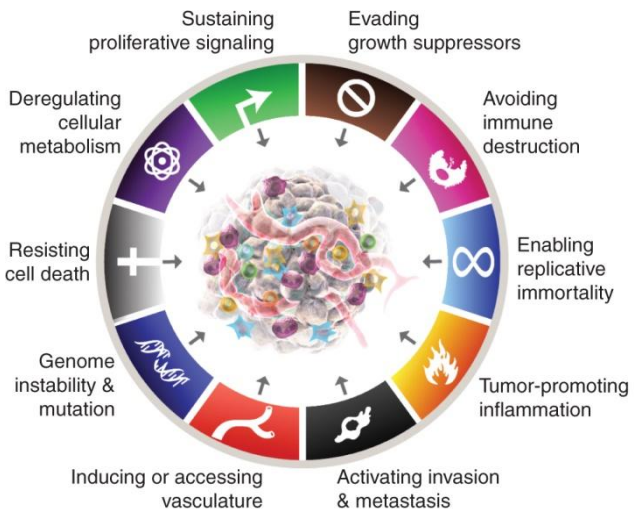

Figure 4: The hallmarks of cancer.

The capabilities of neoplastic disease to form malignant tumours can be summarized in ten different categorize. (modified according to Hanahan, 2022)

Especially deregulation of cellular energetics has been described for a long time, as Warburg *et al.* discovered the so-called Warburg effect in 1924 (Warburg, 1924). This effect is based on the observation that tumours produce high amounts of lactate in the presence of oxygen by a process called “aerobic glycolysis”, while normal cells produce energy by the mitochondria related oxidative phosphorylation (Liberti & Locasale, 2016; Wallace, 2012; Warburg, 1924). Although the aerobic glycolysis is energy inefficient in comparison to the oxidative phosphorylation, it can be beneficial for cancer cell development through the increased glycolytic flux that supports cell proliferation by providing biosynthetic precursors (Liberti & Locasale, 2016). However, new research has shown that not all tumours shift to glycolysis for energy production. In fact, there is a huge heterogeneity in cellular energetics in different

tumours or tumour classes, where in most of them glycolysis does not occur instead of mitochondrial respiration (Koppenol et al., 2011). Although Warburg's observation was made a long time ago, it forms the basis for the observation that metabolic signaling pathways and glycolysis may represent a promising approach to the treatment of cancer.

In general, mitochondria are the main energy source in most eukaryotic cells as these organelles harbor the oxidative phosphorylation system (OXPHOS) that generates the energy currency ATP. Moreover, they also play an important role in many other biological processes like calcium signaling, apoptosis or cellular senescence (Habbane et al., 2021; Osellame et al., 2012). Mitochondria are unique organelles as they contain their own 16,569 bp long DNA, known as the mitochondrial DNA (mtDNA) or mitogenome (Habbane et al., 2021). This genome encodes 37 genes, including 22 transfer RNAs and 2 ribosomal RNAs that are essential for mitochondrial respiration and ATP production (Habbane et al., 2021). In recent years, a wide variety of somatic mutations have been described in these genes in different tumour entities and have been connected to dysregulation of the OXPHOS (Schon et al., 2012; Stewart et al., 2015). It has been reported that these mutations may stimulate the neoplastic formation of tumours and facilitate the adaption to changing bioenergetics (Brandon et al., 2006; Wallace, 2012). Although the role of mtDNA mutations in pancreatic cancer is not well understood, it has been reported that mutations in different genes of the mtDNA occur in a variety of pancreatic cancer cell lines and that these changes may be beneficial for formation and invasion of pancreatic tumours (Jones et al., 2001; Moro, 2021).

Besides the OXPHOS related genes, the mtDNA harbours two non-coding regions that are called control region and displacement loop (Habbane et al., 2021). These secondary structures of the DNA are important for the replication and transcription of the genome as they temporarily contain a short complimentary DNA strand that leads to separation of the double-stranded DNA molecule (Nicholls & Minczuk, 2014). Additionally to these regions, the replication and transcription of the mtDNA depends on nuclear encoded proteins like the Peroxisome proliferator-activated receptor gamma coactivator 1-alpha (PGC1α) or the mitochondrial transcription factor A (TFAM) (Habbane et al., 2021).

1.3.1 mTOR and mitochondria

Given the central role of mTOR in different biological processes, it is not surprising that there is some evidence that the protein impacts the mitochondrial biogenesis. Genome-wide polysome profiling of translational targets of rapalogs revealed, that the inhibition of mTOR impacts a wide variety of mRNAs related to nucleus encoded mitochondrial proteins (Larsson et al., 2012). In total, 14 % of all identified mRNAs were associated with mitochondrial functions (Larsson et al., 2012). These mRNAs included mRNAs encoding for components of the oxidative phosphorylation (mainly complex V (ATP synthase)) and proteins that are involved in the transcription and translation of the mtDNA (for example TFAM) (Larsson et al., 2012; Morita et al., 2013). In addition to these observations, Morita *et al*. showed that inhibition of mTOR leads to reduced mitochondrial mass, mtDNA content and up to 35 % reduced mitochondrial respiration in breast cancer cells, underlying the impact of mTORc1 on a variety of mitochondrial parameters (Morita et al., 2013). The study attributes the effect of mTORC1 on mitochondria to its interaction with 4EBP, which influences the eIF4F initiation complex (Morita et al., 2013).

Another process regulated by mTORC1 are mitochondrial dynamics, which includes the processes of mitochondrial fusion and fission (Trotta & Chipuk, 2017). Fusion refers to the merging of two mitochondria into a single organelle, while fission describes the process by which one mitochondrion divides into two separate mitochondria (Trotta & Chipuk, 2017). In general, mitochondrial dynamics are important for the information exchange between organelles during stress situations, mtDNA replication and cell division (Trotta & Chipuk, 2017). A key regulator of mitochondrial fission is the mitochondrial fission process protein 1 (MTFP1), which is located at the inner mitochondrial membrane (Tondera et al., 2005). The translation of this protein has been shown to be impacted by mTORc1 via 4E-BP and that inhibition of mTORC1 suppresses this process, leading to mitochondrial elongation (Morita et al., 2017). Notably, mTOR inhibitors like rapamycin slow down cell growth by regulating metabolism and protein synthesis, which has cytostatic effects on cells. When mitochondrial fission is additionally enhanced, the mitochondrial structure is altered to such an extent that it triggers stress and activates apoptosis (Morita et al., 2017). As a result, the combination of mTOR inhibition and increased fission becomes cytotoxic (Morita et al., 2017).

1.4 Aim of the work

Neuroendocrine tumours are a rare malignancy that is difficult to medicate as the treatment options mainly include classical cancer treatments such as chemotherapy or surgery. Therefore, the discovery of targeted drug therapy was a great breaking point for the treatment of NETs. They offered the opportunity to specifically target cell growth or cell proliferation related proteins with less side effects for the patient in comparison to common chemotherapy drugs. In NETs one of the main targets for this form of therapy is the mTOR signalling pathway, which is based on the observation that this pathway is highly activated in a great number of NETs. As it has also been shown that mTOR impacts mitochondrial function and the expression of nuclear-encoded mitochondria-related genes, there have been recent discussions regarding the potential benefits of combined treatment with inhibitors targeting cellular metabolism in patients. However, there remains limited understanding of the interplay between mTOR and mitochondria, particularly within NETs. Therefore, the objective of this study was to identify proteins that connect these two systems, with a primary focus on panNETs due to the heterogeneity of NETs.

For this propose, a cohort of 157 panNET was established and the activity of the mTOR signalling pathway determined by expression analysis of the phosphorylated ribosomal protein S6 in a tissue micro array (TMA). In the next step, RNA sequencing was performed on 69 panNET samples from the initial cohort, both with and without mTOR pathway activity, to identify targets associated with both mTOR and mitochondrial function. The expression of the identified genes that was subsequently examined using quantitative PCR. Functional consequences of the observed molecular alterations were assessed in cellular assays using BON1 and QGPT1 cells.

2. Material and methods

2.1 Material

2.1.1 Chemical

Chemical	Manufacturer
Acrylamid Mix, Rotiphorese®Gel 30 (37, 5:1)	Carl Roth, Karlsruhe, Germany
Deoxyribonucleotide triphosphate (dNTP) mix	Thermo Fisher, Waltham , USA
Dimethyl sulfoxide (DMSO)	Thermo Fisher, Waltham , USA
Dulbecco's Phosphate Buffered Saline (PBS)	Sigma-Aldrich, St. Louis, USA
Fetal calf serum (FCS)	Sigma-Aldrich, St. Louis, USA
Gel Loading Dye, Purple (6X)	New England, Frankfurt aM, Germany
Isopropanol	Merck, Darmstadt, Germany
L-Glutamin, 200 Mm Stock	Thermo Fisher, Waltham, USA
Lysis buffer (10x)	Cell Signaling, Frankfurt aM, Germany
M-MLV Reverse Transcriptase	Promega, Walldorf, Germany
Penicillin-Streptomycin	Sigma-Aldrich, St. Louis, USA
Protease/Phosphatase Inhibitor Cocktail (100X)	Thermo Fisher, Waltham, USA
Protein Assay Reagent	Bio-Rad, California, USA
Proteinase K from Tritirachium album	Sigma-Aldrich, St. Louis, USA
Pyruvat	Sigma-Aldrich, St. Louis, USA
Random Primers	Promega, Walldorf, Germany
Bovine serum albumin (BSA)	Roth, Karlsruhe, Germany
RNasin®Plus Rnase Inhibitor	Promega, Walldorf, Germany
RPMI 1640 Medium, GlutaMAX™ Supplement	Thermo Fisher, Waltham, USA
Sodium dodecyl sulfate (SDS)	Serva, Heidelberg, Germany
Sodium Hydroxide Solution, 2 M NaOH	Thermo Fisher, Waltham, USA
SYBR™Green PCR Master Mix	Thermo Fisher, Waltham, USA
TRIS-Acetat-EDTA (TAE)-buffer	Thermo Fisher, Waltham, USA
Tris-buffered saline (TBS) 20x powder	ApplieChem GmbH, Darmstadt, Germany
Trizma® base	Merck, Darmstadt, Germany
Trypsin-EDTA	Sigma-Aldrich, St. Louis, USA
UltraPure™ Agarose	Thermo Fisher, Waltham, USA

2.1.2 Buffer and chemical solutions

2.1.2.1 Isolation of the whole cell extract

6x sample buffer	350 mM Tris-HCl; pH 6.8 10,28 % (w/v) SDS 36 % Glycerol 600 mM Dithiothreitol Spatula tip Bromphenol blue ddH_2O
Lysis buffer	10 % (v/v) 10x Lysis buffer 2 % (v/v) Protease/Phosphatase Inhibitor ddH_2O

2.1.2.2 SDS-Page und Western Blotting

Blocking solution	5 % (w/v) Nonfat dried milk powder in TBS-T
Enhanced chemiluminescence (ECL) detection solution	10 ml Tris-HCl 100 Mm; pH 8.5 50 µl Luminol (250 mM in DMSO) 25 µl Coumaric acid (90 mM in DMSO) 4 µl H_2O_2 (30 % (v/v))
PBS (10x)	140 mM NaCl 8 mM $Na_2HPO_4 \cdot 7H_2O$ 2 mM $NaH_2PO_4 \cdot 7H_2O$ ddH_2O
PBS-T	0,1 % (v/v) Tween 20 in PBS (1x)
Ponceau S staining solution	0,5 % (w/v) Ponceau S 1 % (v/v) Concentrated acetic acid
SDS-Page Running buffer (10 x); pH 8.3	250 mM Tris 1.92 M Glycine 1 % (w/v) SDS ddH_2O

Stacking buffer, pH 6.8	500 mM Tris-HCl ddH_2O
Resolving buffer; pH 8.8	1,5 M Tris-HCl ddH_2O
Semi-dry blotting buffer (1 x)	10 % (v/v) Semi-dry blotting buffer (10 x) 20 % (v/v) Methanol ddH_2O
Semi-dry blotting buffer (10 x); pH 9-9.2	480 mM Tris 390 mM Glycine 0,375 % (w/v) SDS ddH_2O
TBS (10 x); pH 7.6	200 mM Tris 1.38 M NaCl ddH_2O
TBS-T	0,1 % (v/v) Tween 20 in TBS (1x)

2.1.3 Oligonukleotides

2.1.3.1 Oligonucleotides used as qPCR-primer.

Primer	Primer sequence	Manufacturer
HPRT	forward: 5'-TTG CTG ACC TGC TGG ATT AC-3' reverse: 5'-TTT TTG GTT GAG CAC AGG-3'	self-designed
Actin	forward: 5'-CCT AAA AGC CAC CCC ACT TCT C-3' reverse: 5'-ATG CTA TCA CCT CCC CTG TGT G-3'	self-designed
GAPDH	forward: 5'-ACA GTT GCC ATG TAG ACC-3' reverse: 5'-TTT TTG GTT GAG CAC AGG-3'	self-designed
PGC1A	forward: 5´-TGA AGA CGG ATT GCC CTC ATT-3´ reverse: 5´-GCT GGT GCC AGT AAG AGC TT-3´	self-designed
mortalin	forward: 5´-GCC TTG CTA CGG CAC ATT GTG A-3´ reverse: 5´- CTG CAC AGA TGA GGA GAG TTC AC-3´	OriGene Technologies, Rockville, USA

2.1.3.2 Oligonucleotides used as siRNAs.

Target (Gene symbol/ Ensembl ID)	Designation	Company	Article number
PPARGC1A/ ENSG00000109819	PGC1α-si1	Thermo Fisher, Waltham, USA	s21393
PPARGC1A/ ENSG00000109819	PGC1α-si2	Thermo Fisher, Waltham, USA	s21394
MORTALIN/ ENSG00000113013	mortalin-si1 mortalin-si2 mortalin-si3	MedChemExpress, NJ, USA	HY-RS06437
Non-targeting control siRNA	Scram	Dharmacon, CO, USA	D-001810-10-20

2.1.4 DNA- und Protein-marker

Marker	Manufacturer
1 kb DNA Ladder	New England, Frankfurt aM, Germany
100 bp DNA Ladder	New England, Frankfurt aM, Germany
50 bp DNA Ladder	New England, Frankfurt aM, Germany
PageRuler™ Prestained Protein Ladder	Thermo Fisher, Waltham, USA

2.1.5 Kits

Kit	Manufacturer
AmpliSeq™ Library PLUS Kit	Illumina, San Diego, USA
AmpliSeq™ Transcriptome Human Gene Expression Panel	Illumina, San Diego, USA
Maxwell® RSC DNA FFPE Kit	Promega, Heidelberg, Germany
Maxwell® RSC RNA FFPE Kit	Promega, Heidelberg, Germany
ProtoScript® II First Strand cDNA Synthesis Kit	New England, Frankfurt aM, Germany
QIAmp®DNA Mini Kit	Qiagen, Hilden, Germany
QIAseq Targeted DNA 29 Human Mitochondria Panel (DHS-105Z)	Qiagen, Hilden, Germany
Qubit® dsDNA-BR-Assay-Kit	Thermo Fisher, Waltham, USA
Qubit® dsDNA-HS-Assay-Kit	Thermo Fisher, Waltham, USA
RNeasy®Plus Mini Kit	Qiagen, Hilden, Germany
WesternBright™ Sirius™ Detection Kit	advansta, San José, USA

2.1.6 Antibody

All primary antibodies were diluted in PBS-T with 5 % BSA. All secondary antibodies were diluted in TBS-T with 5 % nonfat dry milk.

Primary antibodies	Manufacturer	Working solution Western Blotting	Working solution immunhistochemistry
Monoclonal antibody against human Actin (#MAB1501)	Merck, Darmstadt	1:10.000	-
Monoclonal antibody against human Phospho-S6 Ribosomal Protein (pS6) (#4858)	Cell Signaling, Frankfurt aM	1:2.000	1:400
Monoclonal antibody against human S6 Ribosomal Protein (S6) (#2317)	Cell Signaling, Frankfurt aM	1:1.000	1:200
Monoclonal antibody against human PGC1α (#2178S)	Cell Signaling, Frankfurt aM	1:1.000	-
Monoclonal antibody against human MORTALIN/ Mortalin (#3593)	Cell Signaling, Frankfurt aM	1:1.000	-

Secondary antibody	Manufacturer	Working solution Western Blotting
Rabbit-Antibody (#170-6515)	Bio-Rad, California, USA	1:3.000
Maus-Antikörper (#170-6516)	Bio-Rad, California, USA	1:3.000

2.1.7 Cell lines und cultivation

The adherent human cell lines BON1 and QGP1 which originate from neuroendocrine tumours located in the pancreas were used for all cell biological assays.

Standard growth medium for adherent panNET cell lines

The used panNET cell lines were cultured in RPMI 1640 Medium, GlutaMAX™ Supplement Medium with 10 % FBS, 1 % Penicillin-Streptomycin and 10 % L-Glutamin.

Freezing medium for adherent panNET cell lines

For cryopreservation, the adherent panNET cell lines were stored in freezing medium containing 10 % DMSO and 90 % FBS.

2.1.8 Software

Software	Version	Company
Citavi	6	Swiss Academic Software (Wädenswil, Switzerland)
CLC Genomics Workbench	12.0	Qiagen (Hilden, Germany)
Fusion© Software	v.2.0.19941	Evolution-Capt, (Vilber Lourmat, Eberhardtzell, Germany)
g:profiler online tool		Kolberg et al., 2023
GSEA software		Subramanian et al., 2005
Illumina Experiment Manager	1.15.1	Illumina (San Diego, CA, USA)
ImageJ	1.48	Wayne Rasband (National Institutes of Health, USA)
Inkscape	1.3.2	Inkscape Project, 2020
Maxwell® RSC Application Software		Promega (Madison, WI, USA)
Microsoft ® Excel, PowerPoint, Word for Microsoft 365	2110	Microsoft (Redmond, WA, USA)
MiSeqReporter	2.6.2.3	Illumina (San Diego, CA, USA)
ND-1000	V3.81	Thermo Fisher (Waltham, USA)
NDP.view2	U12388-01	Hamamatsu (Shizuoka, Japan)
NextSeq Control Software	4.0	Illumina (San Diego, CA, USA)
PathoPro	9.0.9070	ifms (Saarbrücken, Germany)
Primer3Plus		Untergasser et al., 2012
Primer-BLAST		Ye et al., 2012
QuantStudio™ Design & Analysis Software	1.5.1	Applied Biosystem/Thermo Fisher (Waltham, USA)
Qubit Data Logger	1.1.7	Thermo Fisher (Waltham, USA)
QuPath	V0.5.1	Bankhead et al., 2017
R	4.3.0	R Core Team (https://www.r-project.org/ (accessed: 15.01.25))
R-Studio	2023.09.1	RStudio (Boston, MA, USA)
SPSS	22.0	IBM (Armonk, NY, USA)
VariantStudioTM	3.0.12	Illumina (San Diego, CA, USA)

2.2.1 Cohort of panNET for the selection of panNET with activated mTOR pathway signaling

To identify panNET with activated mTOR pathway, a well-characterized cohort of 157 panNETs was established. The tumour stage of patients was classified based on the ENETS/ UICC and the grading of the tumours was classified based on the WHO (Klöppel et al., 2010; Rindi et al., 2022). Detailed patient characteristics are displayed in Table 4. The local ethics committee (Ethics Committee of the Rhineland-Palatinate State Medical Association, Mainz, Germany) approved the study design, and all samples were handled in compliance with the standards proposed by the Declaration of Helsinki

Table 4: Summary of clinic pathological features in the study population (n = 157).

Parameter	Samples	
	n	%
Number of patients	157	100
Gender		
Male	80	51
Female	77	49
Age, year	59	
Range	18 - 88	
Primary Tumour (T)		
T1	56	36
T2	37	24
T3	53	34
T4	4	2
TX	7	5
Regional lymph nodes (N)		
N0	53	34
N1	47	30
N2	1	1
NX	56	36
Distant metastasis (M)		
M0	29	19
M1	19	12
MX	109	69

Parameter	Samples	
	n	%
TNM classification		
I	25	16
II	23	15
III	2	1
IV	19	12
unknown	88	56
Grading (G)		
G1	66	42
G2	60	38
G3	14	9
GX	17	11
Functional status		
Functional	34*	22
Non-functional	123	78

* 26 Insulinoma (17 %), 5 Glucagonoma (3 %) und 3 Gastrinoma (2 %)

2.2.1.2 Cohort of panNET for the identification of molecular alterations

For the following molecular analyses, the number of panNET cases had to be adjusted due to low RNA quality and quantity. Therefore, all assays expect the immunohistochemical staining were performed using 69 of the initially 157 panNET cases. All clinical pathological features of this population are listed in Table 5.

Table 5: Summary of clinic pathological features in the experimental population (n = 69).

Parameter	Samples	
	n	%
Number of patients	69	100
Gender		
Male	35	51
Female	34	50
Age, year	59	
Range	25 - 87	
Primary Tumour (T)		
T1	22	32
T2	17	25
T3	24	35
T4	3	4
TX	3	4
Regional lymph nodes (N)		
N0	20	29
N1	26	38
N2	1	1
NX	22	32
Distant metastasis (M)		
M0	29	42
M1	6	9
MX	34	49

Parameter	Samples	
	n	%
TNM classification		
I	14	20
II	13	19
III	7	10
IV	13	19
Unknown	22	32
Grading (G)		
G1	30	44
G2	28	41
G3	5	7
GX	6	8
Functional status		
Functional	19*	28
Non-functional	50	72

* 14 Insulinoma (21 %), 2 Glucagonoma (3 %) und 3 Gastrinoma (4 %)

2.2.2 Immunohistochemistry

2.2.2.1 Tissue microarray (TMA)

To analyse the molecular interaction between mTOR signaling and mitochondria in neuroendocrine tissue, the mTOR activity had to be determined for the established cohort of panNET. Since phosphorylated S6 has been demonstrated to be a good indicator for the activity of mTOR signalling in cancer cells and mice tissue (Knoll et

al., 2016; Stelzer et al., 2010), the expression of the protein was analyzed in a TMA compromising all 157 paraffin blocks of the cohort. Therefore, hematoxylin and eosin stained tissue sections were cut from these blocks and the tumour area was marked by a pathologist. Two tissue cores per patient within the marked area were then removed and assembled on a new paraffin block in an array pattern. In total, 80 tissue cores with 1.5 mm in diameter could be collected on one paraffin block and two samples from muscle tissue were included as quality control. The new paraffin block was cut using a microtome, resulting in sections that were transferred to a microscope slide and immunohistochemically stained. The phosphorylated form of S6 was stained as an indicator for mTOR activity and the un-phosphorylated form of the protein was stained as a control. All used antibodies and working solutions are listed in 2.1.6. The TMA was accomplished in cooperation with the BioBank of the university medical center Mainz. Analysis of the immunohistochemical staining was performed using Qupath (Bankhead et al., 2017) and the expertise of a pathologist.

2.2.3 Nucleic acid extraction from FFPE tissue

2.2.3.1 Preparing of tissue sections

Isolation of genomic DNA and RNA from FFPE tissue samples was performed using unstained FFPE tissue sections. These sections were freshly prepared by cutting paraffin blocks. Therefore, these blocks were placed on a cooling plate (-14 °C) for at least 10 minutes and were cut into 8 µm thick sections using a rotary microtome (Microm HM355S, ThermoFisherScientific). These tissue sections were placed into a 37 °C water bath and transferred to a microscope slide. The generated slides were then placed on a heating table (41 °C) for at least 10 minutes. After this drying process, the FFPE tissue sections could be used for DNA and RNA extraction.

2.2.3.2 DNA extraction

For targeted isolation of DNA from the tumour tissue of panNET, the tumour area had to be identified and marked on the freshly prepared FFPE tissue sections. Hematoxylin and eosin stained tissue sections were used as a template for each sample and the tumour area was marked on these sections by a pathologist. This selection was then transferred on the unstained microscope slides and DNA was isolated according to the manufacturer’s protocol with the Maxwell® RSC DNA FFPE Kit from Promega. Therefore, the tumour area of the section was scraped off the

slide with a scalpel and added to a new tube with sample buffer. The isolation of the nucleic acid from the material was carried out through a Proteinase K digestion, which was prepared according to the manufacturer's instructions and incubated overnight at 70 °C. At the beginning of the incubation, the samples were shaken at 500 rpm for 2 to 3 hours for better disruption of the cells. The next day, isolation of the DNA was performed using the Maxwell®RSC from Promega according to the manufacturer's protocol. The isolation is based on paramagnetic particles (beads) that bind nucleic acids and different washing steps for obtaining the optimal purity of DNA (Figure 5). Concentration of the DNA was measured using the Qubit™Fluorometer (2.2.3.4 Measurement of nucleic acid concentration).

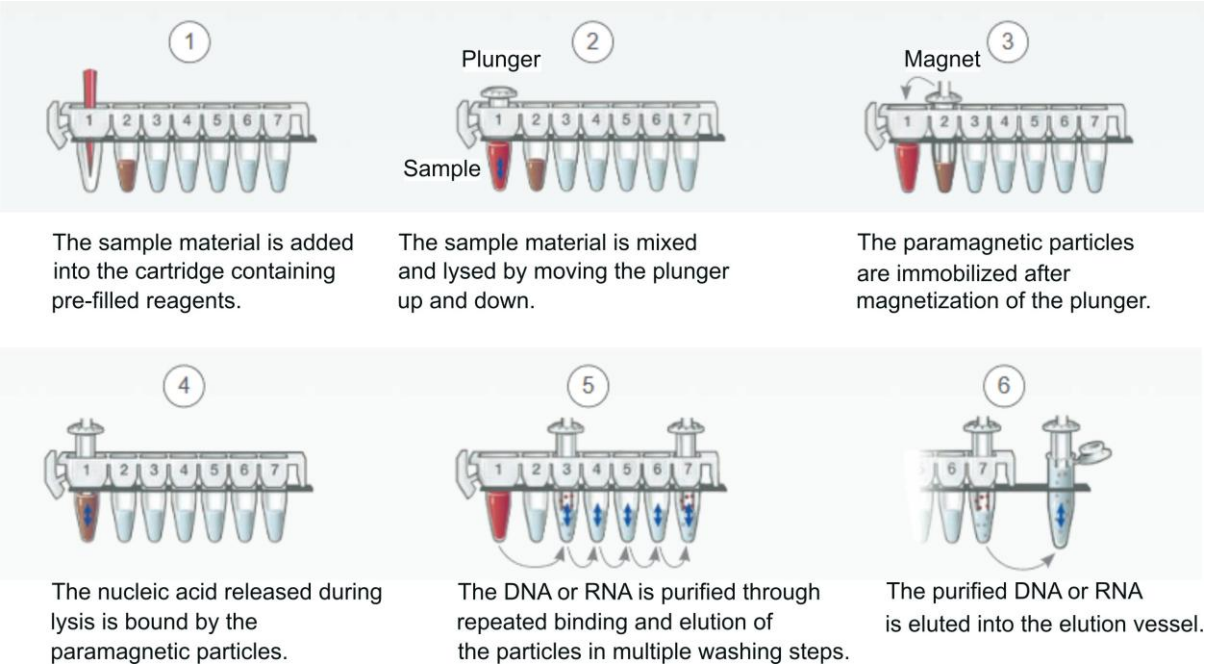

Figure 5: Schematic description of the automated process of DNA/RNA isolation with the Maxwell instrument.

The sample material is added into the cartridge (1) and mixed and lysed by using a plunger (2). The released nucleic acids are bound by beads (3-4) and purified trough different washing steps (5-6). (modified according to Promega)

2.2.3.3 RNA extraction

Isolation of the RNA was performed from the same tumour area as isolation from DNA according to the manufacturer's protocol with the Maxwell® RSC RNA FFPE Kit from Promega. Similar to DNA isolation, the tumour area was scraped off with a scalpel but the resulting sample material was transferred into a new tube with

mineral oil for deparafinization. This step was followed by incubation at 80 °C for two minutes and lysis of the material through Proteinase K digestion. All steps were prepared according to the manufacturer's instructions. The loading of the cartridge and the measurement of the concentration of the RNA were performed equivalent to the DNA isolation (see 2.2.3.2).

2.2.3.4 Measurement of nucleic acid concentration

Table 6: Approach for the concentration measurement of nucleic acids with the Qubit® dsDNA HS or BR Assay Kit.

	Standard 1 or 2 [µl]	**Sample [µl]**
Measurement solution*	190	199
DNA/ RNA	10	1

*Measurement solution = DNA/RNA reagent + buffer (1:200)

Measurement of the concentration of nucleic acids was performed using the Qubit™ 1.0 Fluorometer. For DNA, the Qubit® dsDNA HS Assay Kit (0,2 – 100 ng/µl) or the Qubit® dsDNA BR Assay Kit (2-1.000 ng/µl) from ThermoFisher were used, depending on the expected concentration range. The Qubit™ RNA HS Assay Kit was used for RNA concentration measurement. The samples were prepared according to Table 6. The calculation of the final concentration of the DNA or RNA was performed by the fluorometer using the following formula:

Concentration of the sample = QF value * 200/x

QF value = fluorescence value of the Qubit® Fluorometer

x = used µl of the sample

2.2.4 Next generation sequencing (NGS)

The next generation sequencing is a high-throughput technique for identification of different genomic variations of the DNA in short time. In this work, NGS-analysis was performed according to the bridge amplification form illumina. This system is based

on the following four steps: preparation of the DNA-library, cluster amplification, sequencing and analysis of data.

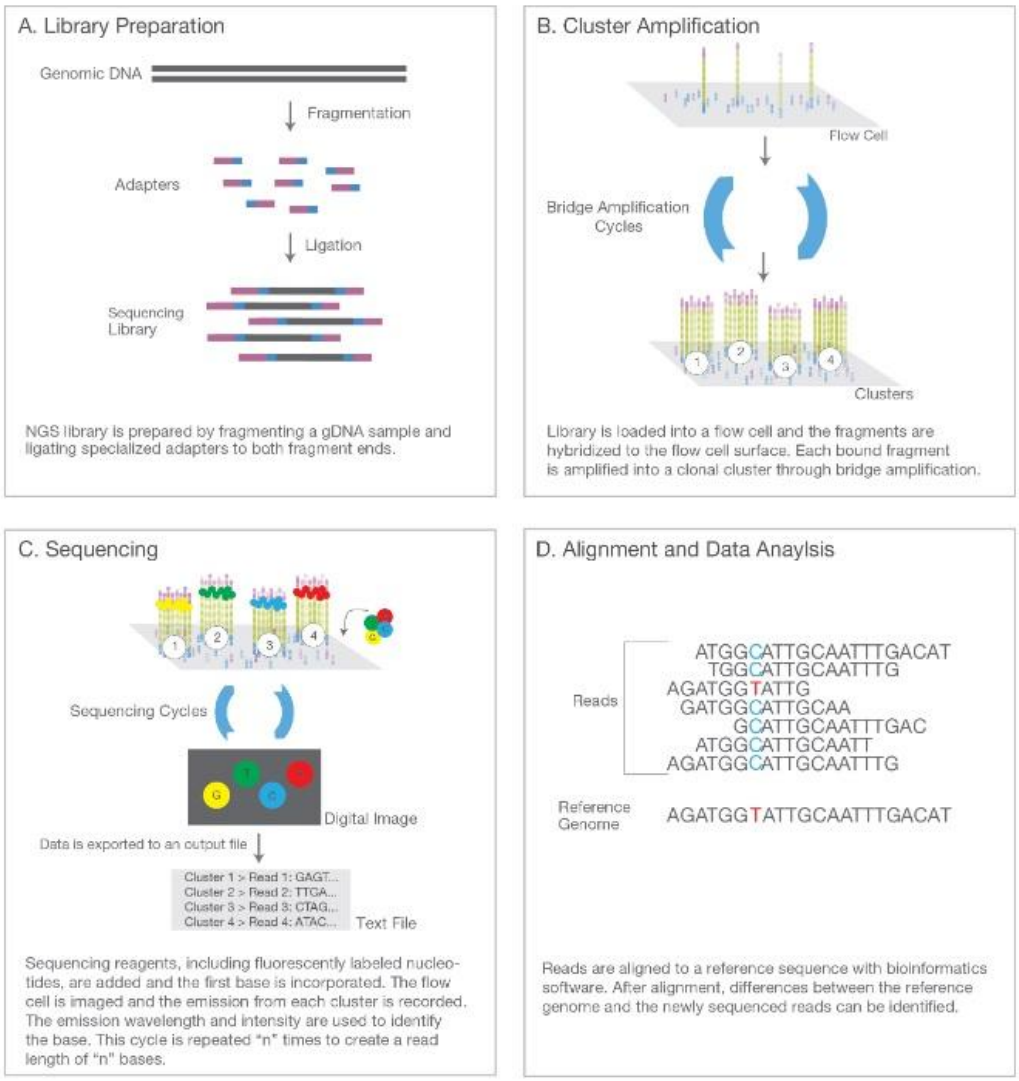

Figure 6: Schematic description of the bridge amplification by Illumina.

The bridge amplification by Illumina is based on the following four steps: (A) preparation of the DNA-library, (B) cluster amplification, (C) sequencing and (D) bioinformatic data analysis. (Illumina, Inc., 2017)

In the first step of NGS-Analysis, a DNA library is generated by fragmentation of the DNA and ligation of adapters on these fragments (Figure 6). The adapters include primer binding sides and so-called unique molecular identifiers sequences (UMIS). These UMIS allow differentiation between artifacts and actual mutations by labelling each DNA library sample. For cluster amplification, the DNA libraries are loaded into a flow cell equipped with complementary adapter oligonucleotides (Figure 6).

Amplification is carried out through the mentioned bridge amplification as described before (Goodwin et al., 2016), resulting in thousands of DNA clusters each originating from a single library fragment. The actual sequencing step is carried out by the sequencing by synthesis (SBS) technology by Illumina. This method requires fluorescence labelled nucleotides that are applied into the nucleic acid chain during each sequencing cycle (Figure 6). The resulting fluorescence signal is detected and documented for each DNA cluster on the flow cell and followed by data analysis (Figure 6).

2.2.4.1 Molecular characterization of the mitochondrial genome of panNET

To analyze the possible impact of the mTOR activity status on the frequency of somatic mutations in the mitochondrial genome, 69 panNET samples from the established cohort were selected for NGS-analysis. The selected samples included 21 panNET with upregulated activity of the mTOR signaling pathway and 48 cases without upregulation of the pathway. The classification of the panNET is based on the results of the immunohistochemistry in 2.2.2. For identification of tumour specific mutations, NGS-analysis was carried out for tumour and normal tissue of each patient. Preparation of DNA libraries was performed using the QIAseq Targeted DNA Human Mitochondria Panel (DHS-105Z, Qiagen), with an average input of 100 ng FFPE-DNA per sample. The DNA libraries were quantified as described in 2.2.3.4 and diluted to a concentration of 4 nM. In the next step, libraries were further diluted by adding 0.2 nM NaOH to a final concentration of 10 pM and pooled, to ensure a sequencing depth of 1 million reads per sample. Sequencing of the mitochondrial genome was performed using the Illumina MiSeq System and paired-end sequencing with 2 x 151 bp reads. For data analysis, the MiSeqReporter Software from Illumina and CLC Workbench from Qiagen were used in combination with an in-house analysis pipeline. This pipeline aligns the generated reads with the Cambridge Reference Sequence (rCRS) of the human mitochondrial DNA (NC_012920) and the detected somatic mutations with the MITOMAP database (Kogelnik et al., 1996).

2.5 RNA-sequencing

To identify differentially expressed genes that are affected by the mTOR activity in panNET, a gene expression profile of 69 panNET cases was created. These included 21 panNET with activated mTOR pathway and 48 panNET without upregulated mTOR activity. RNA sequencing enables the identification of expression

differences in the entirety of all genes in the tissue, whereby in the following we have mainly focused on mitochondria-associated genes and target genes of the mTOR signaling pathway.

2.2.5.1 cDNA synthesis and quantification for RNA-Sequencing

In the first step of the RNA-sequencing, the cDNA synthesis was performed using the ProtoScript® II First Strand cDNA Synthesis Kit (New England Biolabs) according to the manufacturer's instructions. An input of 750 ng RNA per sample was used and the approach for the random primer mix was selected. In deviation from the manufacturer's instructions, only 0.5 µl of the random primer mix were used in the PCR for denaturation of the samples. The concentration of the cDNA was measured according to 2.2.3.4.

2.2.5.2 Library preparation and sequencing

Library preparation was performed using the AmpliSeq™ Transcriptome Human Gene Expression Panel (Illumina, San Diego, CA, USA) and the AmpliSeq™ Library PLUS Kit (Illumina, San Diego, CA, USA) according to the manufacturer's instructions. The amount of cDNA used for amplification of the targets was calculated according to the following formula:

$$\frac{\text{Sample input for library preparation}}{\text{Concentration cDNA} \times (1/\text{Dilution factor cDNA})} = \text{Amount of cDNA for amplification (Max. 8 µl)}$$

Deviating from the protocol, the following PCRs for amplification of the targets and amplification of the libraries were performed.

Table 7: Settings for PCR for amplification of targets and amplification of libraries.
The deviations from the manufacturer's protocol are marked in red

Amplify targets		**Amplify library**	
99 °C for 15 seconds		98 °C for 2 minutes	
99 °C for 15 seconds 60 °C for 16 minutes	13 cycles	98 °C for 15 seconds 64 °C for 1 minute	9 cycles

The quantity and quality of the final libraries was measured using the 2100 Bioanalyzer (Agilent, Santa Clara, CA, USA). Based on this measurement the libraries were diluted to the final loading concentration according to the "Denature

and Dilute Libraries Guide" for the NextSeq500 and 550 (Illumina, San Diego, CA, USA). Library sequencing was performed using the NextSeq500 system (Illumina, San Diego, CA, USA) with single-read sequencing and 76 bp reads. The sequencing depth was 20 million reads per sample.

2.2.5.3 Bioinformatic analysis of data

The generated raw data from the RNA-sequencing were quantified in cooperation with Dr. Michael Kloth of the Institute of Pathology (Mainz). This step included removal of adapter sequences and low-quality reads and was performed using the Salmon tool (Patro et al., 2017).

The following differential expression analysis was carried out with the Bioconductor-DESeq2 package for R (version 4.3.0, R Core Team, 2021) according to the DESeq2 manual (version 1.42.0, Love et al., 2014). As a pre-filter option only samples with a transcript count over 5 were included into analysis. Genes with Benjamin Hochberg adjusted p-value (padj) ≤0.05 were considered significant. The detailed code is described in the supplementary Figure S 1. Stable identifiers (Ensembl ID´s) matching these genes were extracted using the g:Profiler online tool (Kolberg et al., 2023, https://biit.cs.ut.ee/gprofiler/gost (last update: 16.01.25)).

In the next step, Gene Set Enrichment Analysis (GSEA) was performed on the wald-statistic value of all samples using the GSEA software provided by Broad Institutes (Mootha et al., 2003; Subramanian et al., 2005http://www.broad.mit.edu/gsea/ (last update: 08.07.24)). GSEA was run on 1000 permutation mode on gene-set label to generate False Discovery Rate (FDR) and enrichment score (ES) for each gene set. Significant gene sets were filtered based on FDR q-values (cutoff: 0.05). The detailed settings for GSEA are described in the supplementary Figure S 2.

2.6 Gene expression analysis using qPCR

2.6.1 cDNA synthesis and quantification for qPCR-Analysis

For gene expression analysis, 700 to 900 ng of total RNA isolated from tissue slices (2.2.3.3) or from cultivated cells (2.2.8.4) were reverse transcribed into cDNA using the M-MLV Reverse Transcriptase. Therefore, RNA was denatured by adding 11 µl of RNA (700 to 900 ng) and 3 µl Random-Primer together. This mixture was than incubated for 5 minutes at 70 °C and immediately transferred on ice for prevention of renaturation of the RNA. In the next step, 5 µl 5x buffer (Promega, Walldorf,

Germany); 0.8 µl RNAsin-PLUS (Promega, Walldorf, Germany), 1 µl M-MLV Reverse Transcriptase (Promega, Walldorf, Germany) and 4.2 µl of 2.5 mM dNTPs (Invitrogen™ by Thermo Fisher Scientific Waltham, MA, USA) were added to the RNA-Primer-Mix on ice and incubated for 60 minutes at 40 °C.

2.6.2 Primer design

If not stated otherwise, the oligonucleotide primers used in this study were generated using the program Primer3Plus (Untergasser et al., 2012, https://www.primer3plus.com/index.html (last update: 16.01.25)) or Primer-BLAST provided by the National Library of Medicine (Ye et al., 2012, https://www.ncbi.nlm.nih.gov/ (last update: 17.07.24)). The reference sequences for selection of primers in the targeted regions also originated from the National Library of Medicine (https://www.ncbi.nlm.nih.gov/ (last update: 17.07.24)). Primer length was set at 20 bp and the product size ranged between 100 and 150 bp. Melting temperature was set between 58 and 62 °C with an optimal temperature at 60 °C. The percentage of guanine-cytosine content in each primer was set between 50-55 %. All used primers and their origin are listed in 2.1.3. All used primer pairs were diluted to a final concentration of 10 µM with water before use.

2.6.3 qPCR-analysis

The qPCR-analysis of cDNA isolated from the FFPE tissue slices was performed in triplicates for 21 panNET with activated mTOR signaling pathway and 48 panNET with no activation of mTOR. The samples were prepared as followed:

Table 8: The qPCR reaction mix used for gene expression analysis.

	Volume per reaction [µl]
SYBR™ Green PCR Master Mix 5	5
forward primer [10 µM]	0.2
reverse primer [10 µM]	0.2
HPLC-water	3.6
cDNA template (3-5 ng/µl)	1
total volume	10

To measure PCR efficiency, a 1 to 4 dilution series was assayed for every primer starting with a concentration of 3 to 5 ng/µl and ending at 0.04 to 0.07 ng/µl. This dilution series was carried out using a standard consisting of a pool of 10 panNET without mTOR signaling pathway activity. Moreover, a reaction mix with HPLC-water instead of cDNA was assayed as a control against contamination. The following parameters were used for thermal cycling:

Table 9: PCR set up for qPCR.

Temperature	Incubation time	Stage
50 °C 95 °C	2 minutes 10 minutes	Hold Stage
95 °C 60 °C (data acquisition)	15 seconds 1 minute	PCR Stage (40 cycles)
95 °C 60 °C 95 °C (data acquisition)	15 seconds 1 minute 15 seconds	Melt Curve Stage

The qPCR-analysis of cDNA isolated from cultivated cells was performed in a similar way, with a different standard for measuring the PCR efficiency. Instead of a pool of samples, the untreated control of the panNET cells was used as the starting point of the dilution series. Data analysis of all qPCR results was performed using the "$2^{-\Delta\Delta Ct}$-Method" as described previously (Livak & Schmittgen, 2001).

2.2.7 Cell culture assays

All cell culture assays were performed under sterile conditions using a laminar flow cabinet. The used chemicals and media were stored at 4 °C and warmed to 37 °C before use. All cells were considered mycoplasma free before use.

2.2.7.1 Cell culture of human pancreatic neuroendocrine cells

The human pancreatic neuroendocrine cell lines BON1 and QGP1 were considered mycoplasma free before use and authenticated by the Multiplexion GmbH (Heidelberg, Germany; Schmitt & Pawlita, 2009).

According to the growth characteristics and health status, cells were passaged twice a week (average confluency 70 - 80 %) in a ratio of 1:2 to 1:4. Therefore, cells were

washed with PBS (w/o Mg^{2+}/Ca^{2+}) and detached using Trypsin/EDTA-solution for 5 minutes at 37 °C. Cells were then transferred to standard growth medium (see 2.1.7) in a T75 flask and incubated at 37 °C and 5 % CO_2.

For long-term conservation, the cells were stored at -80 °C in freezing medium (see 2.1.7). Therefore, the cells were detached and transferred to growth medium as described before. The cells were then centrifuged at 1,000 rpm for 5 minutes at 4 °C. The medium was aspired, and the resulting cell pellet was resuspended in 1 ml freezing medium and transferred to a cryo vial. For a gentle freezing process, the vial was placed in a freezing box that guarantees freezing of cells at a rate of -1 °C per minute.

2.2.8 Biochemical and molecular biology methods

The preparation of whole cell lysates and the isolation of DNA as well as RNA were carried out after cultivation of the cells at culture dishes with a diameter of 6 cm. For determination of the necessary cell number, cells were counted using a Neubauer chamber (M. Zhang et al., 2020). If not stated otherwise, 1 million cells were seeded per culture dish.

2.2.8.1 Modulation of gene expression

2.2.8.1.1 Transient transfection of siRNA oligonucleotides and modulation of the mTOR pathway activity

For the transient knockdown of different genes, panNET cancer cells were transfected with small interfering RNA (siRNA) oligonucleotides using Lipofectamine®2000 (Invitrogen, Carlsbad, CA, USA). Information's for all used siRNAs are listed in 2.1.3.2. One hour before transfection, growth medium was replaced with Opti-MEM (Invitrogen, Carlsbad, CA, USA) and two solutions were prepared for transfection and incubated separately for 5 minutes at room temperature. One solution contained 5 nM siRNA diluted in 100 µl Opti-MEM and the other solution contained Lipofectamin 2000 (ratio 1:2, DNA:Lipofectamin) diluted in 100 µl Opti-MEM. After the incubation, both solutions were mixed and incubated for 20 minutes at room temperature. In the next step, the transfection mix was added to the cells and incubated at 37 °C and 5 % CO_2. After 5 to 6 hours the Opti-MEM medium was changed to standard growth medium. The cells were incubated for 72 hours before further investigation.

For inhibition of the mTOR signalling pathway, everolimus and temsirolimus were used in a concentration of 1 µM for 72 h.

2.2.8.2 Preparation of whole cell lysate

All following steps were performed on ice. For preparation of whole cell lysates, cells grew to a confluency of 70 to 80 %. The cells were washed with ice-cold PBS and scraped off the culture dish surface with 50 to 70 µl lysis buffer, containing 10x cell lysis buffer (Cell Signaling Technology, Frankfurt aM, Deutschland), 2% Protease/Phosphatase Inhibitor (Cell Signaling Technology, Frankfurt aM, Deutschland) and water. Cell lysates were incubated for 15 minutes on ice. Afterwards, the lysate was centrifuged at 12,700 rpm for 20 minutes at 4 °C, resulting in a sediment part containing cell compartments and the supernatant containing the desired proteins. The sediment was discarded and the concentrations of the proteins in the supernatant were measured using the Bradford protein assay (Thermo Fisher, Waltham, USA) according to the manufacturer's instructions. The quantity of protein per sample was adjusted to 30 µg using 6x protein sample buffer and the samples were incubated at 95 °C for 5 minutes for denaturation.

2.2.8.3 SDS polyacrylamide gel electrophoresis and semi-dry western blotting

Proteins which are contained in the whole cell lysate were separated on 10 to 12 % polyacrylamide gels by using SDS polyacrylamide gel electrophoresis (SDS-page).

Table 10: Composition of SDS polyacrylamide gels for electrophoresis.

	Resolving gel		**Stacking gel**
	10 %	**12 %**	**5 %**
ddH2O [ml]	2	1,7	1.15
Rotiphorese® Gel 30 [ml]	1,7	2	0.33
Stacking buffer [ml]	-	-	0.5
Resolving buffer [ml]	1,3	1,3	-
10 % (w/v) SDS [µl]	50	50	20
10 % (w/v) APS [µl]	50	50	20
TEMED [µl]	2	2	2

The concentration of the gels depended on the molecular weight of the protein of interest, whereby proteins with a low molecular weight are resolved in a high percentage gel. The composition of the used stacking and resolving gels is described in Table 10. The SDS-page was performed using a consistent electric voltage of 120 Volt for 90 minutes.In the next step, the separated proteins were transferred to a nitrocellulose membrane (Bio-Rad, Munich, Germany) using a semidry blotting system. The composition of the semidry blot is described in Figure 7. The proteins were transferred with the Trans-Blot® Turbo™ Blotting System from BioRad using an electric voltage and amperage of 25 Volt and 300 mA for 30 minutes.

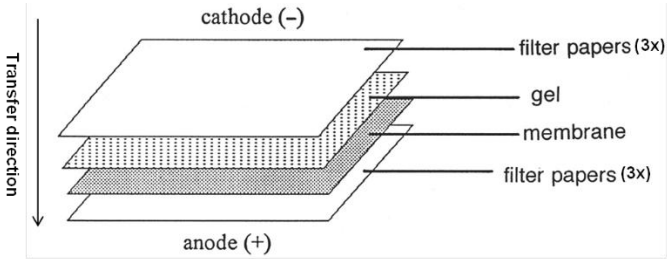

Figure 7: Composition of a semidry blot. (modified according to Gravel, 2009)

2.2.8.4 Immunoblot analysis

The nitrocellulose membrane was incubated and reversibly stained with Ponceau S staining solution. This screening was carried out to guarantee the successful transfer of proteins and to cut the membrane according to the following antibody treatment. Blocking was performed for 1 hour at room temperature with blocking solution to prevent unspecific binding of antibodies. The membrane was than incubated at 4 °C overnight with the primary antibody followed by HRP-labeled secondary antibody for 1 hour at room temperature. Informations for all used antibodies are listed in 2.1.6. Visualization was performed for strong signals with the Enhanced chemiluminescence (ECL) detection solution or for weak signals with the WesternBright™ Sirius™ Detection Kit (advansta, San José, USA) using the chemiluminescence detection system Evolution-Capt (Vilber Lourmat, Eberhardzell, Germany).

2.2.8.5 Nucleic acid extraction from panNET cell lines

Extraction of RNA from cultivated cell lines was performed using the RNeasy® Plus Mini Kit (Qiagen, Hilden, Germany) according to the manufacturer's instructions. To prevent the activity of ribonucleases, cells were scraped of the culture dish surface using 600 µl of a mix of RLTbuffer and β-mercaptoethanol (1:100, β-mercaptoethanol:RLTbuffer). In deviation of the manufacturer´s protocol, all centrifugation steps were set to a minimum of 1 minute. Before eluation of the RNA in 30 µl of water, the columns were centrifuged at 12,700 rpm for 5 minutes for further drying of the membrane. The isolated RNA was stored at -20 °C to -80 °C and for further investigation transcribed into cDNA (see 2.2.5.1 or 2.6.1).

2.2.8.6 Statistical analysis

Statistical analyses were achieved using Microsoft Excel (Microsoft Corporation, Redmond, WA, USA) and RStudio (Version 4.3.2). In total, three experiments were compared for each experimental set up and p-values ≤0.05 were considered significant with the following categories: *p≤0.05, **p≤0.01, and ***p≤0.001. Visualization of data was carried out using Microsoft Excel and Inkscape (Version 1.3.2Inkscape Project, 2020).

3. Results

3.1 The mTOR pathway is activated in a considerable number of panNET

Several studies have shown that the mTOR signaling pathway plays an important role in the pathogenesis of panNET (Chan & Kulke, 2014; Jiao et al., 2011). Particularly interesting in this context is the observation that between 33 to 52 % of panNET exhibit high mTOR pathway activity and that these cases are correlated with increased tumour cell progression and growth (Komori et al., 2014; Giuseppe Lamberti et al., 2018).

To identify tumours with activated mTOR signaling in the established cohort of 157 panNET cases, immunohistochemical staining was performed using a TMA. All selected patients were diagnosed with panNET between 1996 and 2019. They underwent at least one biopsy and the extracted tissue was archived in form of formalin-fixed paraffin-embedded tissue (FFPE) blocks. The cohort included 77 female patients (49 %) and 80 male (51 %) patients with an average age of 59 years

(age-span 18 to 88 years). The panNETs were classified using the TNM staging system (Klöppel et al., 2010), with 25 (16 %) of patients having stage I, 23 (15 %) stage II, 2 (1 %) stage III, and 19 (12 %) stage IV tumours. Staging could not be determined for 88 (56 %) patients due to data limitations. In addition to the staging, all tumours were classified according to the grading system of the WHO (Rindi et al., 2022), with 66 (42 %) being well-differentiated (G1), 60 (38 %) moderately differentiated (G2), and 14 (9 %) poorly differentiated (G3). Grading could not be determined for 17 (11 %) patients due to data limitations. The cohort included 34 functional tumours (22%), with 26 being insulinomas (16.6%), 5 being glucagonomas (3.2%), and 3 being gastrinomas (1.9%). A table of all clinic pathological features in the study population are listed in Table 4 (2.2.1).

As an indicator for the pathway activity, the phosphorylation status of the ribosomal protein S6 (pS6) was investigated (Figure 8). The protein has been described to be a good indicator of the mTOR pathway activity in studies on anal carcinomas and renal cell carcinomas (Knoll et al., 2016; Stelzer et al., 2010). The protein is mainly phosphorylated by different p70 and p90 ribosomal protein S6 kinases as well as the mTOR protein (Ruvinsky et al., 2005; Yi et al., 2021).

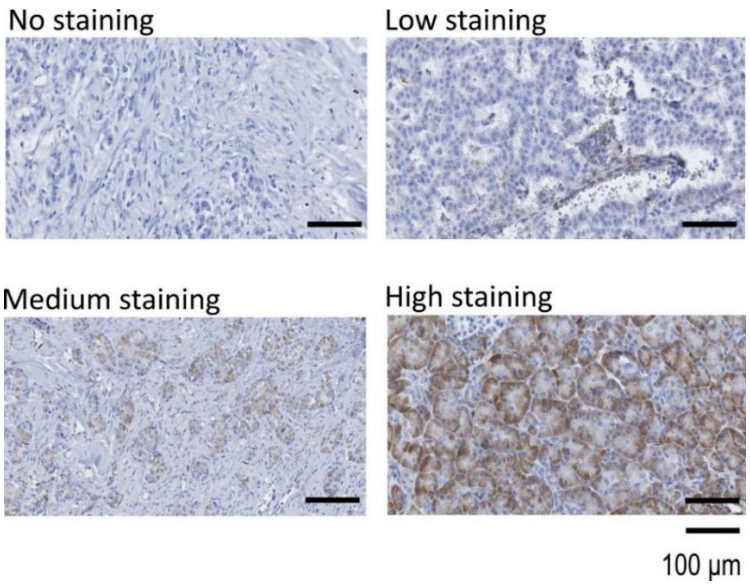

Figure 8: Immunohistochemical staining of panNETs using ati-pS6 antibody.

Representative immunohistochemical staining (brown) for the expression of pS6. Expression levels were quantified into four categories: No staining, low staining, medium staining and high staining based on the expertise of an experienced pathologist.

In this study, 22 % of the investigated panNETs showed alerted pS6 expression and therefore activation of mTOR signalling (Figure 9). That corresponds to 34 out of 157 cases, including 23 cases (15 %) with low mTOR pathway activity, 8 cases (5 %) with medium activity and 3 cases (2 %) with high mTOR activity (Figure 9).

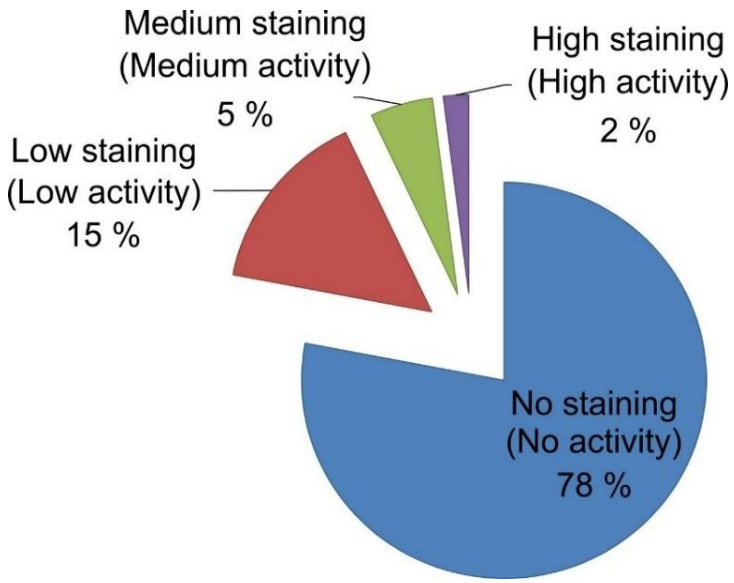

Figure 9: Activity of the mTOR signaling pathway in panNET.

The expression of pS6 was correlated to the mTOR signaling pathway activity in panNET. In total, 22 % of panNET had an activated mTOR signaling pathway. The activity was quantified into four categories: no activity, low activity, medium activity, high activity.

3.2 Molecular characterization of mitochondrial genomes in panNETs

Various somatic mutations of the mitochondrial DNA have been described in tumour entities (Schon et al., 2012; Stewart et al., 2015) and could be correlated with alerted mTOR pathway activity in different cancer cells as well as fibroblasts (Chung et al., 2021). Little is known about the occurrence of mtDNA mutations in panNET due to the low incidence of this entity. Therefore, one aim of the present work was to investigate mtDNA mutations in the established cohort using NGS-analysis and to study the impact of the mTOR pathway activity on these changes. Selected cases for this analysis included 21 mTOR-activated panNETs and 48 panNETs with no mTOR signaling (total 69 panNET). To distinguish inherited from somatic mtDNA mutations; tumour and normal tissue was sequenced and compared for each patient. The total of all cases examined and the corresponding somatic mutations of the mtDNA are listed in the supplementary Table S 1.

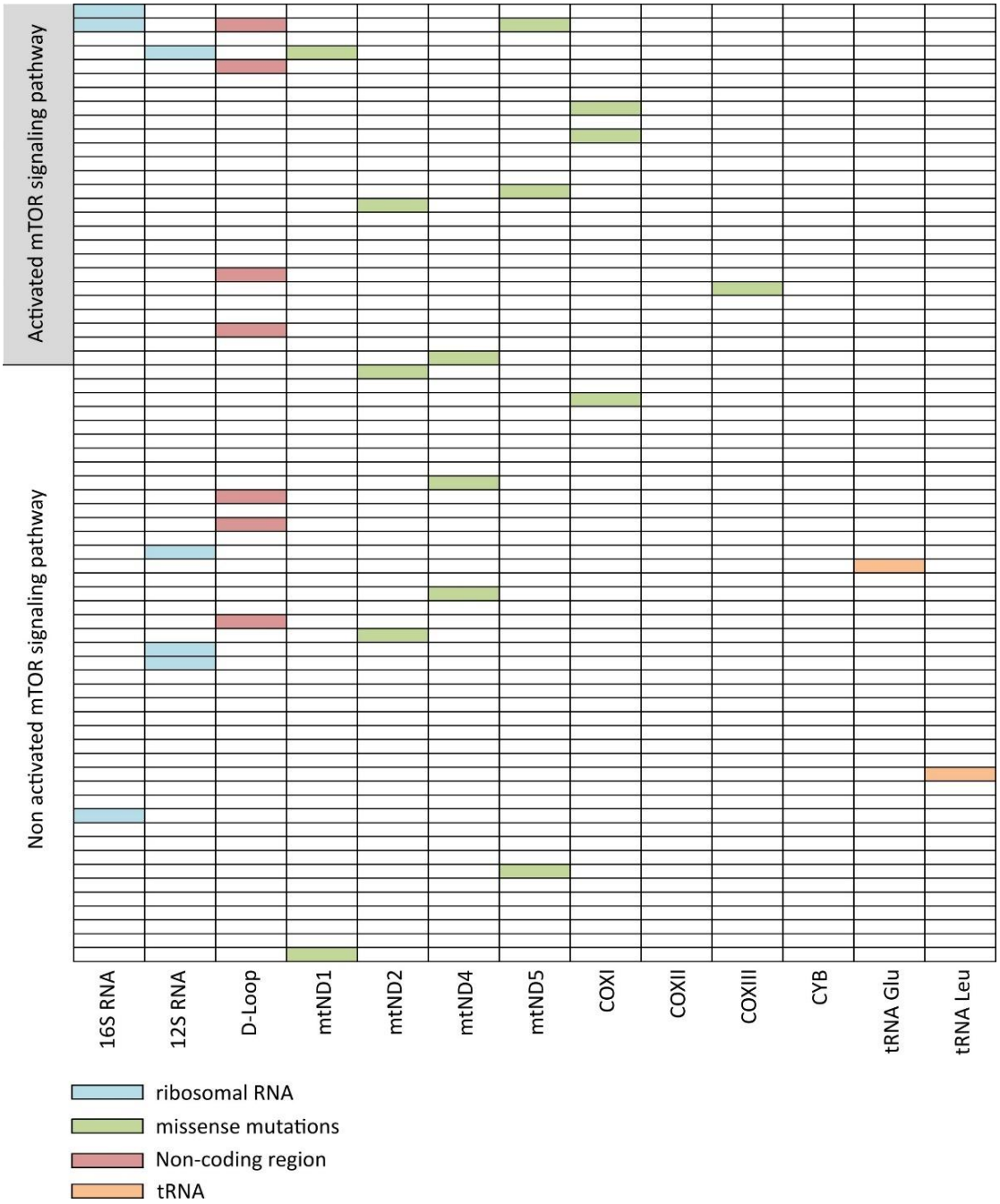

Figure 10: The mTOR signalling pathway activity has no impact on the detected mitochondrial mutations in panNET.

Somatic mutations within the mtDNA were detected using the QIAseq Targeted Panel DHS-105Z which covers the whole mitochondrial genome. In total, 69 panNETs were investigated, including 21 mTOR-activated panNET and 48 cases with no activation of the pathway. A) Heatmap of the identified mutations. All identified mitochondrial mutations were categorized in the following categories: Mutations of the ribosomal RNA (blue), missense-mutations (green), mutations within the non-coding region (red) and mutations of the tRNA (orange). B) Division of the investigated panNET according to the occurrence of the mutations of the mitochondrial genome and the activity of the mTOR signaling pathway.

28 out of 69 panNET (41 %) showed mutations within the mitochondrial genome (Figure 10). These cases included 12 (panNET with activated mTOR pathway signaling and 16 with no activation (Figure 10). Tumour-specific mutations were found in all regions of the mtDNA (non-coding region, genes coding for rRNAs, genes coding for tRNAs and genes coding for respiratory chain complexes) with the most frequent mutations occurring in genes for respiratory chain complexes (Figure 10). In summary, the spectrum of mutational variants varied widely among panNETs and was independent of the mTOR pathway activity.

3.3 Activated mTOR pathway leads to regulation of mitochondria related genes in panNET

One goal of this work was to investigate molecular alterations in panNET that are impacted by the activity of the mTOR signaling pathway. Therefore, RNA sequencing was performed on 69 panNETs. Selected cases for this analysis included 21 panNET with activated mTOR pathway and 48 panNET without mTOR activity.

(A)

(B)

Name of gene set	ES	NES	NOM p-val	FDR q-val
Hallmark_mTORc1_signaling	0.16	2.62	0.000	0.002
Hallmark_KRAS_signaling	0.14	2.17	0.000	0.008
Hallmark_Bile_acid_metabolism	0.12	1.54	0.046	0.148

Figure 11: The mTOR activity impacts different pathways in panNET.

A) Enrichment plot of the mTORc1 gene set in panNET with high mTOR pathway activity. The green line (1) represents the running Enrichment score (ES) for the gene set as the analysis progresses through the ranked list. The black lines (2) highlight the positions of the gene set members within the ranked gene list. B) List of the top 3 gene sets enriched in panNET with high mTOR pathway activity. The ES reflects the degree to which a gene set is overrepresented at the top or bottom of a ranked list of genes. Normalized enrichment score (NES) represents enrichment score normalized across analyzed gene sets. Statistical significance is calculated by nominal p-value of the ES using an

empirical gene-set-based permutation test. A nominal p-value of 0.000 stands for an actual p-value of less than 1/number-of-permutations (in this work: 1/1000 = 0.001). Gene sets from the MSigDB database were tested and gene sets with a false discovery rate (FDR) <0.25 and nominal p-value <0.01 were considered significantly enriched in a prior defined set of genes. All enriched gene sets are listed in the supplementary Table S2.

Gene Set Enrichment Analysis (GSEA) revealed 21 out of 50 hallmark gene sets that were impacted by the mTOR activity status in panNET (list of all enriched gene sets in supplementary Table S2). These 21 gene sets included 3 gene sets that were significantly enriched and 18 gene sets that were significantly decreased in panNET with activated mTOR pathway compared to panNET without activation (FDR < 0.25; nominal p-value < 0.05). As expected, the most significantly enriched hallmark pathway was the mTORc1 signaling pathway (FDR = 0.002; nominal p-value < 0.001; Figure 11). Differentially gene analysis was also performed comparing 21 panNET with activated mTOR pathway and 48 panNET without activation of mTOR. In total, 325 differentially expressed genes were identified comparing these two groups (padj < 0.05; list of all differentially expressed genes in the supplementary Table S 3). These differentially expressed genes included 46 significantly upregulated and 279 significantly downregulated genes in panNET with mTOR pathway activity compared to panNET without mTOR activity (padj < 0.05). The most significantly upregulated gene in panNET with mTOR pathway activity was the *PPARGC1A* gene that encodes for the PGC1α protein (Wald test = 7.16; adjusted p-value < 0.001; Figure 12A, B). This protein is a transcriptional coactivator that plays a key role in the mitochondrial biogenesis through interaction with different transcription factors (Liang & Ward, 2006).

(A)

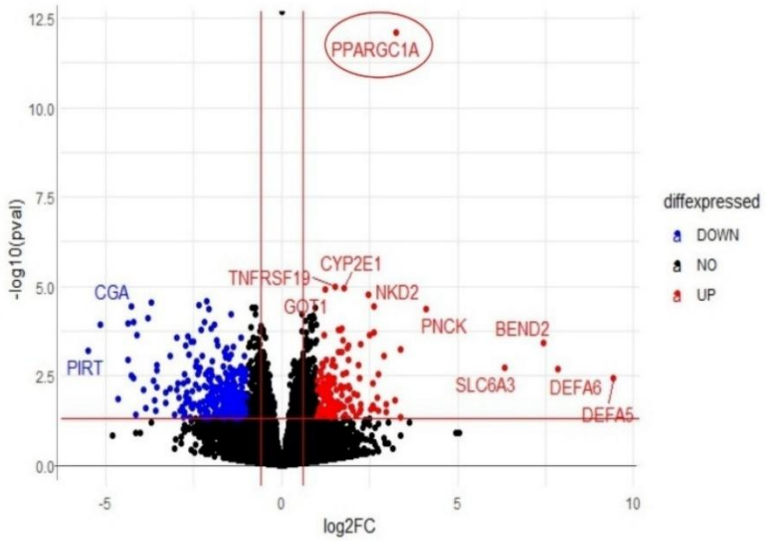

(B)

Gene	Protein	Wald test	adjusted p-val
PPARGC1A	PGC1α	7.16	1.60E-08
LCN1	Lipocalin 1	4.94	2.60E-03
TNFRSF19	Tumor necrosis factor receptor superfamily, member 19	4.42	1.92E-02

Figure 12: Activated mTOR pathway results in increased expression of PGC1α in panNETs.

A) Volcano plot of differentially expressed genes in paNET with activated mTOR pathway compared to panNET without activation of mTOR. Genes with a log2foldchange (log2FC) < -1 or > 1 and a pval < 0.05 were included in the plot. Genes that are down-regulated in panNET with mTOR pathway activity are shown in blue and genes that are upregulated in panNET with mTOR pathway activity are marked in red. B) List of the top 3 genes that are differentially regulated between panNET with activated mTOR pathway and panNET without activation. The genes were determined using the DESeq2 package. All genes with Benjamin Hochberg adjusted p-value (adjusted p-val) < 0.05 were included. The data are represented as Wald-statistic (Wald test). Genes with negative Wald-statistic values are down-regulated in panNET with mTOR pathway activity compared to panNET without activation and genes with positive values are upregulated. All differentially expressed genes are listed in the supplementary Table S 3.

In the second step of the differentially gene analysis, the panNET with mTOR pathway activity were further divided into two groups based on the grading of the cases. This resulted in 10 low grade panNET (G1) with mTOR pathway activity that were compared to 11 high grade panNET (G2 + G3) with mTOR pathway activity. In total, 131 differentially expressed genes were identified comparing these two groups,

including 111 upregulated and 20 downregulated genes in high grade panNET with mTOR activity (padj < 0.05; list of all differentially expressed genes in the supplementary Table S 4). The most significantly upregulated gene in high grade panNET (G2 + G3) compared to low grade panNET (G1) with mTOR pathway activity was the *HSPA9* gene that encodes for the protein mortalin (Wald test = 4.943; adjusted p-value < 0.001; Table 11). This protein is mainly localized to the mitochondria (around 70% of mortalin in the cell) and acts as a mitochondrial chaperon that impacts mitochondrial biogenesis, the formation of reactive oxygen species and glucose metabolism (Esfahanian et al., 2023).

Table 11: Activated mTOR pathway results in increased expression of mortalin in high-grade panNETs.

List of the top 3 genes that are differentially regulated between high grade (G2/G3) panNET with mTOR pathway activity and low grade (G1) panNET with mTOR pathway activity. The genes were determined using the DESeq2 package. All genes with Benjamin Hochberg adjusted p-value (adjusted p-val) < 0.05 were included. The data are represented as Wald-statistic (Wald test). Genes with negative Wald-statistic values are down-regulated in between high grade (G2/G3) panNET with mTOR pathway activity compared to low grade (G1) panNET with mTOR pathway activity and genes with positive values are upregulated. All differentially expressed genes are listed in the supplementary Table S 4.

Gene	Protein	Wald test	adjusted p-val
HSPA9	Mortalin	4.943	0.00019
ZNF702P	Putative zinc finger protein 702	4.903	0.00016
RNF187	Ring Finger Protein 187	4.829	0.00020

Using quantitative PCR it could be confirmed that the expression of *PPARGC1A* (PGC1α) was 2 fold-changes higher in panNET with mTOR pathway activity (21 panNET) when compared to panNET without alerted mTOR activity (49 panNET; p < 0,01; Figure 13A). It could also be confirmed that the *HSPA9* (mortalin) expression was 1.3 fold-changes higher in high grade panNET (G2 + 3) with mTOR pathway activity (11 panNET) when compared to low grade panNET (G1) with mTOR pathway activity (10 panNET; p < 0.05; Figure 13B). These findings underline our results from the differentially gene analysis, identifying two mitochondria related genes as targets of mTOR in panNET.

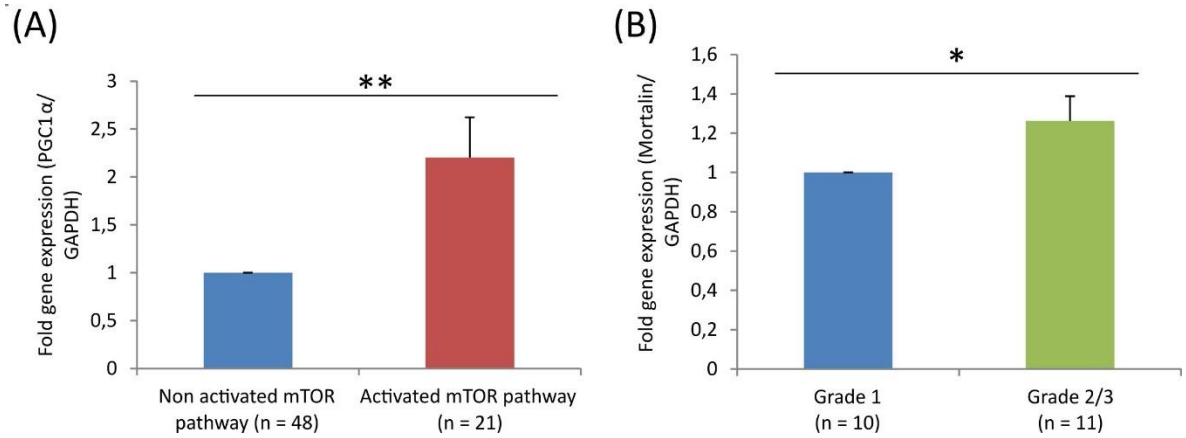

Figure 13: PGC1α and mortalin are targets of mTOR in panNET.

A) Gene expression of PGC1α was measured by qPCR analysis. The expression of the gene was compared between panNET without alerted mTOR pathway activity (non-activated mTOR) and panNET with mTOR pathway activity (activated mTOR). The control group was set to 1 for better representation. Values represent means ± SEM (**p≤0.01, ***p≤0.001; paired t-test (two-tailed)). B) Gene expression of *HSPA9* (mortalin) was measured by qPCR analysis. The expression of the gen was compared between low grade panNET with activated mTOR pathway (mTOR activated G1) and high grade panNET without activation of mTOR (mTOR activated G2/ 3). The control group was set to 1 for better representation. Values represent means ± SEM (**p≤0.01, ***p≤0.001; paired t-test (two-tailed)).

3.4 Regulation of the mTOR pathway activity leads to reduced *PPARGC1A* expression in BON1 cells

To further study the role of mTOR in gene expression of panNET, mTOR pathway activity was inhibited in the cell lines BON1 and QGP1 (Figure 14A - B) using everolimus and temsirolimus. These rapalogues mainly effect the activity of the mTORc1. Initially, the activity of the mTOR pathway was assessed by measuring pS6 expression through immunoblot analysis. Therefore, pS6 levels in BON1 and QGP1 cells were compared with those in two colorectal cancer cell lines (HCT116 and SW480), which are known to exhibit low mTOR pathway activity.

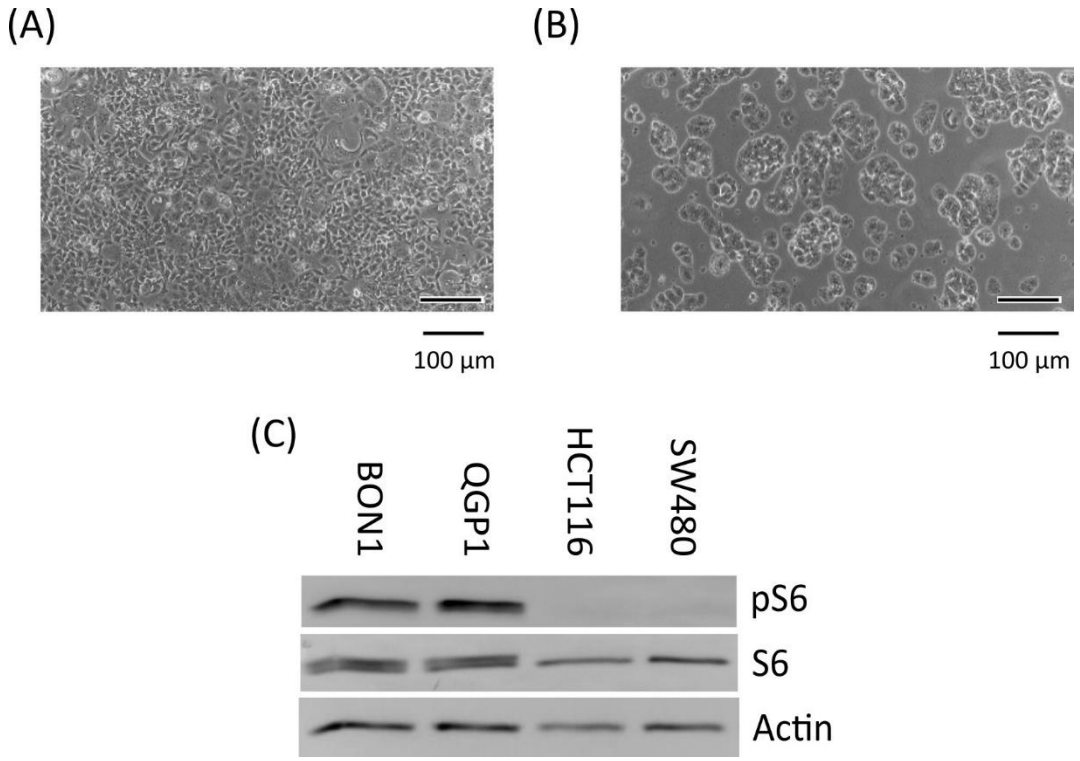

Figure 14: The mTOR pathway is activated in BON1 and QGP1 cell lines.

The activity of the mTOR signalling pathway was investigated using the cell lines BON1 (A) and QGP1 (B), which both originate from neuroendocrine tumours located in the pancreas. C) Representative western blot images for the expression of phosphorylated S6 (32 kDa). The expression of pS6 was correlated to the mTOR signaling pathway activity in panNET cell lines (BON1 and QGP1) and compared to the expression in colorectal cancer cell lines (HCT116 and SW480). The S6 protein (32 kDa) represents the unphosphorylated form of the protein. 30 µg protein was loaded per lane and actin (40 kDa) was used as a loading control. All original, non-cleaved Western Blot images are shown in the supplementary Figure S 3.

As expected, elevated levels of pS6 were observed in both panNET cell lines (BON1 and QGP1) compared to the colorectal cancer cell lines (HCT116 and SW480), indicating the activation of mTOR signalling (Figure 14C). Western Blot analysis at 72 hours after the administration of either 1 µM everolimus or 1 µM temsirolimus revealed a reduction of the pS6 protein level by in BON1 60 to 70 % cells and by 50 % in QGP1 cells, indicating strong inhibition of mTOR signalling (Figure 15).

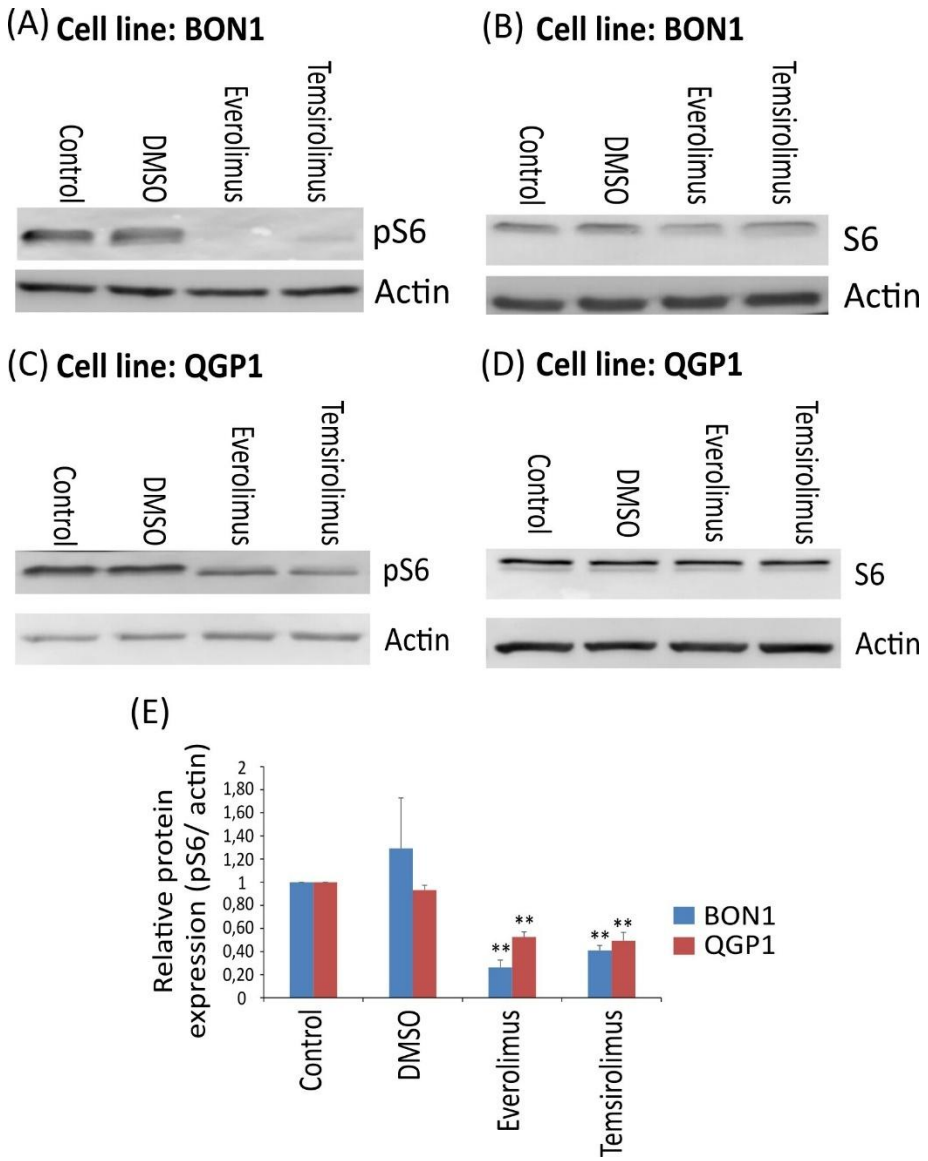

Figure 15: Inhibition of the mTOR signalling pathway in the panNET cell lines BON1 and QGP1.

A - B) Representative western blot images for the expression of phosphorylated S6 (32 kDa) in BON1 treated with the mTOR inhibitors Everolimus (1 µM, 72 hours) or Temsirolimus (1 µM, 7 hours). The S6 protein (32 kDa) represents the unphosphorylated form of the protein. 30 µg protein was loaded per lane and actin (40 kDa) was used as a loading control. All original, non-cleaved Western Blot images are shown in the supplementary Figure S 3. C - D) Representative western blot images for the expression of phosphorylated S6 (32 kDa) in QGP1 treated with the mTOR inhibitors Everolimus (1 µM, 72 hours) or Temsirolimus (1 µM, 7 hours). The S6 protein (32 kDa) represents the unphosphorylated form of the protein. 30 µg protein was loaded per lane and actin (40 kDa) was used as a loading control. All original, non-cleaved Western Blot images are shown in the supplementary Figure S 3. E) Quantification of the protein level of pS6 of the panNET cell lines BON1 and QGP1. Data are shown from three experiments and values represent means ± SEM (*p≤0.05, **p≤0.01; paired t-test (two-tailed)).

To dissect the molecular alterations induced by inhibition of the mTOR signalling pathway, RNA-sequencing was performed on BON1 and QGP1 cells treated with everolimus and temsirolimus. The wild type panNET cells and the panNET cells treated with DMSO served as a control.

In the first step, the general influence of mTOR inhibitors on the expression patterns of genes in panNET was investigated by generating a heatmap with hierarchical clustering for all samples (Figure 16A - B). The color coding of the heatmaps reflects the expression levels of each gene across the different samples, with yellow indicating higher expression and blue indicating lower expression (Figure 16A - B). The expression values were normalized and variance-stabilized to facilitate comparison between samples. Hierarchical clustering was indicated by a dendrogram at the top of each heatmap (Figure 16A - B). As expected, the clustering analysis distinguished the treatment groups (mTOR inhibitors) from the control groups (wild-type and DMSO-treated cells) in both panNET cell lines (BON1 and QGP1, Figure 16A – B). The group of panNET cells treated with everolimus formed a cluster alongside the temsirolimus- treated group, while the wild-type control group exhibited similarities with the DMSO-treated cells (Figure 16A - B). In addition to the heatmaps, a MA-plot was created by categorizing the samples into the two cluster groups: a control group (wild-type panNET cell line and panNET cells treated with DMSO) and an mTOR inhibitor group (panNET cells treated with everolimus or temsirolimus). The plot was used to provide an overview of the distribution of differential expressed genes between these cluster groups. Therefore, the log2 fold change (M) of the differentially expressed genes was plotted against the mean of normalized counts (A, Figure 16C - D). Each point represents a single gene, and the color coding highlights genes with significant difference in expression between the control and mTOR inhibitor-treated groups in red (padj ≤ 0.05, Figure 16C - D). Genes that did not exhibit significant changes are shown as grey points. The MA-plots revealed a clear distinction between the control and treatment groups. Taken together with the results from the heatmaps, this suggests a strong effect of the mTOR inhibitors on gene expression in panNET cell lines (Figure 16).

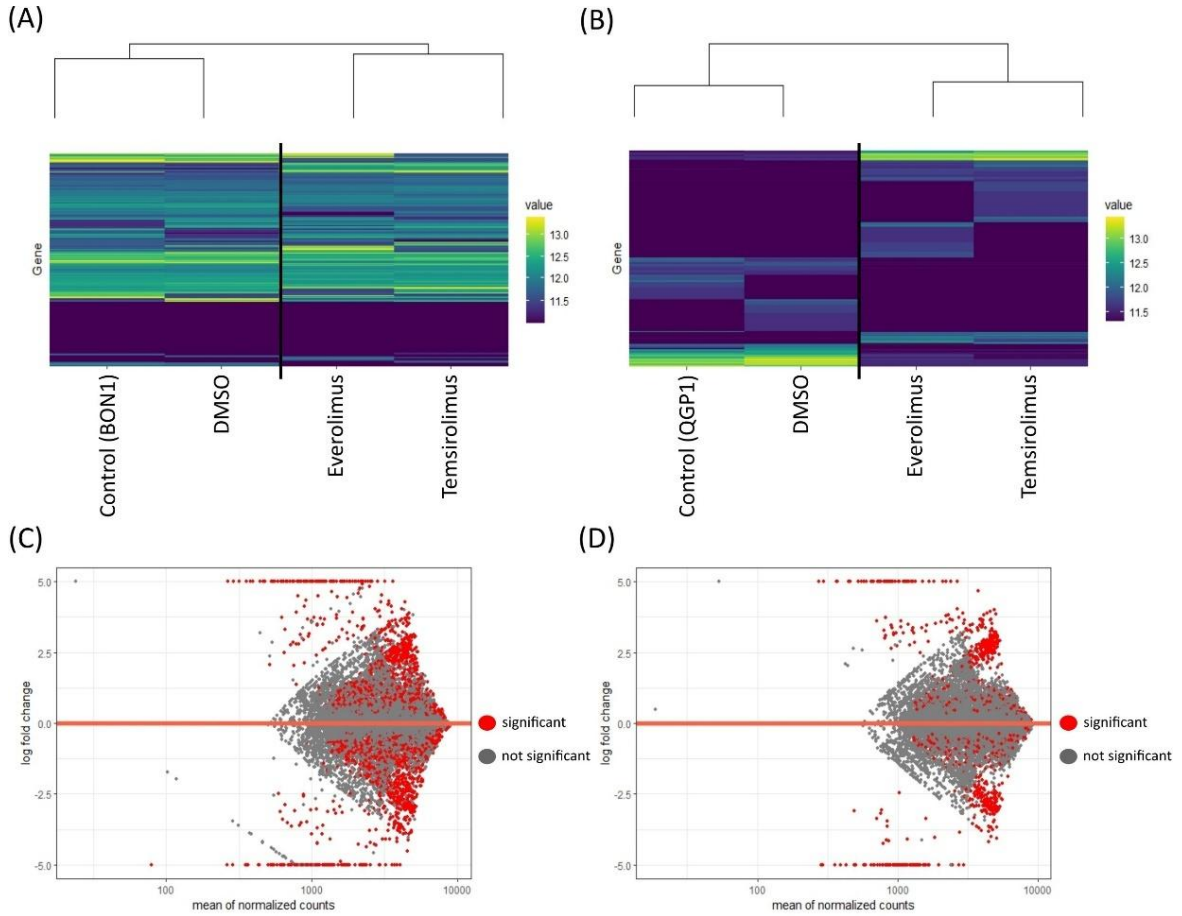

Figure 16: Inhibition of the mTOR pathway activity in panNET cell lines impacts the expression of various genes.

Differential expression analysis was performed using RNA sequencing in the panNET cell lines BON1 and QGP1. A - B) Heatmaps of gene expression data in BON1 (A) and QGP1 (B) cells with sample clustering. Rows represent genes, and columns represent samples. The colour intensity indicates the expression level of each gene in each sample. The value represents the normalized and variance-stabilized expression level of each gene, with darker colours (blue) indicating lower expression and brighter colours (yellow) indicating higher expression. A square root transformation was applied to the values to better highlight differences in lower and intermediate expression levels. The samples are hierarchically clustered based on their gene expression profiles, highlighting patterns of similarity across different experimental groups. Clusters of samples with similar expression profiles are grouped together, as indicated by the dendrogram. C – D) MA-plot of gene expression data in BON1 (C) and QGP1 (D) cells. The x-axis represents the mean of normalized counts, and the y-axis shows the log2fold change between the control group (wild type panNET cells and cells treated with DMSO) and the group treated with the mTOR inhibitors everolimus and temsirolimus. Each point represents a gene, with red-highlighted points indicating genes with significant differential expression (padj ≤ 0.05). A list of all differentially expressed genes is shown in the supplementary Table S 5 (BON1) and Table S 6 (QGP1).

Expression analysis of different genes was performed on the same groups as the MA-plot for both investigated panNET cell lines (BON1 and QGP1). Therefore, gene expression was compared between a control group (wild type panNET cells + DMSO) and a group treated with mTOR inhibitors (panNET cells treated with everolimus or temsirolimus). In general, differential gene analysis (padj ≤ 0.05; differentially expressed genes are listed in supplementary Table S 5 and Table S 6) revealed 1897 regulated genes in BON1 cells and 1129 regulated genes in QGP1 cells treated with mTOR inhibitors. In the mTOR inhibitor group of the BON1 cell line, 923 genes were downregulated, and 974 genes were upregulated in comparison to the control group. In QGP1 cells treated with mTOR inhibitors, 609 genes were downregulated, and 520 genes were upregulated in comparison to the control group. A list of all differentially expressed genes is shown in the supplementary Table S 5 (BON1) and Table S 6 (QGP1). In accordance with the results of the differential gene analysis in NET tissue samples, the *PPARGC1A* gene was downregulated in the mTOR inhibitor group of the BON1 cell line compared to the control group (Wald test = -2.82; padj < 0.001). Using quantitative PCR it could be confirmed that the expression of *PPARGC1A* was 0.3 fold-changes lower in BON1 treated with mTOR inhibitors when compared to the control group (Figure 17A). Western Blot analysis at 72 hours after the administration of either 1 µM everolimus or 1 µM temsirolimus revealed a reduction of the PGC1α protein level by 80 % in BON1 cells treated with mTOR inhibitors (Figure 17B - C). Contrary to the expectations, there were no evidence for an influence of the mTOR pathway activity on the *PPARGC1A* in QGP1 cells and mTOR activity had no impact on the expression of *HSPA9* (padj > 0.05).

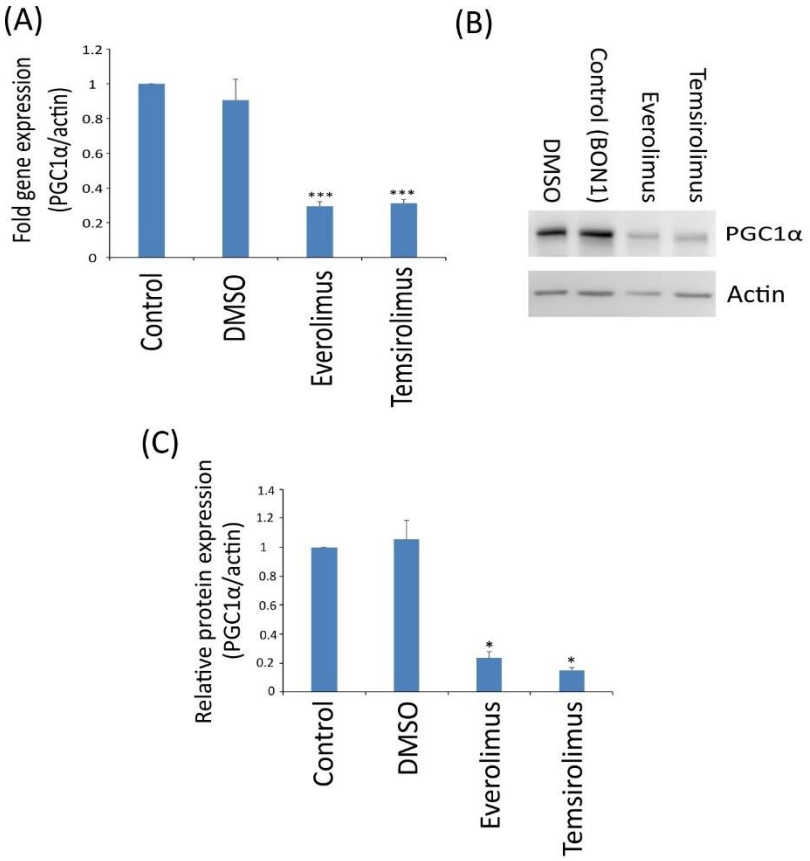

Figure 17: Inhibition of the mTOR pathway activity results in decreased expression of PGC1α in BON cells.

A) Gene expression of PGC1α was measured by qPCR analysis. Cells were treated with 1 µM everolimus or temsirolimus for 72 hours. The control group was set to 1 for better representation. Values represent means ± SEM (***p≤0.001; paired t-test (two-tailed)). B) Representative western blot images for the expression of PGC1α (130 kDa) in BON1 cells. Cells were treated with 1 µM everolimus or temsirolimus for 72 hours. 30 µg protein was loaded per lane and actin (40 kDa) was used as a loading control. All original, non-cleaved Western Blot images are shown in the supplementary Figure S 3. C) Representative western blot images for the expression of PGC1α in BON1 cells. Cells were treated with 1 µM everolimus or temsirolimus for 72 hours. 30 µg protein was loaded per lane and actin was used as a loading control. All original, non-cleaved Western Blot images are shown in the supplementary Figure S 3. D) Quantification of the protein level of PGC1α of the panNET cell line BON1. Data are shown from three experiments and values represent means ± SEM (*p≤0.05; paired t-test (two-tailed)).

3.5 Reduced PGC1α expression leads to reduced mTOR pathway activity in panNET cell lines

In the next step, both mTOR activated cell lines were treated with PGC1α- and mortalin-specific siRNAs and the mRNA and protein levels of both targets were investigated by qPCR analysis and immunoblotting. As expected, all investigated cell lines (BON1, QGP1) treated with PGC1α-specific siRNAs exhibited a reduction in *PGC1α* mRNA by 50 – 80% ($p \leq 0.01$) in comparison to the control (Figure 18A). Moreover, the protein levels of PGC1α were also reduced by 70 – 80% ($p \leq 0.05$) compared to the control (Figure 18C, E). Likewise, all investigated cell lines (BON1, QGP1) treated with mortalin-specific siRNAs exhibited a reduction in *HSPA9* mRNA by 50 – 60% ($p \leq 0.01$, Figure 18B) and reduced mortalin protein level by 50 – 60% ($p \leq 0.05$, Figure 18D, F). Interestingly, both siRNAs (mortalin, PGC1α) appear to also influence the expression of the respective other protein. All investigated cell lines (BON1, QGP1) treated with PGC1α-specific siRNAs also exhibited a reduction in *HSPA9* mRNA by 50 – 70% ($p \leq 0.05$, Figure 18A) and reduced mortalin protein level by 70 – 80% ($p \leq 0.05$, Figure 18C, E) in comparison to the control. Moreover, both panNET cell lines BON1 and QGP1 treated with mortalin-specific siRNAs showed reduced *PGC1α* mRNA by 50 – 60% ($p \leq 0.05$, Figure 18B) and reduced PGC1α protein level by 50 – 60% ($p \leq 0.05$, Figure 18D, E) in comparison to the control.

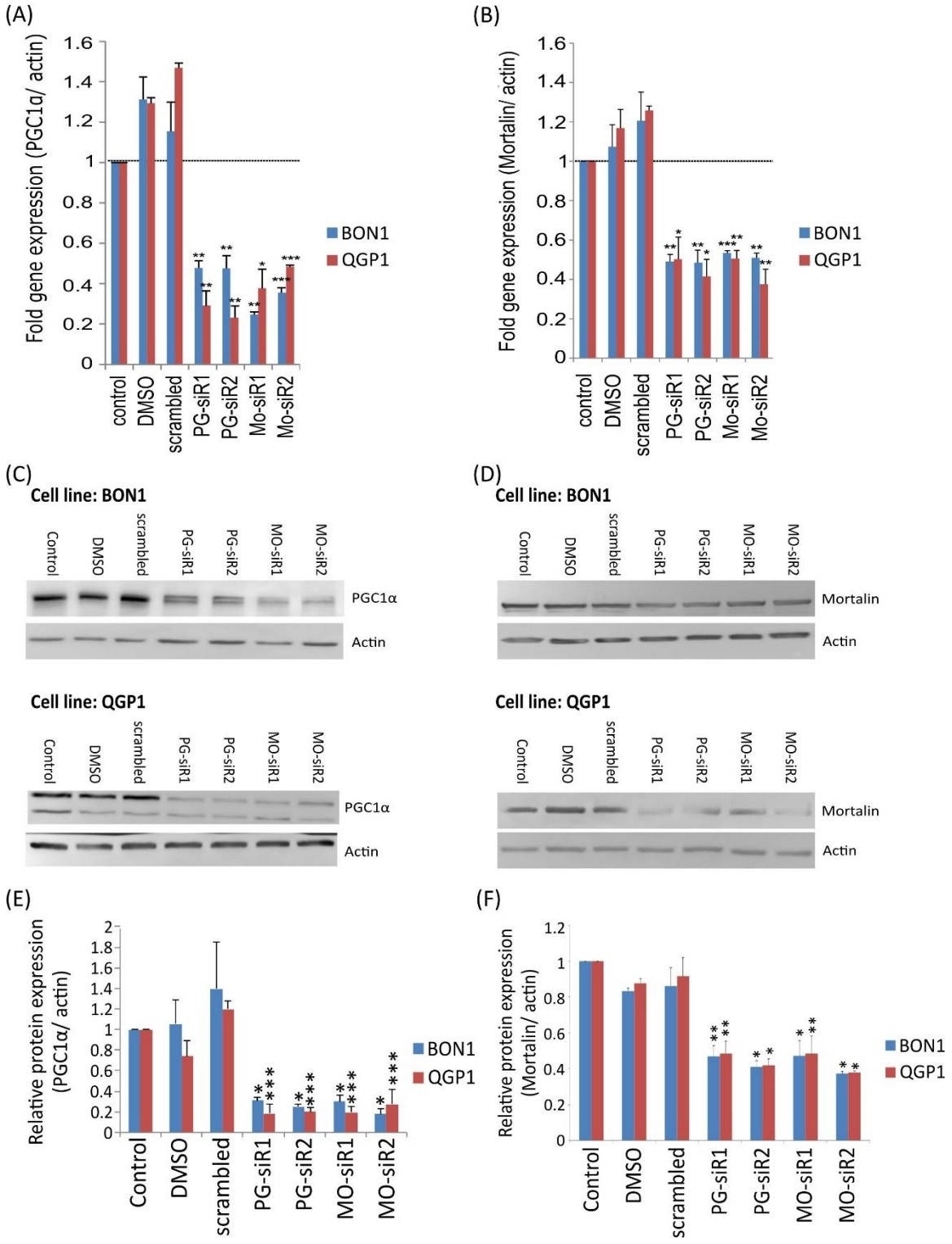

Figure 18: Reduced PGC1α expression leads to reduced mortalin expression in panNET cell lines and vice versa.

A – B) Quantification of the expression of PGC1α (A) and mortalin (B) in the panNET cell lines BON1 and QGP1. The expression of the genes was measured using qPCR analysis and normalized to the reference gene actin. Data were shown from three experiments and values represent means ± SEM

(*p≤0.05, **p≤0.01, ***p≤0.001; paired t-test (two-tailed)). C-D) Representative western blot images for the expression of PGC1α (130 kDa) (C) and mortalin (75 kDa) (D) of the panNET cell lines BON1 and QGP1. 30 µg protein was loaded per lane and actin was used as a loading control. All original, non-cleaved Western Blot images are shown in the supplementary Figure S 3. E-F) Quantification of the protein level of PGC1α (E) and mortalin (F) of the panNET cell lines BON1 and QGP1. Data are shown from three experiments and values represent means ± SEM (*p≤0.05, **p≤0.01, ***p≤0.001; paired t-test (two-tailed)).

As the main goal of this section of the work was to investigate the interaction between mTOR and the two mitochondria related proteins PGC1α and mortalin, it was investigated if these two proteins influence the expression of pS6 in the panNET cell lines BON1 and QGP1 by immunoblotting.

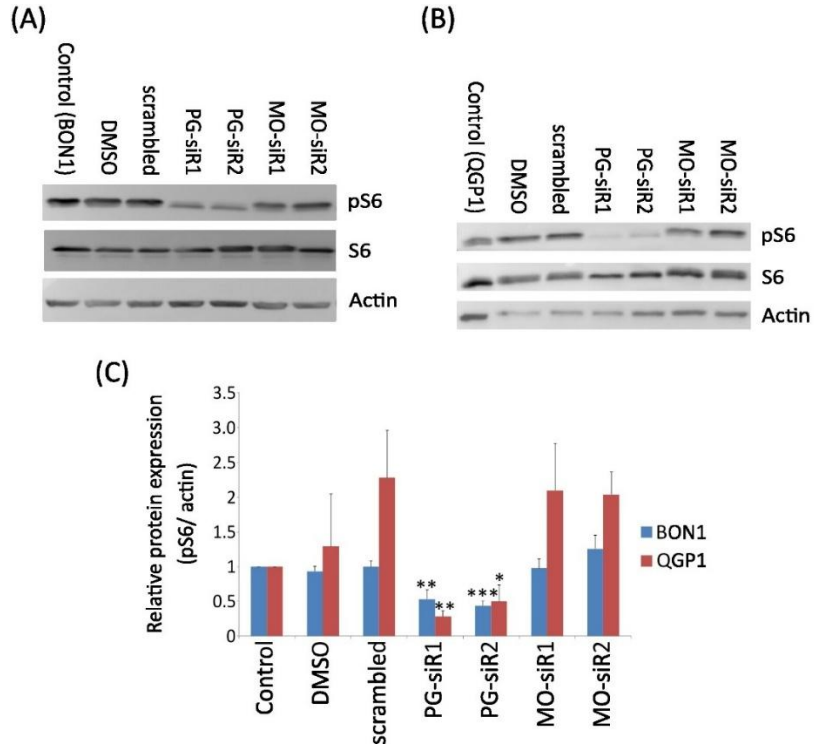

Figure 19: Reduced PGC1α expression impacts the mTOR pathway activity in panNET cell lines.

A-B) Representative western blot images for the expression of pS6 (32 kDa) in the panNET cell lines BON1 and QGP1. The S6 protein (32 kDa) represents the unphosphorylated form of the protein. 30 µg protein was loaded per lane and actin (40 kDa) was used as a loading control. All original, non-cleaved Western Blot images are shown in the supplementary Figure S 3. C) Quantification of the protein level of pS6 measured in the panNET cell lines BON1 and QGP1. Data are shown from three experiments and values represent means ± SEM (*p≤0.05, **p≤0.01, ***p≤0.001; paired t-test (two-tailed)).

The expression of pS6 and therefore the activity of mTOR was reduced by 50 – 60% ($p \leq 0.05$) in all investigated cell lines (BON1, QGP1) treated with PGC1α-specific siRNAs in comparison to the control (Figure 19). In contrast, pS6 expression remained unaffected by mortalin-specific siRNA ($p > 0.05$, Figure 19). These findings suggest that, unlike mortalin, PGC1α plays a regulatory role in mTOR signalling and should be further investigated as a potential functional modulator in pancreatic neuroendocrine tumour cells.

4. Discussion

4.1 Expression analysis of pS6 identifies 22 % of panNET with activated mTOR pathway

Pancreatic neuroendocrine tumours are a relatively rare malignancy, with their incidence increasing over the past decade from 0.42 per 100,000 people per year (2010-2011) to 1.39 per 100,000 people per year (2019-2020, Stensbøl et al., 2021). Due to the low incidence of this tumour type, treatment options are limited, and the therapy of patients remains challenging. The only known potential curative treatment is tumour surgery, which is mainly used for patients with primary, non-metastatic cases (Akirov et al., 2019; Ro et al., 2013; Storni et al., 2021). The success of this treatment depends on the localization, size, and metastatic state of the tumour. It is noteworthy, however, that surgery can also be performed for metastatic cancer, but in such cases, it serves as a palliative treatment aimed at disease control rather than a cure (PDQ Adult Treatment Editorial Board, 2024). In general, therapy of advanced panNETs mainly focuses on improvement of the patient's quality of life by controlling the disease. The two most common treatments in this context are chemotherapy and somatostatin analogues. Chemotherapy is used to prevent further tumour growth, while somatostatin analogues are administered to control symptoms (Megdanova-Chipeva et al., 2020; Ro et al., 2013). However, chemotherapy is associated with high toxicity, and while somatostatin analogues can effectively control symptoms, their antitumour activity is limited (Megdanova-Chipeva et al., 2020; Ro et al., 2013). Therefore, it is not surprising that the introduction of mTOR inhibitors as targeted therapy for panNETs, yield new opportunities for patients with advanced or metastatic tumours. These kind of inhibitors have mainly cytostatic effects, leading to

cell cycle arrest, reduced cell growth and cell proliferation in tumour cells (Exner et al., 2020). A study from Yao *et al.* showed that treatment with the first-generation inhibitor everolimus leads to longer progression-free survival in patients with advanced panNET (Yao et al., 2016). This study is one of the first long-term investigations showing that these inhibitors not only improve patients' quality of life and relieve symptoms but also have the potential to extend their lives by effectively slowing disease progression. Despite these promising findings, the treatment of patients with mTOR inhibitors remains challenging due to certain limitations. One of the major challenges is the lack of reliable biomarkers to guide mTOR-based therapy (Tian et al., 2019). In 2017, Yeung *et al*. highlighted the Kirsten Rat Sarcoma (KRAS) as a potential biomarker for the response of cancer cells to everolimus (Yeung et al., 2017). Their study found that KRAS mutations were associated with resistance to everolimus in 45 % of 20 advanced biliary tract cancer cell lines and this resistance was linked to the activation of the PI3K/AKT/mTOR signalling pathway (Yeung et al., 2017). However, there is still limited evidence and too few studies to consider KRas as a reliable biomarker for predicting resistance to mTOR inhibitors in clinical settings.

Another protein commonly used as an indirect marker for mTOR pathway activity in both research and clinical settings is the S6 protein. S6 is a component of the 40S small ribosomal subunit and acts as a RNA-binding protein in this context (Meyuhas, 2008; Yi et al., 2021). Among its various roles, S6 is involved in the translation of 5′ oligopyrimidine tract mRNAs and the mTOR-mediated regulation of protein synthesis (Dufner & Thomas, 1999; Komori et al., 2014; Ruvinsky et al., 2005; Yi et al., 2021). S6 has been used for a long time as a marker of mTOR pathway activity in research studies involving anal carcinomas (Stelzer et al., 2010), prostate cancer cell lines (Mortensen et al., 2015), and bladder cancer (Svatek et al., 2019). Building on this, a recent genome-wide CRISPR/Cas9 screen identified interleukin enhancer binding factor 3 (ILF3) as an interaction partner of mTORC1 in the context of amino acid sensing, with mTORC1 activity being assessed by pS6 fluorescence (Yan et al., 2023). Moreover, a recent study on uterine leiomyosarcomas showed that aberrant PI3K/mTOR signaling plays a crucial role in immune evasion (Wispelaere et al., 2024), while another study on pediatric malformations of cortical development revealed that mutations in the mTOR pathway lead to dysregulation of different cellular functions (Bakouh et al., 2025), both using pS6 as an indicator of high mTOR

pathway activity. Additionally to the research studies, several clinical trials have utilized S6 as an indicator of mTOR pathway activity, including one of the first blinded studies on patients with sarcomas (Iwenofu et al., 2008), an early trial on glioblastoma (Cloughesy et al., 2008), and a more recent Phase II clinical trial on prostate cancer (George et al., 2020). While the sarcoma trial aimed to investigate S6 as a biomarker of mTOR activity, most clinical trials focus on exploring the potential benefits of first-generation mTOR inhibitors for patients, using S6 as a key biomarker. This makes S6 one of the most important proteins in this research area. However, it has not yet been demonstrated that pS6 serves as an indicator of mTOR activity in panNET. Our findings demonstrate a strong correlation between pS6 expression and mTOR pathway activation in panNET tissue, with 22% of cases showing elevated pS6 levels. These high pS6-expressing cases were further associated with an enrichment of genes related to the mTORC1 pathway during GSEA analysis. Additionally, pS6 expression was found to be upregulated in the panNET cell lines BON1 and QGP1 and treatment with rapalogues led to a 50-70 % decrease of these pS6 levels. Taken together, these findings suggest that pS6 could serve as a potential indicator of mTOR pathway activation in panNET, providing valuable insights for future therapeutic strategies targeting mTOR signaling in these tumors.

Interestingly, there has been recent discussion regarding the potential benefits of S6 kinase inhibitors in cancer patients, with some inhibitors being in preclinical or clinical trial stage (Artemenko et al., 2022). The first reported S6 inhibitor to reach Phase I trials was LY2584702, which has been tested as a monotherapy (Tolcher et al., 2014) or in combination with mTOR inhibitors (Hollebecque et al., 2014) in advanced solid tumours. Unfortunately, the inhibitor demonstrated limited efficacy and was discontinued due to unfavourable pharmacokinetics. However, it has paved the way for the development of other inhibitors, which have not reached clinical trial stages yet (Artemenko et al., 2022). A dual p70S6K/AKT inhibitor showed promising results in a Phase I trial for advanced breast cancer (Tsimberidou et al., 2021) and RNA-based therapies targeting S6, such as miRNA and lncRNA, are being explored (Ma et al., 2018). The present study could also pave the way for the development of more effective therapeutic strategies targeting the S6 pathway, potentially improving treatment outcomes for patients with mTOR pathway-driven cancers.

As we correlated the pS6 expression with the mTOR pathway activity in panNET, we

identified 22 % of tumours with activated mTOR pathway. Previous studies have reported mTOR activity in 33 to 52 % of panNET (Komori et al., 2014; G. Lamberti et al., 2017). The great variability between the percentages can be attributed to variations in study design, pre-existing conditions of patients, patient treatments, and consequently, the quality of the sample material used. While the present study focused solely on panNETs (both poorly and well-differentiated), Lamberti *et al.* exclusively examined tissue from patients with well-differentiated NETs originating from the pancreas and gastrointestinal tract (Giuseppe Lamberti et al., 2018). Furthermore, both Lamberti and Komori examined a smaller number of panNET cases compared to our cohort of 157 cases (Komori et al., 2014; G. Lamberti et al., 2017), which represents one of the largest cohorts studied to date.

4.2 The spectrum of mitochondrial mutations varied widely among panNET and was independent of mTOR signaling

The first somatic point mutations of the mtDNA were discovered by Polyak *et al.*, who analyzed the complete mitochondrial genome of ten colorectal cancer cell lines (Polyak et al., 1998). In the following years, numerous somatic mutations in the mitochondrial genome have been found, with the frequency of these somatic mtDNA mutations varying between different tumour entities (Schon et al., 2012; Stewart et al., 2015). A study of 31 tumour types showed that 59 % of cancer samples harbored at least one somatic mtDNA mutation (Ju et al., 2014), whereby another study on five different cancer types revealed that the frequencies of these deleterious tumour-specific somatic mutations ranged from 13% in glioblastomas to 63% in rectal adenocarcinomas (Larman et al., 2012). The mtDNA and mitochondria have also been shown to play an important role in neuroendocrine tumours. A study by Yang *et al.* investigated a cohort of neuroendocrine tumours and carcinomas and identified four molecular subtypes that differ in their genetic alterations, molecular landscape, and histo-pathological features (Yang et al., 2021). In particular, the Alpha cell-like subtype displayed significantly elevated mitochondrial parameters, including increased mitochondrial-protein content and higher expression of oxidative phosphorylation genes (Maluchenko et al., 2024; Yang et al., 2021). Despite these findings highlighting the importance of mitochondria in NETs, due to the low incidence and heterogeneity of panNET, little is known about the frequency of mtDNA mutations in this tumour type.

In the present study we found that 41 % of the investigated panNET harbour at least one somatic mutation of the mtDNA. The mutations were found in all regions of the mtDNA (non-coding region, genes coding for rRNAs, genes coding for tRNAs and genes coding for respiratory chain complexes) with the most frequent mutations occurring in genes for respiratory chain complexes. Interestingly, these mutations were independent of the mTOR pathway activity in panNET. A possible explanation could lie in the distinct mechanisms that regulate mitochondrial function and genomic stability. While the mTOR pathway plays a central role in regulating cell growth and survival, particularly through the control of autophagy and mitophagy (Bartolomé et al., 2017; Y. C. Kim & Guan, 2015; Qiao et al., 2022), the occurrence of mtDNA mutations depends on other, complex processes that go beyond the mTOR pathway. Although some mtDNA mutations are inherited across generations, a significant number develops over the course of a lifetime (Burr & Chinnery, 2024). In the case of cancer, it has been suggested that somatic mtDNA mutations are acquired during tumorigenesis, as they are absent in the adjacent non-cancerous tissue (Caldıran & Aydemir, 2024; Smith et al., 2022). Due to the lack of a protective histone structure and their proximity to the main site of ROS production in the cell, mtDNA mutations can arise from oxidative stress or damage induced by external agents (K. Chen et al., 2022; Roy et al., 2022; Shokolenko et al., 2009). Moreover, errors in mitochondrial DNA replication, disruptions in mitochondrial biogenesis as well as environmental factors can also cause mutations of the mtDNA (Craigen, 2012). All these processes can take place independently of the mTOR activity and therefore lead to the observed occurrence of mTOR-independent mtDNA mutations in panNET. Although it is still debated whether mtDNA mutations have tumor-promoting (Kim et al., 2016), tumor-suppressing (Iommarini et al., 2014), or neutral effects (Ju et al., 2014) on carcinogenesis, it is most often described that mtDNA mutations occur in cancer cells because they have special energy needs, due to their increased growth and proliferation rates (Hanahan, 2022). In many cases, these mutations lead to enhanced oxidative phosphorylation (OXPHOS), which boosts energy production and helps meet the increased demand (Hanahan, 2022). However, in the case of panNETs, a special scenario arises: A higher percentage of these tumours show increased mTOR pathway activity (Komori et al., 2014; G. Lamberti et al., 2017), which has been connected to high tumour growth and progression in different entities (Hua et al., 2019; Saxton & Sabatini, 2017). It is

possible that panNET cancer cells are not only relying on mitochondrial changes and OXPHOS to meet their elevated energy needs, but are also utilizing mTOR-mediated mechanisms, such as the activation of metabolic pathways for energy production. This could explain why no direct correlation between mTOR activity and mtDNA mutations was observed in our study. The panNETs seem to be using alternative mechanisms for energy supply, allowing mtDNA mutations to occur independently of mTOR pathway activation.

Another possible explanation for the lack of association between mTOR and mtDNA mutations could be that the treatment of patients may have influenced the results. Studies have shown that mTOR inhibition can reduce mtDNA mutations. For example, a study by Chung *et al.* demonstrated that one of the most common disease associated mtDNA mutations, the m.3243 A > G mutation, leads to upregulation of the PI3K-AKT-mTORC1 axis and that inhibition of the mTOR signalling pathway results in reduced mtDNA mutant load in tissue and cell culture experiments (Chung et al., 2021). Similarly, Dai *et al.* showed that rapamycin reduced the G11778A mutation associated with Leber's hereditary optic neuropathy in cybrid cells (Ying Dai et al., 2014). However, since our study lacked sufficient data on whether patients were treated with mTOR inhibitors, it is challenging to determine whether such treatments may have influenced the correlation between mTOR and mtDNA mutations in our cohort.

4.3 Identification of PGC1α as a target of mTOR in panNET with activated mTOR pathway signalling

The next step was to dissect the molecular alterations that were induced by activation of the mTOR signaling pathway in panNET. It is known that mTOR impacts a variety of mRNAs related to nucleus encoded mitochondrial proteins, including mRNAs encoding for components of the oxidative phosphorylation and proteins that are involved in the transcription and translation of the mtDNA (Larsson et al., 2012). For instance, mTORc1 has been shown to regulate the transcription of mitochondrial mRNAs by inhibiting the 4E-binding proteins (4E-BPs) (Morita et al., 2013). This early discovery revealed that mTORC1 affects the expression of mitochondrial ribosomal proteins, components of complexes I and V of the oxidative phosphorylation pathway, as well as the transcription factor TFAM (Morita et al., 2013). More recent studies also underline the role of mTORC1 in regulating

mitochondrial translation. For example, investigations in primary human trophoblast cells demonstrate that inhibition of the mTOR pathway affects the expression of various proteins related to mitochondria and oxidative phosphorylation (OXPHOS) (Rosario et al., 2019; Rosario et al., 2020). Although there has been no direct connection between mTORC2 and the transcription of mitochondrial mRNAs, there is some evidence suggesting that this complex might also influence this process. For instance, mTORC2 has been shown to interact with key molecules such as AKT and Connexin 43, which play significant roles in cellular metabolism or act as structural proteins (Bantug et al., 2018; S. Wang et al., 2022). These interactions have been shown to impact the regulation of mitochondrial gene expression, contributing to mitochondrial integrity and the maintenance of energy homeostasis (Bantug et al., 2018; S. Wang et al., 2022).

One interesting protein family that has been described to connect mTOR and mitochondria in NET before, is the PGC1 family, with PGC1α being the most well-known representative. PGC1α is a 91 kDa protein that is encoded by the *PPARGC1A* gene which consist of 13 exons and is locates on chromosome 4p15.2 (Liang & Ward, 2006). The protein is located in the nucleus and mainly expressed in tissue with high energy demand as it is involved in metabolic key processes, like mitochondrial biogenesis, glucose metabolism and adaptive thermogenesis (Liang & Ward, 2006). PGC1α interacts with at least 20 different nuclear factors and alternative splicing leads to several tissue-specific isoforms of PGC1α, whereby all these isoforms act as transcriptional coactivators (Liang & Ward, 2006; Martínez-Redondo et al., 2015; Mastropasqua et al., 2018; Villena, 2015). In general, members of the PGC1 family are connected to different disease besides cancer, including neurodegenerative diseases, metabolic disorders or cardiovascular diseases (Qian et al., 2024). Interestingly, a study postulates that a considerable number of patients with small cell neuroendocrine tumours exhibit high expression of PGC1α (Varuzhanyan et al., 2024). Varuzhanyan *et al.* showed that high expression of PGC1α leads to enhanced OXPHOS and that PGC1α influences both the progression and subtype determination of small cell neuroendocrine tumours (Varuzhanyan et al., 2024). In the present study, we were able to identify PGC1α as a partner of the mTOR signaling pathway in panNET. The *PPARGC1A* was the most significantly upregulated gene in panNET tissue samples with activated mTOR

pathway and inhibition of mTOR leaded to reduced PGC1α expression in the panNET cell line BON1. Interestingly, we couldn't find any changes in the expression of the protein after inhibition of mTOR in the panNET cell line QGP1. Studies performing comprehensive characterizations of both cell lines revealed significant similarities between them, with one notable difference found in the RAS-pathway between BON1 and QGP1 (Luley et al., 2020; Vandamme et al., 2015). This pathway is a crucial cellular pathway involved in regulating cell growth, cell survival and cell differentiation (Bahar et al., 2023). It is activated by different RAS proteins, which are expressed in various tissues, vary in the frequency of mutations in certain cancers, and have different relevance in specific diseases (Bahar et al., 2023). All RAS proteins act as molecular switches that activate various downstream kinases, such as RAF, MEK, and ERK, that control gene expression and cell functions (Bahar et al., 2023).In the present study, BON1 cells harbor a NRAS mutation, while QGP1 cells carry a KRAS mutation (Vandamme et al., 2015). Mutations in RAS genes are known to drive aberrant activation of downstream signaling cascades, including the PI3K/AKT/mTOR and MAPK/ERK pathways (Prior et al., 2012). These signaling networks can cross-regulate one another and impact the cellular response to mTOR inhibition. In BON1 cells, the NRAS mutation may lead to a more direct and robust activation of the mTOR pathway, making the cells more responsive to mTOR inhibition. Consequently, inhibition of mTOR could more effectively reduce PGC1α expression in these cells. On the other hand, the KRAS mutation in QGP1 cells could activate different compensatory pathways, such as the PI3K/AKT or MEK/ERK axes, which might override or diminish the effect of mTOR inhibition on PGC1α expression. These alternative pathways could maintain cellular homeostasis and prevent a significant decrease in PGC1α levels despite mTOR pathway inhibition. Interestingly, we observed that mTOR inhibition by rapalogues was more effective in BON1 cells at the protein level, with a 60–70% reduction in pS6 expression, compared to a 50% reduction in QGP1 cells. This suggests that KRAS mutations in QGP1 cells might contribute to partial resistance to mTOR inhibition. This hypothesis is further supported by findings from Yeung *et al.* (2017), who demonstrated that KRAS mutations were associated with resistance to everolimus in 45% of 20 advanced biliary tract cancer cell lines (Yeung et al., 2017).

In the present study, not only did mTOR seem to influence PGC1α, but PGC1α also

appeared to have an impact on mTOR signaling. We showed that PGC1α was highly expressed in mTOR-activated panNETs, and that reduction of PGC1α by siRNA led to a 50-60 % reduction in pS6 expression in panNET cell lines. Therefore, PGC1α appears to be more than just a downstream target of mTOR; the reciprocal interaction between these two pathways points to a more dynamic relationship. Previous studies have also described this mTOR-PGC1α axis in various cancer types and biological processes. For example, in lung epithelial cells, the mTOR/PGC1α/β axis was found to be upregulated in senescent cells (Summer et al., 2019), suggesting that this pathway may contribute to cellular aging and senescence. Summer *et al.* proposed that targeting this axis could be beneficial for patients, though preclinical studies have produced mixed results (Houssaini et al., 2018; Summer et al., 2019). Moreover, recent studies of Infectious spleen and kidney necrosis virus and miscarriages have highlighted the involvement of the mTOR-PGC1α axis in regulating cellular metabolism and stress responses (X. Fu et al., 2022; Zhu et al., 2024). In ISKNV-infected cells, mTOR activation promotes the PGC-1α/SIRT3 pathway, influencing viral replication (X. Fu et al., 2022). Similarly, in miscarriage tissue, the mTOR/PGC1α axis is implicated in mitochondrial dysfunction and cell apoptosis, leading to pregnancy loss (Zhu et al., 2024). In addition, the mTOR/PGC1α axis is involved in key metabolic processes such as cellular reprogramming and gluconeogenesis. For instance, studies have shown that suppression of mTORc1 and PGC1α is crucial for mitochondrial remodeling during somatic cell reprogramming (L. Wang et al., 2020). Additionally, mTORc1 plays a critical role in regulating hepatic gluconeogenesis through PGC1α (G. Wang et al., 2022), highlighting the importance of this pathway in energy metabolism and metabolic diseases. Taken together, these studies underscore that the mTOR-PGC1α axis plays a critical role in various pathophysiological conditions, presenting a potential therapeutic target across multiple diseases.

4.4 Identification of mortalin as a target of mTOR in high grade panNET with activated mTOR pathway

To not only dissect molecular alterations that were induced by activation of the mTOR signaling pathway in panNET but to also investigate them in the context of clinic pathological features, high grade (G2/G3) panNET tissue samples with mTOR pathway activity were compared against low grade (G1) panNET tissue samples with

mTOR pathway activity. We identified the *HSPA9* gene as the most upregulated gene in high grade (G2/G3) panNET tissue samples with mTOR pathway activity. In general, *HSPA9* encodes the protein mortalin, which is a member of the HSP70 subfamily. This family is a group of molecular chaperones that are involved in protein folding, regulation of apoptosis and cell survival (Bhattacharya et al., 2020; Esfahanian et al., 2023; Radons, 2016). Although the majority of HSP70 family members share similar structural characteristics, mutations in their coding regions determine their organelle specificity (McCallister et al., 2015). Mortalin contains a mitochondrial-targeting signal peptide at the N terminus, which makes it not surprising that 70 % of the protein is located in the mitochondria (Dahlseid et al., 1994; Esfahanian et al., 2023). In general, mortalin plays a crucial role in mitochondrial processes trough the folding and stabilization of nuclear-encoded mitochondrial proteins and has an impact on different cancer related processes (Esfahanian et al., 2023). For instance, mortalin can bind with p53, a tumour suppressor that is frequently mutated in different cancer types, thereby promoting tumour growth and formation (Sabapathy & Lane, 2019). The binding of mortalin to p53 prevents the tumour suppressor from being transported to the nucleus, impairing its tumour-suppressive functions (Elwakeel, 2022; Gestl & Anne Böttger, 2012). This is in accordance with the observation, that mortalin is upregulated in different tumour types, like breast cancer (R. Zhang et al., 2021), gastric cancer (Yi Dai et al., 2021) or colorectal cancer (Javid et al., 2022), diminishing the overall survival of patients (Esfahanian et al., 2023; Yoon et al., 2022). Moreover, in medullary thyroid carcinoma (a neuroendocrine tumour) reduction of mortalin leads to cell death and decreased proliferation in cell culture experiments (D. Starenki et al., 2015). In line with our findings that mortalin is primarily upregulated in high-grade panNETs with mTOR pathway activity, it has been shown that the upregulation of this protein affects not only patient survival but also tumorigenesis and tumour progression to a more aggressive phenotype (Kaushal et al., 2024).

In contrast to mortalin in cancer, little is known about the relationship between mTOR and the protein so far. A study revealed that loss of mortalin function induces mitochondrial stress and apoptosis in different human cell lines (Burbulla et al., 2014). Burbulla *et al.* postulate that this effect can be rescued by the PTEN-induced kinase 1 (PINK1) in cells with a functional autophagic machinery (Burbulla et al., 2014). Interestingly, this protective effect of PINK1 has been observed in cells

treated with the mTOR inhibitor rapamycin (Sarkar & Rubinsztein, 2008), a compound that inhibits mTORC1 and induces autophagy, suggesting that mTOR may influence the autophagic response to mortalin loss. Taken together, our results highlight that mortalin is not only a critical player in mitochondrial function but also a key regulator within the mTOR signaling pathway in high-grade panNETs, suggesting that targeting mortalin or its interactions with mTOR could offer promising therapeutic strategies for these aggressive tumors.

It is noteworthy that PGC1α, which we show to be generally upregulated in panNET with high mTOR pathway activity, has been reported to correlate with mortalin in some studies. For example, a study by Starenki *et al.* investigated the effect of the mortalin inhibitor MKT-077 on medullary thyroid carcinoma (MTC), a type of neuroendocrine tumour (Dmytro Starenki & Park, 2015). The study found that, in some MTC cells, inhibition of mortalin led to a decrease in the expression of PGC1α, along with other markers of mitochondrial integrity (Dmytro Starenki & Park, 2015). Additionally, another study by Cai *et al.* showed that a decrease in PGC1α in neuroblastoma cells resulted in a reduction of mortalin expression (Cai et al., 2020). Taken together, these studies suggest a complex relationship between PGC1α and mortalin, where changes in one may influence the expression of the other, highlighting their potential interconnected roles in mitochondrial integrity and neuroendocrine tumour biology.

Based on the observation that Mortalin, unlike PGC1α, does not influence pS6 expression in cell culture experiments, it is possible that Mortalin could be a downstream target of mTOR. Additionally, in the tumour microenvironment, factors such as hypoxia or nutrient deprivation could impact mTOR activity and, consequently, the regulation of mortalin in ways that differ from standard cell culture conditions. These stress factors could lead to a differentiated regulation, affecting the direct relationship between mortalin and pS6 observed in specific experiments.

5. Conclusion and future directions

The mTOR signalling pathway plays an important role in targeted drug therapy for panNET, and there has been ongoing discussion about the potential benefits of combination therapy with mTOR inhibitors and drugs targeting mitochondrial pathways. However, investigating this question has proven challenging due to the rarity of panNET, which results in a limited number of available research samples. As

a consequence, our understanding of the impact of mTOR activity on the molecular characteristics of this cancer remains insufficient. In the present study, we established one of the largest cohorts to date, consisting of 157 cases. Despite the challenges in finding reliable biomarkers for mTOR treatment, we identified that 22% of panNET cases with activated mTOR pathway. Additionally, our study demonstrates that pS6 serves as a reliable biomarker for mTOR pathway activity in this tumour entity. Although we did not find any correlation between mTOR signalling activity and somatic mutations in the mtDNA, we successfully identified several mitochondria-related targets of mTOR in panNET. Notably, the most significantly upregulated gene in panNET with mTOR pathway activity was *PPARGC1A*, which encodes PGC1α. This protein is described as the master regulator of mitochondrial biogenesis and has been investigated in some NET before but never in combination with the mTOR pathway activity. Interestingly, cell culture experiments showed that PGC1α also influences the mTOR pathway activity of panNET. Given the possibility that PGC1α may not only be regulated by mTOR but also influence mTOR pathway activity in panNET, future studies should focus on the molecular mechanisms underlying this interaction. Investigating whether PGC1α acts as a downstream target of mTOR or if its role in the mTOR-PGC1α axis involves a reciprocal feedback loop will be crucial in understanding the broader implications for targeted therapies. Additionally, exploring the impact of mTOR-PGC1α interaction on mitochondrial function and panNET progression could provide new insights into potential therapeutic strategies, especially in combination therapies targeting both mTOR and mitochondrial pathways. In addition, mortalin could be identified as a target of mTOR in high-grade mTOR activated panNET in this study. Mortalin is also a mitochondria-related protein that has been associated with aggressive characteristics in other tumour entities. In contrast to PGC1α, mortalin did not affect the mTOR pathway activity in panNET cell lines, indicating that it could be a downstream target of mTOR.

Overall, this study not only highlights key molecular targets involved in mTOR pathway activity but also opens the door to future research on the complex interplay between mTOR signalling and mitochondrial functions in panNET. Investigating this axis in greater detail may provide valuable insights for the development of more effective, targeted therapeutic strategies for this rare and challenging cancer.

References

Akirov, A., Larouche, V., Alshehri, S., Asa, S. L., & Ezzat, S. (2019). Treatment Options for Pancreatic Neuroendocrine Tumors. *Cancers*, *11*(6). https://doi.org/10.3390/cancers11060828

Amin, A. G., Jeong, S. W., Gillick, J. L., Sursal, T., Murali, R., Gandhi, C. D., & Jhanwar-Uniyal, M. (2021). Targeting the mTOR pathway using novel ATP-competitive inhibitors, Torin1, Torin2 and XL388, in the treatment of glioblastoma. *International Journal of Oncology*, *59*(4). https://doi.org/10.3892/ijo.2021.5263

Artemenko, M., Zhong, S. S. W., To, S. K. Y., & Wong, A. S. T. (2022). P70 S6 kinase as a therapeutic target in cancers: More than just an mTOR effector. *Cancer Letters*, *535*, 215593. https://doi.org/10.1016/j.canlet.2022.215593

Bahar, M. E., Kim, H. J., & Kim, D. R. (2023). Targeting the RAS/RAF/MAPK pathway for cancer therapy: From mechanism to clinical studies. *Signal Transduction and Targeted Therapy*, *8*(1), 455. https://doi.org/10.1038/s41392-023-01705-z

Bakouh, N., Castaño-Martín, R., Metais, A., Dan, E. L., Balducci, E., Chhuon, C., Lepicka, J., Barcia, G., Losito, E., Lourdel, S., Planelles, G., Muresan, R. C., Moca, V. V., Kaminska, A., Bourgeois, M., Chemaly, N., Rguez, Y., Auvin, S., Huberfeld, G., . . . Blauwblomme, T. (2025). Chloride deregulation and GABA depolarization in MTOR-related malformations of cortical development. *Brain : A Journal of Neurology*, *148*(2), 549–563. https://doi.org/10.1093/brain/awae262

Bankhead, P., Loughrey, M. B., Fernández, J. A., Dombrowski, Y., McArt, D. G., Dunne, P. D., McQuaid, S., Gray, R. T., Murray, L. J., Coleman, H. G., James, J. A., Salto-Tellez, M., & Hamilton, P. W. (2017). Qupath: Open source software for digital pathology image analysis. *Scientific Reports*, *7*(1), 16878. https://doi.org/10.1038/s41598-017-17204-5

Bantug, G. R., Fischer, M., Grählert, J., Balmer, M. L., Unterstab, G., Develioglu, L., Steiner, R., Zhang, L., Costa, A. S. H., Gubser, P. M., Burgener, A.-V., Sauder, U., Löliger, J., Belle, R., Dimeloe, S., Lötscher, J., Jauch, A., Recher, M., Hönger, G., . . . Hess, C. (2018). Mitochondria-Endoplasmic Reticulum Contact Sites Function as Immunometabolic Hubs that Orchestrate

the Rapid Recall Response of Memory CD8+ T Cells. *Immunity*, *48*(3), 542-555.e6. https://doi.org/10.1016/j.immuni.2018.02.012

Bartolomé, A., García-Aguilar, A., Asahara, S.-I., Kido, Y., Guillén, C., Pajvani, U. B., & Benito, M. (2017). Mtorc1 Regulates both General Autophagy and Mitophagy Induction after Oxidative Phosphorylation Uncoupling. *Molecular and Cellular Biology*, *37*(23). https://doi.org/10.1128/MCB.00441-17

Bhattacharya, K., Weidenauer, L., Luengo, T. M., Pieters, E. C., Echeverría, P. C., Bernasconi, L., Wider, D., Sadian, Y., Koopman, M. B., Villemin, M., Bauer, C., Rüdiger, S. G. D., Quadroni, M., & Picard, D. (2020). The Hsp70-Hsp90 co-chaperone Hop/Stip1 shifts the proteostatic balance from folding towards degradation. *Nature Communications*, *11*(1), 5975. https://doi.org/10.1038/s41467-020-19783-w

Brandon, M., Baldi, P., & Wallace, D. C [D. C.] (2006). Mitochondrial mutations in cancer. *Oncogene*, *25*(34), 4647–4662. https://doi.org/10.1038/sj.onc.1209607

Burbulla, L. F., Fitzgerald, J. C., Stegen, K., Westermeier, J., Thost, A.-K., Kato, H., Mokranjac, D., Sauerwald, J., Martins, L. M., Woitalla, D., Rapaport, D., Riess, O., Proikas-Cezanne, T., Rasse, T. M., & Krüger, R. (2014). Mitochondrial proteolytic stress induced by loss of mortalin function is rescued by Parkin and PINK1. *Cell Death & Disease*, *5*(4), e1180. https://doi.org/10.1038/cddis.2014.103

Burr, S. P., & Chinnery, P. F. (2024). Origins of tissue and cell-type specificity in mitochondrial DNA (mtDNA) disease. *Human Molecular Genetics*, *33*(R1), R3-R11. https://doi.org/10.1093/hmg/ddae059

Cai, Y., Shen, H [Hui], Weng, H., Wang, Y., Cai, G., Chen, X., & Ye, Q. (2020). Overexpression of PGC-1α influences the mitochondrial unfolded protein response (mtUPR) induced by MPP+ in human SH-SY5Y neuroblastoma cells. *Scientific Reports*, *10*(1), 10444. https://doi.org/10.1038/s41598-020-67229-6

Caldıran, F., & Aydemir, M. N. (2024). Exploring the Role of Mitochondrial DNA Mutations in Cancer Development and Diagnosis. In *Interdisciplinary Cancer Research.* Springer International Publishing. https://doi.org/10.1007/16833_2024_270

Chan, J., & Kulke, M. (2014). Targeting the mTOR signaling pathway in neuroendocrine tumors. *Current Treatment Options in Oncology*, *15*(3), 365–379. https://doi.org/10.1007/s11864-014-0294-4

Chen, J [J.], Zheng, X. F., Brown, E. J., & Schreiber, S. L. (1995). Identification of an 11-kDa FKBP12-rapamycin-binding domain within the 289-kDa FKBP12-rapamycin-associated protein and characterization of a critical serine residue. *Proceedings of the National Academy of Sciences of the United States of America*, *92*(11), 4947–4951. https://doi.org/10.1073/pnas.92.11.4947

Chen, K., Lu, P., Beeraka, N. M., Sukocheva, O. A., Madhunapantula, S. V., Liu, J [Junqi], Sinelnikov, M. Y., Nikolenko, V. N., Bulygin, K. V., Mikhaleva, L. M., Reshetov, I. V., Gu, Y., Zhang, J [Jin], Cao, Y., Somasundaram, S. G., Kirkland, C. E., Fan, R., & Aliev, G. (2022). Mitochondrial mutations and mitoepigenetics: Focus on regulation of oxidative stress-induced responses in breast cancers. *Seminars in Cancer Biology*, *83*, 556–569. https://doi.org/10.1016/j.semcancer.2020.09.012

Cheng, H., Zou, Y., Ross, J. S., Wang, K., Liu, X [Xuewen], Halmos, B., Ali, S. M., Liu, H [Huijie], Verma, A., Montagna, C., Chachoua, A., Goel, S., Schwartz, E. L., Zhu, C., Shan, J., Yu, Y., Gritsman, K., Yelensky, R., Lipson, D., . . . Perez-Soler, R. (2015). Rictor Amplification Defines a Novel Subset of Patients with Lung Cancer Who May Benefit from Treatment with mTORC1/2 Inhibitors. *Cancer Discovery*, *5*(12), 1262–1270. https://doi.org/10.1158/2159-8290.CD-14-0971

Chiarini, F., Evangelisti, C., Lattanzi, G., McCubrey, J. A., & Martelli, A. M. (2019). Advances in understanding the mechanisms of evasive and innate resistance to mTOR inhibition in cancer cells. *Biochimica Et Biophysica Acta. Molecular Cell Research*, *1866*(8), 1322–1337. https://doi.org/10.1016/j.bbamcr.2019.03.013

Chow, L. Q. M., & Eckhardt, S. G. (2007). Sunitinib: From rational design to clinical efficacy. *Journal of Clinical Oncology : Official Journal of the American Society of Clinical Oncology*, *25*(7), 884–896. https://doi.org/10.1200/JCO.2006.06.3602

Chung, C.-Y., Singh, K., Kotiadis, V. N., Valdebenito, G. E., Ahn, J. H., Topley, E., Tan, J., Andrews, W. D., Bilanges, B., Pitceathly, R. D. S., Szabadkai, G., Yuneva, M., & Duchen, M. R. (2021). Constitutive activation of the PI3K-Akt-

mTORC1 pathway sustains the m.3243 A G mtDNA mutation. *Nature Communications*, *12*(1), 6409. https://doi.org/10.1038/s41467-021-26746-2

Cloughesy, T. F., Yoshimoto, K., Nghiemphu, P., Brown, K., Dang, J., Zhu, S., Hsueh, T., Chen, Y [Yinan], Wang, W., Youngkin, D., Liau, L., Martin, N., Becker, D., Bergsneider, M., Lai, A., Green, R., Oglesby, T., Koleto, M., Trent, J., . . . Sawyers, C. L. (2008). Antitumor activity of rapamycin in a Phase I trial for patients with recurrent PTEN-deficient glioblastoma. *PLoS Medicine*, *5*(1), e8. https://doi.org/10.1371/journal.pmed.0050008

Conciatori, F., Ciuffreda, L., Bazzichetto, C., Falcone, I., Pilotto, S., Bria, E., Cognetti, F., & Milella, M. (2018). Mtor Cross-Talk in Cancer and Potential for Combination Therapy. *Cancers*, *10*(1). https://doi.org/10.3390/cancers10010023

Craigen, W. J. (2012). Mitochondrial DNA mutations: An overview of clinical and molecular aspects. *Methods in Molecular Biology (Clifton, N.J.)*, *837*, 3–15. https://doi.org/10.1007/978-1-61779-504-6_1

Dahlseid, J. N., Lill, R., Green, J. M., Xu, X [X.], Qiu, Y., & Pierce, S. K. (1994). Pbp74, a new member of the mammalian 70-kDa heat shock protein family, is a mitochondrial protein. *Molecular Biology of the Cell*, *5*(11), 1265–1275. https://doi.org/10.1091/mbc.5.11.1265

Dai, Y [Yi], Li, F., Jiao, Y [Yuwen], Wang, G [Guoguang], Zhan, T., Xia, Y., Liu, H [Hanyang], Yang, H., Zhang, J [Jianping], & Tang, L. (2021). Mortalin/glucose-regulated protein 75 promotes the cisplatin-resistance of gastric cancer via regulating anti-oxidation/apoptosis and metabolic reprogramming. *Cell Death Discovery*, *7*(1), 140. https://doi.org/10.1038/s41420-021-00517-w

Dai, Y [Ying], Zheng, K., Clark, J., Swerdlow, R. H., Pulst, S. M., Sutton, J. P., Shinobu, L. A., & Simon, D. K. (2014). Rapamycin drives selection against a pathogenic heteroplasmic mitochondrial DNA mutation. *Human Molecular Genetics*, *23*(3), 637–647. https://doi.org/10.1093/hmg/ddt450

Dasari, A., Shen, C., Halperin, D., Zhao, B., Zhou, S., Xu, Y., Shih, T., & Yao, J. C. (2017). Trends in the Incidence, Prevalence, and Survival Outcomes in Patients With Neuroendocrine Tumors in the United States. *JAMA Oncology*, *3*(10), 1335–1342. https://doi.org/10.1001/jamaoncol.2017.0589

DeGraffenried, L. A., Fulcher, L., Friedrichs, W. E., Grünwald, V., Ray, R. B., & Hidalgo, M. (2004). Reduced PTEN expression in breast cancer cells confers

susceptibility to inhibitors of the PI3 kinase/Akt pathway. *Annals of Oncology : Official Journal of the European Society for Medical Oncology*, *15*(10), 1510–1516. https://doi.org/10.1093/annonc/mdh388

Dennis, P. B., Pullen, N., Pearson, R. B., Kozma, S. C., & Thomas, G. (1998). Phosphorylation sites in the autoinhibitory domain participate in p70(s6k) activation loop phosphorylation. *The Journal of Biological Chemistry*, *273*(24), 14845–14852. https://doi.org/10.1074/jbc.273.24.14845

Dolly, S. O., Wagner, A. J., Bendell, J. C., Kindler, H. L., Krug, L. M., Seiwert, T. Y., Zauderer, M. G., Lolkema, M. P., Apt, D., Yeh, R.-F., Fredrickson, J. O., Spoerke, J. M., Koeppen, H., Ware, J. A., Lauchle, J. O., Burris, H. A., & Bono, J. S. de (2016). Phase I Study of Apitolisib (GDC-0980), Dual Phosphatidylinositol-3-Kinase and Mammalian Target of Rapamycin Kinase Inhibitor, in Patients with Advanced Solid Tumors. *Clinical Cancer Research : An Official Journal of the American Association for Cancer Research*, *22*(12), 2874–2884. https://doi.org/10.1158/1078-0432.CCR-15-2225

Dufner, A., & Thomas, G. (1999). Ribosomal S6 kinase signaling and the control of translation. *Experimental Cell Research*, *253*(1), 100–109. https://doi.org/10.1006/excr.1999.4683

Düvel, K., Yecies, J. L., Menon, S., Raman, P., Lipovsky, A. I., Souza, A. L., Triantafellow, E., Ma, Q., Gorski, R., Cleaver, S., Vander Heiden, M. G., MacKeigan, J. P., Finan, P. M., Clish, C. B., Murphy, L. O., & Manning, B. D. (2010). Activation of a metabolic gene regulatory network downstream of mTOR complex 1. *Molecular Cell*, *39*(2), 171–183. https://doi.org/10.1016/j.molcel.2010.06.022

Edinger, A. L., & Thompson, C. B. (2004). An activated mTOR mutant supports growth factor-independent, nutrient-dependent cell survival. *Oncogene*, *23*(33), 5654–5663. https://doi.org/10.1038/sj.onc.1207738

Elwakeel, A. (2022). Abrogating the Interaction Between p53 and Mortalin (Grp75/HSPA9/mtHsp70) for Cancer Therapy: The Story so far. *Frontiers in Cell and Developmental Biology*, *10*, 879632. https://doi.org/10.3389/fcell.2022.879632

Esfahanian, N., Knoblich, C. D., Bowman, G. A., & Rezvani, K. (2023). Mortalin: Protein partners, biological impacts, pathological roles, and therapeutic

opportunities. *Frontiers in Cell and Developmental Biology*, *11*, 1028519. https://doi.org/10.3389/fcell.2023.1028519

Exner, S., Arrey, G., Prasad, V., & Grötzinger, C. (2020). Mtor Inhibitors as Radiosensitizers in Neuroendocrine Neoplasms. *Frontiers in Oncology*, *10*, 578380. https://doi.org/10.3389/fonc.2020.578380

Feldman, M. E., & Shokat, K. M. (2010). New inhibitors of the PI3K-Akt-mTOR pathway: Insights into mTOR signaling from a new generation of Tor Kinase Domain Inhibitors (TORKinibs). *Current Topics in Microbiology and Immunology*, *347*, 241–262. https://doi.org/10.1007/82_2010_64

Ferreira-Silva, J., Meireles, S., Falconi, M., Fernandes, A., Vilas-Boas, F., Bispo, M., Rio-Tinto, R., & Rodrigues-Pinto, E. (2024). Portuguese Pancreatic Club Perspectives on Pancreatic Neuroendocrine Neoplasms: Diagnosis and Staging, Associated Genetic Syndromes and Particularities of Their Clinical Approach. *GE Portuguese Journal of Gastroenterology*, *31*(3), 153–164. https://doi.org/10.1159/000534641

Fu, W., & Hall, M. N. (2020). Regulation of mTORC2 Signaling. *Genes*, *11*(9). https://doi.org/10.3390/genes11091045

Fu, X., Li, K., Niu, Y., Lin, Q., Liang, H [Hongru], Luo, X., Liu, L., & Li, N. (2022). The mTOR/PGC-1α/SIRT3 Pathway Drives Reductive Glutamine Metabolism to Reduce Oxidative Stress Caused by ISKNV in CPB Cells. *Microbiology Spectrum*, *10*(1), e0231021. https://doi.org/10.1128/spectrum.02310-21

George, D. J., Halabi, S., Healy, P., Jonasch, D., Anand, M., Rasmussen, J., Wood, S. Y., Spritzer, C., Madden, J. F., & Armstrong, A. J. (2020). Phase 2 clinical trial of TORC1 inhibition with everolimus in men with metastatic castration-resistant prostate cancer. *Urologic Oncology*, *38*(3), 79.e15-79.e22. https://doi.org/10.1016/j.urolonc.2019.08.015

Gestl, E. E., & Anne Böttger, S. (2012). Cytoplasmic sequestration of the tumor suppressor p53 by a heat shock protein 70 family member, mortalin, in human colorectal adenocarcinoma cell lines. *Biochemical and Biophysical Research Communications*, *423*(2), 411–416. https://doi.org/10.1016/j.bbrc.2012.05.139

Gökmen-Polar, Y., Liu, Y [Yi], Toroni, R. A., Sanders, K. L., Mehta, R., Badve, S., Rommel, C., & Sledge, G. W. (2012). Investigational drug MLN0128, a novel TORC1/2 inhibitor, demonstrates potent oral antitumor activity in human

breast cancer xenograft models. *Breast Cancer Research and Treatment*, *136*(3), 673–682. https://doi.org/10.1007/s10549-012-2298-8

Goodwin, S., McPherson, J. D., & McCombie, W. R. (2016). Coming of age: Ten years of next-generation sequencing technologies. *Nature Reviews. Genetics*, *17*(6), 333–351. https://doi.org/10.1038/nrg.2016.49

Grabiner, B. C., Nardi, V., Birsoy, K., Possemato, R., Shen, K., Sinha, S., Jordan, A., Beck, A. H., & Sabatini, D. M. (2014). A diverse array of cancer-associated MTOR mutations are hyperactivating and can predict rapamycin sensitivity. *Cancer Discovery*, *4*(5), 554–563. https://doi.org/10.1158/2159-8290.CD-13-0929

Gravel, P. (2009). Protein Blotting by the Semidry Method. In J. M. Walker (Ed.), *Springer Protocols Handbooks. The Protein Protocols Handbook* (pp. 621–629). Humana Press. https://doi.org/10.1007/978-1-59745-198-7_59

Greenberg, J. A., Ivanov, N. A., Egan, C. E., Lee, Y. J., Zarnegar, R., Fahey, T. J., Finnerty, B. M., & Min, I. M. (2022). Sex-Based Clinicopathologic and Survival Differences Among Patients with Pancreatic Neuroendocrine Tumors. *Journal of Gastrointestinal Surgery : Official Journal of the Society for Surgery of the Alimentary Tract*, *26*(11), 2321–2329. https://doi.org/10.1007/s11605-022-05345-6

Guertin, D. A., Stevens, D. M., Thoreen, C. C., Burds, A. A., Kalaany, N. Y., Moffat, J., Brown, M., Fitzgerald, K. J., & Sabatini, D. M. (2006). Ablation in mice of the mTORC components raptor, rictor, or mLST8 reveals that mTORC2 is required for signaling to Akt-FOXO and PKCalpha, but not S6K1. *Developmental Cell*, *11*(6), 859–871. https://doi.org/10.1016/j.devcel.2006.10.007

Guichard, S. M., Curwen, J., Bihani, T., D'Cruz, C. M., Yates, J. W. T., Grondine, M., Howard, Z., Davies, B. R., Bigley, G., Klinowska, T., Pike, K. G., Pass, M., Chresta, C. M., Polanska, U. M., McEwen, R., Delpuech, O., Green, S., & Cosulich, S. C. (2015). Azd2014, an Inhibitor of mTORC1 and mTORC2, Is Highly Effective in ER+ Breast Cancer When Administered Using Intermittent or Continuous Schedules. *Molecular Cancer Therapeutics*, *14*(11), 2508–2518. https://doi.org/10.1158/1535-7163.MCT-15-0365

Guilmette, J. M., & Nosé, V. (2019). Neoplasms of the Neuroendocrine Pancreas: An Update in the Classification, Definition, and Molecular Genetic Advances.

Advances in Anatomic Pathology, *26*(1), 13–30. https://doi.org/10.1097/PAP.0000000000000201

Habbane, M., Montoya, J., Rhouda, T., Sbaoui, Y., Radallah, D., & Emperador, S. (2021). Human Mitochondrial DNA: Particularities and Diseases. *Biomedicines*, *9*(10). https://doi.org/10.3390/biomedicines9101364

Hanahan, D. (2022). Hallmarks of Cancer: New Dimensions. *Cancer Discovery*, *12*(1), 31–46. https://doi.org/10.1158/2159-8290.CD-21-1059

Hollebecque, A., Houédé, N., Cohen, E. E. W., Massard, C., Italiano, A., Westwood, P., Bumgardner, W., Miller, J., Brail, L. H., Benhadji, K. A., & Soria, J.-C. (2014). A phase Ib trial of LY2584702 tosylate, a p70 S6 inhibitor, in combination with erlotinib or everolimus in patients with solid tumours. *European Journal of Cancer (Oxford, England : 1990)*, *50*(5), 876–884. https://doi.org/10.1016/j.ejca.2013.12.006

Holz, M. K., Ballif, B. A., Gygi, S. P., & Blenis, J. (2021). Mtor and S6K1 mediate assembly of the translation preinitiation complex through dynamic protein interchange and ordered phosphorylation events. *Cell*, *184*(8), 2255. https://doi.org/10.1016/j.cell.2021.03.060

Houssaini, A., Breau, M., Kebe, K., Abid, S., Marcos, E., Lipskaia, L., Rideau, D., Parpaleix, A., Huang, J [Jin], Amsellem, V., Vienney, N., Validire, P., Maitre, B., Attwe, A., Lukas, C., Vindrieux, D., Boczkowski, J., Derumeaux, G., Pende, M., . . . Adnot, S. (2018). Mtor pathway activation drives lung cell senescence and emphysema. *JCI Insight*, *3*(3). https://doi.org/10.1172/jci.insight.93203

Hua, H., Kong, Q., Zhang, H [Hongying], Wang, J., Luo, T., & Jiang, Y [Yangfu] (2019). Targeting mTOR for cancer therapy. *Journal of Hematology & Oncology*, *12*(1), 71. https://doi.org/10.1186/s13045-019-0754-1

Illumina, Inc. (2017). *An introduction to Next-Generation Sequencing Technology*. illumina.com/content/dam/illumina-marketing/documents/products/illumina_sequencing_introduction.pdf

Inkscape Project. (2020). *Inkscape* (Version 1.3.2) [Computer software]. Inkscape Project. https://inkscape.org

Iwenofu, O. H., Lackman, R. D., Staddon, A. P., Goodwin, D. G., Haupt, H. M., & Brooks, J. S. J. (2008). Phospho-S6 ribosomal protein: A potential new predictive sarcoma marker for targeted mTOR therapy. *Modern Pathology :*

An Official Journal of the United States and Canadian Academy of Pathology, Inc, *21*(3), 231–237. https://doi.org/10.1038/modpathol.3800995

Jacinto, E., Facchinetti, V., Liu, D., Soto, N., Wei, S., Jung, S. Y., Huang, Q., Qin, J., & Su, B. (2006). Sin1/mip1 maintains rictor-mTOR complex integrity and regulates Akt phosphorylation and substrate specificity. *Cell*, *127*(1), 125–137. https://doi.org/10.1016/j.cell.2006.08.033

Jacinto, E., Loewith, R., Schmidt, A., Lin, S., Rüegg, M. A., Hall, A., & Hall, M. N. (2004). Mammalian TOR complex 2 controls the actin cytoskeleton and is rapamycin insensitive. *Nature Cell Biology*, *6*(11), 1122–1128. https://doi.org/10.1038/ncb1183

Javid, H., Hashemian, P., Yazdani, S., Sharbaf Mashhad, A., & Karimi-Shahri, M. (2022). The role of heat shock proteins in metastatic colorectal cancer: A review. *Journal of Cellular Biochemistry*, *123*(11), 1704–1735. https://doi.org/10.1002/jcb.30326

Jensen, R. T., Berna, M. J., Bingham, D. B., & Norton, J. A. (2008). Inherited pancreatic endocrine tumor syndromes: Advances in molecular pathogenesis, diagnosis, management, and controversies. *Cancer*, *113*(7 Suppl), 1807–1843. https://doi.org/10.1002/cncr.23648

Jiao, Y [Yuchen], Shi, C., Edil, B. H., Wilde, R. F. de, Klimstra, D. S., Maitra, A., Schulick, R. D., Tang, L. H., Wolfgang, C. L., Choti, M. A., Velculescu, V. E., Diaz, L. A., Vogelstein, B [Bert], Kinzler, K. W [Kenneth W.], Hruban, R. H [Ralph H.], & Papadopoulos, N. (2011). Daxx/atrx, MEN1, and mTOR pathway genes are frequently altered in pancreatic neuroendocrine tumors. *Science (New York, N.Y.)*, *331*(6021), 1199–1203. https://doi.org/10.1126/science.1200609

Jones, J. B., Song, J. J., Hempen, P. M., Parmigiani, G., Hruban, R. H [R. H.], & Kern, S. E. (2001). Detection of mitochondrial DNA mutations in pancreatic cancer offers a "mass"-ive advantage over detection of nuclear DNA mutations. *Cancer Research*, *61*(4), 1299–1304.

Ju, Y. S., Alexandrov, L. B., Gerstung, M., Martincorena, I., Nik-Zainal, S., Ramakrishna, M., Davies, H. R., Papaemmanuil, E., Gundem, G., Shlien, A., Bolli, N., Behjati, S., Tarpey, P. S., Nangalia, J., Massie, C. E., Butler, A. P., Teague, J. W., Vassiliou, G. S., Green, A. R., . . . Campbell, P. J. (2014).

Origins and functional consequences of somatic mitochondrial DNA mutations in human cancer. *ELife*, *3.* https://doi.org/10.7554/eLife.02935

Kang, S. A., Pacold, M. E., Cervantes, C. L., Lim, D., Lou, H. J., Ottina, K., Gray, N. S., Turk, B. E., Yaffe, M. B., & Sabatini, D. M. (2013). Mtorc1 phosphorylation sites encode their sensitivity to starvation and rapamycin. *Science (New York, N.Y.)*, *341*(6144), 1236566. https://doi.org/10.1126/science.1236566

Kaushal, S., Gupta, S., Shefrin, S., Vora, D. S., Kaul, S. C., Sundar, D., Wadhwa, R., & Dhanjal, J. K. (2024). Synthetic and Natural Inhibitors of Mortalin for Cancer Therapy. *Cancers*, *16*(20). https://doi.org/10.3390/cancers16203470

Kim, J., Kundu, M., Viollet, B., & Guan, K.-L. (2011). Ampk and mTOR regulate autophagy through direct phosphorylation of Ulk1. *Nature Cell Biology*, *13*(2), 132–141. https://doi.org/10.1038/ncb2152

Kim, Y. C., & Guan, K.-L. (2015). Mtor: A pharmacologic target for autophagy regulation. *The Journal of Clinical Investigation*, *125*(1), 25–32. https://doi.org/10.1172/JCI73939

Klöppel, G., Rindi, G., Perren, A., Komminoth, P., & Klimstra, D. S. (2010). The ENETS and AJCC/UICC TNM classifications of the neuroendocrine tumors of the gastrointestinal tract and the pancreas: A statement. *Virchows Archiv : An International Journal of Pathology*, *456*(6), 595–597. https://doi.org/10.1007/s00428-010-0924-6

Knoll, M., Macher-Goeppinger, S., Kopitz, J., Duensing, S., Pahernik, S., Hohenfellner, M., Schirmacher, P., & Roth, W. (2016). The ribosomal protein S6 in renal cell carcinoma: Functional relevance and potential as biomarker. *Oncotarget*, *7*(1), 418–432. https://doi.org/10.18632/oncotarget.6225

Kogelnik, A. M., Lott, M. T., Brown, M. D., Navathe, S. B., & Wallace, D. C [D. C.] (1996). Mitomap: A human mitochondrial genome database. *Nucleic Acids Research*, *24*(1), 177–179. https://doi.org/10.1093/nar/24.1.177

Kolberg, L., Raudvere, U., Kuzmin, I., Adler, P., Vilo, J., & Peterson, H. (2023). G:Profiler-interoperable web service for functional enrichment analysis and gene identifier mapping (2023 update). *Nucleic Acids Research*, *51*(W1), W207-W212. https://doi.org/10.1093/nar/gkad347

Komori, Y., Yada, K., Ohta, M., Uchida, H., Iwashita, Y., Fukuzawa, K., Kashima, K., Yokoyama, S., Inomata, M., & Kitano, S. (2014). Mammalian target of

rapamycin signaling activation patterns in pancreatic neuroendocrine tumors. *Journal of Hepato-Biliary-Pancreatic Sciences*, *21*(4), 288–295. https://doi.org/10.1002/jhbp.26

Koppenol, W. H., Bounds, P. L., & Dang, C. V. (2011). Otto Warburg's contributions to current concepts of cancer metabolism. *Nature Reviews. Cancer*, *11*(5), 325–337. https://doi.org/10.1038/nrc3038

Lamberti, G [G.], Ceccarelli, C., Brighi, N [N.], Maggio, I [I.], Santini, D., Mosconi, C., Ricci, C [C.], Biasco, G., & Campana, D [D.] (2017). Determination of Mammalian Target of Rapamycin Hyperactivation as Prognostic Factor in Well-Differentiated Neuroendocrine Tumors. *Gastroenterology Research and Practice*, *2017*, 7872519. https://doi.org/10.1155/2017/7872519

Lamberti, G [Giuseppe], Brighi, N [Nicole], Maggio, I [Ilaria], Manuzzi, L., Peterle, C., Ambrosini, V., Ricci, C [Claudio], Casadei, R., & Campana, D [Davide] (2018). The Role of mTOR in Neuroendocrine Tumors: Future Cornerstone of a Winning Strategy? *International Journal of Molecular Sciences*, *19*(3). https://doi.org/10.3390/ijms19030747

Lamberts, S. W. (1988). Somatostatin analogs in the management of gastrointestinal tumors. *Hormone Research*, *29*(2-3), 118–120. https://doi.org/10.1159/000180985

Laplante, M., & Sabatini, D. M. (2012). Mtor signaling in growth control and disease. *Cell*, *149*(2), 274–293. https://doi.org/10.1016/j.cell.2012.03.017

Larman, T. C., DePalma, S. R., Hadjipanayis, A. G., Protopopov, A., Zhang, J [Jianhua], Gabriel, S. B., Chin, L., Seidman, C. E., Kucherlapati, R., & Seidman, J. G. (2012). Spectrum of somatic mitochondrial mutations in five cancers. *Proceedings of the National Academy of Sciences of the United States of America*, *109*(35), 14087–14091. https://doi.org/10.1073/pnas.1211502109

Larsson, O., Morita, M., Topisirovic, I., Alain, T., Blouin, M.-J., Pollak, M., & Sonenberg, N. (2012). Distinct perturbation of the translatome by the antidiabetic drug metformin. *Proceedings of the National Academy of Sciences of the United States of America*, *109*(23), 8977–8982. https://doi.org/10.1073/pnas.1201689109

Lehnert, H. (Ed.). (2015). *Rationelle Diagnostik und Therapie in Endokrinologie, Diabetologie und Stoffwechsel* (4., vollst. überarb. und aktualisierte Aufl.). Thieme. https://doi.org/10.1055/b-003-104343

Liang, H [Huiyun], & Ward, W. F. (2006). Pgc-1alpha: A key regulator of energy metabolism. *Advances in Physiology Education*, *30*(4), 145–151. https://doi.org/10.1152/advan.00052.2006

Liberti, M. V., & Locasale, J. W. (2016). The Warburg Effect: How Does it Benefit Cancer Cells? *Trends in Biochemical Sciences*, *41*(3), 211–218. https://doi.org/10.1016/j.tibs.2015.12.001

Liu, G. Y., & Sabatini, D. M. (2020). Mtor at the nexus of nutrition, growth, ageing and disease. *Nature Reviews. Molecular Cell Biology*, *21*(4), 183–203. https://doi.org/10.1038/s41580-019-0199-y

Livak, K. J., & Schmittgen, T. D. (2001). Analysis of relative gene expression data using real-time quantitative PCR and the 2(-Delta Delta C(T)) Method. *Methods (San Diego, Calif.)*, *25*(4), 402–408. https://doi.org/10.1006/meth.2001.1262

Love, M. I., Huber, W., & Anders, S. (2014). Moderated estimation of fold change and dispersion for RNA-seq data with DESeq2. *Genome Biology*, *15*(12), 550. https://doi.org/10.1186/s13059-014-0550-8

Luley, K. B., Biedermann, S. B., Künstner, A., Busch, H., Franzenburg, S., Schrader, J., Grabowski, P., Wellner, U. F., Keck, T., Brabant, G., Schmid, S. M., Lehnert, H., & Ungefroren, H. (2020). A Comprehensive Molecular Characterization of the Pancreatic Neuroendocrine Tumor Cell Lines BON-1 and QGP-1. *Cancers*, *12*(3). https://doi.org/10.3390/cancers12030691

Ma, J., Kala, S., Yung, S., Chan, T. M., Cao, Y., Jiang, Y [Yifan], Liu, X [Xiaoxuan], Giorgio, S., Peng, L., & Wong, A. S. T. (2018). Blocking Stemness and Metastatic Properties of Ovarian Cancer Cells by Targeting p70S6K with Dendrimer Nanovector-Based siRNA Delivery. *Molecular Therapy : The Journal of the American Society of Gene Therapy*, *26*(1), 70–83. https://doi.org/10.1016/j.ymthe.2017.11.006

Maharjan, C. K., Ear, P. H., Tran, C. G., Howe, J. R., Chandrasekharan, C., & Quelle, D. E. (2021). Pancreatic Neuroendocrine Tumors: Molecular

Mechanisms and Therapeutic Targets. *Cancers*, *13*(20). https://doi.org/10.3390/cancers13205117

Malley, C. O., & Pidgeon, G. P. (2016). The mTOR pathway in obesity driven gastrointestinal cancers: Potential targets and clinical trials. *BBA Clinical*, *5*, 29–40. https://doi.org/10.1016/j.bbacli.2015.11.003

Maluchenko, A., Maksimov, D., Antysheva, Z., Krupinova, J., Avsievich, E., Glazova, O., Bodunova, N., Karnaukhov, N., Feidorov, I., Salimgereeva, D., Voloshin, M., & Volchkov, P. (2024). Molecular Basis of Pancreatic Neuroendocrine Tumors. *International Journal of Molecular Sciences*, *25*(20). https://doi.org/10.3390/ijms252011017

Manser, C. (2013). Erkrankungen des Pankreas. In M. Fried, M. P. Manns, G. Rogler, T. Luescher, & J. Steffel (Eds.), *Springer-Lehrbuch. Magen-Darm-Trakt* (pp. 73–89). Springer Berlin Heidelberg. https://doi.org/10.1007/978-3-642-29434-1_6

Martina, J. A., Chen, Y [Yong], Gucek, M., & Puertollano, R. (2012). Mtorc1 functions as a transcriptional regulator of autophagy by preventing nuclear transport of TFEB. *Autophagy*, *8*(6), 903–914. https://doi.org/10.4161/auto.19653

Martínez-Redondo, V., Pettersson, A. T., & Ruas, J. L. (2015). The hitchhiker's guide to PGC-1α isoform structure and biological functions. *Diabetologia*, *58*(9), 1969–1977. https://doi.org/10.1007/s00125-015-3671-z

Mastropasqua, F., Girolimetti, G., & Shoshan, M. (2018). Pgc1α: Friend or Foe in Cancer? *Genes*, *9*(1). https://doi.org/10.3390/genes9010048

McCallister, C., Siracusa, M. C., Shirazi, F., Chalkia, D., & Nikolaidis, N. (2015). Functional diversification and specialization of cytosolic 70-kDa heat shock proteins. *Scientific Reports*, *5*, 9363. https://doi.org/10.1038/srep09363

Megdanova-Chipeva, V. G., Lamarca, A., Backen, A., McNamara, M. G., Barriuso, J., Sergieva, S., Gocheva, L., Mansoor, W., Manoharan, P., & Valle, J. W. (2020). Systemic Treatment Selection for Patients with Advanced Pancreatic Neuroendocrine Tumours (PanNETs). *Cancers*, *12*(7). https://doi.org/10.3390/cancers12071988

Meyuhas, O. (2008). Physiological roles of ribosomal protein S6: One of its kind. *International Review of Cell and Molecular Biology*, *268*, 1–37. https://doi.org/10.1016/s1937-6448(08)00801-0

Meyuhas, O. (2015). Ribosomal Protein S6 Phosphorylation: Four Decades of Research. *International Review of Cell and Molecular Biology*, *320*, 41–73. https://doi.org/10.1016/bs.ircmb.2015.07.006

Mootha, V. K., Lindgren, C. M., Eriksson, K.-F., Subramanian, A., Sihag, S., Lehar, J., Puigserver, P., Carlsson, E., Ridderstråle, M., Laurila, E., Houstis, N., Daly, M. J., Patterson, N., Mesirov, J. P., Golub, T. R., Tamayo, P., Spiegelman, B., Lander, E. S., Hirschhorn, J. N., . . . Groop, L. C. (2003). Pgc-1alpha-responsive genes involved in oxidative phosphorylation are coordinately downregulated in human diabetes. *Nature Genetics*, *34*(3), 267–273. https://doi.org/10.1038/ng1180

Morita, M., Gravel, S.-P., Chénard, V., Sikström, K., Zheng, L., Alain, T., Gandin, V., Avizonis, D., Arguello, M., Zakaria, C., McLaughlan, S., Nouet, Y., Pause, A., Pollak, M., Gottlieb, E., Larsson, O., St-Pierre, J., Topisirovic, I., & Sonenberg, N. (2013). Mtorc1 controls mitochondrial activity and biogenesis through 4E-BP-dependent translational regulation. *Cell Metabolism*, *18*(5), 698–711. https://doi.org/10.1016/j.cmet.2013.10.001

Morita, M., Prudent, J., Basu, K., Goyon, V., Katsumura, S., Hulea, L., Pearl, D., Siddiqui, N., Strack, S., McGuirk, S., St-Pierre, J., Larsson, O., Topisirovic, I., Vali, H., McBride, H. M., Bergeron, J. J., & Sonenberg, N. (2017). Mtor Controls Mitochondrial Dynamics and Cell Survival via MTFP1. *Molecular Cell*, *67*(6), 922-935.e5. https://doi.org/10.1016/j.molcel.2017.08.013

Moro, L. (2021). Mitochondrial DNA and MitomiR Variations in Pancreatic Cancer: Potential Diagnostic and Prognostic Biomarkers. *International Journal of Molecular Sciences*, *22*(18), 9692. https://doi.org/10.3390/ijms22189692

Morrison Joly, M., Hicks, D. J., Jones, B., Sanchez, V., Estrada, M. V., Young, C., Williams, M., Rexer, B. N., Sarbassov, D. D [Dos D.], Muller, W. J., Brantley-Sieders, D., & Cook, R. S. (2016). Rictor/mtorc2 Drives Progression and Therapeutic Resistance of HER2-Amplified Breast Cancers. *Cancer Research*, *76*(16), 4752–4764. https://doi.org/10.1158/0008-5472.CAN-15-3393

Mortensen, D. S., Perrin-Ninkovic, S. M., Shevlin, G., Elsner, J., Zhao, J., Whitefield, B., Tehrani, L., Sapienza, J., Riggs, J. R., Parnes, J. S., Papa, P., Packard, G., Lee, B. G. S., Harris, R., Correa, M., Bahmanyar, S., Richardson, S. J., Peng, S. X., Leisten, J., . . . Sankar, S. (2015). Optimization

of a Series of Triazole Containing Mammalian Target of Rapamycin (mTOR) Kinase Inhibitors and the Discovery of CC-115. *Journal of Medicinal Chemistry*, *58*(14), 5599–5608. https://doi.org/10.1021/acs.jmedchem.5b00627

Neil, J., Shannon, C., Mohan, A., Laurent, D., Murali, R., & Jhanwar-Uniyal, M. (2016). Atp-site binding inhibitor effectively targets mTORC1 and mTORC2 complexes in glioblastoma. *International Journal of Oncology*, *48*(3), 1045–1052. https://doi.org/10.3892/ijo.2015.3311

Nicholls, T. J., & Minczuk, M. (2014). In D-loop: 40 years of mitochondrial 7S DNA. *Experimental Gerontology*, *56*, 175–181. https://doi.org/10.1016/j.exger.2014.03.027

Oronsky, B., Ma, P. C., Morgensztern, D., & Carter, C. A. (2017). Nothing But NET: A Review of Neuroendocrine Tumors and Carcinomas. *Neoplasia (New York, N.Y.)*, *19*(12), 991–1002. https://doi.org/10.1016/j.neo.2017.09.002

Osellame, L. D., Blacker, T. S., & Duchen, M. R. (2012). Cellular and molecular mechanisms of mitochondrial function. *Best Practice & Research. Clinical Endocrinology & Metabolism*, *26*(6), 711–723. https://doi.org/10.1016/j.beem.2012.05.003

Paniccia, A., Edil, B. H., & Schulick, R. D. (2015). Pancreatic Neuroendocrine Tumors: An Update. *The Indian Journal of Surgery*, *77*(5), 395–402. https://doi.org/10.1007/s12262-015-1360-2

Panwar, V., Singh, A., Bhatt, M., Tonk, R. K., Azizov, S., Raza, A. S., Sengupta, S [Shinjinee], Kumar, D., & Garg, M. (2023). Multifaceted role of mTOR (mammalian target of rapamycin) signaling pathway in human health and disease. *Signal Transduction and Targeted Therapy*, *8*(1), 375. https://doi.org/10.1038/s41392-023-01608-z

Patro, R., Duggal, G., Love, M. I., Irizarry, R. A., & Kingsford, C. (2017). Salmon provides fast and bias-aware quantification of transcript expression. *Nature Methods*, *14*(4), 417–419. https://doi.org/10.1038/nmeth.4197

PDQ Adult Treatment Editorial Board. (2024). *Pancreatic Neuroendocrine Tumors (Islet Cell Tumors) Treatment (PDQ®): Health Professional Version.* PDQ Cancer Information Summaries [Internet]. https://www.ncbi.nlm.nih.gov/books/NBK65870/

Peterson, T. R., Sengupta, S. S., Harris, T. E., Carmack, A. E., Kang, S. A., Balderas, E., Guertin, D. A., Madden, K. L., Carpenter, A. E., Finck, B. N., & Sabatini, D. M. (2011). Mtor complex 1 regulates lipin 1 localization to control the SREBP pathway. *Cell*, *146*(3), 408–420. https://doi.org/10.1016/j.cell.2011.06.034

Pilotto, S., Simbolo, M., Sperduti, I., Novello, S., Vicentini, C., Peretti, U., Pedron, S., Ferrara, R., Caccese, M., Milella, M., Mafficini, A., Visca, P., Volante, M., Facciolo, F., Santo, A., Carbognin, L., Brunelli, M., Chilosi, M., Scarpa, A., . . . Bria, E. (2017). OA06.06 Druggable Alterations Involving Crucial Carcinogenesis Pathways Drive the Prognosis of Squamous Cell Lung Carcinoma (SqCLC). *Journal of Thoracic Oncology*, *12*(1), S266-S267. https://doi.org/10.1016/j.jtho.2016.11.260

Polyak, K., Li, Y., Zhu, H., Lengauer, C., Willson, J. K., Markowitz, S. D., Trush, M. A., Kinzler, K. W [K. W.], & Vogelstein, B [B.] (1998). Somatic mutations of the mitochondrial genome in human colorectal tumours. *Nature Genetics*, *20*(3), 291–293. https://doi.org/10.1038/3108

Porstmann, T., Santos, C. R., Griffiths, B., Cully, M., Wu, M., Leevers, S., Griffiths, J. R., Chung, Y.-L., & Schulze, A. (2008). Srebp activity is regulated by mTORC1 and contributes to Akt-dependent cell growth. *Cell Metabolism*, *8*(3), 224–236. https://doi.org/10.1016/j.cmet.2008.07.007

Prior, I. A., Lewis, P. D., & Mattos, C. (2012). A comprehensive survey of Ras mutations in cancer. *Cancer Research*, *72*(10), 2457–2467. https://doi.org/10.1158/0008-5472.CAN-11-2612

Promega (Ed.). *Maxwell® Systeme: Produkte und Anwendungen für die Molekulare Diagnostik und Forschung*. https://www.promega.de/resources/guides/maxwell-brochure/

Qian, L., Zhu, Y [Yanli], Deng, C., Liang, Z., Chen, J [Junmin], Chen, Y [Ying], Wang, X., Liu, Y [Yanqing], Tian, Y., & Yang, Y. (2024). Peroxisome proliferator-activated receptor gamma coactivator-1 (PGC-1) family in physiological and pathophysiological process and diseases. *Signal Transduction and Targeted Therapy*, *9*(1), 50. https://doi.org/10.1038/s41392-024-01756-w

Qiao, L., Guo, Z., Liu, H [Haobiao], Liu, J [Jiaxin], Lin, X., Deng, H., Liu, X [Xuan], Zhao, Y., Xiao, X., Lei, J., & Han, J. (2022). Protective Effect of Mitophagy

Regulated by mTOR Signaling Pathway in Liver Fibrosis Associated with Selenium. *Nutrients*, *14*(12). https://doi.org/10.3390/nu14122410

R Core Team. (2021). *R: A Language and Environment for Statistical Computing.* (Version 4.3.0) [Computer software]. R Foundation for Statistical Computing. https://www.R-project.org

Radons, J. (2016). The human HSP70 family of chaperones: Where do we stand? *Cell Stress & Chaperones*, *21*(3), 379–404. https://doi.org/10.1007/s12192-016-0676-6

Rashid, M. M., Lee, H., & Jung, B. H. (2018). Metabolite identification and pharmacokinetic profiling of PP242, an ATP-competitive inhibitor of mTOR using ultra high-performance liquid chromatography and mass spectrometry. *Journal of Chromatography. B, Analytical Technologies in the Biomedical and Life Sciences*, *1072*, 244–251. https://doi.org/10.1016/j.jchromb.2017.11.027

Rindi, G., Mete, O., Uccella, S., Basturk, O., La Rosa, S., Brosens, L. A. A., Ezzat, S., Herder, W. W. de, Klimstra, D. S., Papotti, M., & Asa, S. L. (2022). Overview of the 2022 WHO Classification of Neuroendocrine Neoplasms. *Endocrine Pathology*, *33*(1), 115–154. https://doi.org/10.1007/s12022-022-09708-2

Ro, C., Chai, W., Yu, V. E., & Yu, R. (2013). Pancreatic neuroendocrine tumors: Biology, diagnosis,and treatment. *Chinese Journal of Cancer*, *32*(6), 312–324. https://doi.org/10.5732/cjc.012.10295

Rosario, F. J., Gupta, M. B., Myatt, L., Powell, T. L., Glenn, J. P., Cox, L., & Jansson, T. (2019). Mechanistic Target of Rapamycin Complex 1 Promotes the Expression of Genes Encoding Electron Transport Chain Proteins and Stimulates Oxidative Phosphorylation in Primary Human Trophoblast Cells by Regulating Mitochondrial Biogenesis. *Scientific Reports*, *9*(1), 246. https://doi.org/10.1038/s41598-018-36265-8

Rosario, F. J., Powell, T. L., Gupta, M. B., Cox, L., & Jansson, T. (2020). Mtorc1 Transcriptional Regulation of Ribosome Subunits, Protein Synthesis, and Molecular Transport in Primary Human Trophoblast Cells. *Frontiers in Cell and Developmental Biology*, *8*, 583801. https://doi.org/10.3389/fcell.2020.583801

Roskoski, R. (2022). Properties of FDA-approved small molecule protein kinase inhibitors: A 2022 update. *Pharmacological Research*, *175*, 106037. https://doi.org/10.1016/j.phrs.2021.106037

Roy, A., Kandettu, A., Ray, S., & Chakrabarty, S. (2022). Mitochondrial DNA replication and repair defects: Clinical phenotypes and therapeutic interventions. *Biochimica Et Biophysica Acta. Bioenergetics*, *1863*(5), 148554. https://doi.org/10.1016/j.bbabio.2022.148554

Ruvinsky, I., Sharon, N., Lerer, T., Cohen, H., Stolovich-Rain, M., Nir, T., Dor, Y., Zisman, P., & Meyuhas, O. (2005). Ribosomal protein S6 phosphorylation is a determinant of cell size and glucose homeostasis. *Genes & Development*, *19*(18), 2199–2211. https://doi.org/10.1101/gad.351605

Sabapathy, K., & Lane, D. P. (2019). Understanding p53 functions through p53 antibodies. *Journal of Molecular Cell Biology*, *11*(4), 317–329. https://doi.org/10.1093/jmcb/mjz010

Sarbassov, D. D [D. D.], Guertin, D. A., Ali, S. M., & Sabatini, D. M. (2005). Phosphorylation and regulation of Akt/PKB by the rictor-mTOR complex. *Science (New York, N.Y.)*, *307*(5712), 1098–1101. https://doi.org/10.1126/science.1106148

Sarbassov, D. D [Dos D.], Ali, S. M., Sengupta, S., Sheen, J.-H., Hsu, P. P., Bagley, A. F., Markhard, A. L., & Sabatini, D. M. (2006). Prolonged rapamycin treatment inhibits mTORC2 assembly and Akt/PKB. *Molecular Cell*, *22*(2), 159–168. https://doi.org/10.1016/j.molcel.2006.03.029

Sarkar, S., & Rubinsztein, D. C. (2008). Small molecule enhancers of autophagy for neurodegenerative diseases. *Molecular BioSystems*, *4*(9), 895–901. https://doi.org/10.1039/b804606a

Saxton, R. A., & Sabatini, D. M. (2017). Mtor Signaling in Growth, Metabolism, and Disease. *Cell*, *169*(2), 361–371. https://doi.org/10.1016/j.cell.2017.03.035

Scarpa, A., Chang, D. K., Nones, K., Corbo, V., Patch, A.-M., Bailey, P., Lawlor, R. T., Johns, A. L., Miller, D. K., Mafficini, A., Rusev, B., Scardoni, M., Antonello, D., Barbi, S., Sikora, K. O., Cingarlini, S., Vicentini, C., McKay, S., Quinn, M. C. J., . . . Grimmond, S. M. (2017). Whole-genome landscape of pancreatic neuroendocrine tumours. *Nature*, *543*(7643), 65–71. https://doi.org/10.1038/nature21063

Schenone, S., Brullo, C., Musumeci, F., Radi, M., & Botta, M. (2011). Atp-competitive inhibitors of mTOR: An update. *Current Medicinal Chemistry*, *18*(20), 2995–3014. https://doi.org/10.2174/092986711796391651

Schmitt, M., & Pawlita, M. (2009). High-throughput detection and multiplex identification of cell contaminations. *Nucleic Acids Research*, *37*(18), e119. https://doi.org/10.1093/nar/gkp581

Schon, E. A., DiMauro, S., & Hirano, M. (2012). Human mitochondrial DNA: Roles of inherited and somatic mutations. *Nature Reviews. Genetics*, *13*(12), 878–890. https://doi.org/10.1038/nrg3275

Schünke, M., Schulte, E., Schumacher, U., Voll, M., & Wesker, K. H. (2018). *PROMETHEUS Innere Organe*. Georg Thieme Verlag. https://doi.org/10.1055/b-006-149645

Scott, A. T., & Howe, J. R. (2019). Evaluation and Management of Neuroendocrine Tumors of the Pancreas. *The Surgical Clinics of North America*, *99*(4), 793–814. https://doi.org/10.1016/j.suc.2019.04.014

Sekulić, A., Hudson, C. C., Homme, J. L., Yin, P., Otterness, D. M., Karnitz, L. M., & Abraham, R. T. (2000). A direct linkage between the phosphoinositide 3-kinase-AKT signaling pathway and the mammalian target of rapamycin in mitogen-stimulated and transformed cells. *Cancer Research*, *60*(13), 3504–3513.

Shi, F., Zhang, J [Jinying], Liu, H [Hongyu], Wu, L., Jiang, H., Wu, Q [Qiyan], Liu, T., Lou, M., & Wu, H. (2018). The dual PI3K/mTOR inhibitor dactolisib elicits anti-tumor activity in vitro and in vivo. *Oncotarget*, *9*(1), 706–717. https://doi.org/10.18632/oncotarget.23091

Shokolenko, I., Venediktova, N., Bochkareva, A., Wilson, G. L., & Alexeyev, M. F. (2009). Oxidative stress induces degradation of mitochondrial DNA. *Nucleic Acids Research*, *37*(8), 2539–2548. https://doi.org/10.1093/nar/gkp100

Sidéris, L., Dubé, P., & Rinke, A. (2012). Antitumor effects of somatostatin analogs in neuroendocrine tumors. *The Oncologist*, *17*(6), 747–755. https://doi.org/10.1634/theoncologist.2011-0458

Smith, A. L. M., Whitehall, J. C., & Greaves, L. C. (2022). Mitochondrial DNA mutations in ageing and cancer. *Molecular Oncology*, *16*(18), 3276–3294. https://doi.org/10.1002/1878-0261.13291

Starenki, D [D.], Hong, S.-K., Lloyd, R. V., & Park, J.-I. (2015). Mortalin (GRP75/HSPA9) upregulation promotes survival and proliferation of medullary thyroid carcinoma cells. *Oncogene*, *34*(35), 4624–4634. https://doi.org/10.1038/onc.2014.392

Starenki, D [Dmytro], & Park, J. in (2015). Selective Mitochondrial Uptake of MKT-077 Can Suppress Medullary Thyroid Carcinoma Cell Survival In Vitro and In Vivo. *Endocrinology and Metabolism (Seoul, Korea)*, *30*(4), 593–603. https://doi.org/10.3803/EnM.2015.30.4.593

Stelzer, M. K., Pitot, H. C., Liem, A., Lee, D., Kennedy, G. D., & Lambert, P. F. (2010). Rapamycin inhibits anal carcinogenesis in two preclinical animal models. *Cancer Prevention Research (Philadelphia, Pa.)*, *3*(12), 1542–1551. https://doi.org/10.1158/1940-6207.CAPR-10-0228

Stensbøl, A. B., Krogh, J., Holmager, P., Klose, M., Oturai, P., Kjaer, A., Hansen, C. P., Federspiel, B., Langer, S. W., Knigge, U., & Andreassen, M. (2021). Incidence, Clinical Presentation and Trends in Indication for Diagnostic Work-Up of Small Intestinal and Pancreatic Neuroendocrine Tumors. *Diagnostics (Basel, Switzerland)*, *11*(11). https://doi.org/10.3390/diagnostics11112030

Stewart, J. B., Alaei-Mahabadi, B., Sabarinathan, R., Samuelsson, T., Gorodkin, J., Gustafsson, C. M., & Larsson, E. (2015). Simultaneous DNA and RNA Mapping of Somatic Mitochondrial Mutations across Diverse Human Cancers. *PLoS Genetics*, *11*(6), e1005333. https://doi.org/10.1371/journal.pgen.1005333

Storni, F., Trepp, R., Perren, A., Kollár, A., Gloor, B., & Kim-Fuchs, C. (2021). Neuroendokrine Tumore des Pankreas [Neuroendocrine tumor of the pancreas: What is new?]. *Therapeutische Umschau. Revue therapeutique*, *78*(10), 615–621. https://doi.org/10.1024/0040-5930/a001318

Subramanian, A., Tamayo, P., Mootha, V. K., Mukherjee, S., Ebert, B. L., Gillette, M. A., Paulovich, A., Pomeroy, S. L., Golub, T. R., Lander, E. S., & Mesirov, J. P. (2005). Gene set enrichment analysis: A knowledge-based approach for interpreting genome-wide expression profiles. *Proceedings of the National Academy of Sciences of the United States of America*, *102*(43), 15545–15550. https://doi.org/10.1073/pnas.0506580102

Summer, R., Shaghaghi, H., Schriner, D., Roque, W., Sales, D., Cuevas-Mora, K., Desai, V., Bhushan, A., Ramirez, M. I., & Romero, F. (2019). Activation of the mTORC1/PGC-1 axis promotes mitochondrial biogenesis and induces cellular senescence in the lung epithelium. *American Journal of Physiology. Lung Cellular and Molecular Physiology*, *316*(6), L1049-L1060. https://doi.org/10.1152/ajplung.00244.2018

Svatek, R. S., Ji, N., Leon, E. de, Mukherjee, N. Z., Kabra, A., Hurez, V., Nicolas, M., Michalek, J. E., Javors, M., Wheeler, K., Sharp, Z. D., Livi, C. B., Shu, Z.-J., Henkes, D., & Curiel, T. J. (2019). Rapamycin Prevents Surgery-Induced Immune Dysfunction in Patients with Bladder Cancer. *Cancer Immunology Research*, *7*(3), 466–475. https://doi.org/10.1158/2326-6066.CIR-18-0336

Thomanetz, V., Angliker, N., Cloëtta, D., Lustenberger, R. M., Schweighauser, M., Oliveri, F., Suzuki, N., & Rüegg, M. A. (2013). Ablation of the mTORC2 component rictor in brain or Purkinje cells affects size and neuron morphology. *The Journal of Cell Biology*, *201*(2), 293–308. https://doi.org/10.1083/jcb.201205030

Tian, T., Li, X., & Zhang, J [Jinhua] (2019). Mtor Signaling in Cancer and mTOR Inhibitors in Solid Tumor Targeting Therapy. *International Journal of Molecular Sciences*, *20*(3). https://doi.org/10.3390/ijms20030755

Tolcher, A., Goldman, J., Patnaik, A., Papadopoulos, K. P., Westwood, P., Kelly, C. S., Bumgardner, W., Sams, L., Geeganage, S., Wang, T., Capen, A. R., Huang, J [Jianping], Joseph, S., Miller, J., Benhadji, K. A., Brail, L. H., & Rosen, L. S. (2014). A phase I trial of LY2584702 tosylate, a p70 S6 kinase inhibitor, in patients with advanced solid tumours. *European Journal of Cancer (Oxford, England : 1990)*, *50*(5), 867–875. https://doi.org/10.1016/j.ejca.2013.11.039

Tondera, D., Czauderna, F., Paulick, K., Schwarzer, R., Kaufmann, J., & Santel, A. (2005). The mitochondrial protein MTP18 contributes to mitochondrial fission in mammalian cells. *Journal of Cell Science*, *118*(Pt 14), 3049–3059. https://doi.org/10.1242/jcs.02415

Trotta, A. P., & Chipuk, J. E. (2017). Mitochondrial dynamics as regulators of cancer biology. *Cellular and Molecular Life Sciences : CMLS*, *74*(11), 1999–2017. https://doi.org/10.1007/s00018-016-2451-3

Tsimberidou, A.-M., Shaw, J. V., Juric, D., Verschraegen, C., Weise, A. M., Sarantopoulos, J., Lopes, G., Nemunaitis, J., Mita, M., Park, H., Ellers-Lenz, B., Tian, H., Xiong, W., Kaleta, R., & Kurzrock, R. (2021). Phase 1 study of M2698, a p70S6K/AKT dual inhibitor, in patients with advanced cancer. *Journal of Hematology & Oncology*, *14*(1), 127. https://doi.org/10.1186/s13045-021-01132-z

Tsoli, M., Liu, J [Jie], Franshaw, L., Shen, H [Han], Cheng, C., Jung, M., Joshi, S., Ehteda, A., Khan, A., Montero-Carcabosso, A., Dilda, P. J., Hogg, P., & Ziegler, D. S. (2018). Dual targeting of mitochondrial function and mTOR pathway as a therapeutic strategy for diffuse intrinsic pontine glioma. *Oncotarget*, *9*(7), 7541–7556. https://doi.org/10.18632/oncotarget.24045

Untergasser, A., Cutcutache, I., Koressaar, T., Ye, J., Faircloth, B. C., Remm, M., & Rozen, S. G. (2012). Primer3--new capabilities and interfaces. *Nucleic Acids Research*, *40*(15), e115. https://doi.org/10.1093/nar/gks596

Vandamme, T., Peeters, M., Dogan, F., Pauwels, P., van Assche, E., Beyens, M., Mortier, G., Vandeweyer, G., Herder, W. de, van Camp, G., Hofland, L. J., & Beeck, K. op de (2015). Whole-exome characterization of pancreatic neuroendocrine tumor cell lines BON-1 and QGP-1. *Journal of Molecular Endocrinology*, *54*(2), 137–147. https://doi.org/10.1530/JME-14-0304

Varuzhanyan, G., Chen, C.-C., Freeland, J., He, T., Tran, W., Song, K., Wang, L [Liang], Cheng, D., Xu, S., Dibernardo, G. A., Esedebe, F. N., Bhatia, V., Han, M., Abt, E. R., Park, J. W., Memarzadeh, S., Shackelford, D. B., Lee, J. K., Graeber, T. G., . . . Witte, O. N. (2024). Pgc-1α drives small cell neuroendocrine cancer progression toward an ASCL1-expressing subtype with increased mitochondrial capacity. *Proceedings of the National Academy of Sciences of the United States of America*, *121*(49), e2416882121. https://doi.org/10.1073/pnas.2416882121

Villena, J. A. (2015). New insights into PGC-1 coactivators: Redefining their role in the regulation of mitochondrial function and beyond. *The FEBS Journal*, *282*(4), 647–672. https://doi.org/10.1111/febs.13175

Wallace, D. C [Douglas C.] (2012). Mitochondria and cancer. *Nature Reviews. Cancer*, *12*(10), 685–698. https://doi.org/10.1038/nrc3365

Wang, G [Guoyan], Zhang, J [Jun], Wu, S., Qin, S., Zheng, Y., Xia, C., Geng, H., Yao, J., & Deng, L. (2022). The mechanistic target of rapamycin complex 1

pathway involved in hepatic gluconeogenesis through peroxisome-proliferator-activated receptor γ coactivator-1α. *Animal Nutrition (Zhongguo Xu Mu Shou Yi Xue Hui)*, *11*, 121–131. https://doi.org/10.1016/j.aninu.2022.07.010

Wang, L [Lulu], Xu, X [Xueting], Jiang, C., Ma, G., Huang, Y., Zhang, H [Hui], Lai, Y., Wang, M., Ahmed, T., Lin, R., Guo, W., Luo, Z., Li, W [Wenjuan], Zhang, M [Meng], Ward, C., Qian, M., Liu, B., Esteban, M. A., & Qin, B. (2020). Mtorc1-PGC1 axis regulates mitochondrial remodeling during reprogramming. *The FEBS Journal*, *287*(1), 108–121. https://doi.org/10.1111/febs.15024

Wang, S., Cheng, F., Ji, Q., Song, M., Wu, Z., Zhang, Y [Yiyuan], Ji, Z., Feng, H., Belmonte, J. C. I., Zhou, Q., Qu, J., Li, W [Wei], Liu, G.-H., & Zhang, W. (2022). Hyperthermia differentially affects specific human stem cells and their differentiated derivatives. *Protein & Cell*, *13*(8), 615–622. https://doi.org/10.1007/s13238-021-00887-y

Warburg, O. (1924). ber den Stoffwechsel der Carcinomzelle. *Die Naturwissenschaften*, *12*(50), 1131–1137. https://doi.org/10.1007/BF01504608

Wispelaere, W. de, Annibali, D., Tuyaerts, S., Messiaen, J., Antoranz, A., Shankar, G., Dubroja, N., Herreros-Pomares, A., Baiden-Amissah, R. E. M., Orban, M.-P., Delfini, M., Berardi, E., van Brussel, T., Schepers, R., Philips, G., Boeckx, B., Baietti, M. F., Congedo, L., HoWangYin, K. Y., . . . Amant, F. (2024). Pi3k/mtor inhibition induces tumour microenvironment remodelling and sensitises pS6high uterine leiomyosarcoma to PD-1 blockade. *Clinical and Translational Medicine*, *14*(5), e1655. https://doi.org/10.1002/ctm2.1655

Wittekind, C. (Ed.). (2017). *TNM-Klassifikation maligner Tumoren* (Achte Auflage). Wiley-VCH Verlag GmbH & Co. KGaA; UICC global cancer control.

Yan, G., Yang, J., Li, W [Wen], Guo, A., Guan, J., & Liu, Y [Ying] (2023). Genome-wide CRISPR screens identify ILF3 as a mediator of mTORC1-dependent amino acid sensing. *Nature Cell Biology*, *25*(5), 754–764. https://doi.org/10.1038/s41556-023-01123-x

Yang, K. C., Kalloger, S. E., Aird, J. J., Lee, M. K. C., Rushton, C., Mungall, K. L., Mungall, A. J., Gao, D., Chow, C., Xu, J., Karasinska, J. M., Colborne, S., Jones, S. J. M., Schrader, J., Morin, R. D., Loree, J. M., Marra, M. A., Renouf, D. J., Morin, G. B., . . . Gorski, S. M. (2021). Proteotranscriptomic

classification and characterization of pancreatic neuroendocrine neoplasms. *Cell Reports*, *37*(2), 109817. https://doi.org/10.1016/j.celrep.2021.109817

Yao, J. C., Pavel, M., Lombard-Bohas, C., van Cutsem, E., Voi, M., Brandt, U., He, W., Chen, D., Capdevila, J., Vries, E. G. E. de, Tomassetti, P., Hobday, T., Pommier, R., & Öberg, K. (2016). Everolimus for the Treatment of Advanced Pancreatic Neuroendocrine Tumors: Overall Survival and Circulating Biomarkers From the Randomized, Phase III RADIANT-3 Study. *Journal of Clinical Oncology : Official Journal of the American Society of Clinical Oncology*, *34*(32), 3906–3913. https://doi.org/10.1200/JCO.2016.68.0702

Ye, J., Coulouris, G., Zaretskaya, I., Cutcutache, I., Rozen, S., & Madden, T. L. (2012). Primer-BLAST: A tool to design target-specific primers for polymerase chain reaction. *BMC Bioinformatics*, *13*, 134. https://doi.org/10.1186/1471-2105-13-134

Yeung, Y., Lau, D. K., Chionh, F., Tran, H., Tse, J. W. T., Weickhardt, A. J., Nikfarjam, M., Scott, A. M., Tebbutt, N. C., & Mariadason, J. M. (2017). K-Ras mutation and amplification status is predictive of resistance and high basal pAKT is predictive of sensitivity to everolimus in biliary tract cancer cell lines. *Molecular Oncology*, *11*(9), 1130–1142. https://doi.org/10.1002/1878-0261.12078

Yi, Y. W., You, K. S., Park, J.-S., Lee, S.-G., & Seong, Y.-S. (2021). Ribosomal Protein S6: A Potential Therapeutic Target against Cancer? *International Journal of Molecular Sciences*, *23*(1). https://doi.org/10.3390/ijms23010048

Yoon, A.-R., Wadhwa, R., Kaul, S. C., & Yun, C.-O. (2022). Why is Mortalin a Potential Therapeutic Target for Cancer? *Frontiers in Cell and Developmental Biology*, *10*, 914540. https://doi.org/10.3389/fcell.2022.914540

Zhang, M [Minghao], Gu, L., Zheng, P., Chen, Z., Dou, X., Qin, Q., & Cai, X. (2020). Improvement of cell counting method for Neubauer counting chamber. *Journal of Clinical Laboratory Analysis*, *34*(1), e23024. https://doi.org/10.1002/jcla.23024

Zhang, R., Meng, Z., Wu, X., Zhang, M [Meihua], Zhang, S., & Jin, T. (2021). Mortalin promotes breast cancer malignancy. *Experimental and Molecular Pathology*, *118*, 104593. https://doi.org/10.1016/j.yexmp.2020.104593

Zhu, Y [Yuanchang], Wang, F., Ma, Z., Hou, S., Deng, W., Zhang, Y [Yaou], & Wu, Q [Qiongfang] (2024). Anti-proliferation and apoptosis induced via the mTOR/PGC-1α signaling pathway in trophoblast cells of miscarriage. *Experimental Cell Research*, *436*(2), 113959. https://doi.org/10.1016/j.yexcr.2024.113959

Zoncu, R., Efeyan, A., & Sabatini, D. M. (2011). Mtor: From growth signal integration to cancer, diabetes and ageing. *Nature Reviews. Molecular Cell Biology*, *12*(1), 21–35. https://doi.org/10.1038/nrm3025

Supplementary

```
#Gennamen anpassen
rna <- read.csv(file.choose(),header=TRUE,sep=";")
rna <- data.frame(rna, row.names = 1)
rna <- tibble::rownames_to_column(rna, "VALUE")
rna$VALUE <- gsub(":chr.*", "",rna$VALUE)
rna$VALUE <- gsub(".*\\:", "",rna$VALUE)
rna <- rna[!duplicated(rna[c("VALUE")]),]
rna <- data.frame(rna, row.names = 1)

#Import Counts
rawCounts <- read.csv(file.choose(),header=TRUE,sep=";")
head(rawCounts)
geneID <- rawCounts$Gene.ID
rawCounts <- data.frame(rawCounts, row.names = 1)
head(rawCounts)

#Import Sample Information
sampleData <- read.csv(file.choose(),header=TRUE,sep=";")
head(sampleData)
sampleData <- data.frame(sampleData, row.names = 1)

#Vorbereitung Matrix
sampleIndex <- grepl("H\\d+", colnames(rawCounts))+ grepl("SS\\d+", colnames(rawCounts))
rownames(rawCounts) <- geneID
rawCounts <- rawCounts[,unique(rownames(sampleData))]
all(colnames(rawCounts) == rownames(sampleData))
deseq2Data <- DESeqDataSetFromMatrix(countData = rawCounts, colData = sampleData, design = ~condition)
dim(deseq2Data)
dim(deseq2Data[rowSums(counts(deseq2Data)) > 5, ])
library(BiocParallel)
register(SnowParam(4))
deseq2Data <- DESeq(deseq2Data)

#Vergleich Expression active vs inactive
deseq2Results <- results(deseq2Data, contrast = c("condition", "active", "inactive"))
View(deseq2Results)
deseq2Results_save <- deseq2Results
deseq2Results <- results(deseq2Data, contrast = c("condition", "active", "inactive"))
summary(deseq2Results)

#Daten speichern
write.csv(deseq2Results, "deseq2Results.NET.csv")

#Extraktion normalized counts von DESeq2
norm_counts <- counts(deseq2Data, normalized = T)

#Speichern normalized counts
write.csv(norm_counts, "norm_counts.NET.activity.csv")
```

Figure S 1: Bioinformatic code for differentially expression analysis of RNA-sequencing data. The expression analysis was performed using the DESeq2 package in R.

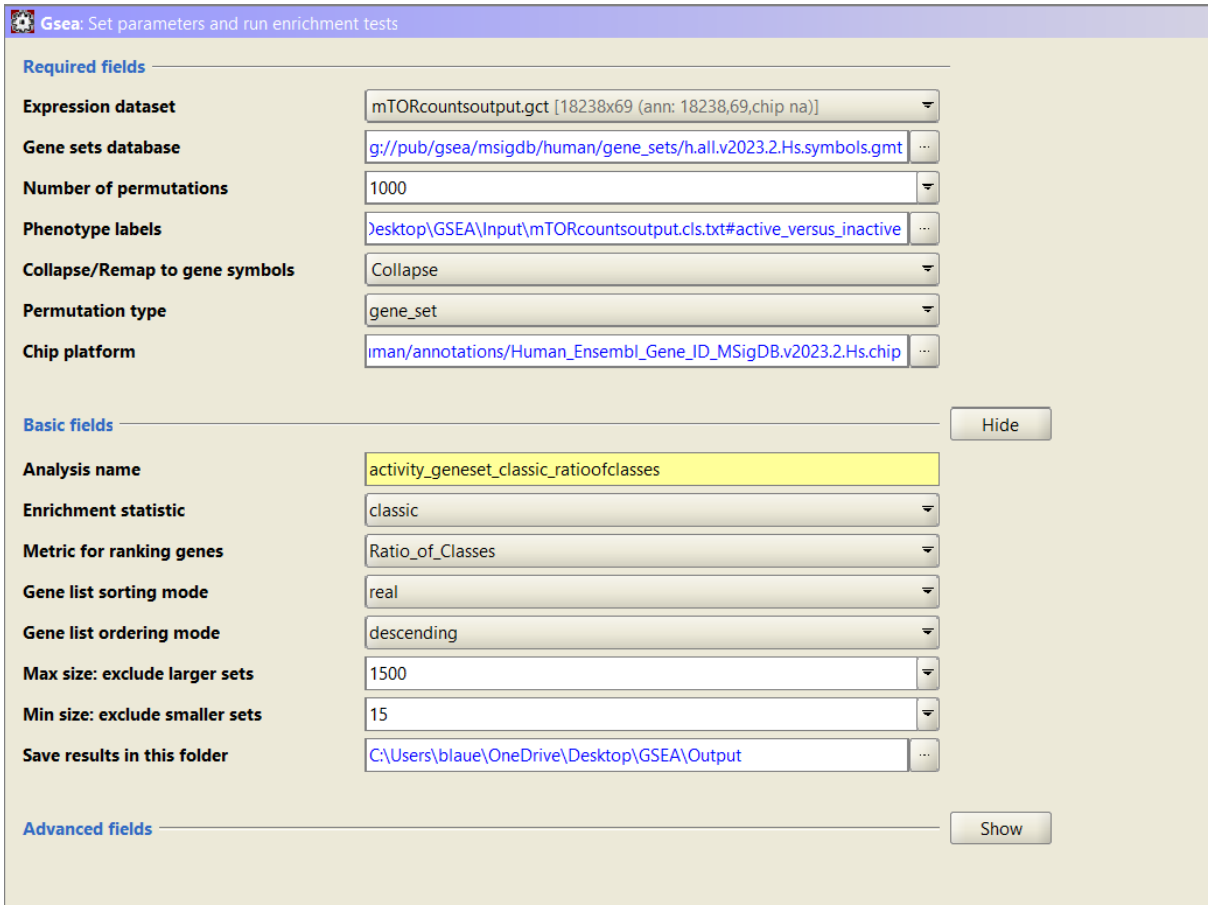

Figure S 2: System settings for GSEA.

The analysis was performed using the GSEA software provided by Broad Institutes.

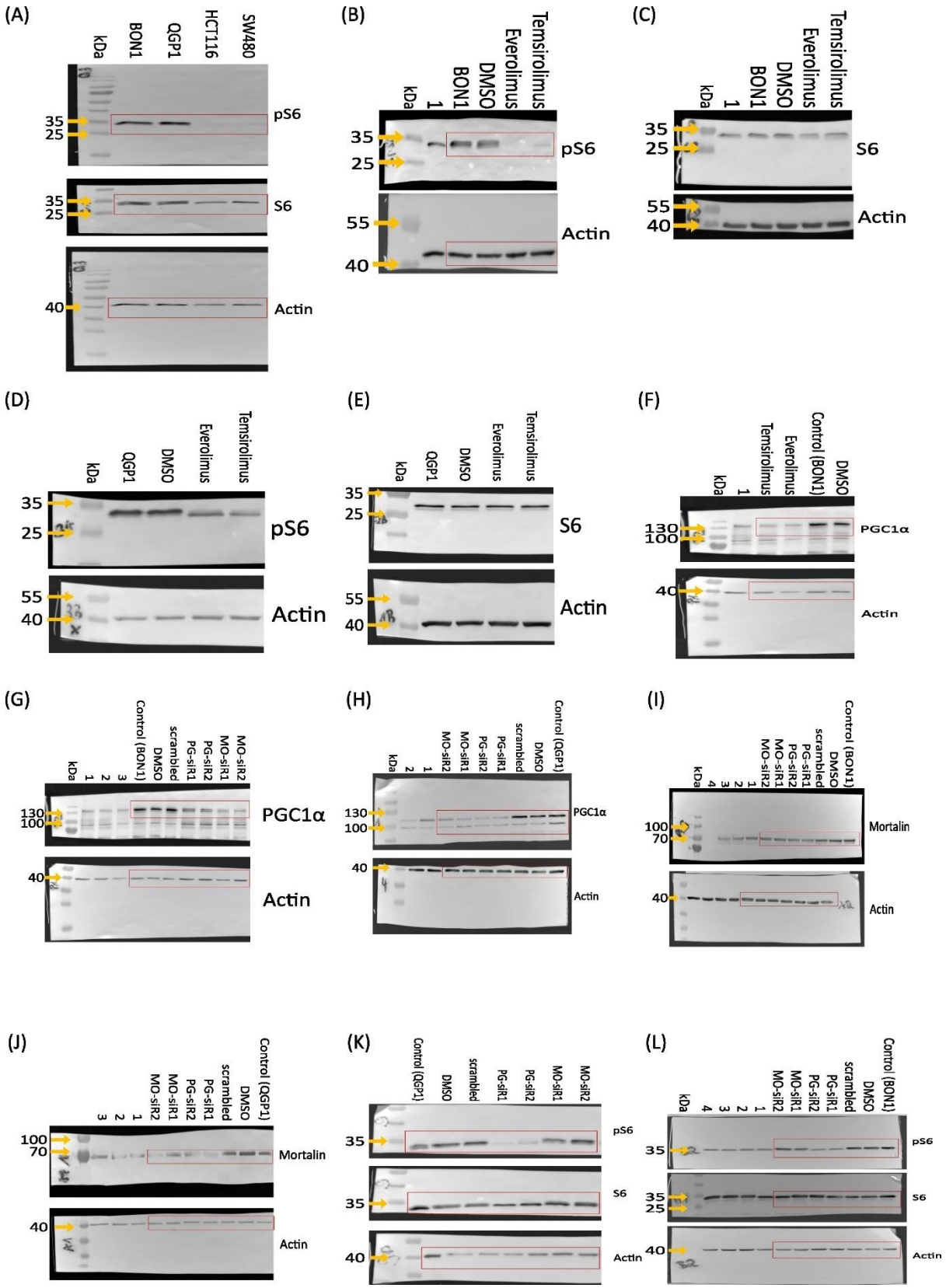

Figure S 3: Original, non-cleaved Western Blot images.

The red boxes indicate the regions of the original blots used for the main figures. A) The image shows the original Western Blot for the detection of pS6 in the main figure 15A. Due to secondary antibodies

from different host species, pS6 (rabbit) and S6 (mouse) could be detected on the same membrane without any signal interferences. Due to secondary antibodies from different host species and different molecular weights, pS6 (rabbit, 35 kDa) and Actin (mouse, 40 kDa) could be detected on the same membrane without any signal interferences. B) The image shows the original Western Blot for the detection of pS6 in the main figure 15B. The sample 1 was excluded from the main figure. C) The image shows the original Western Blot for the detection of S6 in the main figure 15C. The sample 1 was excluded from the main figure. D) The image shows the original Western Blot for the detection of pS6 in the main figure 15D. E) The image shows the original Western Blot for the detection of S6 in the main figure 15E. F) The image shows the original Western Blot for the detection of PGC1α in the main figure 17B. The sample 1 was excluded from the main figure. For a better understanding, the Western Blot image has been mirrored in the main figure. G) The image shows the original Western Blot for the detection of PGC1α (BON1 cell line) in the main figure 17C. The samples 1 - 3 were excluded from the main figure. The shown blot is the same blot as in F, but other samples of the blot are focused. H) The image shows the original Western Blot for the detection of PGC1α (QGP1 cell line) in the main figure 17C. The samples 1 and 2 were excluded from the main figure. For a better understanding, the Western Blot image has been mirrored in the main figure. I) The image shows the original Western Blot for the detection of Mortalin (BON1 cell line) in the main figure 17D. The samples 1 - 4 were excluded from the main figure. For a better understanding, the Western Blot image has been mirrored in the main figure. J) The image shows the original Western Blot for the detection of Mortalin (QGP1 cell line) in the main figure 17D. The samples 1 - 3 were excluded from the main figure. For a better understanding, the Western Blot image has been mirrored in the main figure. K) The image shows the original Western Blot for the detection of pS6 in the main figure 19A. Due to secondary antibodies from different host species, pS6 (rabbit) and S6 (mouse) could be detected on the same membrane without any signal interferences. Due to secondary antibodies from different host species and different molecular weights, pS6 (rabbit, 35 kDa) and Actin (mouse, 40 kDa) could be detected on the same membrane without any signal interferences. L) The image shows the original Western Blot for the detection of pS6 in the main figure 19B. Due to secondary antibodies from different host species, pS6 (rabbit) and S6 (mouse) could be detected on the same membrane without any signal interferences. Due to secondary antibodies from different host species and different molecular weights, pS6 (rabbit, 35 kDa) and Actin (mouse, 40 kDa) could be detected on the same membrane without any signal interferences.

Table S 1: List of all mtDNA mutations detected in the panNET collective.

All cases with activated mTOR pathway are marked in grey.

ID	Lokus	Position on the mtDNA	Amino acid change	Reference	Detected	Impact	Frequency	Coding region change
2	16S RNA	2553	SNV	G	A		28,24	m.2553G>A RNR2
4	16S RNA	3107	del	N	-		98,58	m.3107delN RNR2
5	D-Loop	310^318	del	TCCCCCGCT	-		10,16	m.310^318delTCCCCCGCT
	16S RNA	2053	SNV	T	C		41,10	m.2053T>C RNR2
	mtND5	13958	SNV	G	A	non-synonymous	21,58	m.13958G>A mtND5
22	16S RNA	3107	del	N	-		99,10	m.3107delN RNR2
25	16S RNA	3107	del	N	-		98,90	m.3107delN RNR2
27								
32	12S RNA	1447	SNV	G	A		12,61	m.1447G>A RNR1
	16S RNA	3107	del	N	-		98,44	m.3107delN RNR2
	mtND1	3918	SNV	G	C	non-synonymous	14,63	m.3918G>C mtND1
	mtND1	4238	SNV	T	G	non-synonymous	10,09	m.4238T>G mtND1
37	D-Loop	309^316	del	CTCCCCCG	-		44,18	m.309^316delCTCCCCCG
44								
46								
51	COXI	6004	SNV	G	C	non-synonymous	40,47	m.6004G>C COXI
56								
61	16S RNA	3107	del	N	-		98,85	m.3107delN RNR2
64	COXI	5917	SNV	G	A	non-synonymous	83,89	m.5917G>A COXI
68								
81								
96								
154	16S RNA	2492	SNV	G	A		86,49	m.2492G>A RNR2
	16S RNA	2926	SNV	A	G		90,84	m.2926A>G RNR2
	16S RNA	3107	del	N	-		98,53	m.3107delN RNR2
	mtND5	13171	SNV	T	C	non-synonymous	92,12	m.13171T>C mtND5
161	mtND	4768^4769	MNV	TA	CG	non-	15,71	m.4768^4769

	2					synonymous		mtND2
165								
167								
179								
182								
13								
84								
10	D-Loop	432^433	ins	-	C	synonymous	57,20	m.432^433insC (s)
	16S RNA	3107	del	N	-		98,85	m.3107delN RNR2
12	COX3	9478	del	T	-	non-synonymous	97,30	m.9478delT COXIII
20								
15								
26								
28	mtND4	10972	SNV	A	T	non-synonymous	44,99	m.10972A>T mtND4
29	mtND1	3418	SNV	A	T	non-synonymous	15,79	m.3418A>T mtND1
31	mtND2	4905	SNV	T	C	non-synonymous	94,6	m.4905T>C mtND2
	mtND2	5221	SNV	T	C	non-synonymous	23,56	m.5221T>C mtND2
35								
36	COXI	7342^7343	ins	-	A	non-synonymous	35,74	m.7342^7343insA COXI
38								
39								
40								
41								
45								
47	mtND4	11693	SNV	G	A	non-synonymous	93,64	m.11693G>A mtND4
48	D-Loop	310	Replacement	T	CCTC		63,07	m.310T>CCTC
50								
55	D-Loop	451^452	ins	-	T		95,8	m.451^452insT
59		1975	SNV	T	C		59,22	m.1975T>C
14								
62	12S RNA	879	SNV	T	T		96,97	m.879T>T RNR1
	16S RNA	2099	SNV	T	T		97,89	m.2099T>T RNR2
	16S RNA	2457	SNV	A	A		98,62	m.2457A>A RNR2
	COXI	6379^6380	MNV	TA	TA	synonymous	90,92	m.6379^6380TA>TA COXI
	COXI	6409^6410	MNV	TC	TC	synonymous	90,05	m.6409^6410TC>TC COXI

	ND4	10880	SNV	T	T	synonymous	97,85	m.10880T>T mtND4
	ND4	10983	SNV	T	T	synonymous	93,04	m.10983T>T mtND4
	tRNA Leu	12271	SNV	T	T		97,34	m.12271T>T tRNA Leu
	mtND 5	12417^12418	ins	-	-	synonymous	99,49	m.12417^12418ins
	mtND 5	13231	SNV	A	A	synonymous	98,7	m.13231A>A mtND5
21	mtND 4	11274	SNV	G	A	non-synonymous	82,36	m.11274G>A mtND4
63								
65	D-Loop	310	Rep	T	CCTC		53,92	m.310T>CCTC
70	mtND 2	4867	SNV	G	A	non-synonymous	82,65	m.4867G>A mtND2
82	12S RNA	1082	SNV	A	G		23,28	m.1082A>G RNR1
115	12S RNA	1202	SNV	G	A		86,34	m.1202G>ARNR1
	16S RNA	3107	del	N	-		98,82	m.3107delN RNR2
122								
135								
136								
138								
139								
141								
142	16S RNA	3107	del	N	-		97,73	m.3107delN RNR2
143								
146	16S RNA	3107	del	N	-		99,17	m.3107delN RNR2
147	tRNA Leu	12283	SNV	G	T		10,52	m.12283G>T tRNA Leu
153								
158	16S RNA	3107	del	N	-		99,13	m.3107delN RNR2
163								
164	16S RNA	3075	SNV	G	A		47,46	m.3075G>A RNR2
173								
174	16S RNA	3107	del	N	-		99,03	m.3107delN RNR2
	CYB	15366	SNV	A	G	non-synonymous	29,64	m.15366A>G CYB
175								
176	16S RNA	3107	Deletion	N	-		98,74	m.3107delN RNR2
	COXII	8143^8144	MNV	TA	AC	non-synonymous	12	m.8143^8144TA>AC COXII

180								
181	mtND 5	12979	SNV	G	A	non-synonymous	21,77	m.12979G>A mtND5
183								
184								
185								
187								
188								
189	mtND 1	3667	SNV	T	C	non-synonymous	56,13	m.3667T>C mtND1
190								
9	12S RNA	1129	SNV	T	C		85	m.1129T>C RNR1
18	tRNA Glu	14741	SNV	A	G		65	m.1447G>A RNR1
17								

del: Deletion; ins: Insertion; SNV: Single nucleotide variant; MNV: Multi-nucleotide variant, Rep: Replacement

Table S 2: Gene sets enriched in panNET with high mTOR pathway activity.

Enrichment score (ES) reflects the degree to which a gene set is overrepresented at the top or bottom of a ranked list of genes. Normalized enrichment score (NES) represents enrichment score normalized across analyzed gene sets. Statistical significance is calculated by nominal p-value of the ES using an empirical phenotype-based permutation test. Gene sets from the MSigDB database were tested and gene sets with a false discovery rate (FDR) <0.25 and nominal p-value <0.01 were considered significantly enriched in a prior defined set of genes. A nominal p-value of 0.000 stands for an actual p-value of less than 1/number-of-permutations (in this work: 1/1000 = 0.001).

Name of gene set	ES	NES	NOM p-val	FDR q-val
HALLMARK_MTORC1_SIGNALING	0.16	2.62	0.000	0.002
HALLMARK_KRAS_SIGNALING	0.14	2.17	0.000	0.008
HALLMARK_BILE_ACID_METABOLISM	0.12	1.54	0.046	0.148
HALLMARK_UV_RESPONSE_DN	-0.23	-3.16	0.0000	0.0000
HALLMARK_OXIDATIVE_PHOSPHORYLATION	-0.19	-3.08	0.0000	0.0000
HALLMARK_MYC_TARGETS_V1	-0.16	-2.58	0.0029	0.0050
HALLMARK_EPITHELIAL_MESENCHYMAL_TRANSITION	-0.15	-2.44	0.0057	0.0130
HALLMARK_ANGIOGENESIS	-0.34	-2.40	0.0049	0.0140
HALLMARK_UV_RESPONSE_UP	-0.17	-2.39	0.0043	0.0150
HALLMARK_UNFOLDED_PROTEIN_RESPONSE	-0.19	-2.27	0.0068	0.0270
HALLMARK_FATTY_ACID_METABOLISM	-0.14	-2.08	0.0175	0.0810
HALLMARK_P53_PATHWAY	-0.13	-2.05	0.0169	0.0890
HALLMARK_ANDROGEN_RESPONSE	-0.18	-2.02	0.0172	0.1020
HALLMARK_APOPTOSIS	-0.13	-1.95	0.0235	0.1430
HALLMARK_APICAL_JUNCTION	-0.12	-1.93	0.0247	0.1620
HALLMARK_PROTEIN_SECRETION	-0.17	-1.91	0.0269	0.1870

HALLMARK_MITOTIC_SPINDLE	-0.11	-1.82	0.0414	0.2950
HALLMARK_G2M_CHECKPOINT	-0.11	-1.81	0.0402	0.3030
HALLMARK_ESTROGEN_RESPONSE_EARLY	-0.11	-1.79	0.0417	0.3330
HALLMARK_COMPLEMENT	-0.11	-1.74	0.0522	0.4090
HALLMARK_HEME_METABOLISM	-0.11	-1.73	0.0508	0.4190

Table S 3: List of genes that are differentially regulated between panNET with high mTOR pathway activity and panNET without activation.

The genes were determined using the DESeq2 package. All genes with Benjamin Hochberg adjusted p-value (padj) < 0.05 were included. The data are represented as Wald-statistic (stat). Genes with negative Wald-statistic values are down-regulated in panNET with high mTOR pathway activity compared to panNET without activation and genes with positive values are upregulated.

$$\text{Wald} - \text{statistic} = \frac{\text{log2FoldChange}}{\text{standard error of log2FoldChange}}$$

Ensembl_ ID	Gene_ symbol	Stat_active_ inactive	padj_active_ inactive
ENSG00000104872	PIH1D1	-6,07	8,08E-06
ENSG00000138207	RBP4	-5,8	3,24E-05
ENSG00000133636	NTS	-5,05	1,74E-03
ENSG00000111319	SCNN1A	-4,6	9,28E-03
ENSG00000162630	B3GALT2	-4,21	3,48E-02
ENSG00000181617	FDCSP	-4,19	3,52E-02
ENSG00000135346	CGA	-4,14	3,52E-02
ENSG00000198203	SULT1C2	-4,14	3,52E-02
ENSG00000189320	FAM188A	-4,11	3,52E-02
ENSG00000119048	UBE2B	-4,11	3,52E-02
ENSG00000121621	KIF18A	-4,09	3,52E-02
ENSG00000178607	ERN1	-4,01	4,46E-02
ENSG00000066455	GOLGA5	-4,01	4,46E-02
ENSG00000165409	TSHR	-3,96	4,94E-02

Ensembl_ ID	Gene_ symbol	Stat_active_ inactive	padj_active_ inactive
ENSG00000113013	MORTALIN	3,97	4,84E-02
ENSG00000067365	METTL22	3,98	4,73E-02
ENSG00000099797	TECR	4,01	4,46E-02
ENSG00000130822	PNCK	4,1	3,52E-02
ENSG00000130255	RPL36	4,1	3,52E-02
ENSG00000291029	FKBP9L	4,13	3,52E-02
ENSG00000145506	NKD2	4,3	2,58E-02
ENSG00000120053	GOT1	4,38	1,93E-02
ENSG00000130649	CYP2E1	4,4	1,92E-02
ENSG00000127863	TNFRSF19	4,42	1,92E-02
ENSG00000160349	LCN1	4,94	2,60E-03
ENSG00000109819	PPARGC1A	7,16	1,60E-08

Table S 4: List of genes that are differentially regulated between high grade (G2/G3) panNET with high mTOR pathway activity and low grade (G1) panNET with high mTOR pathway activity.

The genes were determined using the DESeq2 package. All genes with Benjamin Hochberg adjusted p-value (padj) < 0.05 were included. The data are represented as Wald-statistic (stat). Genes with negative Wald-statistic values are down-regulated in high grade (G2/G3) panNET with high mTOR pathway activity compared to low grade (G1) panNET with high mTOR pathway activity.

$$\text{Wald} - \text{statistic} = \frac{\text{log2FoldChange}}{\text{standard error of log2FoldChange}}$$

Ensembl_ ID	Gene_ symbol	Stat_active_inactive	padj_active_inactive
ENSG00000120899	PTK2B	-4,408	0,002
ENSG00000136143	SUCLA2	-4,249	0,003
ENSG00000121988	ZRANB3	-4,221	0,003
ENSG00000205078	SYCE1L	-4,018	0,008
ENSG00000189013	KIR2DL4	-3,966	0,009
ENSG00000143156	NME7	-3,837	0,014
ENSG00000170619	COMMD5	-3,834	0,014
ENSG00000180440	SERTM1	-3,768	0,017
ENSG00000147133	TAF1	-3,604	0,028
ENSG00000143479	DYRK3	-3,567	0,032
ENSG00000126878	AIF1L	-3,559	0,032
ENSG00000276581	SPATA31A5	-3,541	0,033
ENSG00000133961	NUMB	-3,521	0,035
ENSG00000236901	MIR600HG	-3,448	0,043
ENSG00000147649	MTDH	-3,446	0,043
ENSG00000106636	YKT6	-3,443	0,043
ENSG00000115592	PRKAG3	-3,44	0,043
ENSG00000161973	CCDC42	-3,435	0,044
ENSG00000204410	MSH5	-3,426	0,045
ENSG00000171496	OR1L8	-3,405	0,047

Ensembl_ ID	Gene_ symbol	Stat_active_inactive	padj_active_inactive
ENSG00000111203	ITFG2	3,392	0,048
ENSG00000109063	MYH3	3,394	0,048
ENSG00000177853	ZNF518A	3,397	0,048
ENSG00000126010	GRPR	3,403	0,047
ENSG00000076706	MCAM	3,41	0,046
ENSG00000181616	OR52H1	3,41	0,046
ENSG00000137880	GCHFR	3,413	0,046
ENSG00000067606	PRKCZ	3,416	0,046
ENSG00000138777	PPA2	3,418	0,046
ENSG00000204314	PRRT1	3,424	0,045
ENSG00000221859	KRTAP10-10	3,431	0,044
ENSG00000008838	MED24	3,434	0,044
ENSG00000198105	ZNF248	3,463	0,041
ENSG00000105127	AKAP8	3,465	0,040
ENSG00000117016	RIMS3	3,465	0,040
ENSG00000070985	TRPM5	3,475	0,039
ENSG00000104946	TBC1D17	3,477	0,039
ENSG00000136514	RTP4	3,485	0,038
ENSG00000184840	TMED9	3,495	0,037
ENSG00000288649	ACTL10	3,498	0,037
ENSG00000113621	TXNDC15	3,508	0,036
ENSG00000212807	OR2A1	3,509	0,036
ENSG00000100577	GSTZ1	3,517	0,035
ENSG0000010	RRN3P2	3,517	0,035

3472			
ENSG00000221869	CEBPD	3,518	0,035
ENSG00000118004	COLEC11	3,52	0,035
ENSG00000109576	AADAT	3,525	0,035
ENSG00000225781	OR6V1	3,527	0,034
ENSG00000179855	GIPC3	3,53	0,034
ENSG00000004059	ARF5	3,534	0,034
ENSG00000293358	LOC653653	3,537	0,034
ENSG00000177189	RPS6KA3	3,541	0,033
ENSG00000104951	IL4I1	3,542	0,033
ENSG00000108953	YWHAE	3,546	0,033
ENSG00000137673	MMP7	3,55	0,033
ENSG00000179348	GATA2	3,551	0,033
ENSG00000144362	PHOSPHO2	3,552	0,033
ENSG00000168769	TET2	3,556	0,033
ENSG00000054967	RELT	3,598	0,029
ENSG00000245748	LOC100129931	3,603	0,028
ENSG00000108963	DPH1	3,61	0,028
ENSG00000100906	NFKBIA	3,618	0,027
ENSG00000155729	KCTD18	3,62	0,027
ENSG00000232629	HLA-DQB2	3,632	0,026
ENSG00000152455	SUV39H2	3,647	0,025
ENSG00000154917	RAB6B	3,652	0,024
ENSG00000106236	NPTX2	3,653	0,024
ENSG00000183258	DDX41	3,666	0,023
ENSG00000136937	NCBP1	3,673	0,023
ENSG00000151233	GXYLT1	3,686	0,022
ENSG00000136783	NIPSNAP3A	3,695	0,021
ENSG00000212724	KRTAP2-3	3,705	0,021
ENSG00000135617	PRADC1	3,713	0,020
ENSG00000157657	ZNF618	3,729	0,019
ENSG00000100124	ANKRD54	3,734	0,019
ENSG00000182512	GLRX5	3,735	0,019
ENSG00000110076	NRXN2	3,735	0,019
ENSG00000196678	ERI2	3,743	0,019

ENSG00000166448	TMEM130	3,748	0,018
ENSG00000184530	C6orf58	3,753	0,018
ENSG00000132640	BTBD3	3,758	0,018
ENSG00000111087	GLI1	3,764	0,018
ENSG00000149150	SLC43A1	3,769	0,017
ENSG00000172967	XKR3	3,772	0,017
ENSG00000106028	SSBP1	3,782	0,017
ENSG00000158497	HMHB1	3,794	0,016
ENSG00000108424	KPNB1	3,802	0,016
ENSG00000149798	CDC42EP2	3,806	0,016
ENSG00000138834	MAPK8IP3	3,815	0,015
ENSG00000064687	ABCA7	3,819	0,015
ENSG00000230530	LIMD1-AS1	3,836	0,014
ENSG00000074201	CLNS1A	3,886	0,012
ENSG00000148411	NACC2	3,928	0,010
ENSG00000107560	RAB11FIP2	3,93	0,010
ENSG00000048707	VPS13D	3,93	0,010
ENSG00000146067	FAM193B	3,957	0,009
ENSG00000173611	SCAI	3,958	0,009
ENSG00000102010	BMX	3,977	0,009
ENSG00000073067	CYP2W1	4,015	0,008
ENSG00000046774	MAGEC2	4,036	0,007
ENSG00000226761	TAS2R46	4,108	0,005
ENSG00000244694	PTCHD4	4,173	0,004
ENSG00000175215	CTDSP2	4,196	0,004
ENSG00000168646	AXIN2	4,226	0,003
ENSG00000127529	OR7C2	4,233	0,003
ENSG00000102078	SLC25A14	4,233	0,003
ENSG00000013374	NUB1	4,25	0,003
ENSG00000102524	TNFSF13B	4,25	0,003
ENSG00000212124	TAS2R19	4,277	0,003
ENSG00000106648	GALNTL5	4,292	0,003
ENSG00000120910	PPP3CC	4,293	0,003
ENSG00000237945	LINC00649	4,308	0,003
ENSG0000021	TM6SF2	4,376	0,002

3996			
ENSG00000109436	TBC1D9	4,403	0,002
ENSG00000165194	PCDH19	4,412	0,002
ENSG00000108242	CYP2C18	4,436	0,001
ENSG00000119686	FLVCR2	4,44	0,001
ENSG00000112494	UNC93A	4,471	0,001
ENSG00000185873	TMPRSS11B	4,485	0,001
ENSG00000242802	AP5Z1	4,493	0,001
ENSG00000104897	SF3A2	4,587	0,001
ENSG00000104679	R3HCC1	4,601	0,001
ENSG00000087842	PIR	4,663	0,001
ENSG00000154640	BTG3	4,686	0,001
ENSG00000152939	MARVELD2	4,712	0,000
ENSG00000166634	SERPINB12	4,762	0,000
ENSG00000115705	TPO	4,802	0,000
ENSG00000101057	MYBL2	4,806	0,000
ENSG00000168159	RNF187	4,829	0,000
ENSG00000242779	ZNF702P	4,903	0,000
ENSG00000113013	MORTALIN	4,943	0,000

Table S 5: List of genes that are differentially regulated between BON1 cells treated with the mTOR inhibitors everolimus and temsirolimus and the control.

For simplified evaluation, the control group included wild-type BON1 cells and BON1 treated with DMSO, while the inhibitor group included BON1 cells that were treated with 1 µM everolimus and temsirolimus for 72 hours. The genes were determined using the DESeq2 package. All genes with Benjamin Hochberg adjusted p-value (padj) < 0.05 were included. The data are represented as Wald-statistic (stat). Genes with negative Wald-statistic values are down-regulated in BON1 cells treated with mTOR inhibitors compared to the control group.

$$\text{Wald} - \text{statistic} = \frac{\text{log2FoldChange}}{\text{standard error of log2FoldChange}}$$

Ensembl_ID	Gene_symbol	Stat_control_inhibitor	padj_control_inhibitor
ENSG00000138107	ACTR1A	-22,32	1,06E-106
ENSG0000012	TUBGCP6	-21,719	4,61E-101

Ensembl_ID	Gene_symbol	Stat_control_inhibitor	padj_control_inhibitor
ENSG00000173281	PPP1R3B	2,656	4,97E-02
ENSG0000012	MYO1B	2,657	4,97E-02

8159				8641			
ENSG00000137714	FDX1	-19,114	3,73E-78	ENSG00000134056	MRPS36	2,658	4,96E-02
ENSG00000196591	HDAC2	-18,661	1,72E-74	ENSG00000134248	LAMTOR5	2,658	4,95E-02
ENSG00000102978	POLR2C	-16,856	9,75E-61	ENSG00000185668	POU3F1	2,661	4,92E-02
ENSG00000184160	ADRA2C	-16,486	3,64E-58	ENSG00000128656	CHN1	2,661	4,92E-02
ENSG00000120805	ARL1	-16,34	3,63E-57	ENSG00000113966	ARL6	2,661	4,92E-02
ENSG00000101439	CST3	-15,93	2,51E-54	ENSG00000138316	ADAMTS14	2,661	4,92E-02
ENSG00000143158	MPC2	-15,856	7,50E-54	ENSG00000166435	XRRA1	2,661	4,92E-02
ENSG00000122359	ANXA11	-15,683	1,10E-52	ENSG00000121749	TBC1D15	2,661	4,92E-02
ENSG00000168137	SETD5	-15,592	4,25E-52	ENSG00000075399	VPS9D1	2,662	4,92E-02
ENSG00000136271	DDX56	-15,518	1,22E-51	ENSG00000171223	JUNB	2,663	4,92E-02
ENSG00000069849	ATP1B3	-15,368	1,20E-50	ENSG00000134215	VAV3	2,663	4,92E-02
ENSG00000100461	RBM23	-15,22	1,09E-49	ENSG00000087263	OGFOD1	2,669	4,85E-02
ENSG00000112977	DAP	-15,062	1,18E-48	ENSG00000116161	CACYBP	2,67	4,83E-02
ENSG00000176903	PNMA1	-14,641	5,57E-46	ENSG00000152952	PLOD2	2,675	4,78E-02
ENSG00000146963	LUC7L2	-14,603	9,26E-46	ENSG00000167107	ACSF2	2,676	4,77E-02
ENSG00000126261	UBA2	-14,545	2,11E-45	ENSG00000051382	PIK3CB	2,677	4,75E-02
ENSG00000254986	DPP3	-14,441	9,39E-45	ENSG00000101367	MAPRE1	2,679	4,74E-02
ENSG00000204310	AGPAT1	-13,74	1,72E-40	ENSG00000170876	TMEM43	2,681	4,72E-02
ENSG00000189171	S100A13	-13,698	2,97E-40	ENSG00000127533	F2RL3	2,681	4,72E-02
ENSG00000125534	PPDPF	-13,629	7,39E-40	ENSG00000166965	RCCD1	2,685	4,67E-02
ENSG00000204304	PBX2	-13,46	7,06E-39	ENSG00000208772	SNORD94	2,691	4,60E-02
ENSG00000105618	PRPF31	-13,446	8,40E-39	ENSG00000156642	NPTN	2,691	4,60E-02
ENSG00000067560	RHOA	-13,355	2,81E-38	ENSG00000075426	FOSL2	2,692	4,60E-02
ENSG00000104093	DMXL2	-13,234	1,36E-37	ENSG00000115761	NOL10	2,695	4,55E-02
ENSG00000205155	PSENEN	-13,015	2,39E-36	ENSG00000127946	HIP1	2,696	4,54E-02
ENSG00000104973	MED25	-13,007	2,58E-36	ENSG00000115464	USP34	2,699	4,51E-02
ENSG00000165609	NUDT5	-12,798	3,71E-35	ENSG00000137770	CTDSPL2	2,699	4,50E-02
ENSG00000143569	UBAP2L	-12,775	4,86E-35	ENSG00000146109	ABT1	2,699	4,50E-02
ENSG00000117713	ARID1A	-12,691	1,37E-34	ENSG00000198569	SLC34A3	2,7	4,50E-02
ENSG00000162704	ARPC5	-12,406	4,64E-33	ENSG00000120088	CRHR1	2,7	4,50E-02
ENSG00000070950	RAD18	-12,312	1,48E-32	ENSG00000170703	TTLL6	2,7	4,50E-02
ENSG00000064651	SLC12A2	-12,207	5,26E-32	ENSG00000139746	RBM26	2,702	4,48E-02
ENSG00000187079	TEAD1	-12,121	1,46E-31	ENSG00000115525	ST3GAL5	2,704	4,46E-02
ENSG00000075131	TIPIN	-12,058	3,07E-31	ENSG00000144362	PHOSPHO2	2,704	4,46E-02

ENSG00000254911	SCARNA9	-12,013	5,25E-31
ENSG00000110651	CD81	-11,773	9,06E-30
ENSG00000124562	SNRPC	-11,734	1,42E-29
ENSG00000158710	TAGLN2	-11,683	2,56E-29
ENSG00000112699	GMDS	-11,527	1,46E-28
ENSG00000142892	PIGK	-11,511	1,73E-28
ENSG00000175115	PACS1	-11,507	1,80E-28
ENSG00000196700	ZNF512B	-11,418	4,86E-28
ENSG00000121390	PSPC1	-11,007	4,62E-26
ENSG00000170889	RPS9	-10,979	6,16E-26
ENSG00000197077	KIAA1671	-10,922	1,15E-25
ENSG00000163527	STT3B	-10,92	1,17E-25
ENSG00000141985	SH3GL1	-10,837	2,85E-25
ENSG00000204946	ZNF783	-10,406	2,79E-23
ENSG00000149257	SERPINH1	-10,313	7,23E-23
ENSG00000183684	ALYREF	-10,302	8,00E-23
ENSG00000103855	CD276	-10,299	8,20E-23
ENSG00000155363	MOV10	-10,244	1,42E-22
ENSG00000074370	ATP2A3	-10,216	1,89E-22
ENSG00000164307	ERAP1	-10,177	2,81E-22
ENSG00000100124	ANKRD54	-10,147	3,73E-22
ENSG00000173064	HECTD4	-10,082	7,10E-22
ENSG00000221978	CCNL2	-9,988	1,83E-21
ENSG00000108961	RANGRF	-9,96	2,38E-21
ENSG00000160803	UBQLN4	-9,917	3,58E-21
ENSG00000154723	ATP5J	-9,791	1,21E-20
ENSG00000160062	ZBTB8A	-9,715	2,49E-20
ENSG00000109436	TBC1D9	-9,668	3,90E-20
ENSG00000213977	TAX1BP3	-9,583	8,78E-20
ENSG00000184924	PTRHD1	-9,559	1,09E-19
ENSG00000105619	TFPT	-9,54	1,31E-19
ENSG00000132481	TRIM47	-9,344	8,00E-19
ENSG00000031081	ARHGAP31	-9,253	1,83E-18
ENSG00000143178	TBX19	-9,24	2,04E-18
ENSG0000012	MTRF1	-9,24	2,04E-18
ENSG00000156564	LRFN2	2,704	4,46E-02
ENSG00000070388	FGF22	2,704	4,46E-02
ENSG00000126756	UXT	2,704	4,46E-02
ENSG00000134072	CAMK1	2,706	4,46E-02
ENSG00000204070	SYS1	2,706	4,46E-02
ENSG00000152082	MZT2B	2,707	4,45E-02
ENSG00000104812	GYS1	2,708	4,44E-02
ENSG00000108474	PIGL	2,709	4,44E-02
ENSG00000123104	ITPR2	2,709	4,43E-02
ENSG00000243927	MRPS6	2,71	4,43E-02
ENSG00000158796	DEDD	2,71	4,42E-02
ENSG00000108179	PPIF	2,711	4,42E-02
ENSG00000163629	PTPN13	2,713	4,40E-02
ENSG00000107105	ELAVL2	2,713	4,40E-02
ENSG00000174799	CEP135	2,714	4,39E-02
ENSG00000117411	B4GALT2	2,717	4,36E-02
ENSG00000128951	DUT	2,72	4,33E-02
ENSG00000164484	TMEM200A	2,721	4,32E-02
ENSG00000075073	TACR2	2,73	4,21E-02
ENSG00000077097	TOP2B	2,733	4,17E-02
ENSG00000105519	CAPS	2,734	4,17E-02
ENSG00000099341	PSMD8	2,736	4,15E-02
ENSG00000136021	SCYL2	2,737	4,14E-02
ENSG00000166033	HTRA1	2,738	4,14E-02
ENSG00000124493	GRM4	2,74	4,11E-02
ENSG00000090097	PCBP4	2,74	4,11E-02
ENSG00000119986	AVPI1	2,743	4,09E-02
ENSG00000186350	RXRA	2,744	4,07E-02
ENSG00000270647	TAF15	2,747	4,05E-02
ENSG00000106771	TMEM245	2,748	4,03E-02
ENSG00000213190	MLLT11	2,749	4,03E-02
ENSG00000092470	WDR76	2,752	4,00E-02
ENSG00000165997	ARL5B	2,752	4,00E-02
ENSG00000117523	PRRC2C	2,756	3,96E-02
ENSG0000013	KIF20B	2,757	3,96E-02

0662				8182			
ENSG00000136478	TEX2	-9,229	2,24E-18	ENSG00000136960	ENPP2	2,757	3,95E-02
ENSG00000198961	PJA2	-9,146	4,67E-18	ENSG00000103653	CSK	2,758	3,95E-02
ENSG00000119431	HDHD3	-9,092	7,36E-18	ENSG00000167985	SDHAF2	2,763	3,89E-02
ENSG00000286760	LOC100289495	-9,089	7,48E-18	ENSG00000103260	METRN	2,765	3,87E-02
ENSG00000135722	FBXL8	-9,035	1,19E-17	ENSG00000157978	LDLRAP1	2,766	3,86E-02
ENSG00000138468	SENP7	-9,026	1,28E-17	ENSG00000204347	BTBD17	2,768	3,84E-02
ENSG00000078081	LAMP3	-9,018	1,37E-17	ENSG00000102575	ACP5	2,768	3,84E-02
ENSG00000105705	SUGP1	-9,012	1,45E-17	ENSG00000091640	SPAG7	2,772	3,81E-02
ENSG00000099282	TSPAN15	-9,006	1,52E-17	ENSG00000183814	LIN9	2,772	3,81E-02
ENSG00000115295	CLIP4	-9,002	1,56E-17	ENSG00000049283	EPN3	2,773	3,81E-02
ENSG00000196684	HSH2D	-8,953	2,31E-17	ENSG00000196419	XRCC6	2,774	3,80E-02
ENSG00000181192	DHTKD1	-8,94	2,57E-17	ENSG00000151503	NCAPD3	2,776	3,78E-02
ENSG00000004139	SARM1	-8,921	3,01E-17	ENSG00000137563	GGH	2,78	3,74E-02
ENSG00000178445	GLDC	-8,916	3,16E-17	ENSG00000227036	LINC00673	2,781	3,74E-02
ENSG00000121101	TEX14	-8,858	5,24E-17	ENSG00000184203	PPP1R2	2,786	3,68E-02
ENSG00000104427	ZC2HC1A	-8,858	5,24E-17	ENSG00000120526	NUDCD1	2,787	3,68E-02
ENSG00000186007	LEMD1	-8,835	6,25E-17	ENSG00000131477	RAMP2	2,79	3,65E-02
ENSG00000177728	KIAA0195	-8,783	9,62E-17	ENSG00000035499	DEPDC1B	2,79	3,65E-02
ENSG00000163666	HESX1	-8,779	9,95E-17	ENSG00000198074	AKR1B10	2,79	3,65E-02
ENSG00000119922	IFIT2	-8,739	1,40E-16	ENSG00000135407	AVIL	2,791	3,65E-02
ENSG00000130768	SMPDL3B	-8,68	2,25E-16	ENSG00000131389	SLC6A6	2,793	3,63E-02
ENSG00000173083	HPSE	-8,652	2,83E-16	ENSG00000171311	EXOSC1	2,794	3,62E-02
ENSG00000275395	FCGBP	-8,643	3,03E-16	ENSG00000105982	RNF32	2,795	3,61E-02
ENSG00000142544	CTU1	-8,636	3,19E-16	ENSG00000051180	RAD51	2,795	3,61E-02
ENSG00000237190	CDKN2AIPNL	-8,633	3,25E-16	ENSG00000131791	PRKAB2	2,8	3,57E-02
ENSG00000185519	FAM131C	-8,608	3,99E-16	ENSG00000143067	ZNF697	2,806	3,50E-02
ENSG00000066468	FGFR2	-8,608	3,99E-16	ENSG00000104312	RIPK2	2,807	3,50E-02
ENSG00000122417	ODF2L	-8,593	4,49E-16	ENSG00000159055	MIS18A	2,813	3,44E-02
ENSG00000135314	KHDC1	-8,591	4,53E-16	ENSG00000154473	BUB3	2,814	3,43E-02
ENSG00000185842	DNAH14	-8,571	5,34E-16	ENSG00000153071	DAB2	2,814	3,43E-02
ENSG00000134013	LOXL2	-8,539	6,99E-16	ENSG00000068305	MEF2A	2,817	3,40E-02
ENSG00000268061	NAPA-AS1	-8,538	6,99E-16	ENSG00000113758	DBN1	2,818	3,40E-02
ENSG00000157510	AFAP1L1	-8,537	7,04E-16	ENSG00000134824	FADS2	2,819	3,39E-02
ENSG00000156587	UBE2L6	-8,529	7,56E-16	ENSG00000132466	ANKRD17	2,819	3,39E-02

ENSG00000157111	TMEM171	-8,526	7,70E-16	ENSG00000120055	C10orf95	2,821	3,38E-02
ENSG00000111845	PAK1IP1	-8,512	8,60E-16	ENSG00000136527	TRA2B	2,821	3,38E-02
ENSG00000138604	GLCE	-8,501	9,48E-16	ENSG00000133243	BTBD2	2,824	3,34E-02
ENSG00000168040	FADD	-8,472	1,20E-15	ENSG00000188483	IER5L	2,825	3,34E-02
ENSG00000116761	CTH	-8,463	1,28E-15	ENSG00000133115	STOML3	2,825	3,34E-02
ENSG00000103811	CTSH	-8,459	1,32E-15	ENSG00000163468	CCT3	2,828	3,31E-02
ENSG00000276550	HERC2P2	-8,453	1,39E-15	ENSG00000070444	MNT	2,83	3,30E-02
ENSG00000127720	METTL25	-8,441	1,53E-15	ENSG00000105559	PLEKHA4	2,833	3,27E-02
ENSG00000008441	NFIX	-8,424	1,74E-15	ENSG00000119689	DLST	2,837	3,24E-02
ENSG00000132837	DMGDH	-8,424	1,74E-15	ENSG00000119397	CNTRL	2,839	3,21E-02
ENSG00000117586	TNFSF4	-8,414	1,89E-15	ENSG00000126878	AIF1L	2,844	3,17E-02
ENSG00000157514	TSC22D3	-8,409	1,96E-15	ENSG00000159720	ATP6V0D1	2,845	3,16E-02
ENSG00000163975	MFI2	-8,407	1,99E-15	ENSG00000184545	DUSP8	2,848	3,14E-02
ENSG00000027075	PRKCH	-8,4	2,10E-15	ENSG00000177731	FLII	2,852	3,11E-02
ENSG00000147509	RGS20	-8,398	2,13E-15	ENSG00000135269	TES	2,853	3,11E-02
ENSG00000134470	IL15RA	-8,396	2,15E-15	ENSG00000137807	KIF23	2,853	3,10E-02
ENSG00000171346	KRT15	-8,384	2,38E-15	ENSG00000100077	ADRBK2	2,858	3,05E-02
ENSG00000082014	SMARCD3	-8,382	2,41E-15	ENSG00000158793	NIT1	2,869	2,96E-02
ENSG00000164687	FABP5	-8,371	2,61E-15	ENSG00000133835	HSD17B4	2,869	2,96E-02
ENSG00000139211	AMIGO2	-8,36	2,83E-15	ENSG00000004777	ARHGAP33	2,875	2,91E-02
ENSG00000171608	PIK3CD	-8,36	2,84E-15	ENSG00000134222	PSRC1	2,875	2,91E-02
ENSG00000168291	PDHB	-8,349	3,08E-15	ENSG00000122008	POLK	2,882	2,85E-02
ENSG00000150477	KIAA1328	-8,334	3,47E-15	ENSG00000106683	LIMK1	2,886	2,82E-02
ENSG00000169239	CA5B	-8,323	3,79E-15	ENSG00000136848	DAB2IP	2,888	2,80E-02
ENSG00000173210	ABLIM3	-8,307	4,29E-15	ENSG00000169727	GPS1	2,888	2,80E-02
ENSG00000120725	SIL1	-8,306	4,30E-15	ENSG00000065883	CDK13	2,889	2,79E-02
ENSG00000156463	SH3RF2	-8,26	6,22E-15	ENSG00000198855	FICD	2,9	2,70E-02
ENSG00000188051	TMEM221	-8,248	6,82E-15	ENSG00000241697	TMEFF1	2,904	2,67E-02
ENSG00000137936	BCAR3	-8,223	8,38E-15	ENSG00000186222	BLOC1S4	2,911	2,62E-02
ENSG00000164758	MED30	-8,212	9,09E-15	ENSG00000161654	LSM12	2,918	2,57E-02
ENSG00000131508	UBE2D2	-8,212	9,09E-15	ENSG00000095002	MSH2	2,919	2,57E-02
ENSG00000198910	L1CAM	-8,211	9,14E-15	ENSG00000108947	EFNB3	2,923	2,53E-02
ENSG00000127743	IL17B	-8,206	9,56E-15	ENSG00000133226	SRRM1	2,923	2,53E-02
ENSG00000198648	STK39	-8,205	9,56E-15	ENSG00000196453	ZNF777	2,924	2,53E-02
ENSG0000012	TPH1	-8,201	9,88E-15	ENSG0000010	TMEM59L	2,93	2,48E-02

9167				5696			
ENSG00000155846	PPARGC1B	-8,183	1,14E-14	ENSG00000106261	ZKSCAN1	2,934	2,46E-02
ENSG00000139323	POC1B	-8,173	1,23E-14	ENSG00000169180	XPO6	2,936	2,44E-02
ENSG00000134463	ECHDC3	-8,166	1,30E-14	ENSG00000013810	TACC3	2,936	2,44E-02
ENSG00000140961	OSGIN1	-8,152	1,45E-14	ENSG00000123737	EXOSC9	2,938	2,43E-02
ENSG00000145819	ARHGAP26	-8,138	1,62E-14	ENSG00000179933	C14orf119	2,946	2,37E-02
ENSG00000124216	SNAI1	-8,132	1,69E-14	ENSG00000067057	PFKP	2,948	2,36E-02
ENSG00000112394	SLC16A10	-8,114	1,96E-14	ENSG00000119514	GALNT12	2,949	2,35E-02
ENSG00000184588	PDE4B	-8,091	2,36E-14	ENSG00000077152	UBE2T	2,95	2,35E-02
ENSG00000123179	EBPL	-8,079	2,59E-14	ENSG00000184985	SORCS2	2,952	2,34E-02
ENSG00000113108	APBB3	-8,072	2,73E-14	ENSG00000152253	SPC25	2,955	2,31E-02
ENSG00000003137	CYP26B1	-8,055	3,11E-14	ENSG00000160789	LMNA	2,959	2,29E-02
ENSG00000076003	MCM6	-8,04	3,50E-14	ENSG00000038358	EDC4	2,961	2,29E-02
ENSG00000196517	SLC6A9	-8,011	4,38E-14	ENSG00000171094	ALK	2,967	2,24E-02
ENSG00000164683	HEY1	-8	4,78E-14	ENSG00000128536	CDHR3	2,967	2,24E-02
ENSG00000248905	FMN1	-7,979	5,57E-14	ENSG00000260565	ERVK13-1	2,967	2,24E-02
ENSG00000266094	RASSF5	-7,961	6,45E-14	ENSG00000128283	CDC42EP1	2,968	2,24E-02
ENSG00000241852	C8orf58	-7,94	7,61E-14	ENSG00000100485	SOS2	2,97	2,23E-02
ENSG00000263155	MYZAP	-7,89	1,12E-13	ENSG00000183856	IQGAP3	2,973	2,21E-02
ENSG00000175832	ETV4	-7,85	1,53E-13	ENSG00000100749	VRK1	2,977	2,18E-02
ENSG00000128346	C22orf23	-7,828	1,82E-13	ENSG00000213799	ZNF845	2,986	2,12E-02
ENSG00000133818	RRAS2	-7,811	2,06E-13	ENSG00000123374	CDK2	2,991	2,09E-02
ENSG00000105402	NAPA	-7,776	2,71E-13	ENSG00000164904	ALDH7A1	2,991	2,09E-02
ENSG00000182185	RAD51B	-7,73	3,85E-13	ENSG00000165704	HPRT1	2,993	2,09E-02
ENSG00000088367	EPB41L1	-7,685	5,46E-13	ENSG00000171443	ZNF524	3,009	1,98E-02
ENSG00000038274	MAT2B	-7,684	5,47E-13	ENSG00000254618	TMED10P1	3,013	1,96E-02
ENSG00000077713	SLC25A43	-7,678	5,73E-13	ENSG00000151287	TEX30	3,019	1,93E-02
ENSG00000156510	HKDC1	-7,674	5,89E-13	ENSG00000158457	TSPAN33	3,026	1,89E-02
ENSG00000020633	RUNX3	-7,65	7,09E-13	ENSG00000155755	TMEM237	3,033	1,85E-02
ENSG00000067066	SP100	-7,613	9,38E-13	ENSG00000138175	ARL3	3,038	1,82E-02
ENSG00000167785	ZNF558	-7,606	9,94E-13	ENSG00000161011	SQSTM1	3,04	1,81E-02
ENSG00000153029	MR1	-7,605	9,95E-13	ENSG00000265972	TXNIP	3,04	1,81E-02
ENSG00000114346	ECT2	-7,601	1,03E-12	ENSG00000132256	TRIM5	3,042	1,80E-02
ENSG00000103404	USP31	-7,6	1,03E-12	ENSG00000100242	SUN2	3,046	1,77E-02
ENSG00000165475	CRYL1	-7,598	1,04E-12	ENSG00000155906	RMND1	3,047	1,77E-02

ENSG00000131914	LIN28A	-7,578	1,22E-12	ENSG00000137806	NDUFAF1	3,051	1,75E-02
ENSG00000174132	FAM174A	-7,572	1,26E-12	ENSG00000140396	NCOA2	3,051	1,75E-02
ENSG00000167074	TEF	-7,524	1,82E-12	ENSG00000119929	CUTC	3,057	1,72E-02
ENSG00000142279	WTIP	-7,497	2,22E-12	ENSG00000198205	ZXDA	3,059	1,71E-02
ENSG00000183971	NPW	-7,463	2,85E-12	ENSG00000187123	LYPD6	3,06	1,71E-02
ENSG00000173890	GPR160	-7,456	3,00E-12	ENSG00000124181	PLCG1	3,065	1,68E-02
ENSG00000163900	TMEM41A	-7,447	3,21E-12	ENSG00000169710	FASN	3,073	1,64E-02
ENSG00000232956	SNHG15	-7,441	3,34E-12	ENSG00000171530	TBCA	3,073	1,64E-02
ENSG00000188629	ZNF177	-7,361	6,02E-12	ENSG00000170185	USP38	3,074	1,64E-02
ENSG00000137312	FLOT1	-7,24	1,45E-11	ENSG00000128591	FLNC	3,075	1,64E-02
ENSG00000162613	FUBP1	-7,225	1,60E-11	ENSG00000122367	LDB3	3,076	1,63E-02
ENSG00000197483	ZNF628	-7,191	2,05E-11	ENSG00000165449	SLC16A9	3,078	1,62E-02
ENSG00000010803	SCMH1	-7,169	2,40E-11	ENSG00000197841	ZNF181	3,079	1,62E-02
ENSG00000157343	ARMC12	-7,143	2,88E-11	ENSG00000145687	SSBP2	3,08	1,61E-02
ENSG00000102781	KATNAL1	-7,13	3,16E-11	ENSG00000106009	BRAT1	3,087	1,58E-02
ENSG00000135069	PSAT1	-7,119	3,39E-11	ENSG00000198142	SOWAHC	3,087	1,58E-02
ENSG00000123975	CKS2	-7,108	3,65E-11	ENSG00000196151	WDSUB1	3,099	1,52E-02
ENSG00000172766	NAA16	-7,053	5,39E-11	ENSG00000126603	GLIS2	3,102	1,51E-02
ENSG00000011566	MAP4K3	-7,051	5,46E-11	ENSG00000103723	AP3B2	3,105	1,50E-02
ENSG00000110344	UBE4A	-7,049	5,52E-11	ENSG00000197106	SLC6A17	3,108	1,49E-02
ENSG00000085840	ORC1	-6,997	7,95E-11	ENSG00000070214	SLC44A1	3,113	1,47E-02
ENSG00000110060	PUS3	-6,963	1,01E-10	ENSG00000206869	SNORA70F	3,114	1,46E-02
ENSG00000204371	EHMT2	-6,882	1,78E-10	ENSG00000175029	CTBP2	3,116	1,45E-02
ENSG00000172794	RAB37	-6,868	1,95E-10	ENSG00000163636	PSMD6	3,12	1,43E-02
ENSG00000177628	GBA	-6,855	2,12E-10	ENSG00000164111	ANXA5	3,122	1,43E-02
ENSG00000170540	ARL6IP1	-6,853	2,16E-10	ENSG00000116560	SFPQ	3,131	1,38E-02
ENSG00000135373	EHF	-6,831	2,51E-10	ENSG00000180998	GPR137C	3,143	1,33E-02
ENSG00000117480	FAAH	-6,801	3,07E-10	ENSG00000105486	LIG1	3,15	1,30E-02
ENSG00000109911	ELP4	-6,77	3,81E-10	ENSG00000159352	PSMD4	3,151	1,30E-02
ENSG00000106066	CPVL	-6,741	4,60E-10	ENSG00000196220	SRGAP3	3,154	1,29E-02
ENSG00000174808	BTC	-6,727	5,05E-10	ENSG00000129472	RAB2B	3,16	1,27E-02
ENSG00000118579	MED28	-6,703	5,92E-10	ENSG00000080815	PSEN1	3,161	1,26E-02
ENSG00000107404	DVL1	-6,664	7,63E-10	ENSG00000115825	PRKD3	3,168	1,24E-02
ENSG00000168172	HOOK3	-6,601	1,16E-09	ENSG00000164077	MON1A	3,174	1,21E-02
ENSG0000013	LAMC1	-6,561	1,50E-09	ENSG0000010	ZBED4	3,177	1,20E-02

5862				0426			
ENSG00000180773	SLC36A4	-6,536	1,77E-09	ENSG00000167565	SERTAD3	3,18	1,19E-02
ENSG00000133606	MKRN1	-6,5	2,23E-09	ENSG00000107833	NPM3	3,182	1,18E-02
ENSG00000124299	PEPD	-6,498	2,26E-09	ENSG00000140931	CMTM3	3,186	1,17E-02
ENSG00000149573	MPZL2	-6,478	2,57E-09	ENSG00000214736	TOMM6	3,201	1,12E-02
ENSG00000101695	RNF125	-6,477	2,58E-09	ENSG00000168779	SHOX2	3,206	1,10E-02
ENSG00000115266	APC2	-6,464	2,80E-09	ENSG00000164796	CSMD3	3,209	1,09E-02
ENSG00000182836	PLCXD3	-6,426	3,59E-09	ENSG00000126262	FFAR2	3,214	1,07E-02
ENSG00000177238	TRIM72	-6,425	3,60E-09	ENSG00000053524	MCF2L2	3,221	1,05E-02
ENSG00000082397	EPB41L3	-6,424	3,61E-09	ENSG00000135441	BLOC1S1	3,223	1,04E-02
ENSG00000106588	PSMA2	-6,372	5,03E-09	ENSG00000100532	CGRRF1	3,225	1,04E-02
ENSG00000165775	FUNDC2	-6,335	6,34E-09	ENSG00000169093	ASMTL	3,226	1,03E-02
ENSG00000130413	STK33	-6,321	6,92E-09	ENSG00000090661	CERS4	3,229	1,03E-02
ENSG00000176014	TUBB6	-6,303	7,76E-09	ENSG00000091483	FH	3,229	1,03E-02
ENSG00000159314	ARHGAP27	-6,282	8,85E-09	ENSG00000160785	SLC25A44	3,229	1,03E-02
ENSG00000162924	REL	-6,272	9,42E-09	ENSG00000144596	GRIP2	3,23	1,02E-02
ENSG00000177426	TGIF1	-6,184	1,61E-08	ENSG00000139292	LGR5	3,23	1,02E-02
ENSG00000099901	RANBP1	-6,149	1,99E-08	ENSG00000196850	PPTC7	3,233	1,01E-02
ENSG00000103995	CEP152	-6,146	2,03E-08	ENSG00000112242	E2F3	3,236	1,00E-02
ENSG00000004700	RECQL	-6,145	2,04E-08	ENSG00000105835	NAMPT	3,241	9,90E-03
ENSG00000101605	MYOM1	-6,129	2,24E-08	ENSG00000052795	FNIP2	3,249	9,66E-03
ENSG00000245680	ZNF585B	-6,128	2,24E-08	ENSG00000058056	USP13	3,249	9,65E-03
ENSG00000180044	C3orf80	-6,108	2,53E-08	ENSG00000162078	ZG16B	3,253	9,52E-03
ENSG00000197386	HTT	-6,079	2,98E-08	ENSG00000143951	WDPCP	3,257	9,38E-03
ENSG00000114019	AMOTL2	-6,075	3,05E-08	ENSG00000122966	CIT	3,26	9,30E-03
ENSG00000143028	SYPL2	-6,055	3,45E-08	ENSG00000204619	PPP1R11	3,262	9,26E-03
ENSG00000103429	BFAR	-6,035	3,88E-08	ENSG00000173706	HEG1	3,263	9,23E-03
ENSG00000015475	BID	-5,992	4,97E-08	ENSG00000164182	NDUFAF2	3,268	9,08E-03
ENSG00000189143	CLDN4	-5,981	5,28E-08	ENSG00000188681	TEKT4P2	3,268	9,07E-03
ENSG00000175787	ZNF169	-5,969	5,66E-08	ENSG00000114698	PLSCR4	3,269	9,06E-03
ENSG00000156535	CD109	-5,961	5,95E-08	ENSG00000037241	RPL26L1	3,273	8,95E-03
ENSG00000100379	KCTD17	-5,955	6,11E-08	ENSG00000128654	MTX2	3,275	8,92E-03
ENSG00000183098	GPC6	-5,937	6,79E-08	ENSG00000070010	UFD1L	3,276	8,87E-03
ENSG00000119508	NR4A3	-5,929	7,07E-08	ENSG00000161956	SENP3	3,288	8,54E-03
ENSG00000096872	IFT74	-5,922	7,37E-08	ENSG00000160305	DIP2A	3,29	8,49E-03

ENSG00000206755	SNORA30	-5,915	7,69E-08	ENSG00000057608	GDI2	3,296	8,30E-03
ENSG00000167995	BEST1	-5,893	8,74E-08	ENSG00000011347	SYT7	3,301	8,17E-03
ENSG00000164924	YWHAZ	-5,874	9,73E-08	ENSG00000173275	ZNF449	3,309	7,97E-03
ENSG00000010438	PRSS3	-5,861	1,05E-07	ENSG00000113328	CCNG1	3,313	7,87E-03
ENSG00000124613	ZNF391	-5,847	1,13E-07	ENSG00000040608	RTN4R	3,317	7,76E-03
ENSG00000008311	AASS	-5,827	1,27E-07	ENSG00000128218	VPREB3	3,32	7,67E-03
ENSG00000138180	CEP55	-5,817	1,34E-07	ENSG00000137076	TLN1	3,322	7,64E-03
ENSG00000100191	SLC5A4	-5,813	1,36E-07	ENSG00000115827	DCAF17	3,324	7,58E-03
ENSG00000074590	NUAK1	-5,782	1,64E-07	ENSG00000132600	PRMT7	3,324	7,57E-03
ENSG00000001084	GCLC	-5,776	1,68E-07	ENSG00000113658	SMAD5	3,327	7,51E-03
ENSG00000144550	CPNE9	-5,736	2,12E-07	ENSG00000132950	ZMYM5	3,327	7,51E-03
ENSG00000122877	EGR2	-5,735	2,13E-07	ENSG00000142794	NBPF3	3,329	7,47E-03
ENSG00000171617	ENC1	-5,733	2,16E-07	ENSG00000225830	ERCC6	3,33	7,43E-03
ENSG00000072832	CRMP1	-5,73	2,20E-07	ENSG00000115289	PCGF1	3,338	7,25E-03
ENSG00000271303	SRXN1	-5,706	2,51E-07	ENSG00000111275	ALDH2	3,352	6,93E-03
ENSG00000165948	IFI27L1	-5,688	2,78E-07	ENSG00000140259	MFAP1	3,352	6,93E-03
ENSG00000005073	HOXA11	-5,646	3,52E-07	ENSG00000111696	NT5DC3	3,353	6,90E-03
ENSG00000171867	PRNP	-5,645	3,53E-07	ENSG00000162341	TPCN2	3,356	6,84E-03
ENSG00000196653	ZNF502	-5,642	3,58E-07	ENSG00000163393	SLC22A15	3,36	6,76E-03
ENSG00000197385	ZNF860	-5,629	3,85E-07	ENSG00000144354	CDCA7	3,368	6,57E-03
ENSG00000136868	SLC31A1	-5,614	4,20E-07	ENSG00000099954	CECR2	3,371	6,52E-03
ENSG00000159063	ALG8	-5,612	4,24E-07	ENSG00000087245	MMP2	3,372	6,50E-03
ENSG00000135108	FBXO21	-5,605	4,39E-07	ENSG00000100092	SH3BP1	3,374	6,46E-03
ENSG00000124217	MOCS3	-5,575	5,18E-07	ENSG00000164949	GEM	3,376	6,42E-03
ENSG00000110315	RNF141	-5,562	5,57E-07	ENSG00000082068	WDR70	3,393	6,05E-03
ENSG00000081665	ZNF506	-5,556	5,74E-07	ENSG00000119669	IRF2BPL	3,393	6,05E-03
ENSG00000176024	ZNF613	-5,556	5,74E-07	ENSG00000196683	TOMM7	3,394	6,04E-03
ENSG00000173540	GMPPB	-5,556	5,74E-07	ENSG00000188158	NHS	3,409	5,72E-03
ENSG00000169992	NLGN2	-5,54	6,25E-07	ENSG00000104231	ZFAND1	3,412	5,68E-03
ENSG00000187535	IFT140	-5,54	6,27E-07	ENSG00000204052	LRRC73	3,418	5,56E-03
ENSG00000105550	FGF21	-5,512	7,29E-07	ENSG00000154957	ZNF18	3,427	5,41E-03
ENSG00000239149	SNORA59A	-5,511	7,33E-07	ENSG00000090339	ICAM1	3,429	5,37E-03
ENSG00000087995	METTL2A	-5,496	7,96E-07	ENSG00000143252	SDHC	3,429	5,36E-03
ENSG00000183647	ZNF530	-5,474	8,93E-07	ENSG00000133398	MED10	3,433	5,30E-03
ENSG0000016	SPC24	-5,473	8,97E-07	ENSG0000000	SEC62	3,433	5,29E-03

1888				8952			
ENSG00000134668	SPOCD1	-5,47	9,08E-07	ENSG00000196743	GM2A	3,442	5,14E-03
ENSG00000142156	COL6A1	-5,465	9,33E-07	ENSG00000125820	NKX2-2	3,444	5,12E-03
ENSG00000182810	DDX28	-5,447	1,02E-06	ENSG00000156381	ANKRD9	3,447	5,07E-03
ENSG00000159885	ZNF222	-5,438	1,07E-06	ENSG00000221829	FANCG	3,448	5,06E-03
ENSG00000263465	SRSF8	-5,409	1,25E-06	ENSG00000135164	DMTF1	3,45	5,02E-03
ENSG00000114166	KAT2B	-5,401	1,30E-06	ENSG00000156467	UQCRB	3,452	4,99E-03
ENSG00000157423	HYDIN	-5,386	1,41E-06	ENSG00000204335	SP5	3,456	4,91E-03
ENSG00000099840	IZUMO4	-5,386	1,41E-06	ENSG00000012963	UBR7	3,459	4,87E-03
ENSG00000165322	ARHGAP12	-5,377	1,48E-06	ENSG00000162852	CNST	3,47	4,69E-03
ENSG00000073849	ST6GAL1	-5,371	1,52E-06	ENSG00000196169	KIF19	3,472	4,65E-03
ENSG00000164296	TIGD6	-5,368	1,54E-06	ENSG00000171914	TLN2	3,474	4,63E-03
ENSG00000225336	HMGB3P1	-5,363	1,57E-06	ENSG00000156482	RPL30	3,48	4,55E-03
ENSG00000136867	SLC31A2	-5,355	1,63E-06	ENSG00000103184	SEC14L5	3,48	4,55E-03
ENSG00000159307	SCUBE1	-5,347	1,66E-06	ENSG00000239183	SNORA84	3,482	4,51E-03
ENSG00000171365	CLCN5	-5,323	1,85E-06	ENSG00000107104	KANK1	3,483	4,50E-03
ENSG00000135077	HAVCR2	-5,306	2,00E-06	ENSG00000168036	CTNNB1	3,484	4,49E-03
ENSG00000120594	PLXDC2	-5,306	2,00E-06	ENSG00000183258	DDX41	3,49	4,38E-03
ENSG00000135482	ZC3H10	-5,287	2,21E-06	ENSG00000187243	MAGED4B	3,503	4,20E-03
ENSG00000124006	OBSL1	-5,264	2,42E-06	ENSG00000076604	TRAF4	3,508	4,13E-03
ENSG00000121895	TMEM156	-5,261	2,42E-06	ENSG00000005020	SKAP2	3,508	4,12E-03
ENSG00000084110	HAL	-5,252	2,50E-06	ENSG00000140575	IQGAP1	3,509	4,12E-03
ENSG00000152705	CATSPER3	-5,24	2,65E-06	ENSG00000162551	ALPL	3,51	4,10E-03
ENSG00000186364	NUDT17	-5,234	2,73E-06	ENSG00000064989	CALCRL	3,512	4,07E-03
ENSG00000147465	STAR	-5,234	2,73E-06	ENSG00000143228	NUF2	3,514	4,05E-03
ENSG00000104371	DKK4	-5,234	2,73E-06	ENSG00000111450	STX2	3,528	3,85E-03
ENSG00000169918	OTUD7A	-5,234	2,73E-06	ENSG00000127603	MACF1	3,531	3,80E-03
ENSG00000239306	RBM14	-5,207	2,97E-06	ENSG00000187514	PTMA	3,546	3,61E-03
ENSG00000228315	GUSBP11	-5,204	3,01E-06	ENSG00000101337	TM9SF4	3,552	3,53E-03
ENSG00000099875	MKNK2	-5,199	3,08E-06	ENSG00000101844	ATG4A	3,555	3,50E-03
ENSG00000111203	ITFG2	-5,199	3,09E-06	ENSG00000131747	TOP2A	3,561	3,43E-03
ENSG00000149308	NPAT	-5,197	3,11E-06	ENSG00000170619	COMMD5	3,577	3,24E-03
ENSG00000124743	KLHL31	-5,19	3,22E-06	ENSG00000263001	GTF2I	3,59	3,08E-03
ENSG00000115165	CYTIP	-5,178	3,40E-06	ENSG00000155561	NUP205	3,593	3,04E-03
ENSG00000243955	GSTA1	-5,178	3,40E-06	ENSG00000150995	ITPR1	3,598	3,00E-03

ENSG00000223705	NSUN5P1	-5,178	3,40E-06
ENSG00000133962	CATSPERB	-5,178	3,40E-06
ENSG00000174992	ZG16	-5,178	3,40E-06
ENSG00000102174	PHEX	-5,178	3,40E-06
ENSG00000168679	SLC16A4	-5,177	3,40E-06
ENSG00000157150	TIMP4	-5,177	3,40E-06
ENSG00000188573	FBLL1	-5,177	3,40E-06
ENSG00000106686	SPATA6L	-5,177	3,40E-06
ENSG00000242220	TCP10L	-5,177	3,40E-06
ENSG00000179304	FAM156A	-5,177	3,40E-06
ENSG00000147168	IL2RG	-5,177	3,40E-06
ENSG00000175606	TMEM70	-5,15	3,89E-06
ENSG00000215375	MYL5	-5,14	4,03E-06
ENSG00000100601	ALKBH1	-5,136	4,03E-06
ENSG00000254685	FPGT	-5,132	4,03E-06
ENSG00000213075	RPL31P11	-5,132	4,03E-06
ENSG00000197959	DNM3	-5,132	4,03E-06
ENSG00000176732	PFN4	-5,132	4,03E-06
ENSG00000138080	EMILIN1	-5,132	4,03E-06
ENSG00000143994	ABHD1	-5,132	4,03E-06
ENSG00000138079	SLC3A1	-5,132	4,03E-06
ENSG00000118997	DNAH7	-5,132	4,03E-06
ENSG00000230530	LIMD1-AS1	-5,132	4,03E-06
ENSG00000114841	DNAH1	-5,132	4,03E-06
ENSG00000153283	CD96	-5,132	4,03E-06
ENSG00000144857	BOC	-5,132	4,03E-06
ENSG00000145217	SLC26A1	-5,132	4,03E-06
ENSG00000168421	RHOH	-5,132	4,03E-06
ENSG00000112182	BACH2	-5,132	4,03E-06
ENSG00000214338	SOGA3	-5,132	4,03E-06
ENSG00000214309	MBLAC1	-5,132	4,03E-06
ENSG00000205307	SAP25	-5,132	4,03E-06
ENSG00000185267	CDNF	-5,132	4,03E-06
ENSG00000156113	KCNMA1	-5,132	4,03E-06
ENSG0000013	PRR5L	-5,132	4,03E-06
ENSG00000177688	SUMO4	3,599	2,98E-03
ENSG00000135972	MRPS9	3,606	2,91E-03
ENSG00000109072	VTN	3,607	2,90E-03
ENSG00000184489	PTP4A3	3,609	2,89E-03
ENSG00000188021	UBQLN2	3,629	2,68E-03
ENSG00000134262	AP4B1	3,633	2,65E-03
ENSG00000170545	SMAGP	3,652	2,47E-03
ENSG00000145817	YIPF5	3,653	2,46E-03
ENSG00000164985	PSIP1	3,654	2,46E-03
ENSG00000170604	IRF2BP1	3,657	2,43E-03
ENSG00000172354	GNB2	3,658	2,43E-03
ENSG00000118418	HMGN3	3,659	2,41E-03
ENSG00000143442	POGZ	3,659	2,41E-03
ENSG00000117266	CDK18	3,673	2,29E-03
ENSG00000198830	HMGN2	3,676	2,27E-03
ENSG00000039319	ZFYVE16	3,678	2,25E-03
ENSG00000112282	MED23	3,683	2,21E-03
ENSG00000122861	PLAU	3,69	2,15E-03
ENSG00000187109	NAP1L1	3,702	2,06E-03
ENSG00000183891	TTC32	3,713	1,97E-03
ENSG00000111412	C12orf49	3,73	1,85E-03
ENSG00000171824	EXOSC10	3,741	1,77E-03
ENSG00000014216	CAPN1	3,745	1,75E-03
ENSG00000120438	TCP1	3,747	1,74E-03
ENSG00000021355	SERPINB1	3,752	1,71E-03
ENSG00000132780	NASP	3,752	1,71E-03
ENSG00000140365	COMMD4	3,761	1,65E-03
ENSG00000056972	TRAF3IP2	3,764	1,63E-03
ENSG00000148408	CACNA1B	3,77	1,59E-03
ENSG00000196150	ZNF250	3,783	1,52E-03
ENSG00000104738	MCM4	3,795	1,44E-03
ENSG00000109320	NFKB1	3,796	1,44E-03
ENSG00000113141	IK	3,797	1,44E-03
ENSG00000213465	ARL2	3,802	1,41E-03
ENSG00000104	KDM4C	3,808	1,37E-03

5362				7077			
ENSG00000175294	CATSPER1	-5,132	4,03E-06	ENSG00000088727	KIF9	3,809	1,37E-03
ENSG00000174684	B3GNT6	-5,132	4,03E-06	ENSG00000213214	ARHGEF35	3,811	1,36E-03
ENSG00000109927	TECTA	-5,132	4,03E-06	ENSG00000163162	RNF149	3,812	1,36E-03
ENSG00000111729	CLEC4A	-5,132	4,03E-06	ENSG00000196976	LAGE3	3,823	1,30E-03
ENSG00000182544	MFSD5	-5,132	4,03E-06	ENSG00000111641	NOP2	3,828	1,27E-03
ENSG00000125207	PIWIL1	-5,132	4,03E-06	ENSG00000133026	MYH10	3,835	1,24E-03
ENSG00000134874	DZIP1	-5,132	4,03E-06	ENSG00000158106	RHPN1	3,854	1,15E-03
ENSG00000092054	MYH7	-5,132	4,03E-06	ENSG00000142102	ATHL1	3,858	1,13E-03
ENSG00000167195	GOLGA6C	-5,132	4,03E-06	ENSG00000160932	LY6E	3,86	1,13E-03
ENSG00000205923	CEMP1	-5,132	4,03E-06	ENSG00000137161	CNPY3	3,864	1,11E-03
ENSG00000270885	RASL10B	-5,132	4,03E-06	ENSG00000169231	THBS3	3,864	1,11E-03
ENSG00000161664	ASB16	-5,132	4,03E-06	ENSG00000175920	DOK7	3,873	1,07E-03
ENSG00000153822	KCNJ16	-5,132	4,03E-06	ENSG00000204673	AKT1S1	3,881	1,04E-03
ENSG00000116032	GRIN3B	-5,132	4,03E-06	ENSG00000066230	SLC9A3	3,885	1,02E-03
ENSG00000177025	C19orf18	-5,132	4,03E-06	ENSG00000074582	BCS1L	3,899	9,64E-04
ENSG00000083807	SLC27A5	-5,132	4,03E-06	ENSG00000143387	CTSK	3,916	9,00E-04
ENSG00000185019	UBOX5	-5,132	4,03E-06	ENSG00000133687	TMTC1	3,934	8,38E-04
ENSG00000158445	KCNB1	-5,132	4,03E-06	ENSG00000113657	DPYSL3	3,935	8,36E-04
ENSG00000160200	CBS	-5,132	4,03E-06	ENSG00000160439	RDH13	3,949	7,91E-04
ENSG00000158423	RIBC1	-5,132	4,03E-06	ENSG00000149503	INCENP	3,955	7,74E-04
ENSG00000269335	IKBKG	-5,132	4,03E-06	ENSG00000141380	SS18	3,956	7,70E-04
ENSG00000154620	TMSB4Y	-5,132	4,03E-06	ENSG00000008018	PSMB1	3,961	7,56E-04
ENSG00000196214	ZNF766	-5,123	4,22E-06	ENSG00000004799	PDK4	3,984	6,88E-04
ENSG00000136436	CALCOCO2	-5,122	4,24E-06	ENSG00000104897	SF3A2	3,988	6,77E-04
ENSG00000205810	KLRC3	-5,111	4,48E-06	ENSG00000159202	UBE2Z	3,999	6,47E-04
ENSG00000183161	FANCF	-5,102	4,64E-06	ENSG00000179988	PSTK	4,003	6,39E-04
ENSG00000178828	RNF186	-5,1	4,64E-06	ENSG00000123810	B9D2	4,005	6,35E-04
ENSG00000117245	KIF17	-5,1	4,64E-06	ENSG00000172164	SNTB1	4,01	6,21E-04
ENSG00000122224	LY9	-5,1	4,64E-06	ENSG00000241343	RPL36A	4,03	5,72E-04
ENSG00000115221	ITGB6	-5,1	4,64E-06	ENSG00000079246	XRCC5	4,035	5,61E-04
ENSG00000118690	ARMC2	-5,1	4,64E-06	ENSG00000070831	CDC42	4,036	5,57E-04
ENSG00000167653	PSCA	-5,1	4,64E-06	ENSG00000179218	CALR	4,054	5,19E-04
ENSG00000160323	ADAMTS13	-5,1	4,64E-06	ENSG00000116584	ARHGEF2	4,055	5,17E-04
ENSG00000137491	SLCO2B1	-5,1	4,64E-06	ENSG00000141738	GRB7	4,063	5,00E-04

ENSG00000111087	GLI1	-5,1	4,64E-06
ENSG00000197991	PCDH20	-5,1	4,64E-06
ENSG00000099365	STX1B	-5,1	4,64E-06
ENSG00000185666	SYN3	-5,1	4,64E-06
ENSG00000186417	GLDN	-5,07	5,42E-06
ENSG00000170191	NANP	-5,065	5,55E-06
ENSG00000167447	SMG8	-5,061	5,65E-06
ENSG00000145386	CCNA2	-5,058	5,74E-06
ENSG00000061455	PRDM6	-5,056	5,79E-06
ENSG00000137504	CREBZF	-5,052	5,91E-06
ENSG00000102886	GDPD3	-5,051	5,91E-06
ENSG00000185485	SDHAP1	-5,042	6,20E-06
ENSG00000260456	C16orf95	-5,038	6,31E-06
ENSG00000130643	CALY	-5,035	6,41E-06
ENSG00000148572	NRBF2	-5,021	6,87E-06
ENSG00000134864	GGACT	-5,015	7,09E-06
ENSG00000189410	SH2D5	-5,005	7,19E-06
ENSG00000242125	SNHG3	-5,005	7,19E-06
ENSG00000198691	ABCA4	-5,005	7,19E-06
ENSG00000272031	ANKRD34A	-5,005	7,19E-06
ENSG00000132677	RHBG	-5,005	7,19E-06
ENSG00000143858	SYT2	-5,005	7,19E-06
ENSG00000119283	TRIM67	-5,005	7,19E-06
ENSG00000169618	PROKR1	-5,005	7,19E-06
ENSG00000119227	PIGZ	-5,005	7,19E-06
ENSG00000095203	EPB41L4B	-5,005	7,19E-06
ENSG00000205864	KRTAP5-6	-5,005	7,19E-06
ENSG00000165923	AGBL2	-5,005	7,19E-06
ENSG00000167780	SOAT2	-5,005	7,19E-06
ENSG00000120659	TNFSF11	-5,005	7,19E-06
ENSG00000091583	APOH	-5,005	7,19E-06
ENSG00000101470	TNNC2	-5,005	7,19E-06
ENSG00000154736	ADAMTS5	-5,005	7,19E-06
ENSG00000134594	RAB33A	-5,005	7,19E-06
ENSG0000014	OAZ3	-5,004	7,19E-06
ENSG00000137393	RNF144B	4,066	4,94E-04
ENSG00000168237	GLYCTK	4,077	4,71E-04
ENSG00000130702	LAMA5	4,084	4,59E-04
ENSG00000170631	ZNF16	4,084	4,59E-04
ENSG00000114573	ATP6V1A	4,086	4,56E-04
ENSG00000151876	FBXO4	4,093	4,44E-04
ENSG00000142541	RPL13A	4,095	4,40E-04
ENSG00000141873	SLC39A3	4,097	4,36E-04
ENSG00000155959	VBP1	4,106	4,20E-04
ENSG00000120733	KDM3B	4,118	4,00E-04
ENSG00000145494	NDUFS6	4,122	3,94E-04
ENSG00000069329	VPS35	4,13	3,80E-04
ENSG00000172954	LCLAT1	4,13	3,80E-04
ENSG00000179776	CDH5	4,133	3,76E-04
ENSG00000079435	LIPE	4,135	3,72E-04
ENSG00000092969	TGFB2	4,139	3,67E-04
ENSG00000150990	DHX37	4,142	3,62E-04
ENSG00000103199	ZNF500	4,143	3,62E-04
ENSG00000143320	CRABP2	4,154	3,46E-04
ENSG00000173120	KDM2A	4,159	3,37E-04
ENSG00000159556	ISL2	4,163	3,33E-04
ENSG00000132952	USPL1	4,17	3,23E-04
ENSG00000133028	SCO1	4,175	3,16E-04
ENSG00000116741	RGS2	4,183	3,06E-04
ENSG00000185112	FAM43A	4,192	2,94E-04
ENSG00000205060	SLC35B4	4,214	2,68E-04
ENSG00000009694	TENM1	4,247	2,32E-04
ENSG00000175311	ANKS4B	4,25	2,29E-04
ENSG00000221890	NPTXR	4,251	2,28E-04
ENSG00000221914	PPP2R2A	4,259	2,20E-04
ENSG00000179431	FJX1	4,261	2,18E-04
ENSG00000109736	MFSD10	4,279	2,02E-04
ENSG00000153187	HNRNPU	4,305	1,80E-04
ENSG00000125835	SNRPB	4,309	1,77E-04
ENSG0000013	DAGLA	4,314	1,73E-04

3450				4780			
ENSG00000143194	MAEL	-5,004	7,19E-06	ENSG00000196812	ZSCAN16	4,337	1,56E-04
ENSG00000152086	TUBA3E	-5,004	7,19E-06	ENSG00000059145	UNKL	4,361	1,41E-04
ENSG00000163827	LRRC2	-5,004	7,19E-06	ENSG00000186765	FSCN2	4,408	1,14E-04
ENSG00000138769	CDKL2	-5,004	7,19E-06	ENSG00000120437	ACAT2	4,417	1,10E-04
ENSG00000204618	RNF39	-5,004	7,19E-06	ENSG00000161800	RACGAP1	4,429	1,04E-04
ENSG00000196335	STK31	-5,004	7,19E-06	ENSG00000106636	YKT6	4,448	9,55E-05
ENSG00000005981	ASB4	-5,004	7,19E-06	ENSG00000169174	PCSK9	4,457	9,16E-05
ENSG00000158560	DYNC1I1	-5,004	7,19E-06	ENSG00000125430	HS3ST3B1	4,467	8,78E-05
ENSG00000001626	CFTR	-5,004	7,19E-06	ENSG00000121775	TMEM39B	4,471	8,60E-05
ENSG00000181690	PLAG1	-5,004	7,19E-06	ENSG00000235082	SUMO1P3	4,471	8,60E-05
ENSG00000170324	FRMPD2	-5,004	7,19E-06	ENSG00000197208	SLC22A4	4,471	8,60E-05
ENSG00000120054	CPN1	-5,004	7,19E-06	ENSG00000171989	LDHAL6B	4,471	8,60E-05
ENSG00000172572	PDE3A	-5,004	7,19E-06	ENSG00000171793	CTPS1	4,48	8,30E-05
ENSG00000168350	DEGS2	-5,004	7,19E-06	ENSG00000163352	LENEP	4,5	7,56E-05
ENSG00000284837	LOC339166	-5,004	7,19E-06	ENSG00000145911	N4BP3	4,5	7,56E-05
ENSG00000204323	SMIM5	-5,004	7,19E-06	ENSG00000148200	NR6A1	4,5	7,56E-05
ENSG00000212123	PRR22	-5,004	7,19E-06	ENSG00000206622	SNORA69	4,5	7,56E-05
ENSG00000197647	ZNF433	-5,004	7,19E-06	ENSG00000152669	CCNO	4,512	7,17E-05
ENSG00000185437	SH3BGR	-5,004	7,19E-06	ENSG00000166532	RIMKLB	4,513	7,15E-05
ENSG00000179918	SEPHS2	-5,002	7,26E-06	ENSG00000103042	SLC38A7	4,513	7,15E-05
ENSG00000168939	SPRY3	-4,99	7,67E-06	ENSG00000231991	ANXA2P2	4,514	7,14E-05
ENSG00000136295	TTYH3	-4,989	7,73E-06	ENSG00000135960	EDAR	4,515	7,13E-05
ENSG00000180061	TMEM150B	-4,988	7,75E-06	ENSG00000168765	GSTM4	4,515	7,13E-05
ENSG00000013619	MAMLD1	-4,987	7,81E-06	ENSG00000162745	OLFML2B	4,516	7,08E-05
ENSG00000105771	SMG9	-4,979	8,08E-06	ENSG00000196843	ARID5A	4,516	7,08E-05
ENSG00000173389	IQCF1	-4,979	8,10E-06	ENSG00000141028	CDRT15P1	4,516	7,08E-05
ENSG00000204314	LOC100507547	-4,977	8,15E-06	ENSG00000224420	ADM5	4,519	7,01E-05
ENSG00000111215	PRR4	-4,976	8,18E-06	ENSG00000158163	DZIP1L	4,521	6,98E-05
ENSG00000125144	MT1G	-4,966	8,61E-06	ENSG00000123411	IKZF4	4,521	6,98E-05
ENSG00000137310	TCF19	-4,959	8,90E-06	ENSG00000213918	DNASE1	4,528	6,78E-05
ENSG00000177981	ASB8	-4,952	9,19E-06	ENSG00000139625	MAP3K12	4,533	6,62E-05
ENSG00000178999	AURKB	-4,947	9,43E-06	ENSG00000188175	HEPACAM2	4,538	6,47E-05
ENSG00000187840	EIF4EBP1	-4,939	9,79E-06	ENSG00000113161	HMGCR	4,543	6,32E-05
ENSG00000199477	SNORA31	-4,933	1,01E-05	ENSG00000159346	ADIPOR1	4,548	6,20E-05

ENSG00000107242	PIP5K1B	-4,931	1,02E-05	ENSG00000169925	BRD3	4,559	5,89E-05
ENSG00000152683	SLC30A6	-4,93	1,03E-05	ENSG00000181284	TMEM102	4,565	5,72E-05
ENSG00000225470	JPX	-4,93	1,03E-05	ENSG00000162664	ZNF326	4,594	5,00E-05
ENSG00000206937	SNORA70B	-4,928	1,03E-05	ENSG00000167325	RRM1	4,601	4,85E-05
ENSG00000110900	TSPAN11	-4,914	1,11E-05	ENSG00000004487	KDM1A	4,611	4,61E-05
ENSG00000141522	ARHGDIA	-4,913	1,11E-05	ENSG00000086300	SNX10	4,616	4,51E-05
ENSG00000092758	COL9A3	-4,912	1,12E-05	ENSG00000175595	ERCC4	4,617	4,48E-05
ENSG00000213809	KLRK1	-4,909	1,13E-05	ENSG00000106236	NPTX2	4,621	4,41E-05
ENSG00000260287	TBC1D3G	-4,908	1,14E-05	ENSG00000181222	POLR2A	4,623	4,38E-05
ENSG00000128563	PRKRIP1	-4,907	1,14E-05	ENSG00000205581	HMGN1	4,631	4,23E-05
ENSG00000182870	GALNT9	-4,903	1,16E-05	ENSG00000196182	STK40	4,632	4,21E-05
ENSG00000125931	CITED1	-4,903	1,16E-05	ENSG00000164104	HMGB2	4,645	3,97E-05
ENSG00000213139	CRYGS	-4,902	1,16E-05	ENSG00000006625	GGCT	4,648	3,91E-05
ENSG00000174521	TTC9B	-4,902	1,16E-05	ENSG00000112715	VEGFA	4,651	3,86E-05
ENSG00000163762	TM4SF18	-4,9	1,18E-05	ENSG00000088930	XRN2	4,658	3,74E-05
ENSG00000164053	TREX1	-4,899	1,18E-05	ENSG00000176715	ACSF3	4,658	3,73E-05
ENSG00000165113	GKAP1	-4,898	1,19E-05	ENSG00000137642	SORL1	4,662	3,67E-05
ENSG00000119946	CNNM1	-4,897	1,19E-05	ENSG00000178163	ZNF518B	4,667	3,58E-05
ENSG00000196428	TSC22D2	-4,893	1,21E-05	ENSG00000100567	PSMA3	4,67	3,52E-05
ENSG00000198848	CES1	-4,891	1,23E-05	ENSG00000180263	FGD6	4,696	3,12E-05
ENSG00000226887	ERVMER34-1	-4,881	1,29E-05	ENSG00000054267	ARID4B	4,698	3,09E-05
ENSG00000139880	CDH24	-4,862	1,41E-05	ENSG00000141642	ELAC1	4,705	2,98E-05
ENSG00000146674	IGFBP3	-4,861	1,42E-05	ENSG00000149256	TENM4	4,742	2,50E-05
ENSG00000132185	FCRLA	-4,86	1,42E-05	ENSG00000148143	ZNF462	4,767	2,21E-05
ENSG00000070785	EIF2B3	-4,859	1,43E-05	ENSG00000164902	PHAX	4,783	2,05E-05
ENSG00000196821	C6orf106	-4,852	1,48E-05	ENSG00000173846	PLK3	4,793	1,96E-05
ENSG00000257122	RRN3P3	-4,825	1,68E-05	ENSG00000170634	ACYP2	4,796	1,93E-05
ENSG00000204271	SPIN3	-4,825	1,68E-05	ENSG00000180479	ZNF571	4,813	1,78E-05
ENSG00000270441	LAMB2P1	-4,824	1,69E-05	ENSG00000117010	ZNF684	4,819	1,73E-05
ENSG00000136404	TM6SF1	-4,808	1,82E-05	ENSG00000168884	TNIP2	4,845	1,53E-05
ENSG00000160214	RRP1	-4,804	1,86E-05	ENSG00000173852	DPY19L1	4,846	1,52E-05
ENSG00000168924	LETM1	-4,799	1,90E-05	ENSG00000136930	PSMB7	4,856	1,45E-05
ENSG00000163644	PPM1K	-4,789	2,00E-05	ENSG00000185261	KIAA0825	4,866	1,38E-05
ENSG00000101412	E2F1	-4,779	2,09E-05	ENSG00000169418	NPR1	4,869	1,36E-05
ENSG0000011	ACADM	-4,753	2,37E-05	ENSG0000023	HOXB-AS3	4,872	1,35E-05

7054				3101			
ENSG00000183010	PYCR1	-4,749	2,42E-05	ENSG00000064933	PMS1	4,881	1,29E-05
ENSG00000110697	PITPNM1	-4,731	2,64E-05	ENSG00000197046	SIGLEC15	4,886	1,26E-05
ENSG00000167965	MLST8	-4,72	2,78E-05	ENSG00000160194	NDUFV3	4,894	1,21E-05
ENSG00000105516	DBP	-4,686	3,26E-05	ENSG00000169599	NFU1	4,911	1,12E-05
ENSG00000105290	APLP1	-4,649	3,89E-05	ENSG00000197619	ZNF615	4,912	1,12E-05
ENSG00000052749	RRP12	-4,644	3,97E-05	ENSG00000112769	LAMA4	4,946	9,49E-06
ENSG00000161904	LEMD2	-4,627	4,31E-05	ENSG00000185252	ZNF74	4,949	9,34E-06
ENSG00000158292	GPR153	-4,626	4,33E-05	ENSG00000149716	ORAOV1	4,959	8,90E-06
ENSG00000147536	GINS4	-4,623	4,37E-05	ENSG00000130726	TRIM28	4,963	8,72E-06
ENSG00000254402	LRRC24	-4,621	4,42E-05	ENSG00000176840	MIR7-3HG	4,966	8,62E-06
ENSG00000105976	MET	-4,588	5,14E-05	ENSG00000171435	KSR2	4,97	8,43E-06
ENSG00000164611	PTTG1	-4,587	5,16E-05	ENSG00000130005	GAMT	4,983	7,93E-06
ENSG00000155897	ADCY8	-4,558	5,93E-05	ENSG00000101843	PSMD10	4,986	7,81E-06
ENSG00000175426	PCSK1	-4,551	6,10E-05	ENSG00000140263	SORD	4,998	7,40E-06
ENSG00000259494	MRPL46	-4,545	6,29E-05	ENSG00000197978	GOLGA6L9	5,034	6,43E-06
ENSG00000129474	AJUBA	-4,541	6,37E-05	ENSG00000175395	ZNF25	5,059	5,70E-06
ENSG00000139990	DCAF5	-4,535	6,57E-05	ENSG00000131652	THOC6	5,067	5,50E-06
ENSG00000164684	ZNF704	-4,526	6,84E-05	ENSG00000188859	FAM78B	5,068	5,46E-06
ENSG00000155729	KCTD18	-4,519	7,01E-05	ENSG00000132031	MATN3	5,075	5,29E-06
ENSG00000125740	FOSB	-4,519	7,03E-05	ENSG00000137409	MTCH1	5,091	4,86E-06
ENSG00000181649	PHLDA2	-4,517	7,08E-05	ENSG00000137509	PRCP	5,092	4,84E-06
ENSG00000128342	LIF	-4,502	7,53E-05	ENSG00000181826	RELL1	5,098	4,70E-06
ENSG00000164120	HPGD	-4,493	7,81E-05	ENSG00000137571	SLCO5A1	5,099	4,66E-06
ENSG00000082996	RNF13	-4,481	8,24E-05	ENSG00000113569	NUP155	5,105	4,61E-06
ENSG00000102226	USP11	-4,48	8,29E-05	ENSG00000197562	RAB40C	5,114	4,40E-06
ENSG00000132970	WASF3	-4,478	8,35E-05	ENSG00000011478	QPCTL	5,116	4,35E-06
ENSG00000101247	NDUFAF5	-4,46	9,06E-05	ENSG00000079150	FKBP7	5,129	4,08E-06
ENSG00000087086	FTL	-4,453	9,34E-05	ENSG00000111846	GCNT2	5,134	4,03E-06
ENSG00000152147	GEMIN6	-4,451	9,41E-05	ENSG00000196605	ZNF846	5,14	4,03E-06
ENSG00000165879	FRAT1	-4,443	9,73E-05	ENSG00000205710	C17orf107	5,161	3,66E-06
ENSG00000104213	PDGFRL	-4,441	9,85E-05	ENSG00000206948	SNORA36A	5,161	3,66E-06
ENSG00000215915	ATAD3C	-4,408	1,14E-04	ENSG00000147799	ARHGAP39	5,162	3,66E-06
ENSG00000171763	SPATA5L1	-4,392	1,23E-04	ENSG00000149485	FADS1	5,173	3,47E-06
ENSG00000134684	YARS	-4,383	1,28E-04	ENSG00000213693	SEC14L1P1	5,19	3,21E-06

ENSG00000180758	GPR157	-4,382	1,28E-04	ENSG00000143772	ITPKB	5,197	3,11E-06
ENSG00000188566	NDOR1	-4,368	1,37E-04	ENSG00000112852	PCDHB2	5,197	3,11E-06
ENSG00000205220	PSMB10	-4,361	1,41E-04	ENSG00000049089	COL9A2	5,205	3,00E-06
ENSG00000215183	MSMP	-4,353	1,46E-04	ENSG00000273514	FOXD4L6	5,208	2,96E-06
ENSG00000181610	MRPS23	-4,346	1,50E-04	ENSG00000117335	CD46	5,208	2,96E-06
ENSG00000122068	FYTTD1	-4,338	1,56E-04	ENSG00000196233	LCOR	5,209	2,95E-06
ENSG00000132716	DCAF8	-4,337	1,56E-04	ENSG00000259581	TYRO3P	5,209	2,95E-06
ENSG00000107562	CXCL12	-4,329	1,62E-04	ENSG00000215045	GRID2IP	5,212	2,90E-06
ENSG00000178996	SNX18	-4,302	1,82E-04	ENSG00000162571	TTLL10	5,215	2,86E-06
ENSG00000176532	PRR15	-4,285	1,97E-04	ENSG00000177301	KCNA2	5,215	2,86E-06
ENSG00000065833	ME1	-4,269	2,11E-04	ENSG00000236334	PPIAL4G	5,215	2,86E-06
ENSG00000149743	TRPT1	-4,245	2,33E-04	ENSG00000143512	HHIPL2	5,215	2,86E-06
ENSG00000162849	KIF26B	-4,204	2,79E-04	ENSG00000163803	PLB1	5,215	2,86E-06
ENSG00000168282	MGAT2	-4,198	2,87E-04	ENSG00000213901	SLC23A3	5,215	2,86E-06
ENSG00000140807	NKD1	-4,19	2,97E-04	ENSG00000272573	MUSTN1	5,215	2,86E-06
ENSG00000166166	TRMT61A	-4,183	3,06E-04	ENSG00000113231	PDE8B	5,215	2,86E-06
ENSG00000115350	POLE4	-4,18	3,10E-04	ENSG00000232159	RAB9BP1	5,215	2,86E-06
ENSG00000100473	COCH	-4,172	3,20E-04	ENSG00000246334	PRR7-AS1	5,215	2,86E-06
ENSG00000170906	NDUFA3	-4,166	3,28E-04	ENSG00000096088	PGC	5,215	2,86E-06
ENSG00000185634	SHC4	-4,149	3,52E-04	ENSG00000132437	DDC	5,215	2,86E-06
ENSG00000174013	FBXO45	-4,146	3,57E-04	ENSG00000104327	CALB1	5,215	2,86E-06
ENSG00000101665	SMAD7	-4,095	4,40E-04	ENSG00000248599	FLJ42969	5,215	2,86E-06
ENSG00000013583	HEBP1	-4,09	4,50E-04	ENSG00000234618	RPSAP9	5,215	2,86E-06
ENSG00000178934	LGALS7B	-4,088	4,52E-04	ENSG00000136918	WDR38	5,215	2,86E-06
ENSG00000097046	CDC7	-4,086	4,56E-04	ENSG00000198610	AKR1C4	5,215	2,86E-06
ENSG00000071073	MGAT4A	-4,073	4,81E-04	ENSG00000138161	CUZD1	5,215	2,86E-06
ENSG00000123297	TSFM	-4,072	4,81E-04	ENSG00000254827	SLC22A18AS	5,215	2,86E-06
ENSG00000120742	SERP1	-4,066	4,94E-04	ENSG00000166833	NAV2	5,215	2,86E-06
ENSG00000181472	ZBTB2	-4,051	5,24E-04	ENSG00000139194	RBP5	5,215	2,86E-06
ENSG00000234585	CCT6P3	-4,046	5,35E-04	ENSG00000207313	SNORA2B	5,215	2,86E-06
ENSG00000143416	SELENBP1	-4,041	5,46E-04	ENSG00000183092	BEGAIN	5,215	2,86E-06
ENSG00000146063	TRIM41	-4,022	5,91E-04	ENSG00000166143	PPP1R14D	5,215	2,86E-06
ENSG00000084764	MAPRE3	-4,001	6,44E-04	ENSG00000213398	LCAT	5,215	2,86E-06
ENSG00000165731	RET	-3,999	6,49E-04	ENSG00000171431	KRT20	5,215	2,86E-06
ENSG0000016	NRG4	-3,998	6,49E-04	ENSG0000013	MYCBPAP	5,215	2,86E-06

9752				6449			
ENSG00000221963	APOL6	-3,997	6,52E-04	ENSG00000108370	RGS9	5,215	2,86E-06
ENSG00000147224	PRPS1	-3,989	6,73E-04	ENSG00000167216	KATNAL2	5,215	2,86E-06
ENSG00000163743	RCHY1	-3,981	6,95E-04	ENSG00000174788	PCP2	5,215	2,86E-06
ENSG00000165271	NOL6	-3,96	7,59E-04	ENSG00000269304	FKBP1AP1	5,215	2,86E-06
ENSG00000058600	POLR3E	-3,954	7,76E-04	ENSG00000205726	ITSN1	5,215	2,86E-06
ENSG00000133739	LRRCC1	-3,949	7,91E-04	ENSG00000214827	MTCP1	5,215	2,86E-06
ENSG00000140859	KIFC3	-3,938	8,27E-04	ENSG00000174173	TRMT10C	5,229	2,78E-06
ENSG00000122512	PMS2	-3,928	8,59E-04	ENSG00000179750	APOBEC3B	5,233	2,73E-06
ENSG00000141433	ADCYAP1	-3,927	8,61E-04	ENSG00000265293	ARGFXP2	5,236	2,71E-06
ENSG00000068120	COASY	-3,924	8,72E-04	ENSG00000242110	AMACR	5,24	2,66E-06
ENSG00000175931	UBE2O	-3,921	8,85E-04	ENSG00000135736	CCDC102A	5,245	2,59E-06
ENSG00000185015	CA13	-3,918	8,94E-04	ENSG00000205763	RP9P	5,25	2,52E-06
ENSG00000100410	PHF5A	-3,896	9,76E-04	ENSG00000271699	SNX29P2	5,25	2,52E-06
ENSG00000196313	POM121	-3,879	1,04E-03	ENSG00000117643	MAN1C1	5,256	2,44E-06
ENSG00000198743	SLC5A3	-3,863	1,11E-03	ENSG00000197312	DDI2	5,258	2,42E-06
ENSG00000170275	CRTAP	-3,858	1,14E-03	ENSG00000188095	MESP2	5,258	2,42E-06
ENSG00000173013	CCDC96	-3,849	1,17E-03	ENSG00000162733	DDR2	5,258	2,42E-06
ENSG00000252712	SCARNA14	-3,845	1,19E-03	ENSG00000084072	PPIE	5,259	2,42E-06
ENSG00000137843	PAK6	-3,834	1,25E-03	ENSG00000225447	RPS15AP10	5,26	2,42E-06
ENSG00000137804	NUSAP1	-3,833	1,25E-03	ENSG00000115226	FNDC4	5,26	2,42E-06
ENSG00000049883	PTCD2	-3,821	1,31E-03	ENSG00000136546	SCN7A	5,26	2,42E-06
ENSG00000106723	SPIN1	-3,82	1,31E-03	ENSG00000115896	PLCL1	5,26	2,42E-06
ENSG00000188338	SLC38A3	-3,783	1,51E-03	ENSG00000249020	SNORA58	5,26	2,42E-06
ENSG00000089723	OTUB2	-3,774	1,57E-03	ENSG00000196748	CLPSL2	5,26	2,42E-06
ENSG00000060491	OGFR	-3,76	1,66E-03	ENSG00000166106	ADAMTS15	5,26	2,42E-06
ENSG00000175841	FAM172BP	-3,758	1,67E-03	ENSG00000025423	HSD17B6	5,26	2,42E-06
ENSG00000184845	DRD1	-3,758	1,67E-03	ENSG00000111052	LIN7A	5,26	2,42E-06
ENSG00000187735	TCEA1	-3,748	1,73E-03	ENSG00000133106	EPSTI1	5,26	2,42E-06
ENSG00000131781	FMO5	-3,748	1,73E-03	ENSG00000186910	SERPINA11	5,26	2,42E-06
ENSG00000166123	GPT2	-3,739	1,79E-03	ENSG00000177508	IRX3	5,26	2,42E-06
ENSG00000181523	SGSH	-3,737	1,80E-03	ENSG00000180626	ZNF594	5,26	2,42E-06
ENSG00000185946	RNPC3	-3,72	1,92E-03	ENSG00000179761	PIPOX	5,26	2,42E-06
ENSG00000115541	HSPE1	-3,704	2,04E-03	ENSG00000159915	ZNF233	5,26	2,42E-06
ENSG00000112039	FANCE	-3,67	2,31E-03	ENSG00000099326	MZF1	5,26	2,42E-06

ENSG00000173171	MTX1	-3,665	2,37E-03	ENSG00000172264	MACROD2	5,26	2,42E-06
ENSG00000157212	PAXIP1	-3,662	2,38E-03	ENSG00000149634	SPATA25	5,26	2,42E-06
ENSG00000169221	TBC1D10B	-3,654	2,45E-03	ENSG00000131831	RAI2	5,26	2,42E-06
ENSG00000115084	SLC35F5	-3,651	2,48E-03	ENSG00000102078	SLC25A14	5,26	2,42E-06
ENSG00000180329	CCDC43	-3,648	2,51E-03	ENSG00000162129	CLPB	5,26	2,42E-06
ENSG00000113732	ATP6V0E1	-3,647	2,51E-03	ENSG00000132872	SYT4	5,261	2,42E-06
ENSG00000127957	PMS2P3	-3,646	2,52E-03	ENSG00000185758	CLDN24	5,284	2,21E-06
ENSG00000241685	ARPC1A	-3,643	2,55E-03	ENSG00000185379	RAD51D	5,284	2,21E-06
ENSG00000183775	KCTD16	-3,64	2,57E-03	ENSG00000213057	C1orf220	5,285	2,21E-06
ENSG00000124107	SLPI	-3,63	2,67E-03	ENSG00000172771	EFCAB12	5,285	2,21E-06
ENSG00000164039	BDH2	-3,62	2,77E-03	ENSG00000154548	SRSF12	5,285	2,21E-06
ENSG00000140743	CDR2	-3,618	2,79E-03	ENSG00000073067	CYP2W1	5,285	2,21E-06
ENSG00000144655	CSRNP1	-3,618	2,79E-03	ENSG00000241644	INMT	5,285	2,21E-06
ENSG00000149483	TMEM138	-3,615	2,82E-03	ENSG00000235217	TSPY26P	5,285	2,21E-06
ENSG00000115107	STEAP3	-3,614	2,84E-03	ENSG00000240288	GHRLOS	5,291	2,17E-06
ENSG00000164181	ELOVL7	-3,611	2,86E-03	ENSG00000135205	CCDC146	5,294	2,14E-06
ENSG00000169683	LRRC45	-3,61	2,87E-03	ENSG00000176401	EID2B	5,306	2,00E-06
ENSG00000153317	ASAP1	-3,602	2,96E-03	ENSG00000181315	ZNF322	5,32	1,87E-06
ENSG00000185728	YTHDF3	-3,598	2,99E-03	ENSG00000152380	FAM151B	5,321	1,86E-06
ENSG00000253352	TUG1	-3,578	3,22E-03	ENSG00000025434	NR1H3	5,322	1,85E-06
ENSG00000175324	LSM1	-3,57	3,31E-03	ENSG00000181754	AMIGO1	5,322	1,85E-06
ENSG00000196712	NF1	-3,563	3,41E-03	ENSG00000160766	GBAP1	5,322	1,85E-06
ENSG00000205744	DENND1C	-3,558	3,46E-03	ENSG00000118194	TNNT2	5,322	1,85E-06
ENSG00000124279	FASTKD3	-3,558	3,46E-03	ENSG00000171121	KCNMB3	5,322	1,85E-06
ENSG00000102921	N4BP1	-3,554	3,51E-03	ENSG00000081818	PCDHB4	5,322	1,85E-06
ENSG00000107537	PHYH	-3,55	3,55E-03	ENSG00000137273	FOXF2	5,322	1,85E-06
ENSG00000121680	PEX16	-3,533	3,78E-03	ENSG00000146197	SCUBE3	5,322	1,85E-06
ENSG00000106070	GRB10	-3,532	3,80E-03	ENSG00000156509	FBXO43	5,322	1,85E-06
ENSG00000128463	EMC4	-3,525	3,88E-03	ENSG00000197291	RAMP2-AS1	5,322	1,85E-06
ENSG00000136826	KLF4	-3,516	4,03E-03	ENSG00000147251	DOCK11	5,322	1,85E-06
ENSG00000179562	GCC1	-3,507	4,14E-03	ENSG00000171388	APLN	5,322	1,85E-06
ENSG00000106546	AHR	-3,505	4,16E-03	ENSG00000180596	HIST1H2BE	5,325	1,85E-06
ENSG00000162757	C1orf74	-3,503	4,20E-03	ENSG00000207181	SNORA14B	5,326	1,85E-06
ENSG00000173212	MAB21L3	-3,498	4,27E-03	ENSG00000185567	AHNAK2	5,331	1,81E-06
ENSG0000018	SLC51B	-3,495	4,31E-03	ENSG0000022	ZGLP1	5,342	1,70E-06

6198				0201			
ENSG00000162600	OMA1	-3,491	4,38E-03	ENSG00000088881	EBF4	5,344	1,69E-06
ENSG00000168883	USP39	-3,48	4,55E-03	ENSG00000116031	CD207	5,347	1,66E-06
ENSG00000161217	PCYT1A	-3,477	4,58E-03	ENSG00000151292	CSNK1G3	5,347	1,66E-06
ENSG00000101343	CRNKL1	-3,473	4,65E-03	ENSG00000248449	PCDHGB8P	5,347	1,66E-06
ENSG00000125089	SH3TC1	-3,465	4,78E-03	ENSG00000204390	HSPA1L	5,347	1,66E-06
ENSG00000112343	TRIM38	-3,464	4,79E-03	ENSG00000166924	NYAP1	5,347	1,66E-06
ENSG00000148672	GLUD1	-3,46	4,86E-03	ENSG00000090382	LYZ	5,347	1,66E-06
ENSG00000253729	PRKDC	-3,459	4,87E-03	ENSG00000179029	TMEM107	5,347	1,66E-06
ENSG00000108389	MTMR4	-3,457	4,91E-03	ENSG00000175170	FAM182B	5,347	1,66E-06
ENSG00000181798	LINC00471	-3,45	5,02E-03	ENSG00000099998	GGT5	5,347	1,66E-06
ENSG00000219481	NBPF1	-3,444	5,11E-03	ENSG00000158301	GPRASP2	5,347	1,66E-06
ENSG00000162676	GFI1	-3,444	5,11E-03	ENSG00000133142	TCEAL4	5,347	1,66E-06
ENSG00000134369	NAV1	-3,443	5,12E-03	ENSG00000244026	FAM86DP	5,355	1,63E-06
ENSG00000138771	SHROOM3	-3,443	5,13E-03	ENSG00000102878	HSF4	5,355	1,63E-06
ENSG00000160695	VPS11	-3,439	5,19E-03	ENSG00000084628	NKAIN1	5,356	1,63E-06
ENSG00000172331	BPGM	-3,438	5,21E-03	ENSG00000101850	GPR143	5,364	1,57E-06
ENSG00000169957	ZNF768	-3,435	5,25E-03	ENSG00000124939	SCGB2A1	5,364	1,56E-06
ENSG00000106733	NMRK1	-3,425	5,43E-03	ENSG00000205755	CRLF2	5,366	1,56E-06
ENSG00000285077	ARHGAP11B	-3,424	5,46E-03	ENSG00000101306	MYLK2	5,373	1,50E-06
ENSG00000009954	BAZ1B	-3,424	5,46E-03	ENSG00000167711	SERPINF2	5,373	1,50E-06
ENSG00000154545	MAGED4	-3,424	5,46E-03	ENSG00000109089	CDR2L	5,375	1,49E-06
ENSG00000174444	RPL4	-3,415	5,61E-03	ENSG00000140297	GCNT3	5,377	1,48E-06
ENSG00000107863	ARHGAP21	-3,415	5,61E-03	ENSG00000131981	LGALS3	5,394	1,36E-06
ENSG00000214753	HNRNPUL2	-3,401	5,89E-03	ENSG00000128242	GAL3ST1	5,398	1,32E-06
ENSG00000155506	LARP1	-3,398	5,96E-03	ENSG00000200237	SNORA70	5,411	1,24E-06
ENSG00000138231	DBR1	-3,398	5,96E-03	ENSG00000109771	LRP2BP	5,414	1,22E-06
ENSG00000146425	DYNLT1	-3,396	6,00E-03	ENSG00000168661	ZNF30	5,415	1,22E-06
ENSG00000203705	TATDN3	-3,391	6,09E-03	ENSG00000105672	ETV2	5,428	1,13E-06
ENSG00000125812	GZF1	-3,389	6,13E-03	ENSG00000159228	CBR1	5,434	1,10E-06
ENSG00000204568	MRPS18B	-3,387	6,17E-03	ENSG00000132718	SYT11	5,452	9,97E-07
ENSG00000157916	RER1	-3,385	6,22E-03	ENSG00000135773	CAPN9	5,457	9,71E-07
ENSG00000058668	ATP2B4	-3,375	6,44E-03	ENSG00000204934	ATP6V0E2-AS1	5,457	9,71E-07
ENSG00000179913	B3GNT3	-3,371	6,52E-03	ENSG00000172650	AGAP5	5,457	9,71E-07
ENSG00000169439	SDC2	-3,365	6,65E-03	ENSG00000197696	NMB	5,457	9,71E-07

ENSG00000163171	CDC42EP3	-3,363	6,68E-03	ENSG00000139344	AMDHD1	5,469	9,12E-07
ENSG00000196793	ZNF239	-3,362	6,70E-03	ENSG00000101608	MYL12A	5,473	8,97E-07
ENSG00000177311	ZBTB38	-3,36	6,74E-03	ENSG00000140848	CPNE2	5,479	8,70E-07
ENSG00000119844	AFTPH	-3,359	6,76E-03	ENSG00000166529	ZSCAN21	5,48	8,66E-07
ENSG00000146386	ABRACL	-3,354	6,89E-03	ENSG00000250120	PCDHA10	5,488	8,29E-07
ENSG00000177465	ACOT4	-3,35	6,96E-03	ENSG00000132471	WBP2	5,515	7,16E-07
ENSG00000099889	ARVCF	-3,344	7,11E-03	ENSG00000204967	PCDHA4	5,517	7,10E-07
ENSG00000157445	CACNA2D3	-3,343	7,14E-03	ENSG00000118620	ZNF430	5,527	6,73E-07
ENSG00000100813	ACIN1	-3,341	7,19E-03	ENSG00000213760	ATP6V1G2	5,532	6,54E-07
ENSG00000197063	MAFG	-3,34	7,20E-03	ENSG00000117115	PADI2	5,577	5,11E-07
ENSG00000090674	MCOLN1	-3,331	7,41E-03	ENSG00000156531	PHF6	5,583	4,95E-07
ENSG00000155792	DEPTOR	-3,306	8,05E-03	ENSG00000168411	RFWD3	5,589	4,79E-07
ENSG00000126460	PRRG2	-3,302	8,15E-03	ENSG00000196365	LONP1	5,6	4,52E-07
ENSG00000164144	ARFIP1	-3,297	8,30E-03	ENSG00000135486	HNRNPA1	5,602	4,48E-07
ENSG00000262096	PCDHB19P	-3,294	8,37E-03	ENSG00000213741	RPS29	5,613	4,23E-07
ENSG00000099910	KLHL22	-3,284	8,66E-03	ENSG00000196357	ZNF565	5,656	3,32E-07
ENSG00000139977	NAA30	-3,28	8,77E-03	ENSG00000223572	CKMT1A	5,668	3,09E-07
ENSG00000149679	CABLES2	-3,28	8,77E-03	ENSG00000167100	SAMD14	5,683	2,84E-07
ENSG00000120868	APAF1	-3,278	8,82E-03	ENSG00000119878	CRIPT	5,697	2,63E-07
ENSG00000187068	C3orf70	-3,274	8,94E-03	ENSG00000132781	MUTYH	5,707	2,50E-07
ENSG00000075415	SLC25A3	-3,273	8,96E-03	ENSG00000249158	PCDHA11	5,714	2,39E-07
ENSG00000120942	UBIAD1	-3,272	8,97E-03	ENSG00000146556	WASH2P	5,726	2,24E-07
ENSG00000186187	ZNRF1	-3,271	9,00E-03	ENSG00000214013	GANC	5,753	1,93E-07
ENSG00000172336	POP7	-3,27	9,02E-03	ENSG00000138119	MYOF	5,77	1,75E-07
ENSG00000196975	ANXA4	-3,264	9,20E-03	ENSG00000105085	MED26	5,807	1,41E-07
ENSG00000178927	C17orf62	-3,261	9,28E-03	ENSG00000103494	RPGRIP1L	5,807	1,41E-07
ENSG00000067221	STOML1	-3,251	9,60E-03	ENSG00000179010	MRFAP1	5,809	1,40E-07
ENSG00000123836	PFKFB2	-3,248	9,66E-03	ENSG00000159899	NPR2	5,817	1,34E-07
ENSG00000090534	THPO	-3,247	9,71E-03	ENSG00000152240	HAUS1	5,825	1,29E-07
ENSG00000128203	ASPHD2	-3,246	9,74E-03	ENSG00000117152	RGS4	5,829	1,26E-07
ENSG00000109919	MTCH2	-3,239	9,96E-03	ENSG00000184465	WDR27	5,856	1,08E-07
ENSG00000037897	METTL1	-3,237	1,00E-02	ENSG00000147119	CHST7	5,873	9,77E-08
ENSG00000154856	APCDD1	-3,228	1,03E-02	ENSG00000164877	MICALL2	5,876	9,61E-08
ENSG00000133056	PIK3C2B	-3,227	1,03E-02	ENSG00000132740	IGHMBP2	5,886	9,06E-08
ENSG0000017	PFAS	-3,223	1,04E-02	ENSG0000009	HSP90AB1	5,887	9,00E-08

8921				6384			
ENSG00000173011	TADA2B	-3,221	1,05E-02	ENSG00000119673	ACOT2	5,894	8,70E-08
ENSG00000133477	FAM83F	-3,219	1,06E-02	ENSG00000221737	MIR548I1	5,906	8,06E-08
ENSG00000188994	ZNF292	-3,212	1,08E-02	ENSG00000274211	SOCS7	5,93	7,03E-08
ENSG00000152942	RAD17	-3,211	1,08E-02	ENSG00000163694	RBM47	5,931	7,00E-08
ENSG00000196417	ZNF765	-3,208	1,09E-02	ENSG00000170835	CEL	5,932	6,98E-08
ENSG00000077312	SNRPA	-3,207	1,10E-02	ENSG00000167895	TMC8	5,941	6,65E-08
ENSG00000134574	DDB2	-3,204	1,10E-02	ENSG00000160818	GPATCH4	5,943	6,58E-08
ENSG00000175220	ARHGAP1	-3,198	1,13E-02	ENSG00000164855	TMEM184A	5,947	6,43E-08
ENSG00000101210	EEF1A2	-3,194	1,14E-02	ENSG00000165097	KDM1B	5,956	6,10E-08
ENSG00000029993	HMGB3	-3,193	1,15E-02	ENSG00000196611	MMP1	5,976	5,44E-08
ENSG00000132874	SLC14A2	-3,188	1,16E-02	ENSG00000188996	HUS1B	5,982	5,28E-08
ENSG00000168286	THAP11	-3,188	1,16E-02	ENSG00000180423	HARBI1	5,986	5,14E-08
ENSG00000138435	CHRNA1	-3,186	1,17E-02	ENSG00000100994	PYGB	5,996	4,85E-08
ENSG00000168264	IRF2BP2	-3,179	1,20E-02	ENSG00000291107	LOC374443	6,009	4,50E-08
ENSG00000130816	DNMT1	-3,174	1,21E-02	ENSG00000116221	MRPL37	6,012	4,43E-08
ENSG00000070526	ST6GALNAC1	-3,164	1,25E-02	ENSG00000069482	GAL	6,021	4,18E-08
ENSG00000104221	BRF2	-3,163	1,26E-02	ENSG00000116668	SWT1	6,022	4,18E-08
ENSG00000244274	DBNDD2	-3,153	1,29E-02	ENSG00000221916	C19orf73	6,024	4,14E-08
ENSG00000163536	SERPINI1	-3,152	1,30E-02	ENSG00000122970	IFT81	6,025	4,10E-08
ENSG00000143367	TUFT1	-3,147	1,32E-02	ENSG00000185088	RPS27L	6,031	3,97E-08
ENSG00000119760	SUPT7L	-3,139	1,35E-02	ENSG00000099139	PCSK5	6,072	3,10E-08
ENSG00000171492	LRRC8D	-3,137	1,36E-02	ENSG00000104872	PIH1D1	6,083	2,92E-08
ENSG00000153944	MSI2	-3,135	1,37E-02	ENSG00000108852	MPP2	6,091	2,79E-08
ENSG00000114125	RNF7	-3,134	1,37E-02	ENSG00000205885	C1RL-AS1	6,098	2,68E-08
ENSG00000159267	HLCS	-3,132	1,38E-02	ENSG00000100575	TIMM9	6,102	2,61E-08
ENSG00000132405	TBC1D14	-3,131	1,39E-02	ENSG00000152684	PELO	6,105	2,57E-08
ENSG00000240065	PSMB9	-3,123	1,42E-02	ENSG00000196369	SRGAP2B	6,12	2,34E-08
ENSG00000197019	SERTAD1	-3,123	1,42E-02	ENSG00000167889	MGAT5B	6,123	2,30E-08
ENSG00000183155	RABIF	-3,122	1,43E-02	ENSG00000197766	CFD	6,126	2,27E-08
ENSG00000114127	XRN1	-3,121	1,43E-02	ENSG00000154920	EME1	6,126	2,27E-08
ENSG00000054179	ENTPD2	-3,117	1,45E-02	ENSG00000140398	NEIL1	6,132	2,21E-08
ENSG00000169188	APEX2	-3,111	1,47E-02	ENSG00000112033	PPARD	6,152	1,96E-08
ENSG00000213588	ZBTB9	-3,11	1,47E-02	ENSG00000026652	AGPAT4	6,163	1,84E-08
ENSG00000196704	AMZ2	-3,106	1,49E-02	ENSG00000166886	NAB2	6,165	1,82E-08

ENSG00000107816	LZTS2	-3,105	1,50E-02	ENSG00000176020	AMIGO3	6,179	1,66E-08
ENSG00000105656	ELL	-3,105	1,50E-02	ENSG00000137801	THBS1	6,197	1,49E-08
ENSG00000143578	CREB3L4	-3,104	1,50E-02	ENSG00000181982	CCDC149	6,201	1,46E-08
ENSG00000182325	FBXL6	-3,102	1,51E-02	ENSG00000188672	RHCE	6,202	1,45E-08
ENSG00000156802	ATAD2	-3,096	1,54E-02	ENSG00000120158	RCL1	6,204	1,43E-08
ENSG00000189241	TSPYL1	-3,088	1,58E-02	ENSG00000117632	STMN1	6,217	1,32E-08
ENSG00000154059	IMPACT	-3,084	1,59E-02	ENSG00000120053	GOT1	6,245	1,11E-08
ENSG00000185246	PRPF39	-3,082	1,61E-02	ENSG00000106993	CDC37L1	6,256	1,04E-08
ENSG00000108828	VAT1	-3,081	1,61E-02	ENSG00000100344	PNPLA3	6,265	9,82E-09
ENSG00000144837	PLA1A	-3,079	1,62E-02	ENSG00000240386	LCE1F	6,27	9,48E-09
ENSG00000143870	PDIA6	-3,078	1,62E-02	ENSG00000182923	CEP63	6,275	9,23E-09
ENSG00000117036	ETV3	-3,076	1,63E-02	ENSG00000103196	CRISPLD2	6,286	8,68E-09
ENSG00000155329	ZCCHC10	-3,074	1,64E-02	ENSG00000198492	YTHDF2	6,323	6,87E-09
ENSG00000173614	NMNAT1	-3,073	1,64E-02	ENSG00000258289	CHURC1	6,357	5,51E-09
ENSG00000130177	CDC16	-3,073	1,64E-02	ENSG00000261461	UBE2MP1	6,372	5,01E-09
ENSG00000114315	HES1	-3,072	1,64E-02	ENSG00000095752	IL11	6,387	4,56E-09
ENSG00000168393	DTYMK	-3,072	1,64E-02	ENSG00000139725	RHOF	6,389	4,51E-09
ENSG00000198915	RASGEF1A	-3,061	1,70E-02	ENSG00000125898	FAM110A	6,403	4,13E-09
ENSG00000176619	LMNB2	-3,061	1,70E-02	ENSG00000198934	MAGEE1	6,407	4,04E-09
ENSG00000090273	NUDC	-3,054	1,74E-02	ENSG00000106080	FKBP14	6,408	4,01E-09
ENSG00000197903	HIST1H2BK	-3,053	1,75E-02	ENSG00000175895	PLEKHF2	6,428	3,55E-09
ENSG00000176933	TOB2P1	-3,051	1,75E-02	ENSG00000125841	NRSN2	6,436	3,37E-09
ENSG00000256061	DYX1C1	-3,048	1,77E-02	ENSG00000121281	ADCY7	6,477	2,59E-09
ENSG00000055118	KCNH2	-3,048	1,77E-02	ENSG00000120685	PROSER1	6,59	1,24E-09
ENSG00000074201	CLNS1A	-3,047	1,77E-02	ENSG00000128683	GAD1	6,609	1,09E-09
ENSG00000173812	EIF1	-3,046	1,77E-02	ENSG00000188613	NANOS1	6,626	9,78E-10
ENSG00000064999	ANKS1A	-3,045	1,78E-02	ENSG00000138709	LARP1B	6,626	9,78E-10
ENSG00000168818	STX18	-3,039	1,81E-02	ENSG00000213928	IRF9	6,634	9,34E-10
ENSG00000090776	EFNB1	-3,035	1,84E-02	ENSG00000198563	DDX39B	6,662	7,73E-10
ENSG00000129932	DOHH	-3,033	1,85E-02	ENSG00000142684	ZNF593	6,672	7,26E-10
ENSG00000105708	ZNF14	-3,024	1,90E-02	ENSG00000229186	ADAM1A	6,674	7,14E-10
ENSG00000100522	GNPNAT1	-3,022	1,91E-02	ENSG00000168874	ATOH8	6,678	6,96E-10
ENSG00000175213	ZNF408	-3,021	1,92E-02	ENSG00000168297	PXK	6,713	5,52E-10
ENSG00000132470	ITGB4	-3,021	1,92E-02	ENSG00000130749	ZC3H4	6,713	5,52E-10
ENSG0000027	DUSP14	-3,015	1,95E-02	ENSG0000012	ATF4	6,724	5,15E-10

6023				8272			
ENSG00000170860	LSM3	-3,012	1,97E-02	ENSG00000111490	TBC1D30	6,75	4,34E-10
ENSG00000164168	TMEM184C	-3,008	1,99E-02	ENSG00000168216	LMBRD1	6,758	4,10E-10
ENSG00000153130	SCOC	-3,004	2,02E-02	ENSG00000179041	RRS1	6,76	4,07E-10
ENSG00000196387	ZNF140	-3,003	2,02E-02	ENSG00000103034	NDRG4	6,85	2,19E-10
ENSG00000120675	DNAJC15	-2,997	2,06E-02	ENSG00000082805	ERC1	6,868	1,95E-10
ENSG00000136270	TBRG4	-2,995	2,07E-02	ENSG00000203668	CHML	6,87	1,92E-10
ENSG00000135317	SNX14	-2,992	2,09E-02	ENSG00000069188	SDK2	6,875	1,86E-10
ENSG00000174343	CHRNA9	-2,991	2,09E-02	ENSG00000105750	ZNF85	6,882	1,78E-10
ENSG00000052126	PLEKHA5	-2,991	2,10E-02	ENSG00000137094	DNAJB5	6,888	1,72E-10
ENSG00000169021	UQCRFS1	-2,984	2,14E-02	ENSG00000166086	JAM3	7,013	7,15E-11
ENSG00000135392	DNAJC14	-2,984	2,14E-02	ENSG00000152520	PAN3	7,037	5,99E-11
ENSG00000188554	NBR1	-2,977	2,18E-02	ENSG00000173530	TNFRSF10D	7,099	3,91E-11
ENSG00000121350	PYROXD1	-2,977	2,18E-02	ENSG00000168887	C2orf68	7,11	3,60E-11
ENSG00000164674	SYTL3	-2,975	2,19E-02	ENSG00000118496	FBXO30	7,119	3,40E-11
ENSG00000186501	TMEM222	-2,973	2,21E-02	ENSG00000149150	SLC43A1	7,136	3,03E-11
ENSG00000140284	SLC27A2	-2,97	2,23E-02	ENSG00000168026	TTC21A	7,143	2,88E-11
ENSG00000185499	MUC1	-2,97	2,23E-02	ENSG00000072110	ACTN1	7,149	2,76E-11
ENSG00000125434	SLC25A35	-2,964	2,26E-02	ENSG00000104833	TUBB4A	7,195	1,99E-11
ENSG00000119640	ACYP1	-2,962	2,28E-02	ENSG00000188211	NCR3LG1	7,22	1,67E-11
ENSG00000158480	SPATA2	-2,96	2,29E-02	ENSG00000105088	OLFM2	7,244	1,40E-11
ENSG00000141349	G6PC3	-2,958	2,30E-02	ENSG00000119801	YPEL5	7,263	1,23E-11
ENSG00000158113	LRRC43	-2,956	2,31E-02	ENSG00000126778	SIX1	7,276	1,11E-11
ENSG00000064787	BCAS1	-2,956	2,31E-02	ENSG00000187957	DNER	7,289	1,02E-11
ENSG00000067992	PDK3	-2,955	2,32E-02	ENSG00000162702	ZNF281	7,294	9,75E-12
ENSG00000142252	GEMIN7	-2,954	2,32E-02	ENSG00000179833	SERTAD2	7,297	9,61E-12
ENSG00000106927	AMBP	-2,949	2,35E-02	ENSG00000122694	GLIPR2	7,306	8,98E-12
ENSG00000105388	CEACAM5	-2,949	2,36E-02	ENSG00000184436	THAP7	7,345	6,75E-12
ENSG00000105552	BCAT2	-2,943	2,39E-02	ENSG00000172731	LRRC20	7,417	3,98E-12
ENSG00000125817	CENPB	-2,94	2,41E-02	ENSG00000213859	KCTD11	7,419	3,92E-12
ENSG00000125459	MSTO1	-2,933	2,46E-02	ENSG00000146267	FAXC	7,42	3,91E-12
ENSG00000075856	SART3	-2,933	2,46E-02	ENSG00000258366	RTEL1	7,451	3,11E-12
ENSG00000055208	TAB2	-2,927	2,50E-02	ENSG00000182287	AP1S2	7,484	2,45E-12
ENSG00000163072	NOSTRIN	-2,927	2,50E-02	ENSG00000235194	PPP1R3E	7,529	1,75E-12
ENSG00000148153	INIP	-2,923	2,53E-02	ENSG00000204779	FOXD4L5	7,563	1,35E-12

ENSG00000164576	SAP30L	-2,917	2,58E-02	ENSG00000104131	EIF3J	7,586	1,14E-12
ENSG00000054277	OPN3	-2,915	2,59E-02	ENSG00000150401	DCUN1D2	7,679	5,72E-13
ENSG00000166851	PLK1	-2,909	2,63E-02	ENSG00000026950	BTN3A1	7,693	5,13E-13
ENSG00000066279	ASPM	-2,909	2,64E-02	ENSG00000083454	P2RX5	7,731	3,84E-13
ENSG00000090612	ZNF268	-2,906	2,66E-02	ENSG00000167264	DUS2L	7,739	3,61E-13
ENSG00000082641	NFE2L1	-2,905	2,67E-02	ENSG00000168495	POLR3D	7,785	2,53E-13
ENSG00000004142	POLDIP2	-2,901	2,69E-02	ENSG00000251595	ABCA11P	7,786	2,52E-13
ENSG00000147316	MCPH1	-2,897	2,73E-02	ENSG00000188878	FBF1	7,84	1,65E-13
ENSG00000170653	ATF7	-2,893	2,77E-02	ENSG00000141101	NOB1	7,86	1,41E-13
ENSG00000151276	MAGI1	-2,888	2,80E-02	ENSG00000129646	QRICH2	7,861	1,41E-13
ENSG00000132475	H3F3A	-2,886	2,81E-02	ENSG00000173548	SNX33	7,923	8,61E-14
ENSG00000275410	HNF1B	-2,886	2,82E-02	ENSG00000128604	IRF5	7,973	5,86E-14
ENSG00000104408	EIF3E	-2,878	2,88E-02	ENSG00000160087	UBE2J2	7,98	5,57E-14
ENSG00000020129	NCDN	-2,873	2,92E-02	ENSG00000165730	STOX1	7,983	5,46E-14
ENSG00000135336	ORC3	-2,872	2,93E-02	ENSG00000103194	USP10	7,994	4,99E-14
ENSG00000111364	DDX55	-2,864	3,00E-02	ENSG00000087077	TRIP6	8,014	4,28E-14
ENSG00000243646	IL10RB	-2,848	3,15E-02	ENSG00000182534	MXRA7	8,028	3,84E-14
ENSG00000226950	DANCR	-2,847	3,16E-02	ENSG00000117472	TSPAN1	8,04	3,50E-14
ENSG00000185163	DDX51	-2,846	3,16E-02	ENSG00000063587	ZNF275	8,054	3,14E-14
ENSG00000155090	KLF10	-2,845	3,17E-02	ENSG00000126583	PRKCG	8,058	3,06E-14
ENSG00000153904	DDAH1	-2,844	3,17E-02	ENSG00000048162	NOP16	8,079	2,59E-14
ENSG00000085721	RRN3	-2,844	3,17E-02	ENSG00000241404	EGFL8	8,15	1,46E-14
ENSG00000169217	CD2BP2	-2,841	3,20E-02	ENSG00000170037	CNTROB	8,151	1,46E-14
ENSG00000196967	ZNF585A	-2,841	3,20E-02	ENSG00000105447	GRWD1	8,165	1,31E-14
ENSG00000228016	RAPGEF4-AS1	-2,835	3,25E-02	ENSG00000184575	XPOT	8,169	1,27E-14
ENSG00000242485	MRPL20	-2,833	3,27E-02	ENSG00000168734	PKIG	8,18	1,17E-14
ENSG00000146416	AIG1	-2,833	3,27E-02	ENSG00000159905	ZNF221	8,214	9,00E-15
ENSG00000125384	PTGER2	-2,83	3,30E-02	ENSG00000083635	NUFIP1	8,271	5,69E-15
ENSG00000120093	HOXB3	-2,826	3,34E-02	ENSG00000237580	GCSHP3	8,292	4,79E-15
ENSG00000167186	COQ7	-2,825	3,34E-02	ENSG00000181915	ADO	8,306	4,30E-15
ENSG00000109819	PPARGC1A	-2,824	3,34E-02	ENSG00000154310	TNIK	8,322	3,79E-15
ENSG00000070495	JMJD6	-2,82	3,38E-02	ENSG00000116353	MECR	8,355	2,93E-15
ENSG00000114030	KPNA1	-2,818	3,40E-02	ENSG00000168743	NPNT	8,365	2,73E-15
ENSG00000179151	EDC3	-2,817	3,40E-02	ENSG00000127993	RBM48	8,368	2,68E-15
ENSG0000026	DYNLL2	-2,814	3,43E-02	ENSG0000016	ZBTB49	8,378	2,48E-15

4364				8826			
ENSG00000160007	ARHGAP35	-2,812	3,44E-02	ENSG00000134569	LRP4	8,436	1,59E-15
ENSG00000135387	CAPRIN1	-2,804	3,53E-02	ENSG00000081041	CXCL2	8,436	1,59E-15
ENSG00000135297	MTO1	-2,799	3,58E-02	ENSG00000183317	EPHA10	8,449	1,43E-15
ENSG00000179862	CITED4	-2,797	3,60E-02	ENSG00000154102	C16orf74	8,453	1,39E-15
ENSG00000178950	GAK	-2,796	3,60E-02	ENSG00000235631	RNF148	8,47	1,21E-15
ENSG00000151012	SLC7A11	-2,795	3,61E-02	ENSG00000213390	ARHGAP19	8,484	1,09E-15
ENSG00000164932	CTHRC1	-2,794	3,62E-02	ENSG00000129757	CDKN1C	8,518	8,22E-16
ENSG00000121989	ACVR2A	-2,794	3,62E-02	ENSG00000038427	VCAN	8,548	6,51E-16
ENSG00000107554	DNMBP	-2,794	3,62E-02	ENSG00000253958	CLDN23	8,576	5,11E-16
ENSG00000135976	ANKRD36	-2,793	3,63E-02	ENSG00000154359	LONRF1	8,591	4,53E-16
ENSG00000184281	TSSC4	-2,792	3,63E-02	ENSG00000154328	NEIL2	8,597	4,33E-16
ENSG00000251022	THAP9-AS1	-2,792	3,64E-02	ENSG00000075043	KCNQ2	8,605	4,07E-16
ENSG00000163913	IFT122	-2,786	3,68E-02	ENSG00000243509	TNFRSF6B	8,62	3,62E-16
ENSG00000244005	NFS1	-2,785	3,69E-02	ENSG00000174928	C3orf33	8,625	3,48E-16
ENSG00000215717	TMEM167B	-2,783	3,72E-02	ENSG00000265681	RPL17	8,632	3,28E-16
ENSG00000169813	HNRNPF	-2,782	3,72E-02	ENSG00000120709	FAM53C	8,638	3,13E-16
ENSG00000197265	GTF2E2	-2,779	3,76E-02	ENSG00000091879	ANGPT2	8,65	2,86E-16
ENSG00000049768	FOXP3	-2,778	3,76E-02	ENSG00000124787	RPP40	8,663	2,57E-16
ENSG00000147130	ZMYM3	-2,776	3,78E-02	ENSG00000205250	E2F4	8,664	2,57E-16
ENSG00000131873	CHSY1	-2,774	3,79E-02	ENSG00000141622	RNF165	8,667	2,52E-16
ENSG00000174136	RGMB	-2,774	3,80E-02	ENSG00000163481	RNF25	8,667	2,52E-16
ENSG00000274582	SNORA16A	-2,772	3,81E-02	ENSG00000167994	RAB3IL1	8,683	2,21E-16
ENSG00000065882	TBC1D1	-2,771	3,82E-02	ENSG00000135097	MSI1	8,688	2,13E-16
ENSG00000126214	KLC1	-2,771	3,82E-02	ENSG00000258701	LINC00638	8,695	2,02E-16
ENSG00000180357	ZNF609	-2,77	3,82E-02	ENSG00000133138	TBC1D8B	8,699	1,96E-16
ENSG00000163512	AZI2	-2,769	3,83E-02	ENSG00000103978	TMEM87A	8,714	1,72E-16
ENSG00000140307	GTF2A2	-2,767	3,85E-02	ENSG00000090975	PITPNM2	8,733	1,46E-16
ENSG00000101290	CDS2	-2,767	3,85E-02	ENSG00000168505	GBX2	8,767	1,09E-16
ENSG00000189067	LITAF	-2,758	3,95E-02	ENSG00000214401	KANSL1-AS1	8,773	1,04E-16
ENSG00000179869	ABCA13	-2,754	3,99E-02	ENSG00000221303	SNORA79	8,793	8,85E-17
ENSG00000138459	SLC35A5	-2,753	3,99E-02	ENSG00000153814	JAZF1	8,795	8,69E-17
ENSG00000148840	PPRC1	-2,753	3,99E-02	ENSG00000162086	ZNF75A	8,803	8,12E-17
ENSG00000183091	NEB	-2,751	4,00E-02	ENSG00000224940	PRRT4	8,805	8,03E-17
ENSG00000107807	TLX1	-2,751	4,00E-02	ENSG00000186451	SPATA12	8,808	7,87E-17

ENSG00000146859	TMEM140	-2,746	4,05E-02
ENSG00000139187	KLRG1	-2,746	4,05E-02
ENSG00000127334	DYRK2	-2,746	4,05E-02
ENSG00000152192	POU4F1	-2,746	4,05E-02
ENSG00000136485	DCAF7	-2,741	4,10E-02
ENSG00000173110	HSPA6	-2,741	4,11E-02
ENSG00000140988	RPS2	-2,736	4,15E-02
ENSG00000137876	RSL24D1	-2,736	4,15E-02
ENSG00000148459	PDSS1	-2,734	4,17E-02
ENSG00000115446	UNC50	-2,732	4,18E-02
ENSG00000204147	ASAH2B	-2,725	4,27E-02
ENSG00000257923	CUX1	-2,72	4,33E-02
ENSG00000144648	CCBP2	-2,717	4,36E-02
ENSG00000132464	ENAM	-2,717	4,36E-02
ENSG00000129214	SHBG	-2,717	4,36E-02
ENSG00000180305	WFDC10A	-2,717	4,36E-02
ENSG00000000460	C1orf112	-2,717	4,36E-02
ENSG00000171421	MRPL36	-2,715	4,38E-02
ENSG00000197818	SLC9A8	-2,713	4,40E-02
ENSG00000143418	CERS2	-2,713	4,40E-02
ENSG00000182853	VMO1	-2,711	4,41E-02
ENSG00000176222	ZNF404	-2,711	4,41E-02
ENSG00000111247	RAD51AP1	-2,708	4,44E-02
ENSG00000151304	SRFBP1	-2,708	4,44E-02
ENSG00000137074	APTX	-2,707	4,45E-02
ENSG00000148935	GAS2	-2,705	4,46E-02
ENSG00000011677	GABRA3	-2,705	4,46E-02
ENSG00000155961	RAB39B	-2,705	4,46E-02
ENSG00000112365	ZBTB24	-2,701	4,50E-02
ENSG00000175274	TP53I11	-2,7	4,50E-02
ENSG00000157214	STEAP2	-2,7	4,50E-02
ENSG00000164620	RELL2	-2,7	4,50E-02
ENSG00000102265	TIMP1	-2,692	4,59E-02
ENSG00000072274	TFRC	-2,691	4,60E-02
ENSG0000010	ZNF174	-2,689	4,62E-02
ENSG00000169891	REPS2	8,82	7,09E-17
ENSG00000140463	BBS4	8,839	6,10E-17
ENSG00000165806	CASP7	8,839	6,10E-17
ENSG00000206559	ZCWPW2	8,854	5,36E-17
ENSG00000102543	CDADC1	8,856	5,31E-17
ENSG00000153551	CMTM7	8,898	3,68E-17
ENSG00000008256	CYTH3	8,924	2,96E-17
ENSG00000151746	BICD1	8,933	2,74E-17
ENSG00000167772	ANGPTL4	8,956	2,27E-17
ENSG00000026103	FAS	8,964	2,11E-17
ENSG00000008513	ST3GAL1	8,968	2,05E-17
ENSG00000197961	ZNF121	8,978	1,87E-17
ENSG00000134326	CMPK2	8,981	1,84E-17
ENSG00000182240	BACE2	8,983	1,82E-17
ENSG00000138172	CALHM2	8,984	1,81E-17
ENSG00000152256	PDK1	8,999	1,60E-17
ENSG00000183762	KREMEN1	9,047	1,07E-17
ENSG00000009307	CSDE1	9,051	1,03E-17
ENSG00000083828	ZNF586	9,058	9,79E-18
ENSG00000117153	KLHL12	9,066	9,17E-18
ENSG00000105369	CD79A	9,084	7,81E-18
ENSG00000174446	SNAPC5	9,09	7,48E-18
ENSG00000162591	MEGF6	9,092	7,36E-18
ENSG00000258890	CEP95	9,097	7,11E-18
ENSG00000155016	CYP2U1	9,097	7,11E-18
ENSG00000099994	SUSD2	9,101	6,95E-18
ENSG00000134504	KCTD1	9,116	6,08E-18
ENSG00000180340	FZD2	9,136	5,10E-18
ENSG00000152284	TCF7L1	9,162	4,04E-18
ENSG00000088305	DNMT3B	9,186	3,29E-18
ENSG00000184254	ALDH1A3	9,196	3,01E-18
ENSG00000185055	EFCAB10	9,202	2,88E-18
ENSG00000249992	TMEM158	9,264	1,66E-18
ENSG00000100604	CHGA	9,277	1,47E-18
ENSG0000016	AK4	9,3	1,19E-18

3343			
ENSG00000154274	C4orf19	-2,689	4,62E-02
ENSG00000126787	DLGAP5	-2,685	4,67E-02
ENSG00000116922	C1orf109	-2,684	4,68E-02
ENSG00000135116	HRK	-2,681	4,72E-02
ENSG00000114248	LRRC31	-2,679	4,74E-02
ENSG00000029559	IBSP	-2,679	4,74E-02
ENSG00000203907	OOEP	-2,679	4,74E-02
ENSG00000161270	NPHS1	-2,679	4,74E-02
ENSG00000130764	LRRC47	-2,678	4,75E-02
ENSG00000188833	ENTPD8	-2,675	4,78E-02
ENSG00000204983	PRSS1	-2,674	4,79E-02
ENSG00000116183	PAPPA2	-2,672	4,81E-02
ENSG00000164266	SPINK1	-2,672	4,81E-02
ENSG00000187546	AGMO	-2,672	4,81E-02
ENSG00000185681	MORN5	-2,672	4,81E-02
ENSG00000142039	CCDC97	-2,671	4,82E-02
ENSG00000143751	SDE2	-2,671	4,82E-02
ENSG00000071859	FAM50A	-2,668	4,86E-02
ENSG00000134508	CABLES1	-2,666	4,89E-02
ENSG00000128016	ZFP36	-2,663	4,92E-02
ENSG00000136986	DERL1	-2,663	4,92E-02
ENSG00000135631	RAB11FIP5	-2,659	4,94E-02
ENSG00000226742	HSBP1L1	-2,659	4,95E-02
ENSG00000033800	PIAS1	-2,657	4,97E-02

2433			
ENSG00000021762	OSBPL5	9,312	1,07E-18
ENSG00000198824	CHAMP1	9,347	7,81E-19
ENSG00000165006	UBAP1	9,448	3,06E-19
ENSG00000182771	GRID1	9,457	2,81E-19
ENSG00000159433	STARD9	9,478	2,32E-19
ENSG00000100714	MTHFD1	9,487	2,14E-19
ENSG00000234608	MAPKAPK5-AS1	9,625	5,88E-20
ENSG00000068745	IP6K2	9,692	3,12E-20
ENSG00000187372	PCDHB13	9,752	1,75E-20
ENSG00000102924	CBLN1	9,795	1,17E-20
ENSG00000084710	EFR3B	9,807	1,04E-20
ENSG00000150712	MTMR12	9,866	5,90E-21
ENSG00000107521	HPS1	9,91	3,81E-21
ENSG00000217555	CKLF	9,918	3,57E-21
ENSG00000060237	WNK1	9,947	2,69E-21
ENSG00000073060	SCARB1	9,987	1,84E-21
ENSG00000147676	MAL2	10,107	5,57E-22
ENSG00000124786	SLC35B3	10,108	5,55E-22
ENSG00000125630	POLR1B	10,154	3,53E-22
ENSG00000167657	DAPK3	10,265	1,15E-22
ENSG00000119977	TCTN3	10,392	3,17E-23
ENSG00000130479	MAP1S	10,667	1,77E-24
ENSG00000170852	KBTBD2	10,679	1,56E-24
ENSG00000164252	AGGF1	10,841	2,74E-25
ENSG00000080189	SLC35C2	11,164	8,16E-27
ENSG00000065665	SEC61A2	11,185	6,48E-27
ENSG00000197375	SLC22A5	11,187	6,45E-27
ENSG00000143554	SLC27A3	11,187	6,45E-27
ENSG00000160714	UBE2Q1	11,213	4,88E-27
ENSG00000177700	POLR2L	11,276	2,42E-27
ENSG00000162928	PEX13	11,331	1,31E-27
ENSG00000025772	TOMM34	11,477	2,49E-28
ENSG00000091947	TMEM101	11,481	2,40E-28
ENSG00000121892	PDS5A	11,544	1,21E-28

ENSG00000165195	PIGA	11,571	8,95E-29
ENSG00000184178	SCFD2	11,582	7,95E-29
ENSG00000070882	OSBPL3	11,609	5,87E-29
ENSG00000097007	ABL1	11,678	2,67E-29
ENSG00000180667	YOD1	11,804	6,31E-30
ENSG00000149313	AASDHPPT	12,111	1,63E-31
ENSG00000152457	DCLRE1C	12,134	1,28E-31
ENSG00000084652	TXLNA	12,291	1,89E-32
ENSG00000109576	AADAT	12,433	3,37E-33
ENSG00000157869	RAB28	12,524	1,09E-33
ENSG00000136240	KDELR2	12,542	8,87E-34
ENSG00000115170	ACVR1	12,649	2,30E-34
ENSG00000213246	SUPT4H1	12,692	1,37E-34
ENSG00000163605	PPP4R2	12,81	3,24E-35
ENSG00000130810	PPAN	13,18	2,74E-37
ENSG00000146535	GNA12	13,258	1,01E-37
ENSG00000105700	KXD1	13,588	1,28E-39
ENSG00000048828	FAM120A	13,677	3,93E-40
ENSG00000130382	MLLT1	13,743	1,68E-40
ENSG00000067334	DNTTIP2	13,917	1,53E-41
ENSG00000138814	PPP3CA	14,182	3,69E-43
ENSG00000171953	ATPAF2	14,408	1,48E-44
ENSG00000122643	NT5C3	14,638	5,72E-46
ENSG00000123505	AMD1	14,664	4,11E-46
ENSG00000134779	TPGS2	14,767	9,14E-47
ENSG00000182871	COL18A1	14,791	6,60E-47
ENSG00000169241	SLC50A1	15,354	1,45E-50
ENSG00000153561	RMND5A	15,525	1,17E-51
ENSG00000007402	CACNA2D2	15,902	3,75E-54
ENSG00000180921	FAM83H	16,094	1,89E-55
ENSG00000134138	MEIS2	16,44	7,40E-58
ENSG00000119402	FBXW2	16,526	2,02E-58
ENSG00000106344	RBM28	16,548	1,48E-58
ENSG00000137275	RIPK1	16,834	1,33E-60
ENSG0000014	EFHD2	17,185	3,88E-63

2634			
ENSG00000007923	DNAJC11	17,667	1,02E-66
ENSG00000146457	WTAP	17,702	6,07E-67
ENSG00000160211	G6PD	19,658	1,11E-82
ENSG00000182512	GLRX5	21,023	1,08E-94
ENSG00000182199	SHMT2	22,955	8,88E-113
ENSG00000072501	SMC1A	23,777	7,85E-121

Table S 6: List of genes that are differentially regulated between QGP1 cells treated with the mTOR inhibitors everolimus and temsirolimus and the control.

For simplified evaluation, the control group included wild-type QGP1 cells and QGP1 treated with DMSO, while the inhibitor group included QGP1 cells that were treated with 1 µM everolimus and temsirolimus for 72 hours. The genes were determined using the DESeq2 package. All genes with Benjamin Hochberg adjusted p-value (padj) < 0.05 were included. The data are represented as Wald-statistic (stat). Genes with negative Wald-statistic values are down-regulated in QGP1 cells treated with mTOR inhibitors compared to the control group.

$$\text{Wald} - \text{statistic} = \frac{\text{log2FoldChange}}{\text{standard error of log2FoldChange}}$$

Ensembl_ ID	Gene_ symbol	Stat_ control_ inhibitor	padj_ control_ inhibitor
ENSG00000182512	GLRX5	-23,475	9,83E-118
ENSG00000140859	KIFC3	-17,967	7,80E-69
ENSG00000247077	PGAM5	-17,872	3,30E-68
ENSG00000087365	SF3B2	-17,676	9,60E-67
ENSG00000067334	DNTTIP2	-17,571	5,52E-66
ENSG00000142669	SH3BGRL3	-17,419	7,26E-65
ENSG00000106344	RBM28	-15,688	1,53E-52
ENSG00000136522	MRPL47	-15,335	3,36E-50
ENSG00000140263	SORD	-15,315	4,33E-50
ENSG00000153187	HNRNPU	-14,665	6,36E-46
ENSG00000135698	MPHOSPH6	-14,476	9,60E-45
ENSG00000137054	POLR1E	-14,42	2,09E-44
ENSG00000113141	IK	-14,106	1,73E-42
ENSG00000178234	GALNT11	-13,418	2,07E-38
ENSG00000121390	PSPC1	-13,119	1,05E-36
ENSG00000111605	CPSF6	-13,039	2,92E-36
ENSG00000162231	NXF1	-12,879	2,05E-35
ENSG00000107371	EXOSC3	-12,111	2,66E-31
ENSG00000096384	HSP90AB1	-12,047	5,62E-31

Ensembl_ID	Gene_ symbol	Stat_control_ inhibitor	padj_control_ inhibitor
ENSG00000185627	PSMD13	2,824	4,95E-02
ENSG00000122778	KIAA1549	2,834	4,80E-02
ENSG00000028116	VRK2	2,844	4,67E-02
ENSG00000067704	IARS2	2,845	4,66E-02
ENSG00000013810	TACC3	2,846	4,65E-02
ENSG00000232838	CSRP2BP	2,856	4,52E-02
ENSG00000157426	AASDH	2,86	4,47E-02
ENSG00000165861	ZFYVE1	2,866	4,40E-02
ENSG00000142657	PGD	2,87	4,35E-02
ENSG00000130764	LRRC47	2,875	4,28E-02
ENSG00000128951	DUT	2,884	4,18E-02
ENSG00000047644	WWC3	2,887	4,14E-02
ENSG00000145247	OCIAD2	2,891	4,09E-02
ENSG00000164104	HMGB2	2,894	4,06E-02
ENSG00000109576	AADAT	2,902	3,97E-02
ENSG00000088002	SULT2B1	2,91	3,88E-02
ENSG00000174705	SH3PXD2B	2,919	3,80E-02
ENSG00000213853	EMP2	2,921	3,78E-02
ENSG00000140365	COMMD4	2,922	3,77E-02

ENSG00000183207	RUVBL2	-11,9	3,11E-30
ENSG00000108588	CCDC47	-11,537	2,11E-28
ENSG00000133983	COX16	-11,523	2,43E-28
ENSG00000104472	CHRAC1	-11,279	3,82E-27
ENSG00000170779	CDCA4	-11,195	9,39E-27
ENSG00000089220	PEBP1	-11,146	1,61E-26
ENSG00000105618	PRPF31	-10,949	1,32E-25
ENSG00000110321	EIF4G2	-10,9	2,25E-25
ENSG00000174799	CEP135	-10,878	2,81E-25
ENSG00000136527	TRA2B	-10,737	1,26E-24
ENSG00000115053	NCL	-10,73	1,33E-24
ENSG00000184220	CMSS1	-10,675	2,37E-24
ENSG00000245680	ZNF585B	-10,584	6,18E-24
ENSG00000101193	GID8	-10,385	4,75E-23
ENSG00000179041	RRS1	-10,335	7,86E-23
ENSG00000012660	ELOVL5	-10,22	2,49E-22
ENSG00000133606	MKRN1	-10,179	3,78E-22
ENSG00000161888	SPC24	-9,887	6,63E-21
ENSG00000108384	RAD51C	-9,787	1,77E-20
ENSG00000104518	GSDMD	-9,758	2,35E-20
ENSG00000196428	TSC22D2	-9,73	3,01E-20
ENSG00000196653	ZNF502	-9,715	3,48E-20
ENSG00000203761	MSTO2P	-9,613	9,04E-20
ENSG00000180535	BHLHA15	-9,587	1,13E-19
ENSG00000187147	RNF220	-9,546	1,67E-19
ENSG00000008311	AASS	-9,534	1,84E-19
ENSG00000029363	BCLAF1	-9,525	1,97E-19
ENSG00000196504	PRPF40A	-9,516	2,12E-19
ENSG00000145029	NICN1	-9,513	2,14E-19
ENSG00000085465	OVGP1	-9,502	2,37E-19
ENSG00000205250	E2F4	-9,501	2,38E-19
ENSG00000171435	KSR2	-9,404	5,70E-19
ENSG00000162104	ADCY9	-9,389	6,54E-19
ENSG00000110628	SLC22A18	-9,329	1,12E-18
ENSG00000165309	ARMC3	-9,31	1,32E-18
ENSG00000179981	TSHZ1	-9,304	1,38E-18
ENSG00000160862	AZGP1	-9,287	1,60E-18
ENSG00000198879	SFMBT2	-9,278	1,71E-18
ENSG00000151715	TMEM45B	-9,259	2,02E-18
ENSG00000215908	CROCCP2	-9,249	2,18E-18
ENSG00000272674	PCDHB16	-9,248	2,18E-18
ENSG00000114423	CBLB	-9,242	2,28E-18
ENSG00000148082	SHC3	-9,238	2,34E-18
ENSG00000114631	PODXL2	-9,233	2,45E-18
ENSG00000125775	SDCBP2	-9,22	2,68E-18
ENSG00000129946	SHC2	-9,219	2,70E-18
ENSG00000124228	DDX27	2,922	3,77E-02
ENSG00000161800	RACGAP1	2,925	3,74E-02
ENSG00000101849	TBL1X	2,928	3,70E-02
ENSG00000078140	UBE2K	2,946	3,50E-02
ENSG00000163482	STK36	2,956	3,40E-02
ENSG00000136237	RAPGEF5	2,959	3,37E-02
ENSG00000159352	PSMD4	2,966	3,30E-02
ENSG00000122643	NT5C3	2,966	3,30E-02
ENSG00000141994	DUS3L	2,968	3,28E-02
ENSG00000105223	PLD3	2,969	3,27E-02
ENSG00000258102	MAP1LC3B2	2,969	3,27E-02
ENSG00000138670	RASGEF1B	2,97	3,27E-02
ENSG00000146070	PLA2G7	2,979	3,18E-02
ENSG00000091483	FH	2,98	3,17E-02
ENSG00000188681	TEKT4P2	2,994	3,04E-02
ENSG00000186432	KPNA4	2,996	3,03E-02
ENSG00000109458	GAB1	3,022	2,80E-02
ENSG00000128394	APOBEC3F	3,027	2,76E-02
ENSG00000184207	PGP	3,031	2,73E-02
ENSG00000159147	DONSON	3,04	2,65E-02
ENSG00000143919	CAMKMT	3,041	2,65E-02
ENSG00000183684	ALYREF	3,041	2,65E-02
ENSG00000164687	FABP5	3,055	2,54E-02
ENSG00000136271	DDX56	3,056	2,53E-02
ENSG00000105419	MEIS3	3,058	2,51E-02
ENSG00000143061	IGSF3	3,067	2,45E-02
ENSG00000197296	FITM2	3,068	2,44E-02
ENSG00000013563	DNASE1L1	3,077	2,37E-02
ENSG00000198026	ZNF335	3,084	2,32E-02
ENSG00000163848	ZNF148	3,096	2,24E-02
ENSG00000155621	C9orf85	3,114	2,12E-02
ENSG00000156876	SASS6	3,118	2,09E-02
ENSG00000131061	ZNF341	3,127	2,03E-02
ENSG00000077585	GPR137B	3,132	2,00E-02
ENSG00000136153	LMO7	3,133	2,00E-02
ENSG00000177076	ACER2	3,149	1,90E-02
ENSG00000184967	NOC4L	3,171	1,77E-02
ENSG00000145386	CCNA2	3,182	1,70E-02
ENSG00000187514	PTMA	3,196	1,63E-02
ENSG00000130311	DDA1	3,224	1,48E-02
ENSG00000112874	NUDT12	3,232	1,45E-02
ENSG00000170348	TMED10	3,232	1,45E-02
ENSG00000186283	TOR3A	3,24	1,41E-02
ENSG00000032219	ARID4A	3,249	1,37E-02
ENSG00000118162	KPTN	3,258	1,33E-02
ENSG00000081087	OSTM1	3,28	1,24E-02

ENSG00000183018	SPNS2	-9,215	2,77E-18
ENSG00000137825	ITPKA	-9,212	2,81E-18
ENSG00000175175	PPM1E	-9,212	2,81E-18
ENSG00000178538	CA8	-9,202	3,04E-18
ENSG00000197479	PCDHB11	-9,201	3,05E-18
ENSG00000143344	RGL1	-9,18	3,59E-18
ENSG00000033327	GAB2	-9,179	3,59E-18
ENSG00000166503	HDGFRP3	-9,172	3,80E-18
ENSG00000130600	H19	-9,148	4,64E-18
ENSG00000106258	CYP3A5	-9,144	4,78E-18
ENSG00000162613	FUBP1	-9,143	4,78E-18
ENSG00000089127	OAS1	-9,142	4,81E-18
ENSG00000075340	ADD2	-9,138	4,95E-18
ENSG00000162591	MEGF6	-9,114	5,89E-18
ENSG00000161328	LRRC56	-9,113	5,92E-18
ENSG00000205356	TECPR1	-9,109	6,12E-18
ENSG00000152926	ZNF117	-9,096	6,81E-18
ENSG00000198001	IRAK4	-9,085	7,42E-18
ENSG00000246705	H2AFJ	-9,075	8,06E-18
ENSG00000076003	MCM6	-9,033	1,14E-17
ENSG00000101605	MYOM1	-9,031	1,16E-17
ENSG00000206535	LNP1	-9,016	1,33E-17
ENSG00000060982	BCAT1	-8,997	1,56E-17
ENSG00000185442	FAM174B	-8,994	1,59E-17
ENSG00000181031	RPH3AL	-8,966	1,99E-17
ENSG00000157654	PALM2	-8,963	2,05E-17
ENSG00000089199	CHGB	-8,959	2,11E-17
ENSG00000203668	CHML	-8,959	2,11E-17
ENSG00000222009	BTBD19	-8,955	2,17E-17
ENSG00000176714	CCDC121	-8,949	2,28E-17
ENSG00000065534	MYLK	-8,913	3,08E-17
ENSG00000155093	PTPRN2	-8,889	3,76E-17
ENSG00000260456	C16orf95	-8,876	4,17E-17
ENSG00000100505	TRIM9	-8,875	4,19E-17
ENSG00000130294	KIF1A	-8,874	4,22E-17
ENSG00000172803	SNX32	-8,868	4,41E-17
ENSG00000166997	CNPY4	-8,849	5,14E-17
ENSG00000198133	TMEM229B	-8,827	6,16E-17
ENSG00000106541	AGR2	-8,799	7,86E-17
ENSG00000157064	NMNAT2	-8,783	8,84E-17
ENSG00000099337	KCNK6	-8,773	9,59E-17
ENSG00000111704	NANOG	-8,772	9,61E-17
ENSG00000183077	AFMID	-8,757	1,08E-16
ENSG00000237004	ZNRF2P1	-8,748	1,16E-16
ENSG00000155265	GOLGA7B	-8,746	1,17E-16
ENSG00000010310	GIPR	-8,746	1,17E-16

ENSG00000101412	E2F1	3,281	1,23E-02
ENSG00000239306	RBM14	3,285	1,22E-02
ENSG00000116014	KISS1R	3,288	1,21E-02
ENSG00000198912	C1orf174	3,298	1,16E-02
ENSG00000103494	RPGRIP1L	3,31	1,12E-02
ENSG00000083844	ZNF264	3,312	1,11E-02
ENSG00000182004	SNRPE	3,32	1,08E-02
ENSG00000122390	NAA60	3,33	1,05E-02
ENSG00000090924	PLEKHG2	3,356	9,56E-03
ENSG00000068354	TBC1D25	3,368	9,19E-03
ENSG00000025039	RRAGD	3,371	9,14E-03
ENSG00000009954	BAZ1B	3,372	9,11E-03
ENSG00000177732	SOX12	3,373	9,08E-03
ENSG00000184792	OSBP2	3,387	8,62E-03
ENSG00000110074	FOXRED1	3,388	8,61E-03
ENSG00000165501	LRR1	3,394	8,43E-03
ENSG00000117697	NSL1	3,395	8,41E-03
ENSG00000109854	HTATIP2	3,414	7,87E-03
ENSG00000181450	ZNF678	3,418	7,75E-03
ENSG00000126458	RRAS	3,438	7,24E-03
ENSG00000127124	HIVEP3	3,447	7,00E-03
ENSG00000070950	RAD18	3,453	6,85E-03
ENSG00000014824	SLC30A9	3,487	6,09E-03
ENSG00000143545	RAB13	3,505	5,71E-03
ENSG00000185246	PRPF39	3,51	5,61E-03
ENSG00000040275	SPDL1	3,514	5,54E-03
ENSG00000160214	RRP1	3,525	5,33E-03
ENSG00000153774	CFDP1	3,547	4,92E-03
ENSG00000154719	MRPL39	3,557	4,74E-03
ENSG00000125952	MAX	3,575	4,45E-03
ENSG00000156675	RAB11FIP1	3,579	4,38E-03
ENSG00000049541	RFC2	3,601	4,04E-03
ENSG00000149929	HIRIP3	3,609	3,92E-03
ENSG00000185829	ARL17B	3,61	3,92E-03
ENSG00000089063	TMEM230	3,644	3,45E-03
ENSG00000155592	ZKSCAN2	3,652	3,35E-03
ENSG00000130699	TAF4	3,664	3,21E-03
ENSG00000108474	PIGL	3,682	2,99E-03
ENSG00000100714	MTHFD1	3,714	2,64E-03
ENSG00000105649	RAB3A	3,732	2,46E-03
ENSG00000241058	NSUN6	3,758	2,23E-03
ENSG00000060642	PIGV	3,762	2,19E-03
ENSG00000120519	SLC10A7	3,788	1,99E-03
ENSG00000135503	ACVR1B	3,796	1,92E-03
ENSG00000111912	NCOA7	3,805	1,86E-03
ENSG00000215193	PEX26	3,817	1,77E-03

ENSG00000160180	TFF3	-8,719	1,47E-16
ENSG00000169752	NRG4	-8,718	1,48E-16
ENSG00000235169	SMIM1	-8,717	1,49E-16
ENSG00000244694	PTCHD4	-8,707	1,62E-16
ENSG00000174871	CNIH2	-8,701	1,69E-16
ENSG00000105499	PLA2G4C	-8,692	1,81E-16
ENSG00000134668	SPOCD1	-8,685	1,93E-16
ENSG00000018236	CNTN1	-8,682	1,97E-16
ENSG00000134285	FKBP11	-8,677	2,03E-16
ENSG00000134780	DAGLA	-8,676	2,04E-16
ENSG00000123191	ATP7B	-8,668	2,16E-16
ENSG00000164663	USP49	-8,661	2,28E-16
ENSG00000132872	SYT4	-8,656	2,37E-16
ENSG00000257702	LBX2-AS1	-8,652	2,45E-16
ENSG00000183067	IGSF5	-8,652	2,45E-16
ENSG00000132383	RPA1	-8,636	2,80E-16
ENSG00000181444	ZNF467	-8,618	3,22E-16
ENSG00000198346	ZNF813	-8,608	3,49E-16
ENSG00000159307	SCUBE1	-8,608	3,49E-16
ENSG00000121895	TMEM156	-8,589	4,10E-16
ENSG00000126705	AHDC1	-8,586	4,19E-16
ENSG00000196782	MAML3	-8,568	4,85E-16
ENSG00000169856	ONECUT1	-8,545	5,83E-16
ENSG00000137075	RNF38	-8,537	6,24E-16
ENSG00000204977	TRIM13	-8,536	6,27E-16
ENSG00000117461	PIK3R3	-8,533	6,38E-16
ENSG00000129654	FOXJ1	-8,513	7,48E-16
ENSG00000168291	PDHB	-8,51	7,65E-16
ENSG00000189157	FAM47E	-8,503	8,07E-16
ENSG00000181513	ACBD4	-8,456	1,19E-15
ENSG00000129990	SYT5	-8,454	1,21E-15
ENSG00000250510	GPR162	-8,448	1,27E-15
ENSG00000145335	SNCA	-8,444	1,30E-15
ENSG00000231752	EMBP1	-8,431	1,44E-15
ENSG00000087076	HSD17B14	-8,426	1,49E-15
ENSG00000160298	C21orf58	-8,42	1,57E-15
ENSG00000061656	SPAG4	-8,385	2,09E-15
ENSG00000123364	HOXC13	-8,383	2,13E-15
ENSG00000253910	PCDHGB2	-8,381	2,16E-15
ENSG00000164611	PTTG1	-8,363	2,48E-15
ENSG00000063587	ZNF275	-8,354	2,68E-15
ENSG00000079974	RABL2A	-8,331	3,24E-15
ENSG00000116147	TNR	-8,289	4,55E-15
ENSG00000175938	ORAI3	-8,25	6,24E-15
ENSG00000104863	LIN7B	-8,226	7,51E-15
ENSG00000240445	FOXO3B	-8,203	9,09E-15
ENSG00000221909	FAM200A	3,851	1,55E-03
ENSG00000162736	NCSTN	3,882	1,37E-03
ENSG00000120437	ACAT2	3,949	1,04E-03
ENSG00000183864	TOB2	3,965	9,76E-04
ENSG00000133111	RFXAP	3,984	9,03E-04
ENSG00000240053	LY6G5B	4,025	7,60E-04
ENSG00000197226	TBC1D9B	4,066	6,41E-04
ENSG00000132330	SCLY	4,071	6,28E-04
ENSG00000183891	TTC32	4,089	5,81E-04
ENSG00000072501	SMC1A	4,104	5,46E-04
ENSG00000136450	SRSF1	4,107	5,39E-04
ENSG00000157570	TSPAN18	4,207	3,49E-04
ENSG00000175756	AURKAIP1	4,236	3,08E-04
ENSG00000143183	TMCO1	4,293	2,38E-04
ENSG00000100379	KCTD17	4,313	2,18E-04
ENSG00000186638	KIF24	4,35	1,85E-04
ENSG00000187024	PTRH1	4,367	1,71E-04
ENSG00000144452	ABCA12	4,434	1,26E-04
ENSG00000100170	SLC5A1	4,503	9,12E-05
ENSG00000012822	CALCOCO1	4,514	8,70E-05
ENSG00000168461	RAB31	4,651	4,54E-05
ENSG00000134809	TIMM10	4,665	4,24E-05
ENSG00000076067	RBMS2	4,68	3,96E-05
ENSG00000186765	FSCN2	4,753	2,77E-05
ENSG00000104738	MCM4	4,791	2,29E-05
ENSG00000120899	PTK2B	4,968	9,46E-06
ENSG00000128510	CPA4	4,977	9,03E-06
ENSG00000162733	DDR2	5,105	4,64E-06
ENSG00000106617	PRKAG2	5,187	3,00E-06
ENSG00000087085	ACHE	5,195	2,89E-06
ENSG00000175868	CALCB	5,196	2,88E-06
ENSG00000101306	MYLK2	5,198	2,85E-06
ENSG00000248334	WHAMMP2	5,199	2,84E-06
ENSG00000025434	NR1H3	5,2	2,83E-06
ENSG00000240288	GHRLOS	5,202	2,80E-06
ENSG00000185129	PURA	5,204	2,78E-06
ENSG00000197312	DDI2	5,204	2,78E-06
ENSG00000188095	MESP2	5,204	2,78E-06
ENSG00000160781	PAQR6	5,205	2,77E-06
ENSG00000087510	TFAP2C	5,206	2,75E-06
ENSG00000117016	RIMS3	5,209	2,72E-06
ENSG00000084628	NKAIN1	5,214	2,66E-06
ENSG00000180902	D2HGDH	5,217	2,63E-06
ENSG00000112293	GPLD1	5,219	2,60E-06
ENSG00000196233	LCOR	5,224	2,55E-06
ENSG00000259581	TYRO3P	5,224	2,55E-06

ENSG00000124743	KLHL31	-8,195	9,72E-15
ENSG00000162194	C11orf48	-8,154	1,35E-14
ENSG00000143850	PLEKHA6	-8,128	1,67E-14
ENSG00000108786	HSD17B1	-8,125	1,71E-14
ENSG00000111215	PRR4	-8,113	1,88E-14
ENSG00000037757	MRI1	-8,07	2,66E-14
ENSG00000027869	SH2D2A	-8,058	2,92E-14
ENSG00000076351	SLC46A1	-8,054	3,00E-14
ENSG00000076770	MBNL3	-8,027	3,72E-14
ENSG00000185565	LSAMP	-8,014	4,14E-14
ENSG00000256061	DYX1C1	-8,004	4,44E-14
ENSG00000128408	RIBC2	-8,002	4,52E-14
ENSG00000124613	ZNF391	-7,998	4,66E-14
ENSG00000132669	RIN2	-7,955	6,57E-14
ENSG00000198039	ZNF273	-7,943	7,21E-14
ENSG00000101460	MAP1LC3A	-7,911	9,18E-14
ENSG00000167202	TBC1D2B	-7,877	1,20E-13
ENSG00000197172	MAGEA6	-7,832	1,70E-13
ENSG00000263001	GTF2I	-7,822	1,83E-13
ENSG00000146083	RNF44	-7,805	2,09E-13
ENSG00000201643	SNORA14A	-7,785	2,43E-13
ENSG00000204149	AGAP6	-7,731	3,69E-13
ENSG00000196419	XRCC6	-7,714	4,17E-13
ENSG00000228315	GUSBP11	-7,704	4,50E-13
ENSG00000094804	CDC6	-7,668	5,91E-13
ENSG00000026950	BTN3A1	-7,637	7,48E-13
ENSG00000213859	KCTD11	-7,614	8,93E-13
ENSG00000168398	BDKRB2	-7,598	1,00E-12
ENSG00000170381	SEMA3E	-7,591	1,06E-12
ENSG00000167191	GPRC5B	-7,508	1,96E-12
ENSG00000139890	REM2	-7,504	2,02E-12
ENSG00000153956	CACNA2D1	-7,478	2,45E-12
ENSG00000120800	UTP20	-7,477	2,46E-12
ENSG00000142731	PLK4	-7,427	3,55E-12
ENSG00000139352	ASCL1	-7,425	3,61E-12
ENSG00000164053	TREX1	-7,424	3,62E-12
ENSG00000172201	ID4	-7,393	4,55E-12
ENSG00000134986	NREP	-7,349	6,28E-12
ENSG00000159885	ZNF222	-7,34	6,70E-12
ENSG00000152683	SLC30A6	-7,336	6,87E-12
ENSG00000225470	JPX	-7,336	6,87E-12
ENSG00000107242	PIP5K1B	-7,323	7,54E-12
ENSG00000259494	MRPL46	-7,321	7,64E-12
ENSG00000088356	PDRG1	-7,3	8,86E-12
ENSG00000198720	ANKRD13B	-7,293	9,32E-12
ENSG00000166341	DCHS1	-7,275	1,06E-11

ENSG00000198561	CTNND1	5,243	2,32E-06
ENSG00000224420	ADM5	5,251	2,23E-06
ENSG00000172172	MRPL13	5,255	2,19E-06
ENSG00000159640	ACE	5,264	2,09E-06
ENSG00000277161	PIGW	5,27	2,02E-06
ENSG00000176401	EID2B	5,285	1,88E-06
ENSG00000161958	FGF11	5,287	1,87E-06
ENSG00000088881	EBF4	5,291	1,82E-06
ENSG00000163352	LENEP	5,312	1,64E-06
ENSG00000145911	N4BP3	5,312	1,64E-06
ENSG00000148200	NR6A1	5,312	1,64E-06
ENSG00000206622	SNORA69	5,312	1,64E-06
ENSG00000205133	TRIQK	5,324	1,55E-06
ENSG00000109089	CDR2L	5,337	1,44E-06
ENSG00000181315	ZNF322	5,358	1,29E-06
ENSG00000135736	CCDC102A	5,361	1,27E-06
ENSG00000067365	METTL22	5,401	1,02E-06
ENSG00000015153	YAF2	5,403	1,02E-06
ENSG00000185379	RAD51D	5,414	9,59E-07
ENSG00000198960	ARMCX6	5,422	9,19E-07
ENSG00000170291	ELP5	5,43	8,79E-07
ENSG00000180596	HIST1H2BE	5,459	7,50E-07
ENSG00000160469	BRSK1	5,503	5,89E-07
ENSG00000168040	FADD	5,527	5,14E-07
ENSG00000140297	GCNT3	5,558	4,34E-07
ENSG00000012983	MAP4K5	5,591	3,58E-07
ENSG00000005884	ITGA3	5,594	3,53E-07
ENSG00000117115	PADI2	5,689	2,05E-07
ENSG00000196369	SRGAP2B	5,69	2,04E-07
ENSG00000172020	GAP43	5,709	1,83E-07
ENSG00000068078	FGFR3	5,709	1,83E-07
ENSG00000187609	EXD3	5,709	1,83E-07
ENSG00000107859	PITX3	5,709	1,83E-07
ENSG00000181418	DDN	5,709	1,83E-07
ENSG00000234911	TEX21P	5,709	1,83E-07
ENSG00000152315	KCNK13	5,709	1,83E-07
ENSG00000182175	RGMA	5,709	1,83E-07
ENSG00000109113	RAB34	5,709	1,83E-07
ENSG00000160117	ANKLE1	5,709	1,83E-07
ENSG00000197380	DACT3	5,709	1,83E-07
ENSG00000102043	MTMR8	5,709	1,83E-07
ENSG00000171054	OR13H1	5,709	1,83E-07
ENSG00000204421	LY6G6C	5,709	1,83E-07
ENSG00000133195	SLC39A11	5,711	1,83E-07
ENSG00000213928	IRF9	5,741	1,55E-07
ENSG00000263956	NBPF11	5,744	1,53E-07

ENSG00000136367	ZFHX2	-7,262	1,16E-11
ENSG00000125744	RTN2	-7,256	1,21E-11
ENSG00000162630	B3GALT2	-7,247	1,29E-11
ENSG00000186312	CA5BP1	-7,202	1,76E-11
ENSG00000101076	HNF4A	-7,171	2,18E-11
ENSG00000106665	CLIP2	-7,129	2,94E-11
ENSG00000005108	THSD7A	-7,116	3,23E-11
ENSG00000199785	SNORA52	-7,111	3,33E-11
ENSG00000137312	FLOT1	-7,101	3,59E-11
ENSG00000228175	GEMIN8P4	-7,06	4,79E-11
ENSG00000182870	GALNT9	-7,052	5,03E-11
ENSG00000125931	CITED1	-7,052	5,03E-11
ENSG00000260916	CCPG1	-7,011	6,71E-11
ENSG00000169855	ROBO1	-6,953	1,00E-10
ENSG00000134864	GGACT	-6,907	1,38E-10
ENSG00000196417	ZNF765	-6,895	1,49E-10
ENSG00000188818	ZDHHC11	-6,871	1,76E-10
ENSG00000188766	SPRED3	-6,849	2,05E-10
ENSG00000135636	DYSF	-6,837	2,17E-10
ENSG00000224958	PGM5-AS1	-6,837	2,17E-10
ENSG00000149557	FEZ1	-6,837	2,17E-10
ENSG00000205822	TPTE2P6	-6,837	2,17E-10
ENSG00000104154	SLC30A4	-6,837	2,17E-10
ENSG00000091622	PITPNM3	-6,837	2,17E-10
ENSG00000187775	DNAH17	-6,837	2,17E-10
ENSG00000104883	PEX11G	-6,837	2,17E-10
ENSG00000165175	MID1IP1	-6,837	2,17E-10
ENSG00000198157	HMGN5	-6,837	2,17E-10
ENSG00000160716	CHRNB2	-6,837	2,18E-10
ENSG00000186417	GLDN	-6,81	2,63E-10
ENSG00000181798	LINC00471	-6,798	2,83E-10
ENSG00000061455	PRDM6	-6,791	2,96E-10
ENSG00000180884	ZNF792	-6,78	3,19E-10
ENSG00000117407	ARTN	-6,734	4,25E-10
ENSG00000225880	LINC00115	-6,703	5,26E-10
ENSG00000085840	ORC1	-6,7	5,35E-10
ENSG00000173080	RXFP4	-6,694	5,55E-10
ENSG00000205413	SAMD9	-6,67	6,47E-10
ENSG00000157379	DHRS1	-6,665	6,71E-10
ENSG00000169184	MN1	-6,66	6,92E-10
ENSG00000134242	PTPN22	-6,639	7,97E-10
ENSG00000165046	LETM2	-6,597	1,05E-09
ENSG00000175591	P2RY2	-6,556	1,36E-09
ENSG00000164342	TLR3	-6,487	2,14E-09
ENSG00000118557	PMFBP1	-6,4	3,75E-09
ENSG00000111077	TENC1	-6,384	4,15E-09
ENSG00000143702	CEP170P1	5,744	1,53E-07
ENSG00000213760	ATP6V1G2	5,748	1,49E-07
ENSG00000151025	GPR158	5,749	1,49E-07
ENSG00000152556	PFKM	5,831	1,02E-07
ENSG00000166478	ZNF143	5,851	9,08E-08
ENSG00000105865	DUS4L	5,867	8,32E-08
ENSG00000134198	TSPAN2	5,903	6,71E-08
ENSG00000115009	CCL20	5,903	6,71E-08
ENSG00000197415	VEPH1	5,903	6,71E-08
ENSG00000179046	TRIML2	5,903	6,71E-08
ENSG00000129422	MTUS1	5,903	6,71E-08
ENSG00000140006	WDR89	5,903	6,71E-08
ENSG00000103154	NECAB2	5,903	6,71E-08
ENSG00000141639	MAPK4	5,903	6,71E-08
ENSG00000268751	SCGB1B2P	5,903	6,71E-08
ENSG00000162669	HFM1	5,977	4,49E-08
ENSG00000188641	DPYD	5,977	4,49E-08
ENSG00000136689	IL1RN	5,977	4,49E-08
ENSG00000181585	TMIE	5,977	4,49E-08
ENSG00000145536	ADAMTS16	5,977	4,49E-08
ENSG00000164400	CSF2	5,977	4,49E-08
ENSG00000205089	CCNI2	5,977	4,49E-08
ENSG00000078401	EDN1	5,977	4,49E-08
ENSG00000276998	REXO1L2P	5,977	4,49E-08
ENSG00000137070	IL11RA	5,977	4,49E-08
ENSG00000175768	TOMM5	5,977	4,49E-08
ENSG00000173227	SYT12	5,977	4,49E-08
ENSG00000136010	ALDH1L2	5,977	4,49E-08
ENSG00000239827	SUGT1P3	5,977	4,49E-08
ENSG00000129538	RNASE1	5,977	4,49E-08
ENSG00000140092	FBLN5	5,977	4,49E-08
ENSG00000103742	IGDCC4	5,977	4,49E-08
ENSG00000176046	NUPR1	5,977	4,49E-08
ENSG00000221887	HMSD	5,977	4,49E-08
ENSG00000282458	WASH5P	5,977	4,49E-08
ENSG00000186115	CYP4F2	5,977	4,49E-08
ENSG00000105695	MAG	5,977	4,49E-08
ENSG00000196337	CGB7	5,977	4,49E-08
ENSG00000174586	ZNF497	5,977	4,49E-08
ENSG00000100341	PNPLA5	5,977	4,49E-08
ENSG00000102225	CDK16	5,977	4,49E-08
ENSG00000204681	GABBR1	5,977	4,49E-08
ENSG00000188368	PRR19	5,981	4,49E-08
ENSG00000136141	LRCH1	5,995	4,21E-08
ENSG00000169242	EFNA1	5,999	4,11E-08
ENSG00000167588	GPD1	6,003	4,02E-08

ENSG00000184557	SOCS3	-6,354	4,99E-09
ENSG00000224209	LINC00466	-6,353	4,99E-09
ENSG00000182389	CACNB4	-6,353	4,99E-09
ENSG00000173295	FAM86B3P	-6,353	4,99E-09
ENSG00000164741	DLC1	-6,353	4,99E-09
ENSG00000177283	FZD8	-6,353	4,99E-09
ENSG00000240370	RPL13P5	-6,353	4,99E-09
ENSG00000233382	NKAPP1	-6,353	4,99E-09
ENSG00000136167	LCP1	-6,351	5,07E-09
ENSG00000162927	PUS10	-6,318	6,24E-09
ENSG00000114698	PLSCR4	-6,289	7,50E-09
ENSG00000099901	RANBP1	-6,266	8,64E-09
ENSG00000171823	FBXL14	-6,243	1,00E-08
ENSG00000104814	MAP4K1	-6,235	1,05E-08
ENSG00000109079	TNFAIP1	-6,227	1,10E-08
ENSG00000243708	PLA2G4B	-6,226	1,10E-08
ENSG00000056558	TRAF1	-6,224	1,11E-08
ENSG00000126790	L3HYPDH	-6,221	1,14E-08
ENSG00000151224	MAT1A	-6,203	1,27E-08
ENSG00000265763	ZNF488	-6,188	1,35E-08
ENSG00000134321	RSAD2	-6,188	1,35E-08
ENSG00000170745	KCNS3	-6,188	1,35E-08
ENSG00000114771	AADAC	-6,188	1,35E-08
ENSG00000106031	HOXA13	-6,188	1,35E-08
ENSG00000240583	AQP1	-6,188	1,35E-08
ENSG00000002746	HECW1	-6,188	1,35E-08
ENSG00000181085	MAPK15	-6,188	1,35E-08
ENSG00000041982	TNC	-6,188	1,35E-08
ENSG00000174804	FZD4	-6,188	1,35E-08
ENSG00000241749	RPSAP52	-6,188	1,35E-08
ENSG00000198598	MMP17	-6,188	1,35E-08
ENSG00000140459	CYP11A1	-6,188	1,35E-08
ENSG00000127588	GNG13	-6,188	1,35E-08
ENSG00000161405	IKZF3	-6,188	1,35E-08
ENSG00000131943	C19orf12	-6,188	1,35E-08
ENSG00000166619	BLCAP	-6,188	1,35E-08
ENSG00000237438	CECR7	-6,188	1,35E-08
ENSG00000163374	YY1AP1	-6,184	1,38E-08
ENSG00000242110	AMACR	-6,18	1,40E-08
ENSG00000100036	SLC35E4	-6,172	1,47E-08
ENSG00000215218	UBE2QL1	-6,151	1,68E-08
ENSG00000188613	NANOS1	-6,142	1,77E-08
ENSG00000246985	SOCS2-AS1	-6,113	2,12E-08
ENSG00000275111	ZNF2	-6,089	2,43E-08
ENSG00000101294	HM13	-6,081	2,55E-08
ENSG00000124406	ATP8A1	-6,062	2,85E-08

ENSG00000119801	YPEL5	6,011	3,85E-08
ENSG00000151474	FRMD4A	6,023	3,60E-08
ENSG00000115594	IL1R1	6,028	3,49E-08
ENSG00000133640	LRRIQ1	6,038	3,29E-08
ENSG00000170017	ALCAM	6,068	2,76E-08
ENSG00000119013	NDUFB3	6,068	2,75E-08
ENSG00000127324	TSPAN8	6,081	2,55E-08
ENSG00000132952	USPL1	6,093	2,38E-08
ENSG00000132000	PODNL1	6,096	2,34E-08
ENSG00000258920	FOXN3-AS1	6,107	2,18E-08
ENSG00000255150	EID3	6,116	2,07E-08
ENSG00000122970	IFT81	6,117	2,06E-08
ENSG00000168938	PPIC	6,12	2,03E-08
ENSG00000011260	UTP18	6,155	1,63E-08
ENSG00000159899	NPR2	6,159	1,60E-08
ENSG00000207493	SNORA46	6,17	1,49E-08
ENSG00000229186	ADAM1A	6,181	1,40E-08
ENSG00000102302	FGD1	6,182	1,39E-08
ENSG00000105514	RAB3D	6,198	1,31E-08
ENSG00000141837	CACNA1A	6,201	1,28E-08
ENSG00000177971	IMP3	6,211	1,20E-08
ENSG00000145331	TRMT10A	6,226	1,10E-08
ENSG00000161643	SIGLEC16	6,227	1,10E-08
ENSG00000163467	TSACC	6,255	9,30E-09
ENSG00000105388	CEACAM5	6,273	8,28E-09
ENSG00000090905	TNRC6A	6,302	6,89E-09
ENSG00000184698	OR51M1	6,343	5,33E-09
ENSG00000047634	SCML1	6,364	4,73E-09
ENSG00000205002	AARD	6,368	4,61E-09
ENSG00000236200	KDM4A-AS1	6,387	4,07E-09
ENSG00000183647	ZNF530	6,4	3,75E-09
ENSG00000185761	ADAMTSL5	6,426	3,19E-09
ENSG00000068971	PPP2R5B	6,467	2,44E-09
ENSG00000136710	CCDC115	6,515	1,78E-09
ENSG00000070404	FSTL3	6,544	1,47E-09
ENSG00000118292	C1orf54	6,564	1,29E-09
ENSG00000130997	POLN	6,564	1,29E-09
ENSG00000221818	EBF2	6,564	1,29E-09
ENSG00000177042	TMEM80	6,564	1,29E-09
ENSG00000137700	SLC37A4	6,564	1,29E-09
ENSG00000212124	TAS2R19	6,564	1,29E-09
ENSG00000168646	AXIN2	6,564	1,29E-09
ENSG00000184949	FAM227A	6,564	1,29E-09
ENSG00000141294	LRRC46	6,568	1,27E-09
ENSG00000253846	PCDHGA10	6,591	1,09E-09
ENSG00000151846	PABPC3	6,627	8,60E-10

ENSG00000178999	AURKB	-6,061	2,87E-08
ENSG00000153993	SEMA3D	-6,032	3,41E-08
ENSG00000175130	MARCKSL1	-6,025	3,54E-08
ENSG00000136542	GALNT5	-6,019	3,67E-08
ENSG00000213199	ASIC3	-6,01	3,86E-08
ENSG00000007372	PAX6	-6,01	3,86E-08
ENSG00000140465	CYP1A1	-6,009	3,88E-08
ENSG00000167733	HSD11B1L	-5,962	4,89E-08
ENSG00000147144	CCDC120	-5,95	5,26E-08
ENSG00000221916	C19orf73	-5,919	6,34E-08
ENSG00000186854	TRABD2A	-5,91	6,54E-08
ENSG00000138823	MTTP	-5,91	6,54E-08
ENSG00000124507	PACSIN1	-5,91	6,54E-08
ENSG00000184530	C6orf58	-5,91	6,54E-08
ENSG00000006747	SCIN	-5,91	6,54E-08
ENSG00000279012	OR51B2	-5,91	6,54E-08
ENSG00000206192	ANKRD20A9P	-5,91	6,54E-08
ENSG00000180229	HERC2P3	-5,91	6,54E-08
ENSG00000198146	ZNF770	-5,91	6,54E-08
ENSG00000271447	MMP28	-5,91	6,54E-08
ENSG00000188039	NWD1	-5,91	6,54E-08
ENSG00000160396	HIPK4	-5,91	6,54E-08
ENSG00000158164	TMSB15A	-5,91	6,54E-08
ENSG00000198945	L3MBTL3	-5,883	7,54E-08
ENSG00000240386	LCE1F	-5,878	7,79E-08
ENSG00000159388	BTG2	-5,866	8,32E-08
ENSG00000167889	MGAT5B	-5,857	8,74E-08
ENSG00000164761	TNFRSF11B	-5,84	9,67E-08
ENSG00000161955	TNFSF13	-5,828	1,04E-07
ENSG00000162490	DRAXIN	-5,807	1,10E-07
ENSG00000158006	PAFAH2	-5,807	1,10E-07
ENSG00000196189	SEMA4A	-5,807	1,10E-07
ENSG00000163565	IFI16	-5,807	1,10E-07
ENSG00000119771	KLHL29	-5,807	1,10E-07
ENSG00000163817	SLC6A20	-5,807	1,10E-07
ENSG00000163380	LMOD3	-5,807	1,10E-07
ENSG00000145147	SLIT2	-5,807	1,10E-07
ENSG00000181541	MAB21L2	-5,807	1,10E-07
ENSG00000213406	ANXA2P1	-5,807	1,10E-07
ENSG00000198939	ZFP2	-5,807	1,10E-07
ENSG00000087116	ADAMTS2	-5,807	1,10E-07
ENSG00000219607	PPP1R3G	-5,807	1,10E-07
ENSG00000219294	PIP5K1P1	-5,807	1,10E-07
ENSG00000183674	LINC00518	-5,807	1,10E-07
ENSG00000204305	AGER	-5,807	1,10E-07
ENSG00000091137	SLC26A4	-5,807	1,10E-07

ENSG00000102879	CORO1A	6,638	7,98E-10
ENSG00000168026	TTC21A	6,681	6,04E-10
ENSG00000175785	PRIMA1	6,685	5,88E-10
ENSG00000141497	ZMYND15	6,685	5,88E-10
ENSG00000161981	SNRNP25	6,693	5,60E-10
ENSG00000128604	IRF5	6,709	5,07E-10
ENSG00000184047	DIABLO	6,76	3,58E-10
ENSG00000154240	CEP112	6,76	3,58E-10
ENSG00000172731	LRRC20	6,772	3,31E-10
ENSG00000198331	HYLS1	6,772	3,31E-10
ENSG00000248124	RRN3P1	6,772	3,31E-10
ENSG00000167757	KLK11	6,772	3,31E-10
ENSG00000110344	UBE4A	6,772	3,31E-10
ENSG00000134245	WNT2B	6,777	3,23E-10
ENSG00000167311	ART5	6,777	3,23E-10
ENSG00000162241	SLC25A45	6,777	3,23E-10
ENSG00000019144	PHLDB1	6,777	3,23E-10
ENSG00000139970	RTN1	6,777	3,23E-10
ENSG00000183780	SLC35F3	6,883	1,62E-10
ENSG00000157343	ARMC12	6,9	1,45E-10
ENSG00000144355	DLX1	6,901	1,43E-10
ENSG00000181481	RNF135	6,926	1,21E-10
ENSG00000130540	SULT4A1	6,95	1,02E-10
ENSG00000173404	INSM1	6,972	8,78E-11
ENSG00000155158	TTC39B	6,974	8,65E-11
ENSG00000168899	VAMP5	6,981	8,28E-11
ENSG00000152766	ANKRD22	6,992	7,69E-11
ENSG00000152240	HAUS1	7,017	6,44E-11
ENSG00000116138	DNAJC16	7,034	5,73E-11
ENSG00000196214	ZNF766	7,054	4,99E-11
ENSG00000128000	ZNF780B	7,058	4,84E-11
ENSG00000213809	KLRK1	7,145	2,62E-11
ENSG00000106080	FKBP14	7,152	2,50E-11
ENSG00000136295	TTYH3	7,164	2,30E-11
ENSG00000213139	CRYGS	7,173	2,15E-11
ENSG00000174521	TTC9B	7,173	2,15E-11
ENSG00000206755	SNORA30	7,185	1,99E-11
ENSG00000079337	RAPGEF3	7,2	1,78E-11
ENSG00000112561	TFEB	7,203	1,76E-11
ENSG00000197563	PIGN	7,222	1,53E-11
ENSG00000168939	SPRY3	7,23	1,45E-11
ENSG00000040608	RTN4R	7,239	1,36E-11
ENSG00000174721	FGFBP3	7,257	1,20E-11
ENSG00000197483	ZNF628	7,26	1,18E-11
ENSG00000171574	ZNF584	7,299	8,92E-12
ENSG00000128346	C22orf23	7,304	8,64E-12

ENSG00000230316	FEZF1-AS1	-5,807	1,10E-07
ENSG00000158815	FGF17	-5,807	1,10E-07
ENSG00000215187	FAM166B	-5,807	1,10E-07
ENSG00000266412	NCOA4	-5,807	1,10E-07
ENSG00000138131	LOXL4	-5,807	1,10E-07
ENSG00000187908	DMBT1	-5,807	1,10E-07
ENSG00000175264	CHST1	-5,807	1,10E-07
ENSG00000173338	KCNK7	-5,807	1,10E-07
ENSG00000177675	CD163L1	-5,807	1,10E-07
ENSG00000134539	KLRD1	-5,807	1,10E-07
ENSG00000185432	METTL7A	-5,807	1,10E-07
ENSG00000123342	MMP19	-5,807	1,10E-07
ENSG00000238105	GOLGA2P5	-5,807	1,10E-07
ENSG00000167723	TRPV3	-5,807	1,10E-07
ENSG00000173991	TCAP	-5,807	1,10E-07
ENSG00000005961	ITGA2B	-5,807	1,10E-07
ENSG00000293358	LOC653653	-5,807	1,10E-07
ENSG00000183287	CCBE1	-5,807	1,10E-07
ENSG00000125650	PSPN	-5,807	1,10E-07
ENSG00000142303	ADAMTS10	-5,807	1,10E-07
ENSG00000178093	TSSK6	-5,807	1,10E-07
ENSG00000105737	GRIK5	-5,807	1,10E-07
ENSG00000177692	DNAJC28	-5,807	1,10E-07
ENSG00000243279	PRAF2	-5,807	1,10E-07
ENSG00000186416	NKRF	-5,807	1,10E-07
ENSG00000204248	COL11A2	-5,807	1,10E-07
ENSG00000143502	SUSD4	-5,806	1,10E-07
ENSG00000065057	NTHL1	-5,801	1,13E-07
ENSG00000179994	SPDYE7P	-5,799	1,14E-07
ENSG00000187634	SAMD11	-5,794	1,15E-07
ENSG00000196734	LCE1B	-5,794	1,15E-07
ENSG00000115008	IL1A	-5,794	1,15E-07
ENSG00000169432	SCN9A	-5,794	1,15E-07
ENSG00000072195	SPEG	-5,794	1,15E-07
ENSG00000109390	NDUFC1	-5,794	1,15E-07
ENSG00000164136	IL15	-5,794	1,15E-07
ENSG00000173261	PLAC8L1	-5,794	1,15E-07
ENSG00000180938	ZNF572	-5,794	1,15E-07
ENSG00000165995	CACNB2	-5,794	1,15E-07
ENSG00000012779	ALOX5	-5,794	1,15E-07
ENSG00000138326	RPS24	-5,794	1,15E-07
ENSG00000110375	UPK2	-5,794	1,15E-07
ENSG00000140279	DUOX2	-5,794	1,15E-07
ENSG00000214456	PLIN5	-5,794	1,15E-07
ENSG00000124143	ARHGAP40	-5,794	1,15E-07
ENSG00000100031	GGT1	-5,794	1,15E-07
ENSG00000198915	RASGEF1A	7,309	8,34E-12
ENSG00000105750	ZNF85	7,332	7,10E-12
ENSG00000206937	SNORA70B	7,371	5,35E-12
ENSG00000013619	MAMLD1	7,43	3,49E-12
ENSG00000163762	TM4SF18	7,432	3,44E-12
ENSG00000102886	GDPD3	7,514	1,87E-12
ENSG00000158186	MRAS	7,529	1,67E-12
ENSG00000167393	PPP2R3B	7,536	1,60E-12
ENSG00000152219	ARL14EP	7,543	1,52E-12
ENSG00000099840	IZUMO4	7,579	1,16E-12
ENSG00000128607	KLHDC10	7,606	9,46E-13
ENSG00000204516	MICB	7,61	9,18E-13
ENSG00000185485	SDHAP1	7,716	4,10E-13
ENSG00000138834	MAPK8IP3	7,722	3,94E-13
ENSG00000152520	PAN3	7,726	3,82E-13
ENSG00000107282	APBA1	7,741	3,41E-13
ENSG00000096093	EFHC1	7,772	2,67E-13
ENSG00000125741	OPA3	7,789	2,35E-13
ENSG00000164366	CCDC127	7,818	1,89E-13
ENSG00000215375	MYL5	7,827	1,77E-13
ENSG00000144550	CPNE9	7,836	1,65E-13
ENSG00000248905	FMN1	7,843	1,57E-13
ENSG00000136436	CALCOCO2	7,901	9,93E-14
ENSG00000105550	FGF21	7,917	8,76E-14
ENSG00000113318	MSH3	7,939	7,39E-14
ENSG00000152705	CATSPER3	7,939	7,39E-14
ENSG00000117586	TNFSF4	7,95	6,78E-14
ENSG00000186451	SPATA12	8,055	2,98E-14
ENSG00000228409	CCT6P1	8,095	2,17E-14
ENSG00000164241	C5orf63	8,096	2,16E-14
ENSG00000145362	ANK2	8,109	1,93E-14
ENSG00000111145	ELK3	8,237	6,90E-15
ENSG00000132846	ZBED3	8,239	6,80E-15
ENSG00000004948	CALCR	8,242	6,64E-15
ENSG00000004838	ZMYND10	8,272	5,20E-15
ENSG00000183401	CCDC159	8,277	5,02E-15
ENSG00000033170	FUT8	8,287	4,64E-15
ENSG00000187187	ZNF546	8,299	4,22E-15
ENSG00000064687	ABCA7	8,305	4,02E-15
ENSG00000181588	MEX3D	8,307	3,96E-15
ENSG00000171951	SCG2	8,373	2,30E-15
ENSG00000223773	CD99P1	8,411	1,69E-15
ENSG00000159433	STARD9	8,413	1,66E-15
ENSG00000182685	BRICD5	8,426	1,49E-15
ENSG00000084710	EFR3B	8,436	1,38E-15
ENSG00000178104	PDE4DIP	8,443	1,31E-15

ENSG00000085185	BCORL1	-5,794	1,15E-07
ENSG00000274349	ZNF658	-5,777	1,27E-07
ENSG00000144843	ADPRH	-5,775	1,28E-07
ENSG00000205885	C1RL-AS1	-5,772	1,31E-07
ENSG00000108797	CNTNAP1	-5,766	1,35E-07
ENSG00000100604	CHGA	-5,764	1,37E-07
ENSG00000230524	COL6A4P1	-5,752	1,46E-07
ENSG00000092094	OSGEP	-5,705	1,87E-07
ENSG00000221737	MIR548I1	-5,655	2,50E-07
ENSG00000115539	PDCL3	-5,641	2,71E-07
ENSG00000105672	ETV2	-5,621	3,03E-07
ENSG00000101850	GPR143	-5,584	3,74E-07
ENSG00000204315	FKBPL	-5,577	3,88E-07
ENSG00000078804	TP53INP2	-5,543	4,70E-07
ENSG00000215837	SDHAP2	-5,51	5,67E-07
ENSG00000269313	MAGIX	-5,504	5,86E-07
ENSG00000139625	MAP3K12	-5,492	6,24E-07
ENSG00000185758	CLDN24	-5,436	8,51E-07
ENSG00000118620	ZNF430	-5,411	9,77E-07
ENSG00000185250	PPIL6	-5,403	1,02E-06
ENSG00000167100	SAMD14	-5,393	1,07E-06
ENSG00000167711	SERPINF2	-5,366	1,24E-06
ENSG00000162745	OLFML2B	-5,363	1,25E-06
ENSG00000196843	ARID5A	-5,363	1,25E-06
ENSG00000141028	CDRT15P1	-5,363	1,25E-06
ENSG00000271699	SNX29P2	-5,352	1,33E-06
ENSG00000206149	HERC2P9	-5,351	1,33E-06
ENSG00000116396	KCNC4	-5,343	1,39E-06
ENSG00000162129	CLPB	-5,312	1,64E-06
ENSG00000141098	GFOD2	-5,309	1,66E-06
ENSG00000141655	TNFRSF11A	-5,303	1,72E-06
ENSG00000167705	RILP	-5,301	1,73E-06
ENSG00000100100	PIK3IP1	-5,301	1,73E-06
ENSG00000152669	CCNO	-5,298	1,76E-06
ENSG00000204604	ZNF468	-5,281	1,92E-06
ENSG00000153347	FAM81B	-5,279	1,93E-06
ENSG00000244462	RBM12	-5,279	1,94E-06
ENSG00000148516	ZEB1	-5,27	2,03E-06
ENSG00000205755	CRLF2	-5,257	2,17E-06
ENSG00000109686	SH3D19	-5,25	2,24E-06
ENSG00000121775	TMEM39B	-5,242	2,32E-06
ENSG00000235082	SUMO1P3	-5,242	2,32E-06
ENSG00000197208	SLC22A4	-5,242	2,32E-06
ENSG00000171989	LDHAL6B	-5,242	2,32E-06
ENSG00000143772	ITPKB	-5,232	2,45E-06
ENSG00000112852	PCDHB2	-5,232	2,45E-06

ENSG00000122641	INHBA	8,468	1,08E-15
ENSG00000091879	ANGPT2	8,488	9,10E-16
ENSG00000006451	RALA	8,521	7,03E-16
ENSG00000148218	ALAD	8,533	6,36E-16
ENSG00000084676	NCOA1	8,535	6,28E-16
ENSG00000198792	TMEM184B	8,557	5,27E-16
ENSG00000105072	C19orf44	8,557	5,27E-16
ENSG00000111348	ARHGDIB	8,565	4,94E-16
ENSG00000105048	TNNT1	8,572	4,67E-16
ENSG00000104953	TLE6	8,585	4,22E-16
ENSG00000242252	BGLAP	8,619	3,19E-16
ENSG00000167325	RRM1	8,633	2,85E-16
ENSG00000111110	PPM1H	8,642	2,66E-16
ENSG00000136883	KIF12	8,666	2,19E-16
ENSG00000097096	SYDE2	8,675	2,05E-16
ENSG00000115318	LOXL3	8,677	2,03E-16
ENSG00000213906	LTB4R2	8,68	1,98E-16
ENSG00000226823	SUGT1P1	8,692	1,81E-16
ENSG00000247092	SNHG10	8,712	1,54E-16
ENSG00000171097	CCBL1	8,716	1,50E-16
ENSG00000141068	KSR1	8,746	1,17E-16
ENSG00000106701	FSD1L	8,748	1,16E-16
ENSG00000201157	SNORA62	8,755	1,10E-16
ENSG00000198833	UBE2J1	8,778	9,26E-17
ENSG00000150667	FSIP1	8,783	8,84E-17
ENSG00000196388	INCA1	8,784	8,83E-17
ENSG00000196420	S100A5	8,785	8,81E-17
ENSG00000243335	KCTD7	8,793	8,27E-17
ENSG00000170325	PRDM10	8,825	6,23E-17
ENSG00000105204	DYRK1B	8,841	5,46E-17
ENSG00000162924	REL	8,845	5,27E-17
ENSG00000116731	PRDM2	8,856	4,85E-17
ENSG00000176771	NCKAP5	8,862	4,62E-17
ENSG00000231528	FAM225A	8,877	4,17E-17
ENSG00000133121	STARD13	8,89	3,73E-17
ENSG00000185800	DMWD	8,898	3,52E-17
ENSG00000204946	ZNF783	8,934	2,59E-17
ENSG00000171246	NPTX1	8,94	2,45E-17
ENSG00000100221	JOSD1	8,977	1,81E-17
ENSG00000166963	MAP1A	8,978	1,81E-17
ENSG00000103855	CD276	8,983	1,74E-17
ENSG00000204536	CCHCR1	8,994	1,59E-17
ENSG00000203326	ZNF525	9,014	1,34E-17
ENSG00000177628	GBA	9,038	1,10E-17
ENSG00000170011	MYRIP	9,044	1,05E-17
ENSG00000185513	L3MBTL1	9,048	1,01E-17

ENSG00000084072	PPIE	-5,226	2,53E-06
ENSG00000265293	ARGFXP2	-5,224	2,56E-06
ENSG00000117643	MAN1C1	-5,222	2,57E-06
ENSG00000132793	LPIN3	-5,221	2,59E-06
ENSG00000120658	ENOX1	-5,219	2,60E-06
ENSG00000204514	ZNF814	-5,217	2,63E-06
ENSG00000244026	FAM86DP	-5,214	2,65E-06
ENSG00000102878	HSF4	-5,214	2,65E-06
ENSG00000207181	SNORA14B	-5,213	2,66E-06
ENSG00000101608	MYL12A	-5,208	2,73E-06
ENSG00000181826	RELL1	-5,208	2,73E-06
ENSG00000205710	C17orf107	-5,191	2,95E-06
ENSG00000206948	SNORA36A	-5,191	2,95E-06
ENSG00000073921	PICALM	-5,14	3,86E-06
ENSG00000131016	AKAP12	-5,075	5,42E-06
ENSG00000128973	CLN6	-5,06	5,86E-06
ENSG00000135678	CPM	-4,929	1,15E-05
ENSG00000129514	FOXA1	-4,867	1,57E-05
ENSG00000149582	TMEM25	-4,86	1,63E-05
ENSG00000183579	ZNRF3	-4,823	1,97E-05
ENSG00000180658	OR2A4	-4,812	2,07E-05
ENSG00000114861	FOXP1	-4,754	2,75E-05
ENSG00000161277	THAP8	-4,735	3,03E-05
ENSG00000138085	ATRAID	-4,652	4,52E-05
ENSG00000182325	FBXL6	-4,618	5,32E-05
ENSG00000132141	CCT6B	-4,615	5,37E-05
ENSG00000065485	PDIA5	-4,612	5,47E-05
ENSG00000031081	ARHGAP31	-4,538	7,76E-05
ENSG00000199477	SNORA31	-4,416	1,37E-04
ENSG00000131171	SH3BGRL	-4,412	1,40E-04
ENSG00000164932	CTHRC1	-4,305	2,27E-04
ENSG00000131876	SNRPA1	-4,228	3,18E-04
ENSG00000253293	HOXA10	-4,187	3,81E-04
ENSG00000099875	MKNK2	-4,055	6,71E-04
ENSG00000110680	CALCA	-4,048	6,90E-04
ENSG00000189143	CLDN4	-4,039	7,16E-04
ENSG00000123485	HJURP	-3,982	9,07E-04
ENSG00000197933	ZNF823	-3,96	9,97E-04
ENSG00000166938	DIS3L	-3,936	1,10E-03
ENSG00000196139	AKR1C3	-3,916	1,19E-03
ENSG00000100376	FAM118A	-3,908	1,23E-03
ENSG00000168394	TAP1	-3,908	1,23E-03
ENSG00000090470	PDCD7	-3,893	1,31E-03
ENSG00000105696	TMEM59L	-3,842	1,61E-03
ENSG00000147536	GINS4	-3,819	1,76E-03
ENSG00000167608	TMC4	-3,805	1,86E-03

ENSG00000174137	FAM53A	9,051	9,87E-18
ENSG00000182379	NXPH4	9,058	9,34E-18
ENSG00000131944	C19orf40	9,087	7,33E-18
ENSG00000004776	HSPB6	9,095	6,83E-18
ENSG00000164970	FAM219A	9,118	5,75E-18
ENSG00000164749	HNF4G	9,123	5,54E-18
ENSG00000134824	FADS2	9,13	5,24E-18
ENSG00000180730	SHISA2	9,134	5,10E-18
ENSG00000139055	ERP27	9,155	4,34E-18
ENSG00000039139	DNAH5	9,164	4,04E-18
ENSG00000079385	CEACAM1	9,185	3,49E-18
ENSG00000169635	HIC2	9,187	3,45E-18
ENSG00000102678	FGF9	9,205	3,00E-18
ENSG00000139269	INHBE	9,229	2,49E-18
ENSG00000164483	SAMD3	9,229	2,49E-18
ENSG00000155393	HEATR3	9,242	2,28E-18
ENSG00000128917	DLL4	9,253	2,13E-18
ENSG00000132801	ZSWIM3	9,284	1,62E-18
ENSG00000167264	DUS2L	9,293	1,52E-18
ENSG00000110944	IL23A	9,309	1,32E-18
ENSG00000252906	SCARNA3	9,329	1,12E-18
ENSG00000152256	PDK1	9,341	1,01E-18
ENSG00000141522	ARHGDIA	9,408	5,54E-19
ENSG00000135862	LAMC1	9,425	4,74E-19
ENSG00000163644	PPM1K	9,463	3,32E-19
ENSG00000121350	PYROXD1	9,476	2,97E-19
ENSG00000008513	ST3GAL1	9,496	2,48E-19
ENSG00000171466	ZNF562	9,515	2,12E-19
ENSG00000087086	FTL	9,526	1,97E-19
ENSG00000187860	CCDC157	9,537	1,79E-19
ENSG00000124783	SSR1	9,592	1,09E-19
ENSG00000142230	SAE1	9,609	9,32E-20
ENSG00000188215	DCUN1D3	9,631	7,68E-20
ENSG00000114062	UBE3A	9,682	4,72E-20
ENSG00000154380	ENAH	9,691	4,33E-20
ENSG00000172197	MBOAT1	9,919	4,88E-21
ENSG00000159023	EPB41	9,983	2,58E-21
ENSG00000152952	PLOD2	9,99	2,43E-21
ENSG00000131788	PIAS3	9,994	2,37E-21
ENSG00000197321	SVIL	10,055	1,29E-21
ENSG00000165704	HPRT1	10,079	1,02E-21
ENSG00000135048	TMEM2	10,087	9,53E-22
ENSG00000164054	SHISA5	10,265	1,58E-22
ENSG00000109680	TBC1D19	10,378	5,04E-23
ENSG00000142192	APP	10,413	3,59E-23
ENSG00000138604	GLCE	10,436	2,86E-23

ENSG00000165949	IFI27	-3,794	1,94E-03
ENSG00000161904	LEMD2	-3,78	2,04E-03
ENSG00000178057	NDUFAF3	-3,765	2,17E-03
ENSG00000174720	LARP7	-3,756	2,24E-03
ENSG00000212724	KRTAP2-3	-3,743	2,36E-03
ENSG00000002587	HS3ST1	-3,721	2,57E-03
ENSG00000218336	TENM3	-3,71	2,68E-03
ENSG00000185567	AHNAK2	-3,683	2,98E-03
ENSG00000170634	ACYP2	-3,646	3,43E-03
ENSG00000139178	C1RL	-3,642	3,48E-03
ENSG00000121988	ZRANB3	-3,641	3,49E-03
ENSG00000205426	KRT81	-3,64	3,49E-03
ENSG00000143952	VPS54	-3,626	3,69E-03
ENSG00000170776	AKAP13	-3,615	3,84E-03
ENSG00000055332	EIF2AK2	-3,601	4,04E-03
ENSG00000147416	ATP6V1B2	-3,581	4,35E-03
ENSG00000170523	KRT83	-3,574	4,46E-03
ENSG00000196371	FUT4	-3,572	4,49E-03
ENSG00000122406	RPL5	-3,558	4,73E-03
ENSG00000103121	CMC2	-3,545	4,95E-03
ENSG00000120725	SIL1	-3,54	5,05E-03
ENSG00000136152	COG3	-3,532	5,20E-03
ENSG00000188612	SUMO2	-3,519	5,46E-03
ENSG00000291237	SOD2	-3,517	5,49E-03
ENSG00000213963	LOC100130691	-3,516	5,49E-03
ENSG00000186951	PPARA	-3,508	5,64E-03
ENSG00000204386	NEU1	-3,503	5,74E-03
ENSG00000106733	NMRK1	-3,491	6,01E-03
ENSG00000160505	NLRP4	-3,477	6,32E-03
ENSG00000136068	FLNB	-3,474	6,38E-03
ENSG00000178307	TMEM11	-3,469	6,49E-03
ENSG00000141385	AFG3L2	-3,467	6,53E-03
ENSG00000124733	MEA1	-3,457	6,76E-03
ENSG00000109472	CPE	-3,45	6,94E-03
ENSG00000182871	COL18A1	-3,443	7,11E-03
ENSG00000149541	B3GAT3	-3,436	7,27E-03
ENSG00000089057	SLC23A2	-3,424	7,59E-03
ENSG00000176994	SMCR8	-3,408	8,03E-03
ENSG00000114316	USP4	-3,392	8,50E-03
ENSG00000187720	THSD4	-3,37	9,16E-03
ENSG00000173530	TNFRSF10D	-3,368	9,19E-03
ENSG00000173221	GLRX	-3,367	9,22E-03
ENSG00000086232	EIF2AK1	-3,361	9,44E-03
ENSG00000083845	RPS5	-3,358	9,52E-03
ENSG00000156471	PTDSS1	-3,334	1,03E-02
ENSG00000127220	ABHD8	-3,329	1,05E-02

ENSG00000173064	HECTD4	10,497	1,52E-23
ENSG00000066379	ZNRD1	10,509	1,36E-23
ENSG00000108671	PSMD11	10,706	1,71E-24
ENSG00000164307	ERAP1	10,829	4,74E-25
ENSG00000004799	PDK4	10,963	1,16E-25
ENSG00000075856	SART3	11,102	2,59E-26
ENSG00000176871	WSB2	11,198	9,20E-27
ENSG00000186501	TMEM222	11,259	4,72E-27
ENSG00000176142	TMEM39A	11,359	1,56E-27
ENSG00000177688	SUMO4	11,498	3,18E-28
ENSG00000137575	SDCBP	11,616	8,51E-29
ENSG00000120837	NFYB	11,722	2,49E-29
ENSG00000138698	RAP1GDS1	11,734	2,21E-29
ENSG00000136631	VPS45	11,907	2,92E-30
ENSG00000149573	MPZL2	12,193	9,88E-32
ENSG00000133731	IMPA1	12,198	9,50E-32
ENSG00000223509	WHAMMP1	12,249	5,21E-32
ENSG00000054523	KIF1B	12,287	3,32E-32
ENSG00000077147	TM9SF3	12,562	1,09E-33
ENSG00000198876	DCAF12	12,7	1,94E-34
ENSG00000179950	PUF60	12,736	1,26E-34
ENSG00000120709	FAM53C	12,886	1,92E-35
ENSG00000129657	SEC14L1	12,893	1,79E-35
ENSG00000198182	ZNF607	12,921	1,28E-35
ENSG00000166888	STAT6	13,028	3,26E-36
ENSG00000120925	RNF170	13,559	3,13E-39
ENSG00000168615	ADAM9	13,701	4,64E-40
ENSG00000179546	HTR1D	13,849	6,24E-41
ENSG00000173020	ADRBK1	14,178	6,48E-43
ENSG00000169241	SLC50A1	14,967	7,34E-48
ENSG00000113580	NR3C1	15,151	4,81E-49
ENSG00000162086	ZNF75A	15,268	8,44E-50
ENSG00000111424	VDR	15,607	5,17E-52
ENSG00000158623	COPG2	16,341	4,55E-57
ENSG00000139644	TMBIM6	16,575	1,02E-58
ENSG00000174405	LIG4	16,849	1,10E-60
ENSG00000129250	KIF1C	17,283	7,05E-64
ENSG00000162889	MAPKAPK2	17,959	7,80E-69
ENSG00000173456	RNF26	18,277	4,29E-71
ENSG00000100227	POLDIP3	19,127	6,81E-78
ENSG00000106351	AGFG2	19,565	2,06E-81

ENSG00000172137	CALB2	-3,321	1,08E-02
ENSG00000144589	STK11IP	-3,319	1,09E-02
ENSG00000238795	SCARNA12	-3,318	1,09E-02
ENSG00000188976	NOC2L	-3,31	1,12E-02
ENSG00000060971	ACAA1	-3,3	1,16E-02
ENSG00000102316	MAGED2	-3,293	1,19E-02
ENSG00000111863	ADTRP	-3,28	1,23E-02
ENSG00000159346	ADIPOR1	-3,279	1,24E-02
ENSG00000177963	RIC8A	-3,275	1,26E-02
ENSG00000197261	C6orf141	-3,255	1,34E-02
ENSG00000070159	PTPN3	-3,247	1,38E-02
ENSG00000137801	THBS1	-3,245	1,39E-02
ENSG00000090060	PAPOLA	-3,233	1,44E-02
ENSG00000169813	HNRNPF	-3,22	1,50E-02
ENSG00000106123	EPHB6	-3,217	1,51E-02
ENSG00000105443	CYTH2	-3,211	1,54E-02
ENSG00000002549	LAP3	-3,191	1,65E-02
ENSG00000130702	LAMA5	-3,188	1,67E-02
ENSG00000075399	VPS9D1	-3,171	1,77E-02
ENSG00000009780	FAM76A	-3,161	1,83E-02
ENSG00000167904	TMEM68	-3,148	1,90E-02
ENSG00000041357	PSMA4	-3,14	1,95E-02
ENSG00000181523	SGSH	-3,138	1,96E-02
ENSG00000135924	DNAJB2	-3,132	2,00E-02
ENSG00000127884	ECHS1	-3,13	2,01E-02
ENSG00000120337	TNFSF18	-3,128	2,03E-02
ENSG00000102384	CENPI	-3,122	2,07E-02
ENSG00000119335	SET	-3,111	2,13E-02
ENSG00000166226	CCT2	-3,109	2,14E-02
ENSG00000097021	ACOT7	-3,109	2,15E-02
ENSG00000158156	XKR8	-3,099	2,21E-02
ENSG00000170312	CDK1	-3,086	2,31E-02
ENSG00000188342	GTF2F2	-3,085	2,31E-02
ENSG00000162073	PAQR4	-3,084	2,32E-02
ENSG00000119431	HDHD3	-3,083	2,32E-02
ENSG00000104064	GABPB1	-3,078	2,36E-02
ENSG00000145349	CAMK2D	-3,063	2,48E-02
ENSG00000162971	TYW5	-3,05	2,58E-02
ENSG00000106683	LIMK1	-3,041	2,65E-02
ENSG00000136003	ISCU	-3,036	2,68E-02
ENSG00000117280	RAB7L1	-3,031	2,73E-02
ENSG00000106392	C1GALT1	-3,028	2,75E-02
ENSG00000187210	GCNT1	-3,023	2,79E-02
ENSG00000074370	ATP2A3	-3,02	2,81E-02
ENSG00000149150	SLC43A1	-3,015	2,85E-02
ENSG00000119777	TMEM214	-3,001	2,99E-02

ENSG00000184489	PTP4A3	-2,986	3,13E-02
ENSG00000175426	PCSK1	-2,984	3,14E-02
ENSG00000170442	KRT86	-2,984	3,14E-02
ENSG00000060762	MPC1	-2,98	3,18E-02
ENSG00000105991	HOXA1	-2,975	3,22E-02
ENSG00000132646	PCNA	-2,97	3,27E-02
ENSG00000122042	UBL3	-2,963	3,33E-02
ENSG00000173535	TNFRSF10C	-2,95	3,46E-02
ENSG00000000460	C1orf112	-2,941	3,56E-02
ENSG00000105486	LIG1	-2,923	3,76E-02
ENSG00000115204	MPV17	-2,918	3,81E-02
ENSG00000181789	COPG1	-2,918	3,81E-02
ENSG00000178761	FAM219B	-2,916	3,82E-02
ENSG00000251992	SCARNA17	-2,916	3,82E-02
ENSG00000143401	ANP32E	-2,912	3,86E-02
ENSG00000115514	TXNDC9	-2,912	3,86E-02
ENSG00000145741	BTF3	-2,91	3,88E-02
ENSG00000113810	SMC4	-2,904	3,95E-02
ENSG00000129991	TNNI3	-2,904	3,95E-02
ENSG00000196757	ZNF700	-2,9	4,00E-02
ENSG00000120656	TAF12	-2,899	4,00E-02
ENSG00000168887	C2orf68	-2,899	4,00E-02
ENSG00000149483	TMEM138	-2,898	4,00E-02
ENSG00000160803	UBQLN4	-2,893	4,07E-02
ENSG00000076258	FMO4	-2,879	4,24E-02
ENSG00000132698	RAB25	-2,878	4,25E-02
ENSG00000166582	CENPV	-2,872	4,33E-02
ENSG00000112576	CCND3	-2,866	4,40E-02
ENSG00000116133	DHCR24	-2,863	4,44E-02
ENSG00000163947	ARHGEF3	-2,861	4,46E-02
ENSG00000280789	PAGR1	-2,86	4,47E-02
ENSG00000260001	TGFBR3L	-2,859	4,48E-02
ENSG00000100979	PLTP	-2,854	4,54E-02
ENSG00000008988	RPS20	-2,852	4,57E-02
ENSG00000187735	TCEA1	-2,851	4,58E-02
ENSG00000142453	CARM1	-2,838	4,74E-02
ENSG00000181982	CCDC149	-2,836	4,78E-02
ENSG00000133067	LGR6	-2,824	4,95E-02

Acknowledgment

I would like to take this opportunity to thank all those who supported me in the preparation of this dissertation:

- Professor Dr. Wilfried Roth for the opportunity to carry out my dissertation at the Institute of Pathology and for his support during this project.
- Dr. Nils Hartmann for the interesting choice of topic, as well as for the support in planning, conducting, and analyzing my work.
- Dr. Katrin Tagscherer for allowing me to carry out the cell culture experiments of my dissertation in her research group and for her support in planning and conducting the study.
- Professor Dr. Hans Zischler for taking on the secondary review.

I would also like to thank all the members of the Hartmann and Tagscherer research groups for their helpfulness and friendliness.

Special thanks to Doris Dreis, who helped me with all tissue-related experiments with great patience and advice, Dr. Michael Kloth and Nadine Dexheimer, who helped me with the RNA-sequencing experiments and analysis, Dr. Daniel-Christoph Wagner, who helped me with analysis of the TMA, Celine Müller, for providing heir code for the analysis of the RNA sequencing and Jutta Richter, who helped me with cell culture experiments.

My thanks also go to the Biobank of the University Medical Center in Mainz for performing the TMA and to the Wilhelm Sander Foundation for funding this work.

Lastly, my thanks go to my family and friends, who supported and motivated me during this time.

Lebenslauf

Persönliche Angaben

Jessika Buchwaldt

Geburtsdatum: 18.07.1995

Akademischer Werdegang

Oktober.2020 – 2025:
Doktoratsstudium an der Johannes Gutenberg-Universität Mainz, Fachbereich Biologie am Institut für Pathologie

April.2018 – Juli.2020:
Master of Science in Biologie an der Johannes Gutenberg-Universität Mainz, Fachbereich Biologie am Institut für Pathologie

Oktober.2014 – August.2018:
Bachelor of Science in Biologie an der Johannes Gutenberg-Universität Mainz, Fachbereich Biologie am Institut für Pathobiochemie

Berufserfahrung

Oktober.2020 – Dezember.2025:
Wissenschaftliche Mitarbeiterin am Institut für Pathologie, Universitätsmedizin der Johannes Gutenberg-Universität Mainz

Juni.2018 – Januar.2019:
Wissenschaftliche Mitarbeiterin am Institut für Pathobiochemie, Universitätsmedizin der Johannes Gutenberg-Universität Mainz

Curriculum Vitae

Personal Information

Jessika Buchwaldt

Date of Birth: July 18, 1995

Academic Background

October 2020 – 2025:

Doctoral studies in Biology at the Institute of Pathology, Johannes Gutenberg University Mainz

April 2018 – July 2020:

Master of Science in Biology at the Institute of Pathology, Johannes Gutenberg University Mainz

October 2014 – August 2018:

Bachelor of Science in Biology at the Institute of Pathobiochemistry, Johannes Gutenberg University Mainz

Professional Experience

October 2020 – December 2025:

Research Associate at the Institute of Pathology, University Medical Center of the Johannes Gutenberg University Mainz

June 2018 – January 2019:

Research Associate at the Institute of Pathobiochemistry, University Medical Center of the Johannes Gutenberg University Mainz

Eidesstattliche Erklärung

Hiermit versichere ich, dass ich diese Dissertation selbstständig verfasst und keine anderen als die angegebenen Quellen und Hilfsmittel benutzt habe. Außerdem versichere ich, dass diese Arbeit weder in der jetzigen noch in einer abgewandelten Form bei einem anderen Prüfungsausschuss vorgelegt wurde.

Mainz, den _____ _____

Jessika Buchwaldt